INTEGRATED MICROSYSTEMS SERIES

Microfabrication for Microfluidics

Sang-Joon John Lee
Narayan Sundararajan

Microfabrication for Microfluidics

For a listing of recent titles in the
Artech House Integrated Microsystems Series,
turn to the back of this book.

Microfabrication for Microfluidics

Sang-Joon John Lee
Narayan Sundararajan

ARTECH
HOUSE
BOSTON | LONDON
artechhouse.com

Library of Congress Cataloging-in-Publication Data
A catalog record for this book is available from the U.S. Library of Congress.

British Library Cataloguing in Publication Data
A catalogue record for this book is available from the British Library.

Cover design by Vicki Kane

ISBN 13: 978-1-59693-471-9

685 Canton Street
Norwood, MA 02062

10 9 8 7 6 5 4 3 2 1

Contents

Preface

> "You can know the name of a bird in all the languages of the world, but when you're finished, you'll know absolutely nothing whatever about the bird. So let's look at the bird and see what it's doing—that's what counts."
>
> —*Richard Feynman*, 1966

We have long been fascinated with the scaling laws that govern phenomena at micro- and nanodimensional scales. Molecular self-assembly, electrostatic droplet steering, light-guided particle manipulation, and materials that exhibit mechanical response to chemical stimuli comprise just a few examples of phenomena that are exploited in microfluidics. The field of microfluidics is delightfully challenging because it requires a highly multidisciplinary understanding of engineering and science principles. Microfluidics is also an enabling technology that benefits society in diverse areas including health and medicine, energy conversion, and environmental protection.

Theories and principles, however, remain incomplete until manifested in and interrogated by observable phenomena. This is where fabrication serves as a bridge between what is thought to be true and what is in fact true. The authors have often found that lack of fabrication knowledge can present unnecessary obstacles for progress and discovery. This has been a central motivation for writing this book: to overcome such barriers and to help others delve more directly into questions of scientific interest as well as problem-solving for practical applications.

We hope that the top-down, methodical approach taken in this book will accelerate novice readers through learning curves. For more experienced readers and practitioners in the field, it is hoped that this book may provide greater breadth of awareness and possibly uncover alternative solutions. With well over

700 citations to published works in microfluidics, we further hope that this book can be helpful as a starting point to dive deeper into the vast knowledge accumulated in the field over the past several years.

Dr. Lee would like to express gratitude to his wife Jung Ah and their daughter Jin-Hee for unwavering support of this endeavor. Dr. Sundararajan would like to acknowledge his wife Prerana and their son Smaran, who have been his inspiration. We also convey thanks to our mentors and colleagues over the years, not only for exchanging their knowledge with us, but more importantly for instilling and cultivating a passion for sharing knowledge with others.

1

Introduction

Microfluidics is a synergy of science and engineering applied to fluid mechanics, involving characteristic dimensions in the micron scale. Examples of application areas include chemical analysis, biological interfacing, medical diagnostics, energy conversion, and toxin detection. Characteristic dimensions such as channel widths or orifice diameters are typically on the order of 10 to 100 μm (10^{-5} to 10^{-4} m). The fluid volumes of interest are typically measured in nanoliters (10^{-9} L) or picoliters (10^{-12} L), and flow rates generally do not exceed more than a few microliters per minute. Figure 1.1 shows one example of a microfluidic device: a subcutaneous insulin delivery device with integrated pumping actuation.

A volume of 1 nL corresponds to a cube that has dimensions of 100 μm on each side; and objects much smaller than 100 μm fall below the limit of resolution by the human eye. Table 1.1 provides a few additional comparisons for volume in relation to microns.

Working with such minute volumes of fluid, microfluidic devices can often be used to achieve exceptional performance in terms of parameters such as sensitivity, speed, and spatial resolution. At one extreme, a microfluidic chemical sensor can detect a target species with sensitivity as fine as one part per billion [1]. At another extreme, an ink-jet droplet generator can print an image with approximately one million discretely controlled droplets in an area of only one square centimeter.

For the purposes of this book, a microfluidic device is defined as an engineered component or assembly that is designed to perform a designated function related to the manipulation and/or analysis of very small volumes of fluids. Examples of such functions include pumping, metering, mixing, component

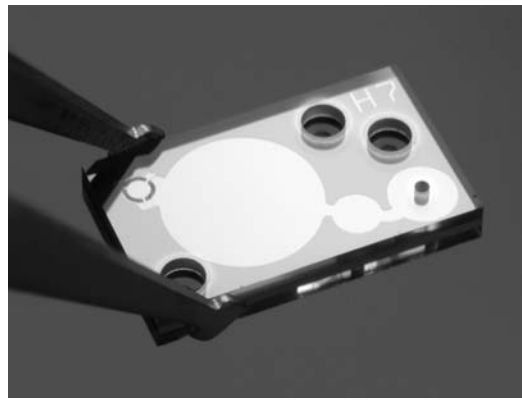

(a)

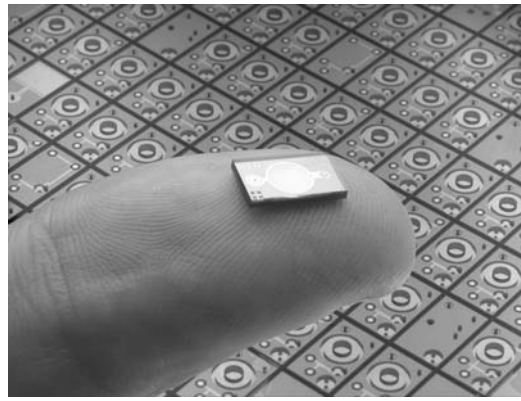

(b)

Figure 1.1 (a, b) Insulin nanopump. (Courtesy of Debiotech S.A.)

Table 1.1
Fluid Volume in Relation to Micron Dimensions and Points of Reference

Size (μm)	Approximate Reference	Volume of a Cube
10,000	Size of a sugar cube	1 milliliter (mL)
1,000	Size of the head of a pin	1 microliter (μL)
100	Diameter of a hair	1 nanoliter (nL)
10	Diameter of a red blood cell	1 picoliter (pL)

separation, and droplet generation. Many microfluidic components perform fluid-related functions that are analogous to macroscale counterparts such as

valves, pumps, and filters. However, scaling laws for microfluidics often dictate that the most relevant physical phenomena can differ vastly for devices in microscale compared to those in macroscale. For example, surface tension dominates over gravitational forces, electric fields tend to be far more influential than pressure gradients, and molecular diffusion becomes more significant relative to bulk fluid displacement.

This book complements a growing knowledge base for microfluidics, as published in books and encyclopedias [2, 3], review articles [4–7], and numerous research papers on the subject. The main purpose of this book, however, is to offer a focused and structured understanding of fabrication aspects in particular. It is intended to serve as an informative guide for readers who may be new to microfabrication processes, as well as a reference for readers with substantial experience in microfluidic device fabrication. With a focus on fabrication, this text does not attempt to discuss fluid dynamics or end applications in depth, and the reader is referred to theory-oriented [8] or applications-oriented materials [9–11], respectively. This book focuses on how to fabricate a wide variety of geometric features using the materials that are most relevant for enabling the functional capabilities required by microfluidic devices.

This introductory chapter establishes the scope of the book. It explains various ways in which microfluidic devices can be classified. This chapter also describes some applications of microfluidics to provide motivating background for the book, without attempting to cover applications comprehensively. Instead, microfluidic functions are discussed at a more generic descriptive level. For example, *electrokinetic pumping* is presented as a microfluidic function, without being restricted specifically to an end application such as *microelectronics cooling*. Examples from the field of microfluidics are presented to illustrate some ways in which these functions have been implemented.

1.1 A Fabrication Perspective

The most appropriate fabrication methods for achieving functional objectives depend on the geometric features that can be produced and what materials properties are needed. Such interdependencies are conceptually illustrated in Figure 1.2. The end application requires one or more microfluidic functions. These functions are made possible by a combination of geometric features and material properties, while taking advantage of physics phenomena in microscale. The microfluidic functions (rather than the end applications per se) are what principally drive the selection of fabrication methods. Suitable fabrication methods are chosen to produce the necessary geometric features with appropriate materials for performing the microfluidic functions. Material properties apply significant constraints on what fabrication methods can be used, and must be

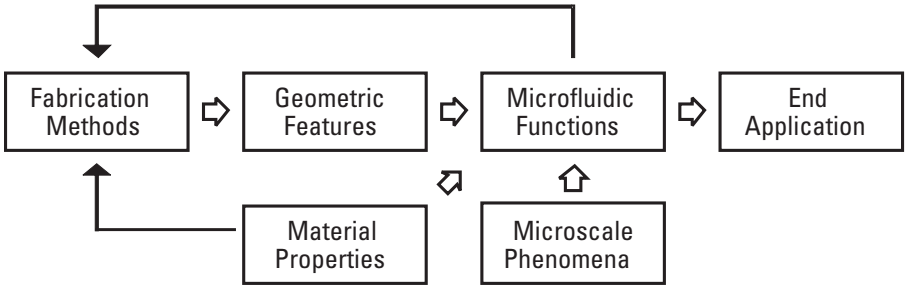

Figure 1.2 Relational map among fabrication methods, geometric features, material properties, microscale phenomena, microfluidic functions, and end applications.

taken into consideration even before attempting to fabricate the desired the geometric features.

As a specific example to illustrate the conceptual framework presented above, consider the end application of insulin delivery. An essential microfluidic function is the pumping of liquid from a reservoir to the point of subcutaneous injection. The function of pumping can be accomplished by several different mechanisms (discussed later in this chapter), but for concise illustration consider the narrow case in which the mechanism of pumping has been selected to be peristaltic action. Having made this initial design decision, there are still several options for the kinds of geometric features that are required and the types of materials that will be involved. One approach has been to use bulk micromachining of etched cavities in stacked silicon wafers [12]. Another approach has been to use surface micromachining of silicon nitride membranes [13]. Yet another approach is to use monolithic elastomer membranes actuated under pneumatic pressure [14, 15]. These all share in common the function of pumping (even more narrowly by peristaltic action), and they can be used for similar end applications. However, the geometric features and materials of construction are very different.

The close interdependency between functional design and fabrication methods is similarly true for MEMS devices [16] as well as for microelectronics [17]. A few microfluidic devices do push the level of large-scale integration [18], but most microfluidic devices tend to be far less complex than microelectronic circuits. However, microelectronic devices are simpler in the limited sense that they are entirely solid-state, have no moving parts, and do not come in contact with fluid media. Some common MEMS transducers (e.g., pressure sensors) do interact with liquid or gaseous media, but many others (e.g., accelerometers) have the advantage of being protected by hermetically sealed packaging. Therefore, it is also the interaction with moving fluids that makes fabrication of microfluidic devices uniquely challenging.

Following the general framework presented above, the next section of this chapter introduces some of the physics phenomena that are exploited for greater functionality and performance in microfluidic devices [19]. It is followed by a description of several engineered functions, with examples from devices that have been demonstrated in the microfluidics field. The main reasons for presenting the physics phenomena and microfluidic functions are to offer background and to set context for examining geometric features, material properties, and fabrication methods presented in the remaining chapters of this book.

1.2 Scaling Laws and Fluid Phenomena

Miniaturization of fluidic devices offers several practical benefits such as using low sample volume, occupying little space, and achieving high throughput. However, these merits alone do not account for the rapidly growing interest in microfluidics in recent years. Many microfluidic devices are not only miniaturized, but are also specifically engineered to take advantage of beneficial scaling phenomena related to the physics of fluid behavior. To help understand why microfluidic devices are designed as they are, this section very briefly introduces a few of the scaling considerations that are important for microfluidic device engineering. For a more thorough understanding of scaling, the reader is referred to a comprehensive discussion on fluid physics at very small dimensions [20].

One very fundamental parameter that needs to be observed when considering dimensional scaling is the surface-to-volume ratio. As the dimensions of a device decrease, the surface area becomes relatively larger compared to the volume. Consequently, parameters such as surface charge and wetting behavior have increasingly greater relevance compared to considerations such as fluid inertia which are based on mass and volume. Figure 1.3 shows how the surface-to-volume ratio rapidly increases as characteristic dimension decreases from 100 μm to below 10 μm. The figure illustrates the case for a microchannel with square cross-section and for a droplet with spherical shape, and both cases exhibit a rapid increase in surface-to-volume ratio as dimensions become smaller.

This observation of surface-to-volume ratio is very important for fluid mechanics at the microscale because forces, whether fluid-related or otherwise, scale differently with diminishing size [21, 22]. Using a generic length variable L, it can be expressed that body forces such as gravity scale as volume (L^3), while surface forces such as those resulting from shear stress along walls are based on area (L^2). In fact, surface tension (as will be discussed later) is even more dependent on geometric scaling because it is a line force that scales linearly with dimension L.

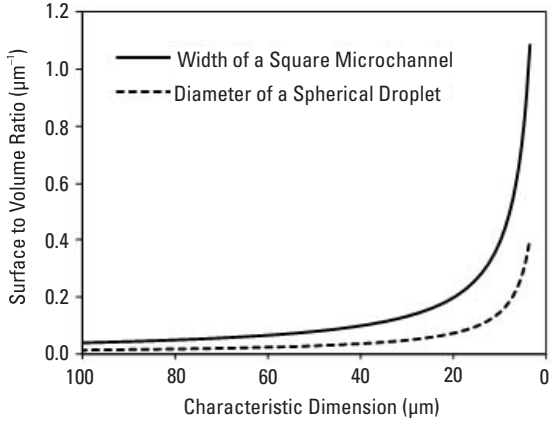

Figure 1.3 Surface-to-volume ratio for microchannels and droplets as dimensions decrease.

As a simplified illustration for conceptual understanding, consider the net one-dimensional force ΣF acting on a fluid element, which is a hypothetical combination of a body force, a surface force, and line force. By Newton's Second Law, the sum of forces equals a change in momentum of the fluid, represented as the mass m times the rate of change of velocity v. In the following relation, this change in momentum is shown to vary as the sum of the body force (represented by density ρ times volume L^3), the surface force (represented by shear stress τ times area L^2), and the line force (represented by surface tension γ times contact perimeter L).

$$m\frac{dv}{dt} \sim \rho(L^3) + \tau(L^2) + \gamma(L) \tag{1.1}$$

As dimensions decrease, body forces diminish more rapidly than surface forces and line forces, and consequently become less significant with respect to the motion $m(dv/dt)$ of the fluid element. For example, if the geometric dimensions of a fluidic device are uniformly reduced by a factor of 10, the first term on the right-hand side of (1.1) (which scales as L^3) decreases by 1/1,000, while the second term (which scales as L^2) decreases by only 1/100. So if the diameter of a microchannel is reduced from 1 mm to 100 μm, surface forces in comparison become 10 times more influential than the weight of the fluid, and surface tension is likewise even more significant.

An example of how a large surface-to-volume ratio is beneficial for microfluidics is *electro-osmotic* flow, in which liquid is dragged along a surface by mobile ions in close proximity to it [23]. Electro-osmotic (EO) flow works

without any moving structures and solves problems that are associated with the high resistance that is typical of pressure-driven flow in microchannels. EO flow is effective in microchannels because all of the fluid throughout the channel is in close proximity to the channel surface, often resulting in a blunt velocity profile as mobile ions closest to the wall drag the entire fluid downstream in response to an applied electric field. This mechanism of fluid transport is not effective in macroscale because as channel size increases the surface-to-volume ratio decreases, and inertia correspondingly overwhelms surface interactions. Another example is the interaction of small liquid droplets and a surface acoustic wave (SAW), for which small volume compared to interfacial area allows acoustic energy to displace droplets [24].

Scaling implications are also revealed in the Navier-Stokes equation, which is the basic differential equation for describing the flow of Newtonian fluids. Per unit volume, it equates fluid acceleration on the left with the sum of forces on the right, in terms of velocity vector **u**, time t, pressure p, dynamic viscosity μ, and body forces (per unit volume) **f**.

$$\rho\left(\frac{\partial \mathbf{u}}{\partial t} + \mathbf{u}\cdot\nabla\mathbf{u}\right) = -\nabla p + \mu\nabla^2\mathbf{u} + \mathbf{f} \tag{1.2}$$

In small dimensions the convective acceleration typically diminishes compared to other terms, leaving the Stokes equation, below. Although expressed as a three-dimensional vector equation per unit volume, still evident is the fact that the motion $\rho(\partial\mathbf{u}/\partial t)$ of fluid depends on a combination of forces that may not scale equally as device dimensions are reduced to microscale.

$$\rho\frac{\partial \mathbf{u}}{\partial t} = -\nabla p + \mu\nabla^2\mathbf{u} + \mathbf{f} \tag{1.3}$$

Having drawn attention to the importance of dimensional scaling, discussed below are some key aspects of fluid flow that are often relevant to the design of microfluidic devices. These are not comprehensive, but rather are provided to offer insight into the unique merits of microfluidic devices as well as some challenges that affect design and manufacturing decisions.

1.2.1 Viscous Flow

A fluid is defined as a substance that continues to exhibit strain when subjected to shear stress [25]. Consequently, viscosity μ is one of the most important fluid properties because it relates shear stress τ to the rate of shearing strain du/dy:

$$\tau = \mu \frac{du}{dy} \tag{1.4}$$

Analysis of fluid mechanics often benefits from dimensionless numbers that describe flow behavior. In microfluidics the most frequently mentioned dimensionless number is the Reynolds number (Re), expressed as a function of density ρ, velocity U, characteristic length L, and dynamic viscosity μ:

$$\mathrm{Re} = \frac{\rho UL}{\mu} \tag{1.5}$$

The Reynolds number compares inertial effects with viscous effects, and the very low values for Re that are typical in microfluidics reveal that microscale flows are greatly dominated by viscous effects. For example, in the case of water ($\rho \approx 1{,}000$ kg/m^3, $\mu \approx 0.001$N·s/m^2 at room temperature) flowing at 1 μL/min through a microchannel of diameter 100 μm, the Reynolds number is only Re = 0.2. The threshold between turbulent flow and laminar flow typically does not occur until Re is at least 10,000 times greater, so microchannel flow is clearly laminar. Detailed considerations beyond this introductory example—such as effects related to entrance regions, non-Newtonian fluids, wall slip, surface roughness, turbulent exceptions, and viscous dissipation—are reported in research literature [26].

Of much practical relevance for microchannel flow is the effect of dimensional scaling on fluidic resistance. Poiseuille's law describes the flow of a Newtonian fluid (one having constant viscosity μ) through a circular tube of length L and radius r, and relates the flow rate Q to the pressure drop Δp across the conduit:

$$Q = \frac{\pi r^4 \Delta p}{8\mu L} \tag{1.6}$$

Fluidic resistance R in a conduit is the pressure drop divided by the volume flow rate, so this shows that the resistance in the channel varies as the inverse of the fourth power of channel radius.

$$R = \frac{8\mu L}{\pi r^4} \tag{1.7}$$

This represents a very unfavorable scaling relationship for pressure-driven flow, because reducing a channel size by a factor of 10 increases the fluidic

resistance by a factor of 10,000. This expression of fluidic resistance is useful even for non-Newtonian fluids such as blood, as long as the apparent viscosity (which may not be constant) can be quantified and appropriately substituted for μ [27]. Not only is it difficult to drive fluid in such a viscosity-dominated flow regime, but also it is nontrivial to achieve mixing of fluids, necessitating alternative three-dimensional flow patterns and/or active cross-flows [28–30].

1.2.2 Surface Tension

Surface tension is a phenomenon in which the intermolecular forces at a fluid boundary maintain a force that depends on the perimeter of that boundary. The coefficient of surface tension γ (also sometimes represented by the symbol σ) has units of force divided by length. The importance of surface tension is often recognized at the three-phase boundary shared by a liquid, a solid, and the surrounding gas (e.g., a water droplet on a glass slide in air), although fundamentally it is also relevant between any two immiscible fluids (e.g., oil in water). The interface between a liquid, solid, and gas is concisely described by the contact angle θ_c, as shown in Figure 1.4.

A classic example illustrates how surface tension and contact angle are affected by dimensional scaling. Figure 1.5 illustrates the capillary rise of a liquid with density ρ inside a circular tube of radius R. The height h of the liquid column is determined by equilibrium resulting from a competition between the force from surface tension and the weight under gravitational acceleration g. Notable is that the left-hand side of (1.8) scales as L^1, while the right-hand side scales as L^3. So if the dimensions of a device are uniformly reduced by a factor of 10, the surface tension decreases by only that same factor of 10 while the weight decreases by 10^3, and in relative comparison surface tension is 1,000 times more influential.

$$2\pi R\gamma \cos\theta = \rho g \pi R^2 h \tag{1.8}$$

For typical values associated with water and glass, if the tube diameter were as small as 1 μm, the column would rise by approximately 30m by capillary

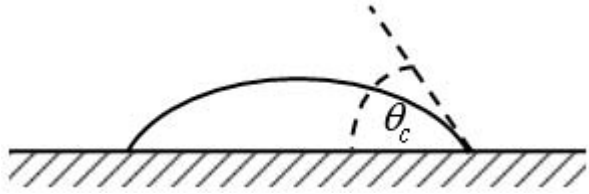

Figure 1.4 Contact angle between a droplet of liquid on a solid surface.

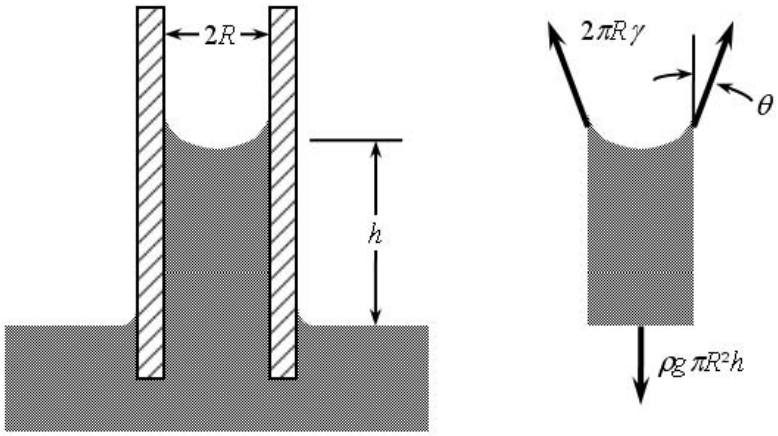

Figure 1.5 Force balance between forces from surface tension and gravity in a capillary tube.

forces alone. This is a clear illustration of how a force that depends on perimeter becomes far more relevant than body forces such as gravity in microscale dimensions. The Weber number (We = $\rho U^2 L/\gamma$) compares inertial effects to surface tension, and in small dimensions the Weber number is also small, revealing the relative insignificance of inertial effects.

Surface tension is an important force that can be used for functional advantages in microfluidics [31], and several examples take advantage of surface wetting phenomena [32, 33]. Electrowetting is a prevalent example of manipulating fluids by locally changing the charge on a surface, which in turn alters the contact angle [34–36]. The contact angle between a liquid and solid can be altered by other mechanisms as well, such as thermal gradients and photo-initiated changes to surface conditions.

1.2.3 Diffusion

Diffusion is another fundamental phenomenon that influences the design and functionality of microfluidic devices. Diffusion pertains to the redistribution of molecules or particles in response to concentration gradients, and microfluidic applications require effective control over molecule or particle concentration, both spatially and temporally.

Fick's first law relates the flux J of molecules (expressed per unit are a per unit time) to the concentration C using a diffusion coefficient D (also called diffusivity). In one dimension x, it is expressed as $J = -D(\partial C/\partial x)$, or in three dimensions (x,y,z) the same equation is expressed in a more general form using the gradient operator ∇:

$$J = -D\nabla C \tag{1.9}$$

The diffusion coefficient D has dimensions of length squared per unit time, and for microfluidics a convenient set of units is $\mu m^2/s$. Considering a suspension of particles in liquid, smaller particles have higher values for diffusion coefficient than larger particles, corresponding to the intuitive understanding that smaller particles more readily redistribute by diffusion than larger ones. Changes in concentration with respect to time are expressed in Fick's second law:

$$\frac{\partial C}{\partial t} = D\nabla^2 C \tag{1.10}$$

Comparing microfluidic flows to macroscale counterparts, diffusion takes a more important role compared to convection and bulk flow. The ratio of convection to diffusion is effectively expressed by the nondimensional Péclet number (Pe), defined in terms of flow velocity U, a characteristic length L, and the diffusion coefficient D:

$$\text{Pe} = \frac{Ul}{D} \tag{1.11}$$

A large value for diffusion coefficient (and thus small Péclet number) can be beneficial for separation and filtering applications, in which the differences in diffusion coefficient alone can be used to separate smaller particles from larger ones in a mixed flow without any need for membranes or centrifuge methods [37]. On the other hand, passive diffusion may be inadequate for rapid mixing applications and must be accelerated by methods such as modifying channel walls to more actively disrupt flow streams [38]. In either case, effective performance requires attention to diffusion phenomena with respect to geometric scaling considerations.

1.3 Microfluidic Functions

The breadth and variety of microfluidic functions are vast, and this section attempts to provide a high-level categorization into three broad areas: flow control within enclosed cavities and conduits, manipulation of particles and cells, and ejection of fluids in the form of droplets or sprays. Each of these is discussed below, along with some lower-level functions that fall within each category. The purpose is to reinforce the fabrication perspective on microfluidics that was presented in Section 1.1. Fabrication decisions can be viewed in terms of suitability

for enabling one or more application-required *functions*. So before proceeding into the subsequent chapters on the details regarding geometric features and materials selection, it is helpful to establish an awareness of variety of the functions that microfluidics technology enables.

There are certainly functions that fall beyond or overlap the categories of flow control, particle/cell manipulation, and droplet/spray generation. For example, one other category that has gained attention is the manipulation of discrete volumes of liquid on an open surface rather than in enclosed channels or cavities [39]. Fluid droplets are also used in novel applications such as reconfigurable optics [40]. So the following three categories are neither comprehensive nor rigidly exclusive of one another, but do attempt to present a high-level grouping of many important functions performed by microfluidic components and devices.

1.3.1 Flow Control

Arguably the most fundamental function of a microfluidic device is to move a volume of fluid from one location to another, and many of the earliest microfluidic devices focused primarily on flow control [41]. Flow control includes a suite of component functions including pumping, isolation, switching, metering, regulating, and mixing. There are numerous approaches to microfluidic pumping, and two most common approaches for are pressure-driven flow and electro-osmotic flow [42–45].

Another very fundamental function for microfluidic devices is control of flow by isolation or switching. These functions are often performed by some sort of deformable surface, but may also include approaches with nonmoving parts based on differences in hydrodynamic behavior or surface tension [46]. Microvalves based on diaphragms or other deflecting surfaces are often advantageous for compatibility with layer-based microfabrication, but there is a wide variety of other approaches that also include sliding or rotating components.

Many microfluidic applications involve analysis for which a discretely controlled sample of interest is transported in a buffer solution, or more than one fluid sample must be allowed to interact. So numerous innovations in mixing and flow injection have been developed [47–49]. Consistent and stable flow is important for many sample analysis applications, and accordingly flow metering, regulation, and stabilization are also important flow control functions [50].

1.3.2 Particle Manipulation

One of the most essential functions for chemical and biochemical analysis is the separation of particles that may include macromolecules, proteins, and other constituents carried by fluids [51–53]. For analysis applications, not only do

particles need to be separated, but functions such as filtering and preconcentrating are typically required as prerequisite steps. For larger particles, sorting rather than filtering may be of greater interest [54–56]. Particle focusing into narrow spatial regions is often essential for high-resolution analysis [57], and one application for which particle focusing is particularly useful is flow cytometry for the counting of particles or cells in a fluid stream [58, 59]. Perhaps the most intriguing set of microfluidic functions for biological applications is the direct manipulation of living cells [60–62]. The variety of cell manipulation functions include not only separation, placement, and confinement, but also more intrusive operations including mechanical stress application, lysing, and neurophysiological probing [63, 64].

1.3.3 Fluid Ejection

In contrast to flow control in confined volumes and fluidic manipulation of particles, a distinct but important category of microfluidic flow involves flow ejection in the form of droplets, jets, and sprays [65]. The most well-established microfluidic function involving external flows is droplet generation for ink-jet printing of digital images on paper [66]. This function has been commercially viable in image printing for so many years and has become so commonplace that it is not always considered under the heading of microfluidics. However, droplet sizes and the characteristic dimensions of printhead components are indeed in the range of microfluidics, and scaling laws associated with factors such as surface tension, capillary adhesion, and drag are very relevant. Moreover, ink-jet methods have expanded beyond image printing to include three-dimensional object printing [67] and biological applications as well [68].

Another important microfluidic function is the generation of fine sprays, in particular by electrospray methods [69, 70]. Microfluidic jets in air are generally not feasible because of the inherent instability in competition with surface tension, but jets can be used to inject fluids into liquid reservoirs to achieve engineered gradients [71]. An example of a microfluidic function that is entirely distinct from those required by the more common biological or chemical applications is satellite propulsion [72].

1.4 Semantics

Microfluidics has been discussed in some contexts as a subset of microelectromechanical systems (MEMS) or microsystems technology (MST) [73, 74]. The description of microsytems technology is sufficiently broad that such categorization of microfluidics as a subset is justified. Many MEMS devices are specifically engineered for microfluidic functions [75], but it is also true that

many microfluidic devices involve no electromechanical transduction whatsoever. To distinguish from microsystems and MEMS transducers that are not directly involved with fluid interaction, the word "microfluidics" will be treated as a separate technology field rather than as a subset of either MEMS or MST in the context of this book.

BioMEMS is a subset of MEMS that focuses on biological applications [76]. As many biological systems are inherently based on fluids, it is no coincidence that the words microfluidics and BioMEMS are often used interchangeably. For distinction, however, it is worth noting that some BioMEMS devices such as neural implant [77] and micromechanical sensors [78] are not directly concerned with fluid dynamics. Therefore, BioMEMS is not limited to the field of microfluidics. Likewise, microfluidics can be viewed as a vital technology for BioMEMS, but should not be exclusively restricted to it. Applications for microfluidics are much more diverse, and include the well-established example of ink-jet printing as well as other applications such as energy conversion [79] and microelectronics cooling [80].

The coined phrases lab-on-a-chip (LoC) [81] and micro total analysis systems (μTAS) [82–84] typically refer to systems that perform multiple operations toward an integrated end-application. By performing important functions such as filtering, mixing, pumping, particle focusing, and so on, microfluidics can be viewed as the most fundamental enabling technology for LoC and μTAS devices. However, the latter terms may also encompass other important functions such as optical detection, signal processing, and other system-level considerations that are not fluidic per se. This offers some distinction from the word microfluidics defined in a more narrow sense. Chapter 10 addresses multifunctional integration issues, focusing on how the microfluidic components fit in the context of system-level requirements that are needed in higher-level LoC and μTAS applications.

Historically the concept of a micro total analysis system originated from a MEMS perspective for miniaturized *chemical* analysis with early devices explored in silicon [85, 86], whereas the concept of lab on a chip was driven more strongly by *biological* applications with the majority of devices in glass and polymer materials [87]. However, these distinctions between LoC and μTAS are neither firm nor absolute. These terms are often used interchangeably and for simplicity will be treated as being effectively synonymous for the purposes of this book.

The term nanofluidics [88] has also been coined to draw attention to fluid phenomena at characteristic length scale even smaller than those for established microfluidic devices. As mentioned previously, however, critical fluid volumes are already sometimes in the picoliter range, so presumably nanofluidics should then be more narrowly restricted to devices with characteristic dimensions less than approximately 100 nm. The distinction between nanofluidics and

microfluidics remains vaguely used, however, and for the purposes of this book the term "nanofluidics" will generally not be used even if some characteristic dimensions are well into the nanometer scale.

1.5 Categorizing Fabrication Processes

Most of the fundamental processes used to fabricate MEMS [89] and semiconductor-based microelectronic devices [90, 91] find utility for microfluidic devices. Books that cover both fundamental and broad aspects of MEMS and microsystems [92–95] accordingly dedicate significant attention to fabrication methods as well. This book complements existing knowledge on the fundamentals of microfabrication processes in general with a specific focus on how such processes have been used to fabricate features that are most relevant to microfluidic devices.

1.5.1 Bulk Micromachining Versus Surface Micromachining

Before the rapid expansion of ever-more diverse processes, microfabrication for MEMS devices could coarsely be divided into two major categories: bulk micromachining and surface micromachining [96]. Bulk micromachining is based on selective removal of material from a substrate such as a silicon wafer or glass slide. The substrate usually remains as an important and functional part of the working device, such as the membrane of a silicon pressure sensor or the main body of a glass microchannel device. Surface micromachining is a combination of film deposition and removal processes. Each layer is selectively patterned, and often one or more sacrificial layers are used to create regions of free space underneath suspended structures. In contrast to bulk micromachining, the underlying substrate may sometimes be entirely passive and used simply as a supporting structure for the surface-micromachined features that are built upon it.

There are several important microfabrication processes that do not fall into either category of bulk or surface micromachining. One common example is masked electroplating, which, although built upon a surface, is typically used for features that are much thicker than those produced by thin-film metal deposition. Furthermore, the rapid growth of interest in polymer materials for microfluidics has put much attention on solidification or reshaping techniques such as casting and hot embossing. With accelerated interest in polymer-based microfluidic systems over silicon and glass devices, it can be argued that a more contemporary way of categorizing fabrication processes for microfluidics is hard micromachining versus soft micromachining [97].

1.5.2 Serial Versus Parallel Fabrication Processes

A broad but important distinction among fabrication processes is the nature of spatial control, sometimes described as *serial* versus *parallel*. Describing a process as serial implies that the material is changed at a localized point, such as the point of incidence of a focused ion beam. Fabrication proceeds in a serial fashion by repositioning of the point of interaction with respect to the working substrate. This can be done either by steering a beam or particle stream, or by moving a substrate on a motorized stage beneath a stationary beam axis. In contrast, describing a process as spatially parallel typically means that a broader area is affected simultaneously. For example, when a wafer is submerged in a liquid etchant, all exposed surfaces of the wafer are subject to etching simultaneously.

A fundamental trade-off between serial and parallel processes is that serial processes tend to offer greater flexibility for producing custom design features and arrangements, while parallel processes are generally superior in terms of productivity. This distinction between serial and parallel spatial control is not always exclusive, and often combinations of serial and parallel strategies are used to balance flexibility and productivity. A multijet printhead is an example of running an essentially serial process (droplet ejection) in a parallel format with several jets active simultaneously. Marching a reticle on a photolithography stepper machine is an example of running an essentially parallel process (UV imaging) in serially incremented steps.

Spatially parallel fabrication methods are very often implemented based on copying from some master pattern. For example, a metal hot embossing tool may have thousands of ridges patterned across its surface. When pressed upon a thermoplastic material, this master produces thousands of grooves in the thermoplastic simultaneously. Effort, time, and expense are invested in the master, and subsequently large numbers of copies are then manufactured with high repeatability, high productivity, and low cost. This is in contrast to patterning the same array of grooves by a spatially serial process such as laser ablation. The latter may offer greater flexibility for custom patterns, but in general serial processes are less repeatable and much slower than parallel processes.

1.5.3 Major Fabrication Process Categories

Microfabrication processes for the purposes of this book are as grouped under four major categories as shown in Figure 1.6. This framework is not intended to set definitive boundaries, but to enable organization of chapters according to broad similarities. There are alternative ways that processes can be grouped based on type of material, serial versus parallel approaches, overall dimensional scale, and other possibilities. While this perspective is thus somewhat arbitrary, it is effective for highlighting fundamental commonalities among the processes as grouped in the figure.

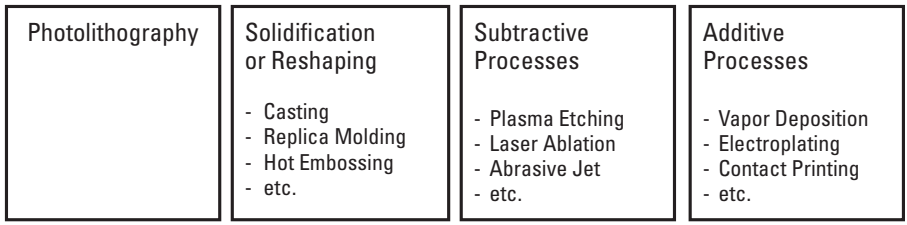

Figure 1.6 Broad categories of microfabrication processes.

In addition to these major categories, other categories include surface modification, bulk properties modification, and assembly processes. Some of the most commonly encountered bulk modification processes in microfabrication are ion implantation, diffusion, and annealing. There are several surface modification processes that do not grossly change geometric feature, but are very important to microfluidic applications. Rather than treating them as separate categories, however, examples of bulk properties modification and surface modification will be distributed within the context of their relevance to other processes and functional requirements.

1.6 Organization of this Book

What has been presented in this chapter is a perspective on microfluidics from a fabrication point of view, in which the ability to fabricate geometric features with desirable material properties directly determines the ability to perform the required microfluidic functions needed by end applications. Some physics phenomena that are exploited for microfluidic functions have been briefly introduced, and some examples of microfluidic functions have been presented. The framework establishes a connection to the main substance of this handbook, which focuses on geometric features, materials, fabrication methods, and functional integration.

Chapter 2 focuses on the actual structures and components that are needed to achieve the various functions that were introduced in this chapter. The main purpose is to reveal the physical similarities among structures such as wells, channels, membranes, and beams. This chapter shows how certain functional structures serve as the essential building blocks for a very wide variety of devices, and thus provides a bridge between the microfluidic functions introduced in this chapter and the more specific fabrication topics detailed in subsequent chapters.

Chapter 3 recognizes fundamentally important ways in which materials dictate not only functional utility, but also the options available for fabrication.

Thus the chapter provides a resource for materials selection in microfluidic device design. Depending on application, some of the critical issues for materials selection include mechanical behavior, thermal stability, chemical compatibility, electrical characteristics, and optical properties. This chapter introduces the most common materials used in microfluidics, and includes examples from published literature to illustrate how material properties specifically impact device functionality. The parts of this chapter that will be of greatest benefit to more experienced readers will be the material properties tables that are drawn from materials handbooks, product datasheets, and other sources with cross-reference citations. There are many important aspects of material surface conditions that are not properties per se, but are still very influential in microfluidics. Several examples of inherent and modified surface conditions will be included in the discussion of materials as well.

Chapter 4 begins the main chapters on fabrication, leading with photolithography. Since the earliest developments in microfabrication, photolithography has served as the most essential and important step for a vast majority of devices. It can actually be described as a combination of subtractive, additive, and selective solidification processes. Readers already familiar with the fundamentals of photolithography may prefer to skip to the later chapters.

Chapter 5 features solidification processes. In terms of organizational sequence, it may be considered somewhat nonconventional to discuss solidification processes ahead of subtractive processes. Etching is traditionally considered to be the most basic type of microfabrication process after photolithography. However, techniques of soft lithography and advances with polymer materials have had a very profound impact on the field of microfluidics in the past several years [98] and are anticipated to continue driving future innovations in the field. Accordingly, the authors feel that it does better justice to present these topics ahead of the more traditional microfabrication processes such as plasma etching and thin-film vapor deposition.

Chapters 6 and 7 present the relatively straightforward topics of subtractive processes and additive processes. These topics coincide with most traditional discussions of microfabrication. Etching as a subtractive process and thin-film vapor deposition as an additive process are two of the most common examples. These chapters also discuss several more subtractive and additive processes along with their application to microfluidic devices. Chapter 8 recognizes that many functional devices cannot be made by subtractive or additive processes independently of each other. Instead, it often takes a combination of additive and subtractive processes to produce useful cavities and to provide proper degrees of freedom for microfluidic devices.

A majority of microfluidic devices are fabricated from planar substrates, and consequently require some form of alignment and assembly of multiple substrates. Chapter 9 surveys the variety of methods by which microfluidic

substrates are bonded and by which fluidic interfacing of chips to the macro world is implemented. These topics primarily address fluidic packaging issues. Chapters 5, 6, and 7 generally address core processes steps and represent the central focus of this book. Chapters 8 and 9 address other important aspects that may be less elementary with respect to creating geometric features, but often are equally important for the fabrication of useful microfluidic devices.

Chapter 10 extends and closes the book with a discussion of system integration and augmented functionality beyond the fluidic domain. Topics in Chapter 10 include integration with electromechanical transducers, optical sensors, and chemical detectors, and biological systems for higher-level device functionality.

References

[1] Timmer, B. H., et al., "Selective Low Concentration Ammonia Sensing in a Microfluidic Lab-on-a-Chip," *IEEE Sensors Journal*, Vol. 6, June 2006, pp. 829–835.

[2] Nguyen, N., and S. T. Wereley, *Fundamentals and Applications of Microfluidics*, 2nd ed., Norwood, MA: Artech House, 2006.

[3] Li, D., (ed.), *Encyclopedia of Microfluidics and Nanofluidics*, New York: Springer, 2008.

[4] Gravesen, P., J. Branebjerg, and O. S. Jensen, "Microfluidics—A Review," *Journal of Micromechanics and Microengineering*, Vol. 3, 1993, pp. 168–182.

[5] Whitesides, G. M., "The Origins and the Future of Microfluidics," *Nature*, Vol. 442, No. 7101, 2006, pp. 368–373.

[6] Ong, S. E., et al., "Fundamental Principles and Applications of Microfluidic Systems," *Frontiers in Bioscience*, 2008, pp. 2757–2773.

[7] Abgrall, P., and A. M. Gué, "Lab-on-Chip Technologies: Making a Microfluidic Network and Coupling It into a Complete Microsystem—A Review," *Journal of Micromechanics and Microengineering*, Vol. 17, No. 5, 2007, pp. R15–R49.

[8] Bruus, H., *Theoretical Microfluidics*, New York: Oxford University Press, 2007.

[9] Tay, F. E. H., (ed.), *Microfluidics and BioMEMS Applications*, New York: Springer, 2002.

[10] Gomez, F. A., *Biological Applications of Microfluidics*, New York: Wiley-Interscience, 2008.

[11] Saliterman, S., *Fundamentals of bioMEMS and Medical Microdevices*, Bellingham, WA: SPIE—The International Society for Optical Engineering, 2006.

[12] Schabmueller, C. G. J., et al., "Self-Aligning Gas/Liquid Micropump," *J. Micromech. Microengineering*, Vol. 12, July 2002, pp. 420–424.

[13] Judy, J. W., T. Tamagawa, and D. L. Polla, "Surface-Machined Micromechanical Membrane Pump," *IEEE Proceedings of Micro Electro Mechanical Systems, 1991, MEMS '91, An Investigation of Micro Structures, Sensors, Actuators, Machines and Robots*, 1991, pp. 182–186.

[14] Unger, M. A., et al., "Monolithic Microfabricated Valves and Pumps by Multilayer Soft Lithography," *Science*, Vol. 288, 2000, pp. 113–116.

[15] Sundararajan, N., D. Kim, and A. A. Berlin, "Microfluidic Operations Using Deformable Polymer Membranes Fabricated by Single Layer Soft Lithography," *Lab on a Chip*, Vol. 3, 2005, pp. 350–354.

[16] Judy, J. W., "Microelectromechanical Systems (MEMS): Fabrication, Design and Applications," *Smart Mater. Struct.*, Vol. 10, December 2001, pp. 1115–1134.

[17] Campbell, S. A., *Fabrication Engineering at the Micro- and Nanoscale*, New York: Oxford University Press, 2008.

[18] Thorsen, T., S. J. Maerkl, and S. R. Quake, "Microfluidic Large-Scale Integration," *Science*, Vol. 298, 2002, pp. 580–584.

[19] Beebe, D. J., G. A. Mensing, and G. M. Walker, "Physics and Applications of Microfluidics in Biology," *Annu. Rev. Biomed. Eng.*, Vol. 4, August 1, 2002, pp. 261–286.

[20] Squires, T. M., and S. R. Quake, "Microfluidics: Fluid Physics at the Nanoliter Scale," *Reviews of Modern Physics*, Vol. 77, 2005, pp. 977–1026.

[21] Trimmer, W. S. N., "Microrobots and Micromechanical Systems," *Sensors and Actuators*, Vol. 19, 1989, pp. 267–287.

[22] Shimoyama, I., "Scaling in Microrobots," *Proceedings of the IEEE/RSJ International Conference on Intelligent Robots and Systems*, 1995, pp. 208–211.

[23] Manz, A., et al., "Electroosmotic Pumping and Electrophoretic Separations for Miniaturized Chemical Analysis Systems," *Journal of Micromechanics and Microengineering*, Vol. 4, 1994, pp. 257–265.

[24] Beyssen, D., et al., "Microfluidic Device Based on Surface Acoustic Wave," *Sensors and Actuators, B: Chemical*, Vol. 118, No. 1-2, 2006, pp. 380–385.

[25] Munson, B. R., D. F. Young, and T. H. Okiishi, *Fundamentals of Fluid Mechanics*, New York: John Wiley & Sons, 2006.

[26] Koo, J., and C. Kleinstreuer, "Liquid Flow in Microchannels: Experimental Observations and Computational Analyses of Microfluidics Effects," *J. Micromech. Microengineering*, Vol. 13, 2003, pp. 568–579.

[27] Sugihara-Seki, M., and B. M. Fu, "Blood Flow and Permeability in Microvessels," *Fluid Dyn. Res.*, Vol. 37, 2005, pp. 82–132.

[28] Lee, S. W., et al., "A Split and Recombination Micromixer Fabricated in a PDMS Three-Dimensional Structure," *J. Micromech. Microengineering*, Vol. 16, 2006, pp. 1067–1072.

[29] Tsouris, C., et al., "Electrohydrodynamic Mixing in Microchannels," *AICHE J.*, Vol. 49, 2003, pp. 2181–2186.

[30] Lynn, N. S., C. S. Henry, and D. S. Dandy, "Microfluidic Mixing Via Transverse Electrokinetic Effects in a Planar Microchannel," *Microfluidics and Nanofluidics*, Vol. 5, 2008, pp. 493–505.

[31] Kim, C. -J., *Microfluidics Using the Surface Tension Force in Microscale,* Vol. 4177, Santa Clara, CA: Society of Photo-Optical Instrumentation Engineers, 2000.

[32] Jokinen, V., and S. Franssila, "Capillarity in Microfluidic Channels with Hydrophilic and Hydrophobic Walls," *Microfluidics and Nanofluidics*, Vol. 5, 2008, pp. 443–448.

[33] Zhao, B., J. S. Moore, and D. J. Beebe, "Surface-Directed Liquid Flow Inside Microchannels," *Science*, Vol. 291, 2001, pp. 1023–1026.

[34] Wang, K. L., and T. B. Jones, "Electrowetting Dynamics of Microfluidic Actuation," *Langmuir*, Vol. 21, No. 9, 2005, pp. 4211–4217.

[35] Pollack, M. G., A. D. Shenderov, and R. B. Fair, "Electrowetting-Based Actuation of Droplets for Integrated Microfluidics," *Lab on a Chip*, Vol. 2, May 2002, pp. 96–101.

[36] Satoh, W., M. Loughran, and H. Suzuki, "Microfluidic Transport Based on Direct Electrowetting," *J. Appl. Phys.*, Vol. 96, 2004, pp. 835–841.

[37] Brody, J. P., and P. Yager, "Diffusion-Based Extraction in a Microfabricated Device," *Sensors and Actuators A: Physical*, Vol. 58, January 1997, pp. 13–18.

[38] Johnson, T. J., D. Ross, and L. E. Locascio, "Rapid Microfluidic Mixing," *Anal. Chem.*, Vol. 74, 2002, pp. 45–51.

[39] Fouillet, Y., et al., "Digital Microfluidic Design and Optimization of Classic and New Fluidic Functions for Lab on a Chip Systems," *Microfluidics and Nanofluidics*, Vol. 4, 2008, pp. 159–165.

[40] Cheng, C., C. A. Chang, and J. A. Yeh, "Variable Focus Dielectric Liquid Droplet Lens," *Optics Express*, Vol. 14, 2006, pp. 4101–4106.

[41] Ho, C., and Y. Tai, "Review: MEMS and Its Applications for Flow Control," *J. Fluids Eng. Trans. ASME*, Vol. 118, 1996, pp. 437–446.

[42] Iverson, B., and S. Garimella, "Recent Advances in Microscale Pumping Technologies: A Review and Evaluation," *Microfluidics and Nanofluidics*, Vol. 5, August 1, 2008, pp. 145–174.

[43] Laser, D. J., and J. G. Santiago, "A Review of Micropumps," *J. Micromech. Microengineering*, Vol. 14, June 2004, pp. 35–64.

[44] Nguyen, N., X. Huang, and T. K. Chuan, "MEMS—Micropumps: A Review," *J. Fluids Eng. Trans. ASME*, Vol. 124, 2002, pp. 384–392.

[45] Chen, L., et al., "Continuous Dynamic Flow Micropumps for Microfluid Manipulation," *Journal of Micromechanics and Microengineering*, Vol. 18, 2008, p. 013001.

[46] Oh, K. W., and C. H. Ahn, "A Review of Microvalves," *Journal of Micromechanics and Microengineering*, Vol. 16, 2006, pp. R13–R39.

[47] Nguyen, N., and Z. Wu, "Micromixers—A Review," *J. Micromech. Microengineering*, Vol. 15, February 2005, pp. 1–16.

[48] Tseng, H. -Y., et al., "Membrane-Activated Microfluidic Rotary Devices for Pumping and Mixing," *Biomed. Microdevices*, Vol. 9, August 2007, pp. 545–554.

[49] Chang, C., and R. Yang, "Electrokinetic Mixing in Microfluidic Systems," *Microfluidics and Nanofluidics*, Vol. 3, 2007, pp. 501–525.

[50] Bozhi, Y., J. W. Levis, and L. Qiao, "A PDMS-Based Constant-Flowrate Microfluidic Control Device," *17th IEEE International Conference on Micro Electro Mechanical Systems (MEMS)*, 2004, pp. 379–382.

[51] Beech, J. P., and J. O. Tegenfeldt, "Tuneable Separation in Elastomeric Microfluidics devices," *Lab on a Chip*, 2008.

[52] Chen, X., et al., "Microfluidic Chip for Blood Cell Separation and Collection Based on Crossflow Filtration," *Sensors and Actuators B: Chemical*, Vol. 130, 2008, pp. 216–221.

[53] Kulrattanarak, T., et al., "Classification and Evaluation of Microfluidic Devices for Continuous Suspension Fractionation," *Adv. Colloid Interface Sci.*, Vol. 142, 2008, pp. 53–66.

[54] Chen, P., et al., "Microfluidic Chips for Cell Sorting," *Front Biosci.*, 2008, pp. 2464–2483.

[55] Fernandez, J. G., et al., "All-Polymer Microfluidic Particle Size Sorter for Biomedical Applications," *Physica Status Solidi (A) Applied Research*, Vol. 203, 2006, pp. 1476–1480.

[56] Sun, Y., et al., "Design, Simulation and Experiment of Electroosmotic Microfluidic Chip for Cell Sorting," *Sensors and Actuators A: Physical*, Vol. 133, 2007, pp. 340–348.

[57] Sundararajan, N., et al., "Three-Dimensional Hydrodynamic Focusing in Polydimethylsiloxane (PDMS) Microchannels," *Journal of Microelectromechanical Systems*, Vol. 13, 2004, pp. 559–567.

[58] Jacobson, S. C., et al., "Flow Cytometry on Microfluidic Devices," *Solid-State Sensor and Actuator Workshop*, 2000, pp. 203–205.

[59] Ateya, D., et al., "The Good, the Bad, and the Tiny: A Review of Microflow Cytometry," *Analytical and Bioanalytical Chemistry*, 2008, pp. 1618–1642.

[60] Griscom, L., et al., "Cell Placement and Neural Guidance Using a Three-Dimensional Microfluidic Array," *Japanese Journal of Applied Physics, Part 1: Regular Papers and Short Notes and Review Papers*, Vol. 40, 2001, pp. 5485–5490.

[61] Tsutsui, H., and C. Ho, "Cell Separation by Non-Inertial Force Fields in Microfluidic Systems," *Mech. Res. Commun.*, 2009, Vol. 36, pp. 92–103.

[62] Lai, C., et al., "A Cell Delivery and Pre-Positioning System Utilizing Microfluidic Devices for Dual-Beam Optical Trap-and-Stretch," *Sensors and Actuators B: Chemical*, Vol. 135, December 10, 2008, pp. 388–397.

[63] Van Vliet, K. J., G. Bao, and S. Suresh, "The Biomechanics Toolbox: Experimental Approaches for Living Cells and Biomolecules," *Acta Materialia*, Vol. 51, 2003, pp. 5881–5905.

[64] Brown, T. D., "Techniques for Mechanical Stimulation of Cells In Vitro: A Review," *Journal of Biomechanics*, Vol. 33, 2000, pp. 3–14.

[65] Guillot, P., et al., "Droplets and Jets in Microfluidic Devices," *Comptes Rendus Chimie*, Vol. 12, 2009, pp. 247–257.

[66] Doane, I. G., "A Review of Ink-Jet Printing," *Journal of Applied Photographic Engineering*, Vol. 7, October 1981, pp. 121–125.

[67] Sachs, E., et al., "Three-Dimensional Printing: The Physics and Implications of Additive Manufacturing," *CIRP Ann. Manuf. Technol.*, Vol. 42, 1993, pp. 257–260.

[68] Cooley, P., D. Wallace, and B. Antohe, "Applications of Ink-Jet Printing Technology to BioMEMS and Microfluidic Systems," *Proceedings of SPIE—The International Society for Optical Engineering, Microfluidics and BioMEMS 2001*, 2001, pp. 177–188.

[69] Shinohara, H., et al., "Polymer Microchip Integrated with Nano-Electrospray Tip for Electrophoresis–Mass Spectrometry," *Sensors and Actuators B: Chemical*, Vol. 132, June 16, 2008, pp. 368–373.

[70] Sen, A. K., J. Darabi, and D. R. Knapp, "Design, Fabrication and Test of a Microfluidic Nebulizer Chip for Desorption Electrospray Ionization Mass Spectrometry," *Sensors Actuators B: Chemical*, Vol. 137, April 2, 2009, pp. 789–796.

[71] Keenan, T. M., C. Hsu, and A. Folch, "Microfluidic 'Jets' for Generating Steady-State Gradients of Soluble Molecules on Open Surfaces," *Appl. Phys. Lett.*, Vol. 89, 2006, p. 114103–1.

[72] Patel, K. D., et al., "Electrokinetic Pumping of Liquid Propellants for Small Satellite Microthruster Applications," *Sensors and Actuators B: Chemical*, Vol. 132, June 16, 2008, pp. 461–470.

[73] Gad-el-Hak, M., *MEMS: Design and Fabrication*, Boca Raton, FL: CRC Press, 2006.

[74] Hsu, T., *MEMS & Microsystems: Design and Manufacture*, New York: McGraw-Hill, 2002.

[75] Henning, A. K., "Microfluidic MEMS," *Proceedings of the 1998 IEEE Aerospace Conference*, Aspen, CO, 1998, pp. 471–486.

[76] Grayson, A. C. R., et al., "A BioMEMS Review: MEMS Technology for Physiologically Integrated Devices," *Proc IEEE*, Vol. 92, January 2004, pp. 6–21.

[77] Spratley, J. P. F., et al., "Flexible SU-8 Microstructures for Neural Implant Design," *Sensors and Actuators A: Physical*, Vol. 147, September 15, 2008, pp. 324–331.

[78] Yang, S., and M. T. A. Saif, "MEMS Based Force Sensors for the Study of Indentation Response of Single Living Cells," *Sensors and Actuators A: Physical*, Vol. 135, March 30, 2007, pp. 16–22.

[79] Lee, S. J., et al., "Design and Fabrication of a Micro Fuel Cell Array with 'Flip-Flop' Interconnection," *Journal of Power Sources*, Vol. 112, 2002, pp. 410–418.

[80] Jiang, L., et al., "Closed-Loop Electro-Osmotic Microchannel Cooling System for VLSI Circuits," *IEEE Transactions on Components and Packaging Technologies*, Vol. 25, 2002, pp. 347–355.

[81] Figeys, D., and D. Pinto, "Lab-on-a-Chip: A Revolution in Biological and Medical Sciences," *Anal. Chem.*, Vol. 72, May 1, 2000, pp. 330A–335A.

[82] West, J., et al., "Micro Total Analysis Systems: Latest Achievements," *Anal. Chem.*, Vol. 80, June 1, 2008, pp. 4403–4419.

[83] Dittrich, P. S., K. Tachikawa, and A. Manz, "Micro Total Analysis Systems. Latest Advancements and Trends," *Anal. Chem.*, Vol. 78, June 1, 2006, pp. 3887–3908.

[84] Vilkner, T., D. Janasek, and A. Manz, "Micro Total Analysis Systems. Recent Developments," *Anal. Chem.*, Vol. 76, June 1, 2004, pp. 3373–3386.

[85] Manz, A., N. Graber, and H. M. Widmer, "Miniaturized Total Chemical Analysis Systems: A Novel Concept for Chemical Sensing," *5th International Conference on Solid-State Sensors and Actuators and Eurosensors III*, 1990, pp. 244–248.

[86] Reyes, D. R., et al., "Micro Total Analysis Systems. 1. Introduction, Theory, and Technology," *Anal. Chem.*, Vol. 74, June 1, 2002, pp. 2623–2636.

[87] Salimi-Moosavi, H., et al., "Biology Lab-on-a-Chip for Drug Screening," *Technical Digest Solid-State Sensor and Actuator Workshop*, 1998, pp. 350–353.

[88] Craighead, H. G., "Nanoelectromechanical Systems," *Science*, Vol. 290, 2000, pp. 1532–1535.

[89] Madou, M. J., *Fundamentals of Microfabrication: The Science of Miniaturization*, 2nd ed., Boca Raton, FL: CRC Press, 2002.

[90] Campbell, S. A., *The Science and Engineering of Microelectronic Fabrication*, 2nd ed., New York: Oxford University Press, 2001.

[91] Wolf, S., and R. N. Tauber, *Silicon Processing for the VLSI Era, Volume 1: Process Technology*, 2nd ed., Sunset Beach, CA: Lattice Press, 2000.

[92] Kovacs, G. T. A., *Micromachined Transducers Sourcebook*, New York: McGraw-Hill, 1998.

[93] Hsu, T.-R., *MEMS and Microsystems: Design Manufacture, and Nanoscale Engineering*, 2nd ed., New York: John Wiley & Sons, 2001.

[94] Maluf, N., *An Introduction to Microelectromechanical Systems Engineering*, 2nd ed., Norwood, MA: Artech House, 2004.

[95] Gad-el-Hak, M., (ed.), *MEMS: Design and Fabrication*, 2nd ed., Boca Raton, FL: CRC Press, 2005.

[96] Bustillo, J. M., R. T. Howe, and R. S. Muller, "Surface Micromachining for Microelectromechanical Systems," *Proceedings of the IEEE*, Vol. 86, No. 8, 1998, pp. 1552–1573.

[97] Ziaie, B., et al., "Hard and Soft Micromachining for BioMEMS: Review of Techniques and Examples of Applications in Microfluidics and Drug Delivery," *Advanced Drug Delivery Reviews*, Vol., 56, No. 2, 2004, pp. 145–172.

[98] Whitesides, G. M., "The Origins and the Future of Microfluidics," *Nature*, Vol. 442, No. 7101, 2006, pp. 368–373.

2

Geometric Features

Engineered functions are enabled by devices with appropriate combinations of geometric features and material properties. Microfluidic devices furthermore often take advantage of scaling phenomena, as introduced in Chapter 1. This chapter focuses on geometric features and surveys a wide variety of geometric features that have been fabricated in microfluidics research and development. It is followed by a discussion of materials in Chapter 3 and fabrication methods in Chapters 4 through 7. The concept map showing how geometry, materials, phenomena, and fabrication methods relate to microfluidic functions is reviewed in Figure 2.1. To achieve the desired geometric features, fabrication methods must encompass and take into account not only material behavior, but also other factors such as equipment capabilities and environmental conditions (temperature, moisture, and so forth).

This chapter also intends to serve as motivation for understanding the different approaches to microfabrication that have been innovated in order to produce a great variety of geometric features. For the purposes of this book, a geometric feature will be defined as a deliberately designed collection of points that distinguishes solid material from void space. Common examples in microfluidic devices include wells, orifices, channels, and membranes. One very basic distinction is whether a feature is a negative feature or a positive feature. Wells, orifices, and channels are examples of negative features because they are defined by regions of vacant space; while membranes, beams, and pillars are examples of positive features because they are defined by regions of solid matter. Figure 2.2 shows an example of a microfluidic device used for biochemical detection. The device performs a variety of functions including metering, mixing, sample injection, separation, and detection. These functions are achieved

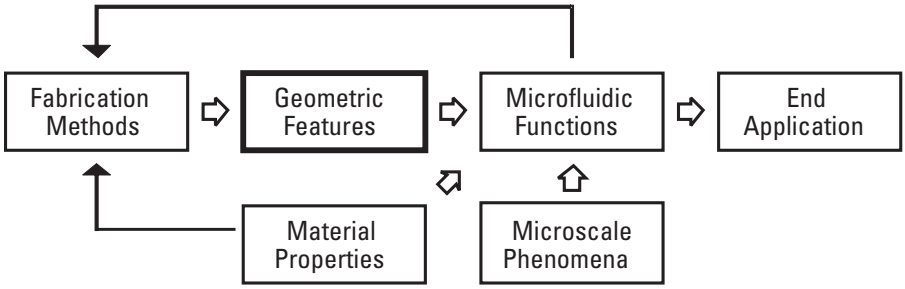

Figure 2.1 Concept map highlighting geometric features for enabling microfluidic functions.

with geometric features, including wells, vents, and a combination of liquid flow channels and pneumatic control channels.

As is the case for the example in Figure 2.2, the majority of microfluidic devices are fabricated using planar substrates such as silicon wafers, glass slides, polymer chips, or some combination thereof. The use of planar substrates is influenced heavily by mature technologies that have been developed for fabrication of microelectronic devices. Photolithography, the selective patterning of light-sensitive material through a mask, plays an especially vital role throughout microfabrication and will be discussed in greater detail in Chapter 4. In this chapter a spatial reference frame that orients the *z*-axis perpendicular to the broad substrate plane will be used. For cases in which there is a primary flow direction or an elongated geometric feature, the *x*-axis will be aligned to that longitudinal direction, with the y-axis aligned laterally. Figure 2.3 presents a generic reference frame for discussing the wide variety of geometric features used in microfluidic devices. A very simple microchannel is oriented within the frame, with the broadest plane perpendicular to the *z*-axis and the straight microchannel aligned with the *x*-axis.

There are only two types of features in the example of Figure 2.3: an open channel connecting two wells. The wells can be described as features having some specified depth along the *z*-axis. The lateral dimensions of each well along the *x* and *y* directions are of similar magnitude but substantially larger than the depth. In contrast, the channel is a feature for which the length along the *x*-axis is substantially much larger than the transverse width along the *y*-axis. The width of the channel, however, is on the same order of magnitude as the depth along the *z*-axis.

Although a single microchannel is a very simple example, this terminology for discussing orientation and relative size along directional axes will be helpful as other features are described throughout the remainder of this chapter. The terminology will be augmented to address more interesting features that

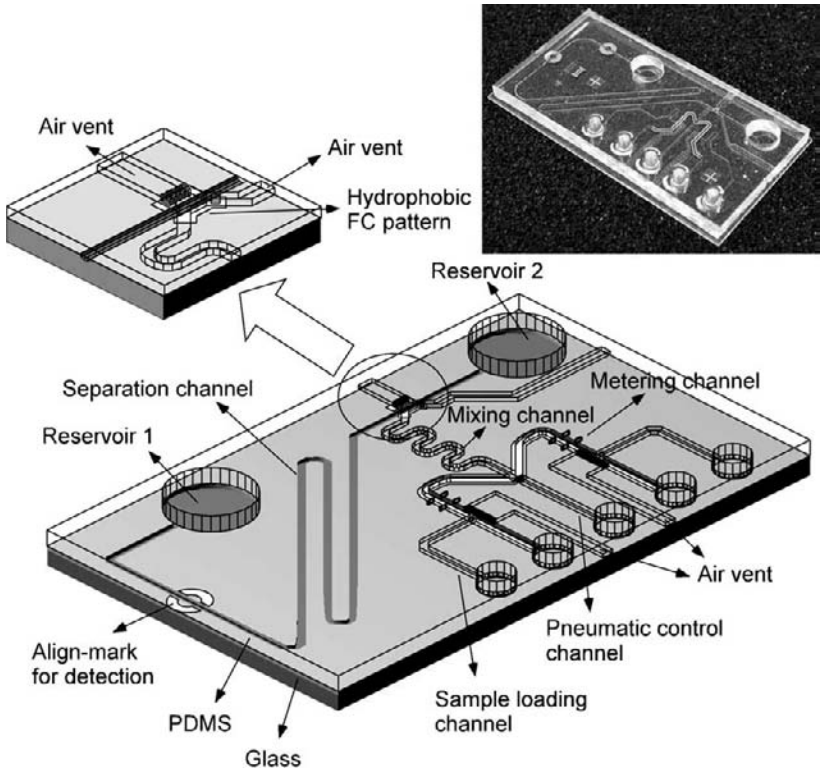

Figure 2.2 Microfluidic chip for biochemical reaction and species separation. Reprinted from [1]. Copyright 2005, with permission from Elsevier.

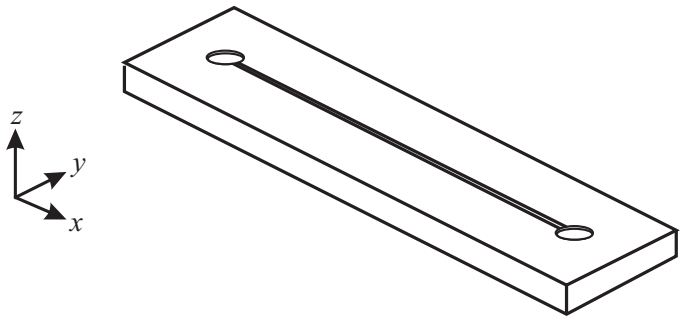

Figure 2.3 Reference frame and orientation for a generic microchannel.

may include inclined surfaces, curved profiles, and other geometric complexities. The next section showcases several examples of common types of geometric features from developments in the field of microfluidics. The basic microfluidic

functions enabled by these features will be explained, but fabrication details will be deferred until Chapters 4 through 7.

2.1 Common Types of Features

The types of features used in microfluidic devices are so diverse that it would be impossible to categorize with consistent detail beyond a few broad generalizations. Still, some types of features are so common that they can be presented here as basic building blocks that are used to achieve many essential microfluidic functions. As the types of features are described, it will be helpful to notice that many of the features are prismatic. A prismatic feature is one that has constant cross-section along a given axis. Influenced heavily by photolithography and related microfabrication processing, many microfluidic components have reduced shape complexity in three-dimensional (3D) space and accordingly are described as having only 2.5D complexity.

2.1.1 Cavities and Orifices

Perhaps the most basic example of a negative feature is a recessed cavity or orifice. Orifices are distinguished from cavities in general in that they pass entirely through the base material. Most commonly cavities and orifices have similar dimensional size in lateral directions, and are projected along the axis perpendicular to the substrate plane. Cavities and orifices can be fabricated by a multitude of options including silicon etching [2], electrical discharge machining [3], electrochemical machining [4], laser drilling [5], abrasive jet machining [6], and direct photo-patterning [7].

Figure 2.4 shows some common profiles for simple cavities. Shown in side view, these are representative profiles based on some of the most common fabrication techniques, including etching and ablation. If the cavities are completely extended through the material, the profiles would likewise extend and form orifices. Some other achievable profiles are discussed in this chapter, while the process mechanisms behind these and other profiles are discussed in Chapters 5 through 7.

In terms of the achievable shapes when viewed perpendicular to the *x-y* plane, there is almost no limit to shape complexity. There are a few fabrication subtleties discussed in Chapters 5 through 7 and resolution limits are discussed below, but otherwise there is tremendous design freedom for shaped features within the *x-y* plane. Figure 2.5 shows a combination of cavities, orifices, and flow channels used for studying the growth and survivability of osteoblastic cells for bone tissue engineering. The cavities are used as culture chambers for

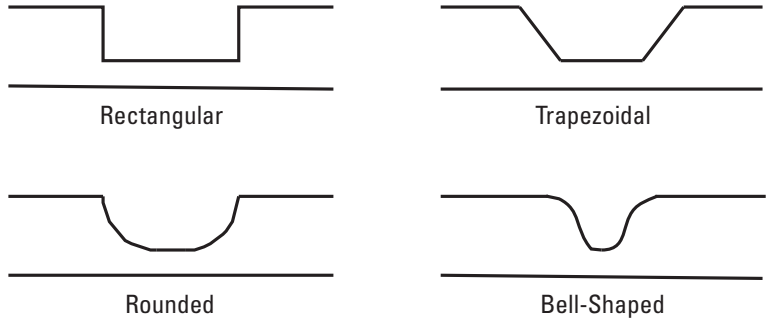

Figure 2.4 Common profiles for microfabricated cavities.

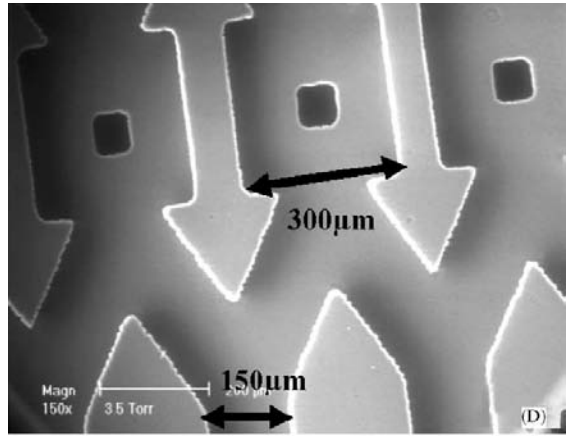

Figure 2.5 Culture chamber for study of cell growth under dynamic flow conditions. (Reprinted from [8]. Copyright 2006, with permission from Elsevier.)

observing cell behavior, and the 3D structure provides scaffolding to maintain cell adhesion under dynamic flow conditions that favor cell growth.

Although it is most intuitive to consider the fabrication of cavities (as well as microchannels described in the next section) in terms of material removal, Chapter 5 in particular will show that this is not always the case. Many fabrication strategies use a (positive) master pattern to replicate features from one material into another. In some cases, such pattern transfer is motivated by the freedom to have different material properties, as will be discussed further in Chapter 3. It is also beneficial from a low-cost manufacturing standpoint, in which time and expense is invested in a high-quality master, and the master is used subsequently to produce larger quantities of units by replication methods such as casting, embossing, or injection molding.

2.1.2 Microchannels

Microchannels are geometrically characterized by having one dimension significantly larger than the other two dimensions (i.e., length greater than width or height). In planar microfluidic chips, microchannels are almost exclusively oriented with longitudinal axis parallel to the substrate plane, with channel depth parallel to the *z*-axis. As conduits for fluid flow from one location to another, microchannels are fundamental features incorporated into many microfluidic devices.

In microfluidics, channels often serve more significant roles that mere conductance of fluid from one point to another. Capillary electrophoresis (CE) is a good example of an application for which microscale features combine with scaling phenomena to achieve meaningful functionality [9]. A typical chip layout is shown in Figure 2.6, in which a separation channel runs along the length of the chip. A shorter inject channel is oriented perpendicular to the separation channel near the inlet. After filling the transverse inject channel with a sample liquid, a precise volume at the junction between channels is pushed down the separation channel. While moving along the separation channel under and electric field, the various species within the sample separate by differences in mass and charge. The species within the sample can be detected based on UV absorbance or fluorescence signatures, by observing the difference in time of arrival near the outlet.

Another good example of relatively simple channel features that achieve meaningful functionality by taking advantage of scaling phenomena is the H-shaped channel shown in Figure 2.7 [10], which can be used for separation,

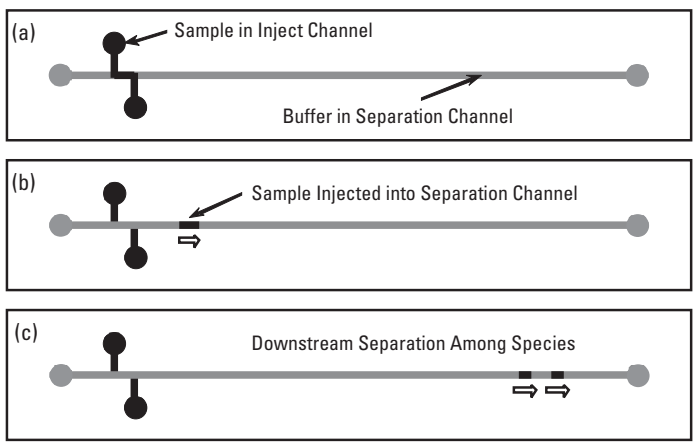

Figure 2.6 Capillary electrophoresis chip. (a) A sample to be analyzed fills the inject channel, and (b) a precise volume is injected by initiating flow in the separation channel, after which (c) differences in mobility result in the separation of species downstream.

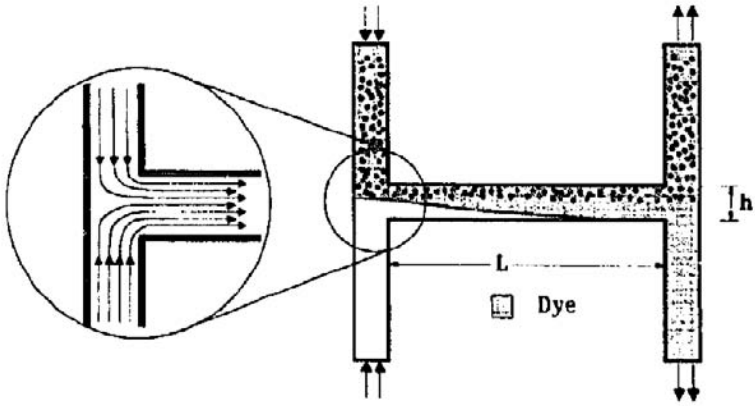

Figure 2.7 Diffusion-based separation of particles in an H channel. (Reprinted from [10]. Copyright 1997, with permission from Elsevier.)

extraction, or filtering. A fluid with mixed particle contents joins another carrier fluid at the inlet, and while traversing across the common channel the smaller particles diffuse faster into the second fluid. The highly laminar nature of flow in microchannels prevents bulk mixing, so diffusion is the dominant mechanism of interaction between the two fluids as they move in parallel along the common channel. At the exit, the common stream splits, leaving two streams with smaller particles having been extracted from the original fluid.

The previous two examples illustrate meaningful functionality from elegantly simple microchannel features. When needed, however, almost limitless complexity within the *x-y* plane can be fabricated for channel designs based on photolithography. Figure 2.8 [11] shows a device that is able to generate smooth concentration gradients as distinct fluids meander and mix through a dense network of branched microchannels.

As is the case for producing cavities, there are many different approaches for fabricating microchannels. Relatively common methods include etching, casting, embossing, and laser ablation. A variety of alternative methods have been demonstrated, however, and these include surface micromachining [12, 13], multilevel UV curing [14], and investment molding with fugitive inserts [15].

Channel passages are often augmented with protrusions or other obstacles for functional purposes such as mixing [16]. Figure 2.9 [17] shows an example of using protrusions to facilitate sorting of particles by size. In the figure, stationary obstructions C have spacing such that only smaller particles B are permitted to pass through, while larger particles A are blocked.

Another novel enhancement to conventional flow channels is the inclusion of a pillar array to take advantage of liquid retention by capillary forces. In the

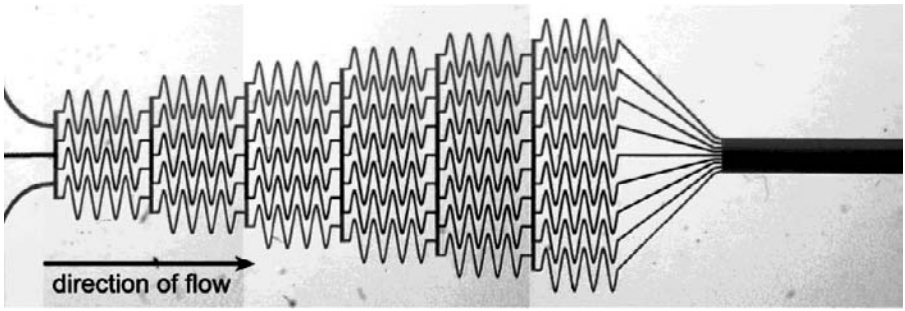

Figure 2.8 Branched network of microchannels for generation of concentration gradients. (Reprinted with permission from [11]. Copyright 2001 American Chemical Society.)

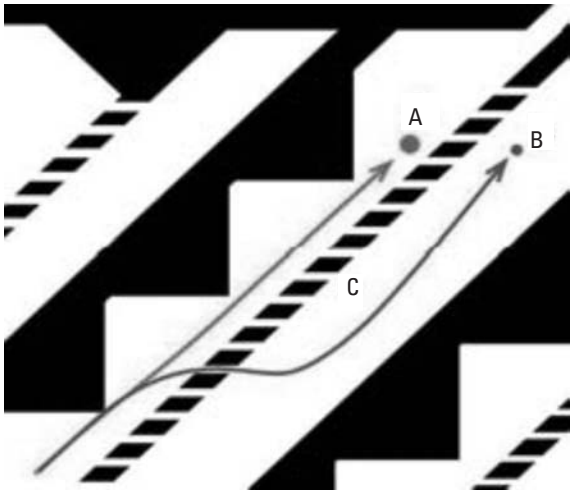

Figure 2.9 Microfluidic particle size sorter based on gaps between obstructions. (*Source:* [17] Copyright Wiley-VCH Verlag GmbH & Co. KGaA. Reproduced with permission.)

device shown in Figure 2.10 [18], external pumping is not required to fill the flow channel because capillary forces allow the microchannel to fill spontaneously based on surface energy. Once liquid fills to the tip, a concentrated electric field can then be used to spray the sample as extremely fine ionized droplets.

Capillary tubing with constant annular cross-section also deserves mention in the discussion of microchannels. Capillary tubing in materials such as fused silica and polyetheretherketone (PEEK) are commercially available with inner diameter as small as a few tens of microns. Fluid flow within these capillaries certainly qualifies as microfluidic, but integration of tubing into multifunctional

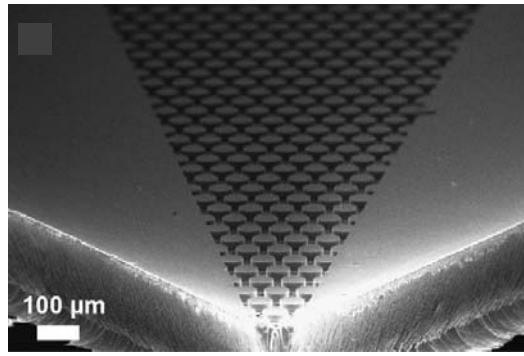

(a)

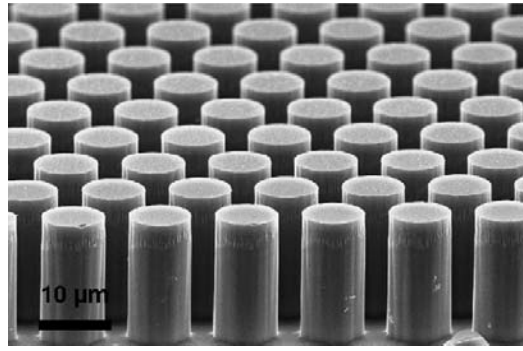

(b)

Figure 2.10 Electrospray tip with channel filled by a pillar array (a) and close-up of pillars (b). (Reprinted from [18]. Copyright 2008, with permission from Elsevier.)

devices tends to be very indirect compared to integration of microchannels fabricated in planar substrates.

A example of highly integrated functionality using microchannels is shown in Figure 2.11 [19]. Microfluidic chips such as these have been demonstrated with thousands of valves and hundreds of independently addressable chambers. The particular device shown in the figure is a microfluidic comparator, capable of performing operations analogous to microelectronic devices. A fundamental building block for the integrated chip above is the switching action provided at the intersection of two crossing microchannels, fabricated on different layers with flexible material separating the crossing channels.

The material between the pneumatic control lines and fluid channels is capable of achieving significantly large deformation not only because the material is a soft elastomer (discussed in more detail in Chapter 3), but also because the geometric proportions are such that the thickness is relatively small

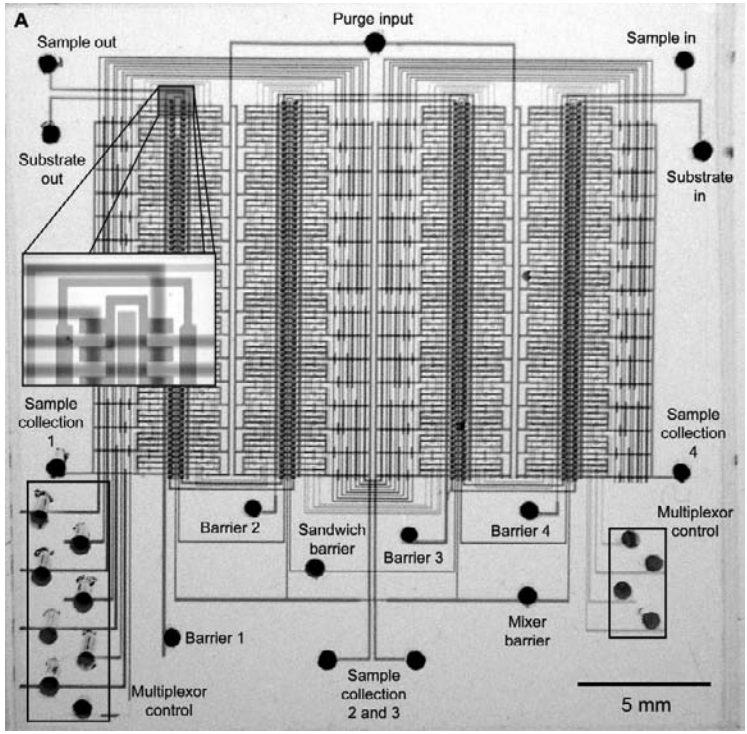

Figure 2.11 Microfluidic large scale integration. (*From:* [19]. Reprinted with permission from AAAS.)

compared to lateral size dimensions. So locally, the crossing region may be described as a membrane, another very common type of geometric feature that is presented next.

2.1.3 Membranes

Membranes are ubiquitous throughout microfluidic design [20], and in the context of geometric features membranes will for convenience be defined as structures that have one size dimension much smaller than the other two dimensions. In terms of geometrical description, membranes will also be considered synonymous with diaphragms. Very often these kinds of structures are used to take advantage of compliance in the direction parallel to the thinnest dimension. Several of the earliest MEMS devices engineered for functions related to flow control were based on a thin silicon membrane, typically tens of microns thick, deflecting perpendicular to the wafer plane. One of the most basic of such devices is illustrated in Figure 2.12 [21], in which the deformation of the thin membrane expands or contracts a fluid-filled cavity.

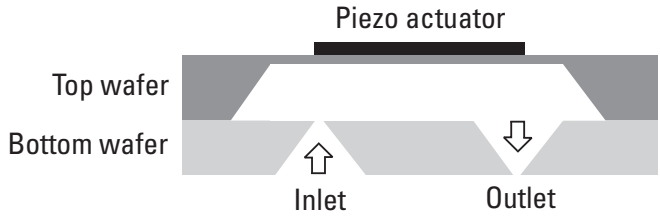

Figure 2.12 Reciprocating micropump with bulk-micromachined silicon membrane. (*After:* [21].)

Reciprocating action of the membrane enables fluid pumping when combined with opposing tapered passages that favor one-directional flow. Multiple variants on this design have been developed, including the addition of check-valve flaps [22], use of electrostatic actuation [23] or thermopneumatic actuation [24], and insertion of polymer diaphragms [25].

A different approach to fabricating devices with membrane features has been to design with thin-film structures, as shown in the peristaltic pump in Figure 2.13 [26]. As will be discussed more directly in Chapter 8, these types of structures are typically fabricated by thin-film deposition methods and result in membranes that are typically on the order of 1 micron thick.

Not all membranes are used as actuators. Passive compliant membranes have been used for functions such as flow regulation and flow rate stabilization [27]. Figure 2.14 shows an example of a single membrane sheet used for the dual purpose of pneumatic pumping followed by flow regulation through a downstream fluidic capacitor. The fluidic capacitance and fluidic resistance are elemental components that can be used to design dynamic response of a fluidic circuit, analogous to circuit design with electrical components [28].

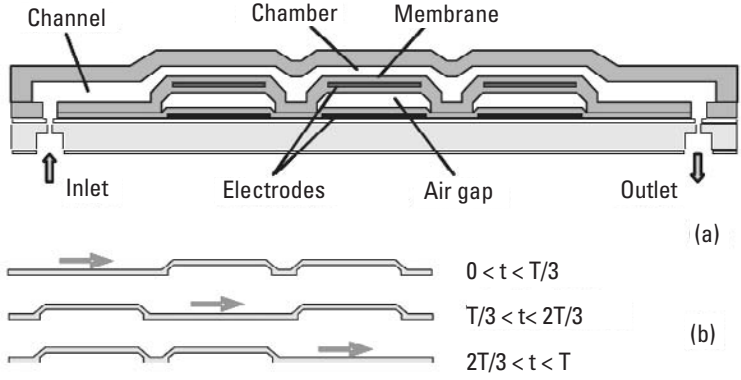

Figure 2.13 (a, b) Peristaltic micropump with surface-micromachined thin-film membranes. (Reprinted from [26]., with permission from IOP Publishing.)

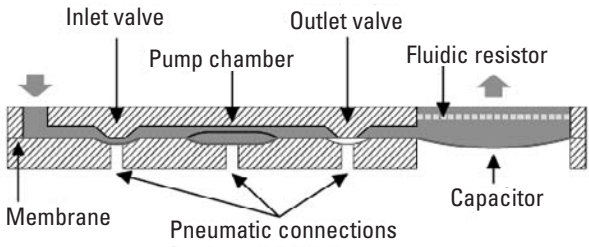

Figure 2.14 Micropump with pneumatic actuation and flow regulation. (Reprinted from [29], with permission from IOP Publishing).

Although it is most straightforward to have the thinnest dimension of membranes oriented for deflection perpendicular of the substrate plane, as shown in the prior examples above, some membranes are engineered for lateral deflection instead. Figure 2.15 shows a peristaltic pump with three pairs of pneumatically actuated membranes along a fluid channel. Similar approaches using lateral deflection membranes have also been demonstrated for other microfluidic functions including mixing [30] and droplet generation [31].

2.2 Geometric Characteristics

This section presents some geometric characteristics that can be used to categorize and compare not only the relatively common features already introduced thus far, but also a much wider variety of geometric features. Understanding these important geometric characteristics provides more meaningfully descriptive dialog for evaluating criteria and trade-offs that are important for design and fabrication decisions.

2.2.1 Profile

As discussed more thoroughly in Chapters 5 through 7, there are uniquely fundamental ways of fabricating features: material removal, material addition, plastic deformation, or phase change. Each approach offers different characteristic profiles that can be produced. Common removal processes such as etching or ablation typically produce trench-like features, inherently useful for microchannel cavities. However, positive features also play important roles for functions such as mixing, filtering, and manipulation of liquids by surface energy (as in the example of Figure 2.10). Removal processes can be used to create positive features, by creating substantial regions of negative space (by etching, for example), such that what remains is positive. Illustrative examples are shown in

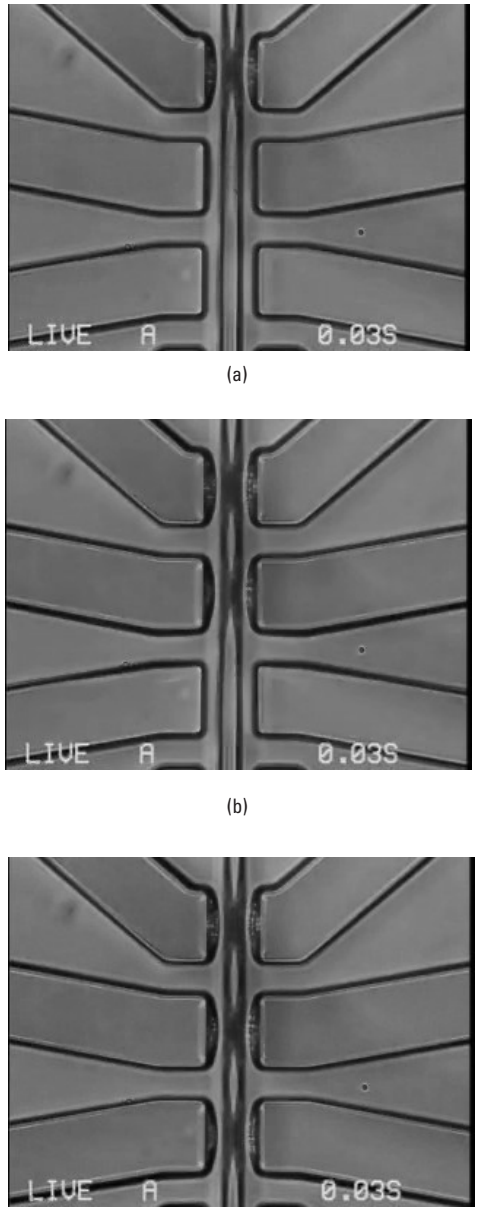

Figure 2.15 Peristaltic pump with laterally deflecting membrane pairs. (*Source:* [32]. Reproduced by permission of the Royal Society of Chemistry.)

Figure 2.16, and while rectangular profiles remain rectangular, implications for the shapes of curved profiles become more relevant.

Figure 2.16 Examples of isolated positive features produced by regions of empty space.

Positive features and different profiles can also be fabricated by pattern transfer. Figure 2.17 shows some representative examples of positive features produced by pattern transfer from what were originally negative feature profiles. These are typically produced by fabrication methods such as casting, injection molding, and hot embossing.

Figure 2.18 illustrates a specific example of microscale lenses, which are rounded convex features. These lenses have variable focusing capability, enabled by pneumatic pressure in a backside cavity to alter the convex profile. The features are produced by a two-step pattern transfer process, beginning with an initial photoresist pattern, casting of a master mold (with concave cavities), and making a second casting for the final material.

Especially evident for features that involve pattern transfer is the fact that most geometric features used in microfluidic devices have limited orientation with respect to the substrate plane. Most features are produced using planar interfaces such as a metal embossing tool pressed against a thermoplastic polymer. Such limitations are not absolute, however. A novel approach for producing features that do not have orthogonal orientation with respect to the substrate is to use UV polymerization with inclined exposure. For example, Figure 2.19

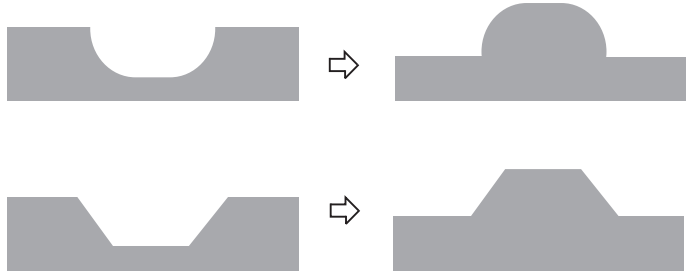

Figure 2.17 Examples of complementary (positive) features by pattern transfer from (negative) features.

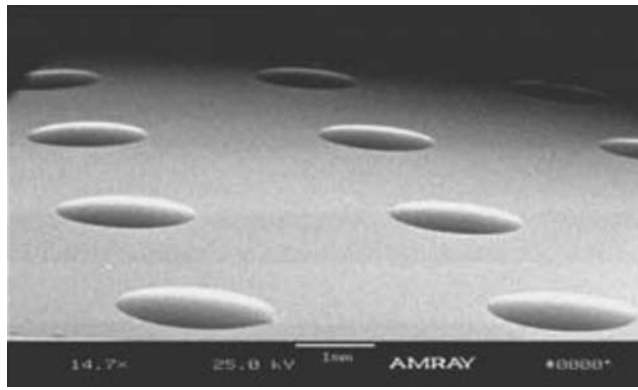

Figure 2.18 Variable-focusing microlens by two-step casting process. (Reprinted from [33], with permission from IOP Publishing.)

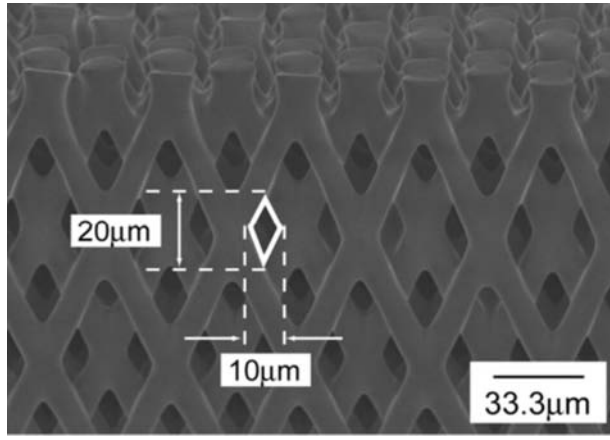

Figure 2.19 Micromesh by an all SU-8 microfluidic chip with built-in 3D fine microstructures. (Reprinted from [34], with permission from IOP Publishing.)

shows a fine crossing mesh that has been demonstrated for droplet fragmentation in two-phase flow.

Even more complex 3D profiles can be fabricated with fine control over the substrate positioning stage and/or the energy source. For example, the wine glass in Figure 2.20 was produced by focused ion beam (FIB) machining with a precision rotating stage.

Scalability of FIB methods for high-volume manufacturing remains limited for reasons discussed more thoroughly in Chapters 4 through 7. However, the narrowest part of the neck of the glass was only 400 nm in diameter,

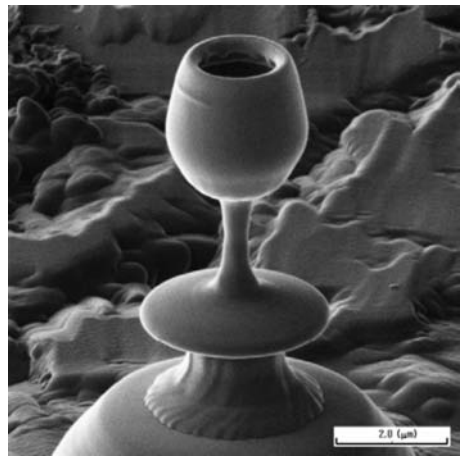

Figure 2.20 Three-dimensionally complex fabrication by focused ion beam. (Reprinted from [35], with permissions from IOP Publishing.)

exceeding the resolution capabilities of most conventional fabrication methods for objects with this degree of three-dimensional complexity. Resolution is therefore recognized as a very fundamental consideration for feature geometry, and this is addressed next.

2.2.2 Feature Resolution

In microelectronics, the critical dimension (CD) is a popular and effectively concise geometric parameter used to describe the sophistication of a fabrication process (or set of processes). Smaller values of CD correspond to finer resolution. A CD such as 65 nm or 45 nm typically describes the width of a transistor gate or the width of a metallic conductor. This includes both positive features (e.g., lines) and negative features (e.g., spaces). The CD of a microelectronics fabrication process communicates the resolution of achievable features, and this is also fundamentally important for microfluidics. Spatial resolution is defined in general terms as the ability to distinguish an individual entity or adjacent separate entities clearly. In microfabrication, spatial resolution in terms of geometric features can often be simplified to an indication of the smallest positive feature or the smallest negative feature that can be produced.

Feature proximity and density are related considerations that are dependent on resolution. High feature density requires fine resolution, but not vice versa. This is analogous to the line-space (L/S) ratio, which is an important parameter in microelectronics fabrication [36]. A problem that limits L/S ratio is the possibility of interaction among distinct features. For features that have short height or depth compared to their width, lateral interaction among

features is generally not a concern. However, as thin features become taller or deeper, opportunities for failure increase. The relative magnitude of lateral versus vertical dimensions is most effectively described in terms of aspect ratio, discussed next.

2.2.3 Aspect Ratio

Aspect ratio in general can be defined as the dimension along one directional axis in comparison to the dimension along another. For microelectromechanical systems (MEMS) in particular, high aspect ratio is very desirable for the performance of many sensors and actuators such as comb-drive actuators [37]. In microfabrication based on planar substrates, high aspect ratio almost invariably refers to a lateral dimension (such as trench width or wall width) compared to the vertical height or depth. Examples of high aspect ratio features are shown in Figure 2.21 [38].

Producing structures with high aspect ratio, however, presents a difficult fabrication challenge because of the extreme process anisotropy required, as highlighted in Chapter 6. Many microfluidic devices such as simple channels do not demand the same extremes in high aspect ratio as silicon-based MEMS sensors and actuators, but there are instances such as vertically oriented deformable membranes [39] for which high aspect ratio is also functionally desirable. High aspect ratio features also provide structural design flexibility within channels, and the extremely fine pillar arrays in Figure 2.22 [40] have been applied to the study of DNA separation and kinetics.

2.2.4 Degrees of Freedom

Some features by design are intended to move or deform substantially as an essential part of their functionality. One basic example of a microfluidic device that requires freedom of motion is the passive valve shown in Figure 2.23 [41]. The plate-like feature is micromachined from polysilicon and it is designed to cover an orifice. As pressure increases in the cavity behind the orifice, the plate-like feature is lifted such that flow can pass through the resulting space around the perimeter.

An alternative to the same basic concept is shown in Figure 2.24 [42]. In this case the greater compliance afforded by folded beam supports allows this valve to be opened with relatively low pressure. Greater compliance is also achieved by a change in material properties (addressed more specifically in Chapter 3), but these two implementations of a planar check valve concept illustrate how geometric features can be used to offer different ranges of operation. Both examples have their primary degree of freedom along the z-axis perpendicular to the substrate plane.

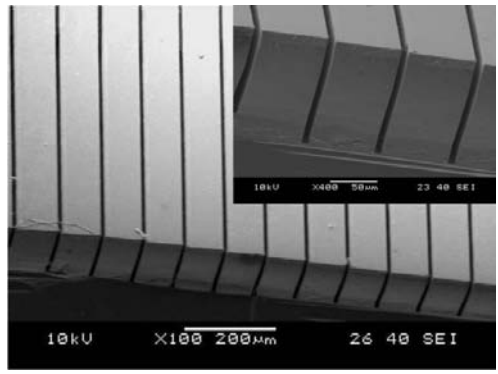

(a)

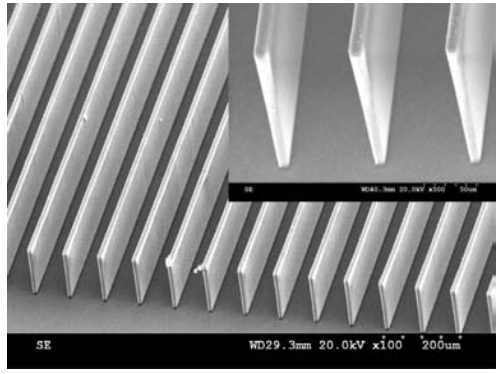

(b)

Figure 2.21 High-aspect ratio negative features in photoresist (SU-8, a) and corresponding positive replica features in elastomer (PDMS, b). (*Source:* [38]. Reproduced by permission of the Royal Society of Chemistry.)

Design with compliant members is also useful for degrees of freedom parallel to substrate plane. Figure 2.25 [43] shows yet another check valve concept in line with a microchannel. While fabricating in line with a flow channel may be advantageous for design simplicity, this type of structure is different from the previous examples because it mandates structures with a high aspect ratio.

Figure 2.26 [44] shows a geometrically simpler device with similar functionality: the venous valve using a compliant elastomer. The thickness and length are designed to block flow in one direction, but to allow flow in the other direction if the fluid pressure is sufficient for splitting the opposing flaps. This design is an example of biomimetic design, imitating nature (venous valves in blood vessels, for example) to achieve engineered functionality.

Valves represent a very common but not exclusive category of microfluidic components that are based on compliance. A different way of taking advantage

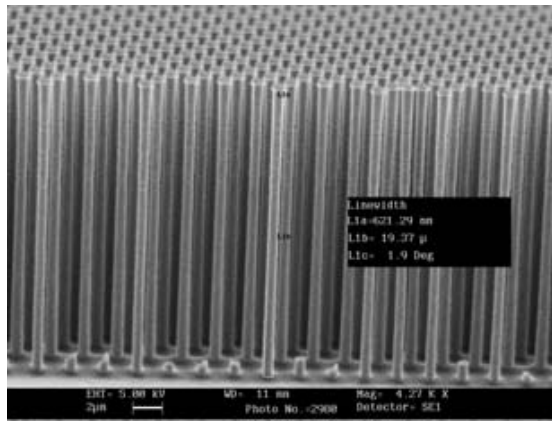

Figure 2.22 High aspect ratio submicron pillar array for DNA separation. (Reprinted from [40], with permission from IOP Publishing.)

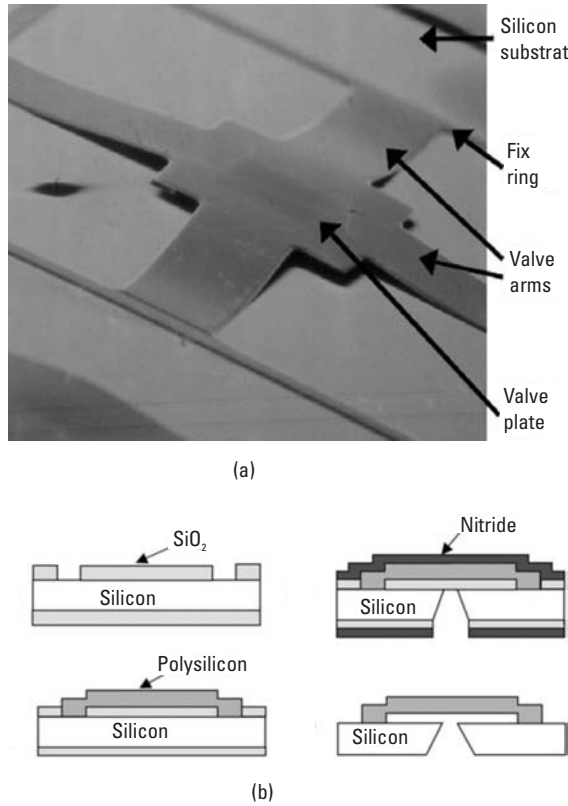

Figure 2.23 (a, b) Micromachined passive valve. (Reprinted from [41], with permission from IOP Publishing.)

Figure 2.24 Microcheck valves with compliant folded beams. (Reprinted from [42], with permission from IOP Publishing.)

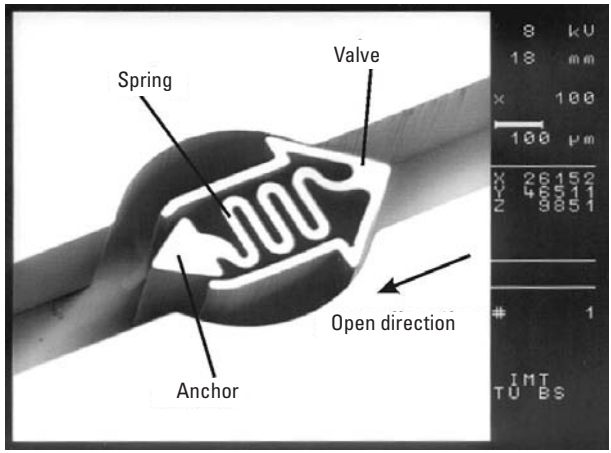

Figure 2.25 Spring-actuated check valve. (Reprinted from [43]. Copyright 2002, with permission from Elsevier.)

of compliance is shown in Figure 2.27 [45]. This device also has primary degree of freedom along the longitudinal axis of a microchannel, and it includes a tethered body attached to an anchor. As flow rate increases, the corresponding increase of drag on the tethered body elongates the highly compliant spring-like structure and thereby serves as a flow rate measurement device.

Another degree of freedom is curvature out of the substrate plane. Even though many geometric features are fabricated as thin, layered structures, some can be designed to actuate out-of-plane. Figure 2.28 [46] shows a set of thin beam-like features that active out-of-plane motion by electrostatic actuation.

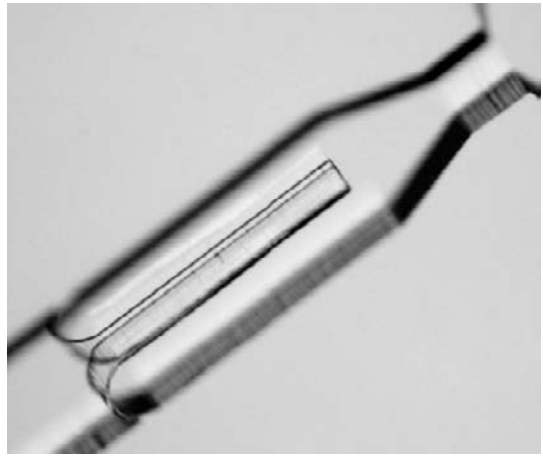

Figure 2.26 Venous valve with flexible elastomer flaps. (Reprinted from [44], with permission from IOP Publishing.)

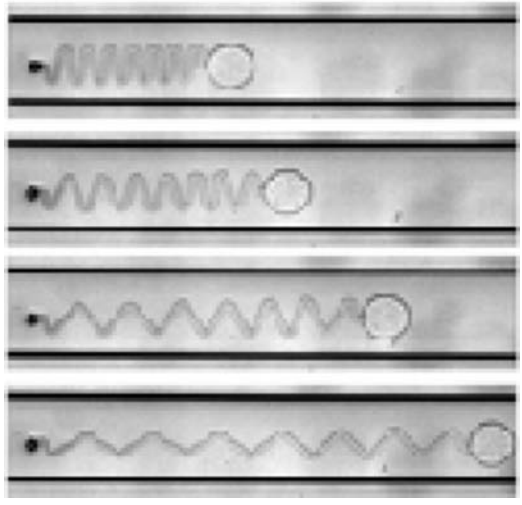

Figure 2.27 Flow rate measurement with an in-line tethered body. (*Source:* [45]. Reproduced by permission of The Royal Society of Chemistry.)

When actuated, these beams move like cilia (another example of bimimetic design) to produce turbulent mixing.

A seemingly similar cluster of features is present in the microcage shown in Figure 2.29 [47]. However, these are distinct in that the primary curvature of the fingers is caused by residual stress between chromium and aluminum materials. Actuation is not electrostatic, but rather pneumatic, with deflection

(a)

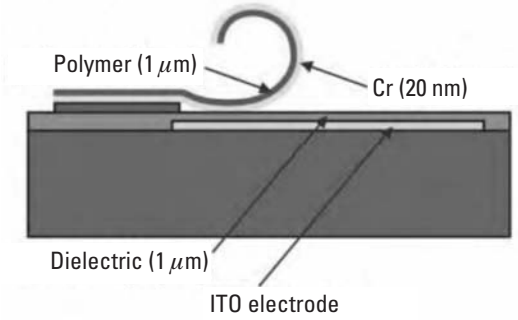

(b)

Figure 2.28 (a, b) Out-of-plane thin beams actuated for fluid mixing. (*Source:* [46]. Reproduced by permission of The Royal Society of Chemistry.)

occurring in the base. A motivation for choosing pneumatic actuation is compatibility with the liquid environments in which the microbes are manipulated.

Some nonstationary structures may even be floating, in the sense that they are not physically anchored to the substrate or other larger objects, but rather are simply retained to move within confined space. Figure 2.30 [48] shows microstirrers that have a rotational degree of freedom about the z-axis. These are actuated by an external rotating magnetic field from a conventional (macroscale) hotplate stirrer typically used in benchtop applications.

Another example of a floating structure is the microgate valve shown in Figure 2.31 [49]. This structure has a single linear degree of freedom transverse to the longitudinal axis of a fluid microchannel. Gate valves have a relative advantage of sustaining very high holding force because the force from fluid

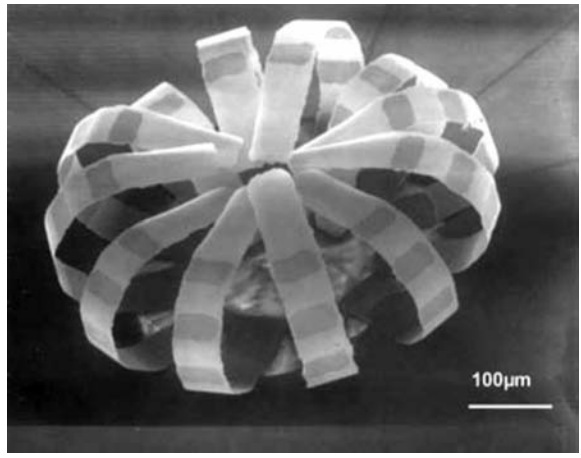

(a)

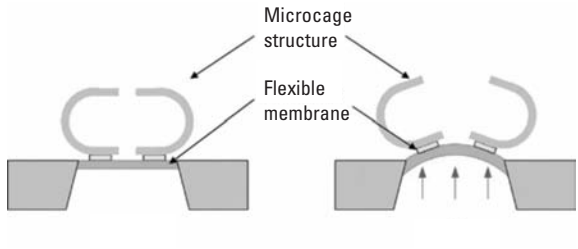

(b)

Figure 2.29 Out-of-plane microcage for retention of microbes. (© 2006 IEEE. Reprinted with permission from [47].)

pressure acts primarily in a perpendicular direction. The valve shown in the figure is actuated by thermally generated vapor bubbles in the chambers in front of and behind the crossbar. As will be discussed in Chapter 8, it is especially important to plan an integrated process strategy for the fabrication of geometric features that involve the release of moving components.

2.2.5 Surface Roughness

Surface roughness is another geometric parameter that plays an important role in microfluidics. Roughness significantly affects the wetting behavior of liquids [50] and the flow of fluid within microchannels [51]. In microfluidic applications that are based on surface chemistry and/or biomolecule interactions, roughness can be advantageous because it provides greater surface area between the stationary and nonstationary phases involved [52].

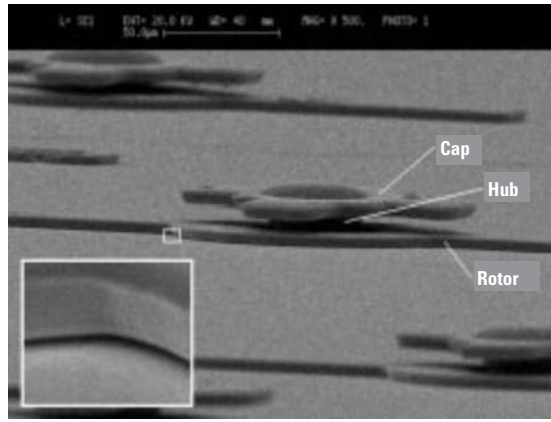

Figure 2.30 Microstirrer array for microfluidic mixing. (©2002 IEEE. Reprinted with permission from [48].)

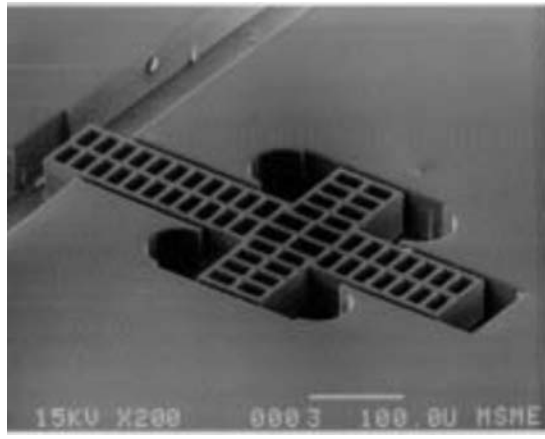

Figure 2.31 Silicon microgate valve. (© 1999 ASME. Reprinted with permission from [49].)

Different combinations of fabrication processes and materials naturally result in a wide variety of surface textures. Etch processing for silicon or glass microchannels can be optimized to achieve very smooth surfaces, but etched polymers or materials subject to laser ablation tend to produce significantly rougher texture, as illustrated by the example in Figure 2.32 [53].

Surface roughness is often expressed in terms of the average roughness R_a or the root-mean-square (RMS) roughness R_q. Average roughness (R_a) is routinely used to describe machined surfaces on macroscale components, and it is computed as the average differences between surface points and the mean:

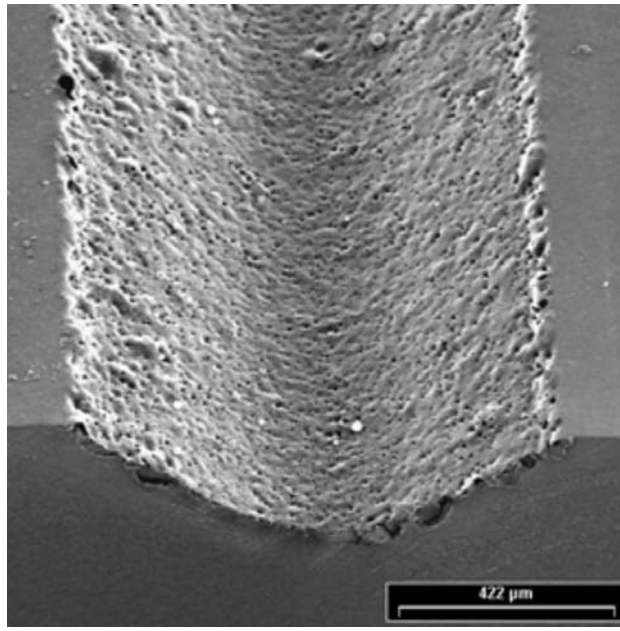

Figure 2.32 Surface roughness inside laser-patterned polymethylmetacrylate microchannel. (Reprinted from [53], with permission from IOP Publishing.)

$$R_a = \frac{1}{n}\sum_{i=1}^{n}\left|z_i - \bar{z}\right| \tag{2.1}$$

Average roughness R_a is adequate for relative comparisons, but for microscale process characterization and for very smooth surfaces, RMS roughness is often preferred because it tends to more accurately convey magnitude for upper and lower bounds of the actual physical profile [54]. The RMS roughness (or R_q) represents the standard deviation of differences between surface points and the mean:

$$R_q = \sqrt{\frac{1}{n}\sum_{i=1}^{n}\left(z_i - \bar{z}\right)^2} \tag{2.2}$$

The greater availability in recent years of a variety of 3D surface metrology techniques [55] makes it routinely possible to acquire area-based measurements analogous to the more simple line-based equations provided above.

References

[1] Lee, S. -H., et al., "Microfluidic Chip for Biochemical Reaction and Electrophoretic Separation By Quantitative Volume Control," *Sensors and Actuators B: Chemical*, Vol. 110, No. 1, 2005, pp. 164–173.

[2] Smith, L., A. Soderbarg, and U. Bjorkengren, "Continuous Ink-Jet Print Head Utilizing Silicon Micromachined Nozzles," *Sensors and Actuators, A: Physical*, Vol. 43, No. 1–3, 1994, pp. 311–316.

[3] Allen, D. M., and A. Lecheheb, "Micro Electro-Discharge Machining of Ink Jet Nozzles: Optimum Selection of Material and Machining Parameters," J*ournal of Materials Processing Technology*, Vol. 58, No. 1, 1996, pp. 53–66.

[4] Datta, M., "Fabrication of an Array of Precision Nozzles by Through-Mask Electrochemical Micromachining," *Journal of the Electrochemical Society*, Vol. 142, No. 11, 1995, pp. 3801–3805.

[5] Kim, K. R., S. C. Ko, and S. Shin, "Laser Micromachining of Inkjet Nozzles," *Proceedings of International Congress on Applications of Lasers and Electro-Optics,* Orlando, FL, 2001, pp. 1603–1611.

[6] Park, D. -S., et al., "Micro-Grooving of Glass Using Micro-Abrasive Jet Machining," *Journal of Materials Processing Technology,* Vol. 146, No. 2, 2004, pp. 234–240.

[7] Kukharenka, E., et al., "Electroplating Moulds Using Dry Film Thick Negative Photoresist," *Journal of Micromechanics and Microengineering,* Vol. 13, No. 4, 2003, pp. 67–74.

[8] Leclerc, E., et al., "Study of Osteoblastic Cells in a Microfluidic Environment," *Biomaterials*, Vol. 27, No. 4, 2006, pp. 586–595.

[9] Chan, Y. C., et al., "Design and Fabrication of an Integrated Microsystem for Microcapillary Electrophoresis," *Journal of Micromechanics and Microengineering*, Vol. 13, No. 6, 2003, pp. 914–921.

[10] Brody, J. P., and P. Yager, "Diffusion-Based Extraction in a Microfabricated Device," *Sensors and Actuators A: Physical*, Vol. 58, No. 1, 1997, pp. 13–18.

[11] Dertinger, S. K. W., et al., "Generation of Gradients Having Complex Shapes Using Microfluidic Networks," *Analytical Chemistry*, Vol. 73, No. 6, 2001, pp. 1240–1246.

[12] Bhusari, D., et al., "Fabrication of Air-Channel Structures for Microfluidic, Microelectromechanical, and Microelectronic Applications," *Journal of Microelectromechanical Systems*, Vol. 10, No. 3, 2001, pp. 400–408.

[13] Lee, K. B., and L. Lin, "Surface Micromachined Glass and Polysilicon Microchannels Using MUMPs for BioMEMS Applications," *Sensors and Actuators, A: Physical,* Vol. 111, No. 1, 2004, pp. 44–50.

[14] Yao, P., G. J. Schneider, and D. W. Prather, "Three-Dimensional Lithographical Fabrication of Microchannels," *Journal of Microelectromechanical Systems,* Vol. 14, No. 4, 2005, pp. 799–805.

[15] Lippmann, J. M., E. J. Geiger, and A. P. Pisano, "Polymer Investment Molding: Method for Fabricating Hollow, Microscale Parts," *Sensors and Actuators A: Physical*, Vol. 134, No.1 , 2007, pp. 2–10.

[16] Wang, H., et al., "Mixing of Liquids Using Obstacles in Microchannels," *Proceedings of SPIE—The International Society for Optical Engineering*, Vol. 4590, 2001, pp. 204–212.

[17] Fernandez, J. G., et al., "All-Polymer Microfluidic Particle Size Sorter for Biomedical Applications," *Physica Status Solidi (A) Applied Research,* Vol. 203, No. 6, 2006, pp. 1476–1480.

[18] Sainiemi, L., et al., "Fabrication and Fluidic Characterization of Silicon Micropillar Array Electrospray Ionization Chip," *Sensors and Actuators B: Chemical*, Vol. 132, No. 2, June 16, 2008, pp. 380–387.

[19] Thorsen, T., S. J. Maerkl, and S. R. Quake, "Microfluidic Large-Scale Integration," Science, Vol. 298, No. 5593, 2002, pp. 580–584.

[20] de Jong, J., R. G. H. Lammertink, and M. Wessling, "Membranes and Microfluidics: A Review," *Lab on a Chip*, Vol. 6, No. 9, 2006, pp. 1125–1139.

[21] Gerlach, T., M. Schuenemann, and H. Wurmus, "New Micropump Principle of the Reciprocating Type Using Pyramidic Micro Flowchannels as Passive Valves," *Journal of Micromechanics and Microengineering*, Vol. 5, No. 2, 1995, pp. 199–201.

[22] Koch, M., A. G. R. Evans, and A. Brunnschweiler, "Characterization of Micromachined Cantilever Valves," *Journal of Micromechanics and Microengineering,* Vol. 7, No. 3, 1997, pp. 221–223.

[23] Zengerle, R., A. Richter, and H. Sandmaier, "A Micro Membrane Pump with Electrostatic Actuation," *Proceedings of the IEEE Micro Electro Mechanical Systems Workshop*, Travemuende, Germany, 1992.

[24] Henning, A. K., et al., "Thermopneumatically Actuated Microvalve for Liquid Expansion and Proportional Control," *Proceedings of the 1997 International Conference on Solid-State Sensors and Actuators,* Vol. 2, Chicago, IL, 1992.

[25] Benard, W. L., et al., "Thin-Film Shape-Memory Alloy Actuated Micropumps," *Journal of Microelectromechanical Systems,* Vol. 7, No. 2, 1998, pp. 245–251.

[26] Lin, Q., et al., "Dynamic Simulation of a Peristaltic Micropump Considering Coupled Fluid Flow and Structural Motion," *Journal of Micromechanics and Microengineering*, Vol. 17, No. 2, 2007, pp. 220–228.

[27] Yang, B., J. L. Metter, and Q. Lin, "Using Compliant Membranes for Dynamic Flow Stabilization in Microfluidic Systems," *MEMS 2005: 18th IEEE International Conference on Micro Electro Mechanical Systems*, 2005.

[28] Kim, D., N. C. Chester, and D. J. Beebe, "A Method for Dynamic System Characterization Using Hydraulic Series Resistance," *Lab on a Chip*, Vol. 6, 2006, No. 5, pp. 639–644.

[29] Inman, W., et al., "Design, Modeling and Fabrication of a Constant Flow Pneumatic Micropump," *Journal of Micromechanics and Microengineering*, Vol. 17, 2007, No. 5, pp. 891–899.

[30] Hsiung, S. -K., et al., "Active Micro-Mixers Utilizing Moving Wall Structures Activated Pneumatically by Buried Side Chambers," *Journal of Micromechanics and Microengineering*, Vol. 17, No. 1, 2007, pp. 129–138.

[31] Lee, C. -Y., Y. -H. Lin, and G. -B. Lee, "A Droplet-Based Microfluidic System Capable of Droplet Formation and Manipulation," *Microfluidics and Nanofluidics*, Vol. 6, No. 5, 2009, pp. 599–610.

[32] Sundararajan, N., D. Kim, and A. A. Berlin, "Microfluidic Operations Using Deformable Polymer Membranes Fabricated by Single Layer Soft Lithography," *Lab-on-a-Chip*, Vol. 3, 2005, pp. 350–354.

[33] Chen, J., et al., "Variable-Focusing Microlens with Microfluidic Chip," *Journal of Micromechanics and Microengineering*, Vol. 14, No. 5, 2004, pp. 675–680.

[34] Sato, H., et al., "An All SU-8 Microfluidic Chip with Built-In 3D Fine Microstructures," *Journal of Micromechanics and Microengineering*, Vol. 16, No. 11, 2006, pp. 2318–2322.

[35] Fujii, T., et al., "A Nanofactory by Focused Ion Beam," *Journal of Micromechanics and Microengineering,* Vol. 15, No. 10, 2005, pp. S286–S291.

[36] Naulleau, P., et al., "Extreme Ultraviolet Lithography Capabilities at the Advanced Light Source Using a 0.3-NA Optic," *IEEE Journal of Quantum Electronics*, Vol. 42, No. 1, 2006, pp. 44–50.

[37] Sun, Y., et al., "A Bulk Microfabricated Multi-Axis Capacitive Cellular Force Sensor Using Transverse Comb Drives," *Journal of Micromechanics and Microengineering*, Vol. 12, No. 6, 2002, pp. 832–840.

[38] Zhang, J., M. B. Chan-Park, and S. R. Conner, "Effect of Exposure Dose on the Replication Fidelity and Profile of Very High Aspect Ratio Microchannels in SU-8," *Lab on a Chip*, Vol. 4, No. 6, 2004, pp. 646–653.

[39] Lee, S. J., et al., "Characterization of Laterally Deformable Elastomer Membranes for Microfluidics," *Journal of Micromechanics and Microengineering*, Vol. 17, No. 5, 2007, pp. 843–851.

[40] Chan, Y. C., Y. -K. Lee, and Y. Zohar, "High-Throughput Design and Fabrication of an Integrated Microsystem with High Aspect-Ratio Sub-Micron Pillar Arrays for Free-Solution Micro Capillary Electrophoresis," *Journal of Micromechanics and Microengineering*, Vol. 16, No. 4, 2006, pp. 699–707.

[41] Bien, D. C. S., S. J. N. Mitchell, and H. S. Gamble, "Fabrication and Characterization of a Micromachined Passive Valve," *Journal of Micromechanics and Microengineering,* Vol. 13, No. 5, 2003, pp. 557–562.

[42] Nguyen, N. -T., et al., "Micro Check Valves for Integration into Polymeric Microfluidic Devices," *Journal of Micromechanics and Microengineering*, Vol. 14, No. 1, 2004, pp. 69–75.

[43] Seidemann, V., S. Butefisch, and S. Buttgenbach, "Fabrication and Investigation of In-Plane Compliant SU8 Structures for MEMS and Their Application to Micro Valves and Micro Grippers," *Sensors and Actuators, A: Physical*, Vol. 97-98, 2002, pp. 457–461.

[44] Klammer, I., et al., "Numerical Analysis and Characterization of Bionic Valves for Microfluidic PDMS-Based Systems," *Journal of Micromechanics and Microengineering*, Vol. 17, No. 7, 2007, pp. S122–S127.

[45] Attia, R., et al., "Soft Microflow Sensors," *Lab on a Chip*, Vol. 9, 2009, pp. 1213–1218.

[46] Toonder, J. D., et al., "Artificial Cilia for Active Micro-Fluidic Mixing," *Lab on a Chip*, Vol. 8, No. 4, 2008, pp. 533–541.

[47] Ok, J., Y. W. Lu, and C. J. Kim, "Pneumatically Driven Microcage for Microbe Manipulation in a Biological Liquid Environment," *Journal of Microelectromechanical Systems*, Vol. 15, No. 6, 2006, pp. 1499–1505.

[48] Lu, L. -H., K. S. Ryu, and C. Liu, "A Magnetic Microstirrer and Array for Microfluidic Mixing," *Journal of Microelectromechanical Systems*, Vol. 11, No. 5, 2002, pp. 462–469.

[49] Papavasiliou, A. P., D. Liepmann, and A. P. Pisano, "Fabrication of a Free Floating Silicon Gate Valve," *Proceedings of ASME International Mechanical Engineering Congress and Exposition*, 1999.

[50] Busscher, H. J., et al., "The Effect of Surface Roughening of Polymers on Measured Contact Angles of Liquids," *Colloids and Surfaces*, Vol. 9, No. 4, 1984, pp. 319–331.

[51] Celata, G. P., et al., "Characterization of Fluid Dynamic Behaviour and Channel Wall Effects in Microtube," *International Journal of Heat and Fluid Flow*, Vol. 27, No. 1, 2006, pp. 135–143.

[52] Pullen, P. E., et al., "Characterization by Atomic Force Microscopy of Fused-Silica Capillaries Chemically Modified for Capillary Electrokinetic Chromatography," *Analytical Chemistry*, Vol. 72, No. 13, 2000, pp. 2751–2757.

[53] Luo, L. W., et al., "Rapid Prototyping of Microfluidic Systems Using a Laser-Patterned Tape," *Journal of Micromechanics and Microengineering*, Vol. 17, No. 12, 2007, pp. N107–N111.

[54] Creath, K., and J. C. Wyant, "Absolute Measurement of Surface Roughness," *Applied Optics*, Vol. 29, No. 26, 1990, pp. 3823–3827.

[55] Beraldin, J. A., "Basic Theory on Surface Measurement Uncertainty of 3D Imaging Systems," *SPIE—The International Society for Optical Engineering*, Vol. 7239, 2009.

3

Materials for Microfluidic Devices

Material properties fundamentally affect both *functionality* and *manufacturability*, making material selection inseparable from successful design and fabrication. This dual importance is highlighted in the relational map shown in Figure 3.1. In terms of device performance, proper material selection is critical for balancing functional requirements such as biocompatibility, mechanical resilience, optical transparency, and chemical resistance. From a fabrication perspective, the behavior of material dictates which processes are favorable, unfavorable, or outright impossible.

This chapter is divided into three sections. Section 3.1 arranges materials in major categories and discusses some of the most common materials used in microfluidic devices. Relative merits among different materials are presented,

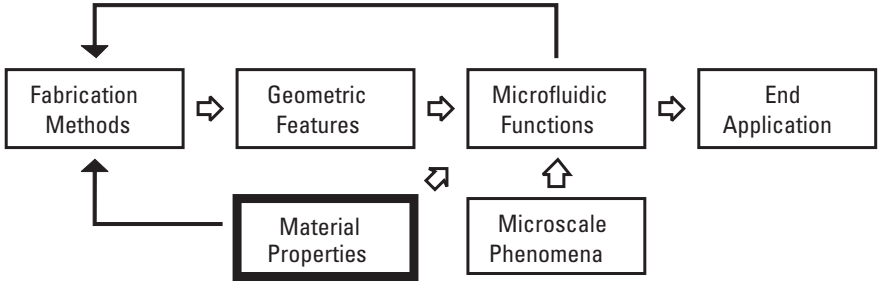

Figure 3.1 Relational map highlighting importance of material properties with respect to both fabrication methods and microfluidic functions.

and examples are cited to illustrate how these relative merits influence fabrication and functionality. In Section 3.1, properties are discussed informally in terms of qualitative mechanical, thermal, electrical, chemical, and optical characteristics. Section 3.2 addresses specific material properties more formally, and it provides quantitative comparisons among materials according to properties that are often of critical interest for microfluidic device fabrication. Section 3.3 draws special attention to the very influential role of material surface conditions in microfluidics.

3.1 Types of Materials

Materials commonly used for microfluidic devices may be divided into major categories of polymers, silicon, glass, and metals. Each of these is discussed in the following sections. Ceramics, composites, and other materials are less prevalent but are also discussed briefly.

3.1.1 Polymers

Polymers present an extremely diverse set of material characteristics for microfluidic devices [1, 2]. Compared to other types of materials, polymers have relatively low mechanical strength, low melting point, and high electrical resistance. The main advantage that polymers offer is that they can be engineered or synthesized to exhibit properties required for targeted functionality. For example, polycarbonate has excellent mechanical toughness and polytetrafluoroethylene (PTFE) has exceptional chemical resistance. Furthermore, many polymers can be surface-modified for greater biocompatibility, more effective surface chemistry, solvent resistance, and so on. In microfluidics, some of the more common polymer materials include polydimethylsiloxane (PDMS), SU-8, polymethyl methacrylate (PMMA), and polyimide. Several others polymers have also been used in microfluidic applications, as discussed later.

The geometry and distribution of materials for a vast majority of microfluidic devices are defined by photolithography. Photoresists are arguably the most important materials in microfabrication of fluidic devices, even though in most cases they are used only as an intermediate material during fabrication and do not remain in final devices. As discussed more thoroughly in Chapter 4, photolithography is the process by which selected regions of a photoresist layer are patterned through a mask, based on sensitivity to radiation—either ultraviolet (UV) or X-ray. Photoresist materials are used during the patterning steps of fabrication but are typically removed before the overall fabrication sequence is completed. This chapter focuses primarily on materials that remain permanent

in completed devices. One exception is SU-8, which is a photoresist material yet has been used extensively for structural purposes in a variety of microfluidic devices.

From a manufacturing perspective, a very important distinction among polymers is whether they are *thermoplastic* or *thermoset*. Thermoplastics are characterized by the ability to be reshaped at elevated temperature. This may be an advantage or disadvantage for final devices, depending on functional requirements. If dimensional stability at high temperature is required, thermosets such as polyimide are generally superior. For manufacturing, however, thermoplastics are desirable because they can be manufactured using a wide variety of rapid and low-cost fabrication methods including thermoforming and hot embossing [3]. The cyclic olefin polymer (COP) ZEONOR and the cyclic olefin copolymer (COC) TOPAS are examples of materials that combine advantages of functional merits such as UV transparency and chemical resistance with the ease of thermoplastic manufacturing for microfluidic chips [4–6]. Elastomers like PDMS are sometimes categorized in a third category apart from thermoplastic or thermoset, but in the context of this book elastomers will be considered thermoset because they generally cannot be plastically reshaped simply by elevating temperature.

Polydimethylsiloxane (PDMS) is the most widely investigated polymer material in microfluidics [7]. It belongs to the broader class of polymers known as polysiloxanes and more generally silicones, which are characterized by a siloxane backbone of silicon and oxygen atoms. PDMS is inexpensive, nontoxic, and optically transparent. It is also chemically stable in a wide range of environments. Although PDMS is subject to swelling in solvents, additives have been shown to be effective in reducing swelling [8]. Two of the most frequently used commercial PDMS products used in microfluidics are Sylgard 184 from Dow Corning (Midland, Michigan) and RTV 615 from Momentive Performance Materials, Inc. (Albany, New York), formerly GE Silicones.

A major reason for the popularity of PDMS is its ease of fabrication by a diverse set of replication methods collectively described as soft lithography [9], detailed further in Chapter 5. A unique benefit of fabricating structures by casting is the opportunity to embed functional components within the structure. For example, an electromagnetic coil can be embedded within PDMS to produce a compact electromagnetically actuated membrane device [10]. Although casting is more common, PDMS can also be patterned by plasma etching [11]. Like many polymers, the properties of PDMS can be altered, for example to make it photopatternable or conductive [12]. Mechanically, PDMS is described as a hyperelastic material, meaning that it may undergo very large strains and still have full elastic recovery. This makes it very attractive for use as membrane or flexure components [13, 14]. The stress-strain relationship of PDMS is

nonlinear over the full range of strain, but for limited range the behavior is close to being linearly elastic [15, 16].

SU-8 is an epoxy-based photocurable resin that has gained widespread use in microfabrication particularly because of the high aspect ratio that can be achieved [17]. It is a negative-tone resist, meaning that regions that are exposed to UV radiation are subject to curing, while masked regions remain soluble and are removed during the developing step of photolithography. SU-8 is an extremely diverse material for fabrication of microfluidic devices. It is used for direct fabrication of microchannels [18, 19] and embedded flexible structures [20], as well as for sacrificial layers [21], electroplating templates [22] and masks for etching [23] or abrasive machining [24]. As a photosensitive yet mechanically resilient material, SU-8 is used frequently as a master relief pattern for casting or molding microfluidic devices in other materials such as PDMS [25]. SU-8 is also capable of supporting electro-osmotic flow [26] with performance similar to that of glass. A major U.S. supplier of SU-8 is MicroChem Corporation (Newton, Massachusetts).

Polymethyl methacrylate (PMMA) is another diversely functional material for microfluidics. PMMA is a common base material for high-resolution photoresists. PMMA is also a thermoplastic material, and therefore can be patterned with microchannels or other structures by fast manufacturing methods such as hot embossing. It is optically transparent and can be patterned effectively by laser cutting [27]. PMMA is opaque to light transmission in the UV range, which limits its applicability for some approaches to sensing applications. However, it can still be used for microchannel separations by laser-induced fluorescence methods [28]. It can be integrated with metal electrodes and its surface can be functionalized for electrochemical sensing applications [29]. PMMA is also used advantageously as an intermediate material for some fabrication strategies. For example, although PDMS as a thermoset is constrained to relatively slower curing methods, PMMA masters can be produced rapidly in high volume by hot embossing, and these masters can be used for manufacturing of PDMS chips with better productivity [30]. PMMA is amenable to bonding with other materials including SU-8 [31]. It can also be used as an intermediate layer in novel ways such as enabling the integration of gold electrodes within microchannels between silicon and glass [32].

Polyimides are generally regarded as high-performance engineering polymers, because, compared to many other polymers, they have higher mechanical strength, heat resistance, and dielectric strength [33]. Polyimide has been used as a highly flexible substrate for MEMS sensors [34], and is compatible with microfabrication processes including laser ablation [35], plasma etching [36], as well as direct photopatterning [37]. Dimensional stability of polyimide is superior to many other polymers, making it commercially viable for multifunctional chips used in liquid chromatography and electrospray applications [38].

Examples of commercial polyimides engineered for microfabrication applications include the PI-2600 series (nonphotodefinable) and HD-4100 series (photodefinable) from HD Microsystems (Parlin, New Jersey).

Fluoropolymers have exceptional chemical resistance, as well as favorable thermal and electrical properties compared to many other polymers. Fluoropolymers can be integrated as functional components or coatings for biocompatible microfluidic systems [39]. The most well known among flouropolymers is polytetrafluoroethylene (PTFE), under the trade name Teflon by DuPont (Wilmington, Delaware). Other fluoropolymers include fluorinated ethylene propylene (FEP), ethylene-tetrafluoroethylene (ETFE), and perfluoroalkoxy copolymer (PFA).

Compared to other important types of materials such as silicon, glass, and metals, polymers have tremendous functional diversity. In addition to the relatively common polymers already discussed above, there are several others with unique functional merits that have been explored for microfluidics. The cyclic olefin copolymer (COC) TOPAZ is a thermoplastic material that exhibits optical transmission superior to PMMA and many other polymers [40]. Polyvinylidene fluoride (PVDF) exhibits piezoelectric response [41] and poly(vinylidene fluoride-trifluoroethylene) exhibits electrostrictive response [42], making these materials useful for electromechanical actuation of microfluidic devices. The reversible sol-gel transition of methyl cellulose has been used for microvalve actuation [43]. The low melting point and high expansion of paraffin upon changing from solid to liquid can be used to an advantage, for example, as the basis for actuation of valves [44] or high-pressure micropumps [45]. The surface of polymethylhydrosiloxane (PMHS) can be readily modified by hydrosilation for analytical chemistry applications [46]. Polycaprolactone is a biodegradable polymer that can be of interest for implantable biomedical microdevices [47].

Several other polymers are used routinely for ancillary purposes, such as fittings and tubing for laboratory testing. Some of the more common materials include polypropylene (PP), polyetheretherketone (PEEK), and polyoxymethylene (also known as polyacetal or commercially as Delrin). For example, polypropylene is inexpensive but is limited to low temperatures, PEEK can be manufactured in extremely fine tubing dimensions but is subject to solvent absorption, and polyoxymethylene has favorable mechanical properties but has poor resistance against corrosives.

3.1.2 Silicon

The wide variety of microfabrication processes for microfluidic and MEMS devices are largely inherited from microelectronics fabrication, for which silicon is by far the most prevalent substrate material in use. Silicon is most

fundamentally important for microelectronics because of its semiconductor properties. Not only can the resistivity of silicon can be altered by many orders of magnitude by doping [48], but differences in spatial arrangement of dopant concentration can fundamentally enable the functionality of diodes and transistors—the basic building blocks for integrated circuits. As discussed later silicon also has several merits as a functional material beyond its importance as a semiconductor.

Before the rapid growth of interest in polymer materials for microfluidics, silicon received the greatest early attention because silicon-based MEMS technology had already been a very active field of research and development. Numerous innovations were explored to apply MEMS technology to flow control devices including valves, pumps, and mixers [49]. Although brittle when stressed to the point of fracture, silicon is remarkably effective as a mechanical material [50]. It exhibits linearly elastic behavior below its yield strength with no hysteresis, and suffers no plastic deformation or creep except under very extreme temperatures well beyond relevance to microfluidic applications. Silicon has a high melting temperature (1,410°C) comparable to many engineering metals, and relatively low coefficient of thermal expansion. With proper design, silicon is very reliable and commercially successful in a wide variety of MEMS transducers such as accelerometers, pressure sensors, and micromirrors [51].

Distinct from other materials used in microfluidics is the importance of crystal orientation for silicon. Silicon wafers have single-crystal structure, formed by a cubic diamond arrangement of covalently bonded silicon atoms in overlapping cubic unit cells [52]. This single crystal structure is what makes bulk micromachining of silicon very predictable and consistent. Wafers are cut from ingots based on specific orientation with respect to crystal planes, as shown labeled with Miller indices in Figure 3.2.

Single-crystal silicon is an isotropic material for which its properties are not identical in all directions. Therefore, crystal plane orientation is often very relevant for silicon micromachining. In particular, the (111) plane has a higher packing density of atoms and is significantly more resistant to some types of chemical etchants. This is what makes it possible to design very precise trapezoidal features, with sloped (111) planes inclined with respect to the (100) plane at an angle of 54.74°. Details of anisotropic wet etching of silicon are discussed further in Chapter 6. Other anisotropic characteristics are difference in mechanical stiffness and rate of surface oxidation.

Silicon is also prevalent in microsystems in the form of *polysilicon* (i.e., polycrystalline silicon) and amorphous silicon. In both cases, the silicon is typically deposited as thin films by vapor deposition, and can be doped for electronic device functionality. Polysilicon is used in many diverse ways for surface micromachined sensors and actuators. For example, in the case of actuation, polysilicon has been used for electrostatic diaphragms [53] and as heating

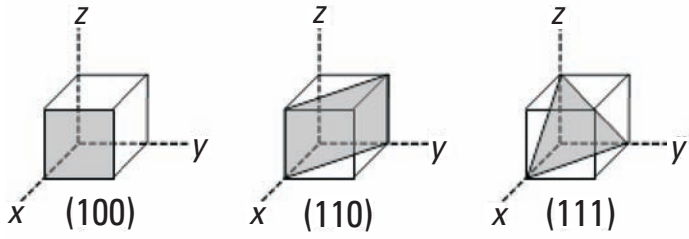

Figure 3.2 Silicon crystal planes and Miller indices. (*After:* [52].)

elements [54] for micropumps. Properly doped polysilicon is also effective for sensing elements based on capacitive displacement [55] and piezoresistive strain measurement [56]. Amorphous silicon has a functional advantage of lower processing temperature for deposition, but is not common in microfluidic devices.

Another unique aspect of silicon is that it can be made highly porous with good uniformity by an anodic electrochemical etch process [57]. Porous silicon has extremely high surface-to-volume ratio, which is particularly advantageous for applications with surface reactions involving catalysis, adsorption, and/or desorption [58]. Porous silicon has also been explored as scaffolding for studies on cell adhesion [59] and scaffolding for tissue engineering [60].

3.1.3 Glass

The term glass conventionally refers to materials that are predominately amorphous silicon dioxide (SiO_2), also known as silica. Varieties of glass are made by including other compounds such as sodium carbonate, calcium oxide, and boron oxide to produce different thermal, mechanical, and optical characteristics. Like silicon, glass is rigid, dimensionally stable, and relatively brittle. Many common types of glass are optically transparent, making glass favorable for applications that require imaging or optical methods of detection for fluids and/or suspended particles. Glass is a very convenient substrate for microfluidic devices because it is readily available in flat form, typically cut into rectangular slides or circular wafers. For applications such as capillary electrophoresis, glass microchannel chips are routinely produced as either commercial off-the-shelf products or even semi-custom layouts [61, 62]. Unless specifically engineered for electrical conductivity, conventional glass exhibits sufficient electrical insulation such that it can serve as a substrate for direct patterning of conductive metal lines and functional electrodes [63, 64].

Borosilicate glass substrates are routinely available in R&D laboratories as microscope slides and are frequently used as substrates for supporting polymer microfluidic structures involving other materials such as PDMS. PYREX by

Corning Incorporated (Corning, New York) and BOROFLOAT by SCHOTT AG (Mainz, Germany) are types of borosilicate glass that are commercially produced in a variety of forms, including thin circular wafers. PYREX 7740 is a formulation favorable for wafer-scale bonding to silicon [65], using an anodic bonding process described in Chapter 9. Soda-lime glass is another common type of glass that has been used in some microfabrication applications. Borosilicate glass, however, is superior to soda-lime glass in terms of dimensional stability at elevated temperature. Fused silica is a form of amorphous silicon dioxide that is typically synthesized for ultra high purity. Like natural quartz, fused silica is notable among other materials for its exceptional thermal and optical properties. Fused silica maintains dimensional stability above 1,500°C and is transparent even in the low UV spectrum.

A common way of creating channels in glass substrates is by wet etching, typically with concentrated hydrofluoric acid [66]. Wet etching of glass occurs isotropically and typically produces rounded profiles with low aspect ratio. However, more directional profiles by plasma etching are also achievable [67] and techniques have also been developed specifically for high-aspect ratio features in glass [68] as well as quartz [69]. Holes and channels in glass substrates can be fabricated by ultrasonic drilling [70] and laser ablation [71]. There are also formulations of photosensitive glass that exhibit spatial etch selectivity when exposed to UV radiation through a mask [72]. Although the majority of glass microfluidic devices use slides or wafers, glass in other forms can also be used to fabricate channel-like structures using spin-on-glass [73] or sputtered films [74].

3.1.4 Metals

Metals are clearly distinguished by having significantly higher electrical conductivity than other types of materials used in microfluidics. Accordingly, metals are frequently used for functional electrical components such as electrodes, conducing lines, or signal interface contacts. As conductors of electricicty, metals may also be used to modify electromagnetic fields, which may subsequently be used in novel ways for applications such as biological cell manipulation [75]. Another functional merit for metals is high thermal conductivity. For example, a heat spreader based on micro heat pipe design has been constructed from layers of copper and brass for microprocessor cooling [76]. The relatively high mechanical strength of metals favors their use for high-pressure applications [77], compared to polymer materials. Some metal alloys that have favorable magnetic properties have been incorporated into functional components such as nickel-iron rotors for active mixing [78]. Magnetic components have also been combined with deformable polymer structures for functionality as micropumps [79] and microvalves [80, 81]. Some microfluidic devices also take advantage of shape-memory alloys. Nickel-titanium (NiTi), for example, changes from its

austenite phase to its martensite phase upon cooling, and the corresponding shape change can be used for device actuation [82, 83].

Gold, nickel, and copper are among the most commonly used metals in microfluidic devices. Gold is often the material of choice for electrical purposes because of superior resistance to corrosion and oxidation, even though other materials such as copper have lower electrical resistivity (1.7×10^{-6} Ω·cm for copper versus 2.2×10^{-6} Ω·cm for gold). Especially for silicon substrates and silicon dioxide surfaces, chromium is frequently used as an effective adhesion layer for gold [84]. Nickel, copper, and alloys based on nickel or copper are favorable for structures made by electroplating and electroforming. An example of a commercially successful metal microfluidic structure is the orifice array for ink-jet printheads, made in a single nickel electroforming step [85]. In contrast to gold and copper, the much higher resistivity of platinum (10.6×10^{-6} Ω·cm) makes it favorable for resistive heating. Other metals such as aluminum and tungsten are prevalent in microelectronics but less common in microfluidic devices. Aluminum has relatively low melting point (660°C), high electrical conductivity, and high thermal conductivity. Tungsten has very high melting point (3,410°C) and modest electrical conductivity, but has been very popular in microelectronics fabrication for its ability to fill narrow trenches and gaps.

As detailed in Chapters 4 through 8, several techniques inherited from microelectronics fabrication are routinely available for patterning thin-film metal layers. Thin-film deposition techniques offer the option of surface micromachined channels in metal, with the potential benefit of integration with microelectronic device circuitry [86]. A different approach to fabricating larger microchannels is to use fugitive inserts, followed by selective etching [87].

Another important role of metals in microfluidic device fabrication is tooling. Even if the final device made of a different material, it is sometimes beneficial to have finely patterned tooling to transfer the relevant geometry by hot embossing or other molding technique. This facilitates more rapid high-volume manufacturing with good repeatability. One approach, for example, is to begin with laser micromachining of patterned tooling in a thin metallic sheet, then to transfer the pattern by hot embossing onto a thermoplastic (PMMA) master, and to complete the process with casting of PDMS atop the PMMA master [88].

3.1.5 Other Materials

Polymers, silicon, glass, and metals comprise the majority of material types used in microfluidic devices. However, other materials play important functional roles as well. Silicon compounds such as silicon nitride and silicon dioxide (SiO_2) films are also used extensively in microfabrication. Silicon nitride in its stoichiometrically balanced form is Si_3N_4, although SiN_x is used as the

abbreviation for more general cases. In the context of microfabrication, these are often abbreviated as nitride and oxide, respectively. Both silicon nitride and silicon dioxide are effective electrical and thermal insulators. In silicon micromachining, nitride or oxide films are routinely used as temporary masking layers for etch processes. In addition, however, nitride and oxide are sometimes used for permanent functional components such as microchannels [89] and membranes [90]. Nitride has good chemical resistance and is often used as a protective passivation layer. Neither nitride nor oxide is used very commonly as the structural basis for microchannels, although there is some precedent [91]. Silicon carbide (SiC) is another silicon compound noteworthy for having exceptionally high melting temperature (2,300°C). Silicon carbide is not as commonplace as nitride or oxide for microfabrication in general, but can be advantageous for high-temperature and corrosive applications [92].

Among the most well-known engineering ceramics are silicon dioxide (SiO_2, or silica), aluminum oxide (Al_2O_3, or alumina), and zirconium dioxide (ZrO_2, or zirconia). Low-temperature cofired ceramics (LTCC) are advantageous from a manufacturing standpoint because they can be used to fabricate laminate structures [93, 94]. Ceramics can also be bulk-manufactured in very fine particle form, which can be useful for manufacturing strategies that involve solid particles. For example, silica nanoparticles have been used to produce well-ordered nanoscale porosity inside fluidic microchannels [95]. Composite materials represent another important category of materials. In particular, materials such as lead zirconate titanate (PZT) that exhibit a strong piezoelectric effect are often used for electromechanical actuation [96, 97] of microfluidic components. Hydrogels that exhibit dramatic change in volume and porosity in response to changes in environmental conditions like temperature or pH level can also offer unique functionality for fluidic purposes, such as valve actuation [98]. Indium tin oxide (ITO) has a unique advantage in microfluidic devices as a conductive electrode, because it is optically transparent and therefore allows observation of particle and cell manipulations under optical microscopes.

3.2 Material Properties

In this book material properties are categorized as mechanical, thermal, electrical, optical, magnetic, and chemical. The majority of material properties in this section are referenced from the *CRC Handbook of Chemistry and Physics* [99], the *CRC Materials Science and Engineering Handbook* [100], the *CRC Handbook of Mechanical Engineering* [101], and the *Polymer Data Handbook* [102], which offer relatively comprehensive databases for material properties data. Some information is also drawn from online references or product datasheets, as noted by citation in the figures. The materials shown focus on those that are relatively

common in microfluidics fabrication, as were discussed above. Bar charts are used throughout this chapter for the benefit of graphical comparison, with sources cited for each row entry in the respective charts.

As shown in the following comparison figures, some of the properties are not narrow, constant values, but vary within a range of values depending on exact formulation, processing conditions, and even directional orientation. Furthermore, different methods of quantifying properties can produce slightly different values. Organizations such as the International Organization for Standardization (ISO) and ASTM International (originally known as the American Society for Testing and Materials) serve a vital role of establishing well-documented testing standards. In general the properties described next assume that the materials are homogeneous, isotropic, and at room temperature, unless noted by exception.

3.2.1 Mechanical Properties

Mechanical properties focus on relationships among stress, strain, and structural failure of materials. The mechanical properties of a microfluidic device are particularly important for flexures, flaps, membranes, and other structures for which deformation is an essential part of their functionality (see examples in Chapter 2). The deformation of surfaces in response to fluid pressure is particularly relevant for very soft materials like PDMS, as channel deformation alters flow dynamics [103]. In some cases, however, this deflection may be used as an advantage, if it is desirable to change channel geometry for tunable flow [104]. Mechanical properties are generally temperature dependent, although the degree of dependency varies significantly depending on type of material. Most materials tend to exhibit higher ductility and lower stiffness with increasing temperature, with thermoplastics being most extreme in these regards.

3.2.1.1 Elastic Properties

There are multiple moduli that describe the elastic behavior of materials, and fundamentally these moduli are expressions of the ratio of stress versus strain. The most well known is Young's modulus E, which is the ratio of stress versus strain in the linear elastic region of a stress-strain curve. It is often used synonymously with modulus of elasticity or elastic modulus, even though more narrowly E refers to the ratio of tensile stress to tensile strain. Shear modulus and bulk modulus are other elastic moduli, discussed further later. Figure 3.3 compares values for Young's modulus of some materials commonly used in microfluidic devices.

Poisson's ratio ν is the ratio of transverse strain versus axial strain. Most common engineering materials have values between 0.2 and 0.5, with elastomers like PDMS approaching the upper extreme near 0.5. Shear modulus G,

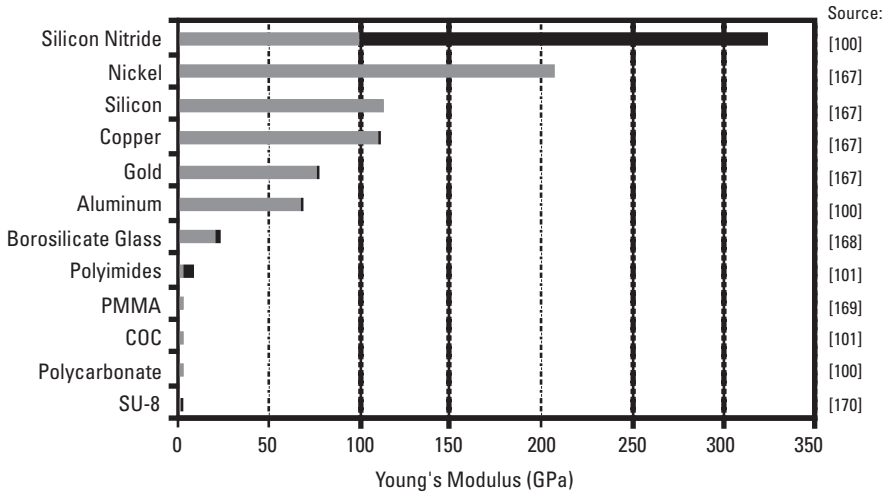

Figure 3.3 Comparison of Young's modulus for selected materials.

sometimes called the modulus of rigidity, is the ratio of shear stress to shear strain. For homogeneous linearly elastic materials, the shear modulus is related to Young's modulus and Poisson's ratio by the following equation:

$$G = \frac{E}{2(1+\upsilon)} \tag{3.1}$$

The bulk modulus K represents a resistance to compression under uniform pressure. It is defined in terms of applied pressure P and material volume V as shown in (3.2). A material with low bulk modulus is more compressible than a material with high bulk modulus.

$$K = V\frac{\partial P}{\partial V} \tag{3.2}$$

For homogeneous linearly elastic materials, the bulk modulus is related to Young's modulus and Poisson's ratio by (3.3). This reveals that from the four properties E, ν, G, and K, only three are actually needed to calculate the remaining one, as long as the material is homogeneous, isotropic, and linearly elastic.

$$K = \frac{E}{3(1-2\upsilon)} \tag{3.3}$$

3.2.1.2 Strength Properties

The strength of a material is a general term used to describe some characteristic limits with respect to the ability to sustain load. It is most often associated with the concept of material failure, and units are typically those of stress (N/m^2 or Pa). Ductile materials are often considered to have failed if plastic deformation occurs, and this is commonly characterized by yield strength S_y. The yield strength of most materials decreases with increasing temperature. Flexural strength measures the limiting ability of a material to sustain transverse load before fracture, and is useful for quantifying the strength of brittle materials that do not exhibit significant plastic deformation before failure. Flexural strength is typically measured by loading in three-point or four-point bend tests, and is also known as the modulus of rupture (MOR). Ultimate tensile strength (UTS), compressive strength, and impact strength are other examples of characteristic stress limits.

In microfabricated structures it is important to recognize that the strength of thin films is highly dependent on factors such as residual stress, impurities, and localized geometric irregularities including surface roughness. Therefore any reference values for properties such as UTS and MOR based on macroscopic specimen testing should be used only for very coarse relative comparisons, with failure tested directly for microscale components based on actual processing conditions and resulting geometry. For some materials, direct mechanical testing of microscale specimens has been conducted using techniques such as atomic force microscopy [105] and nanoindentation [106]. Figure 3.4 offers coarse comparison of tensile strength based on macroscale specimen testing.

Many polymers exhibit nonlinear mechanical behavior for which it becomes impractical to characterize stiffness by elastic properties such as Young's modulus. In such cases, the percent elongation before failure is a more useful indicator of pliability. PTFE is notable for having extreme pliability, with total elongation in excess of 300% before failure. PDMS is also remarkable for not only sustaining over 100% elongation before failure, but also having the ability to elastically recover over much of this range. Figure 3.5 compares total elongation for selected polymers.

3.2.1.3 Fatigue Life

Fatigue strength may be important for flexure components, especially if they are subject to high cycling. Quantified values for fatigue strength depend on specimen geometry, loading magnitude, and numbers of cycles. Available data for macroscale test specimens typically provide only coarse comparisons among materials rather than accurate predictions. Consequently, fatigue performance is referenced in this section by citations rather than data tables.

Some thermosets have been reported to exhibit endurance limit behavior in the range between 10^4 and 10^7 cycles [107]. Crack propagation under fatigue

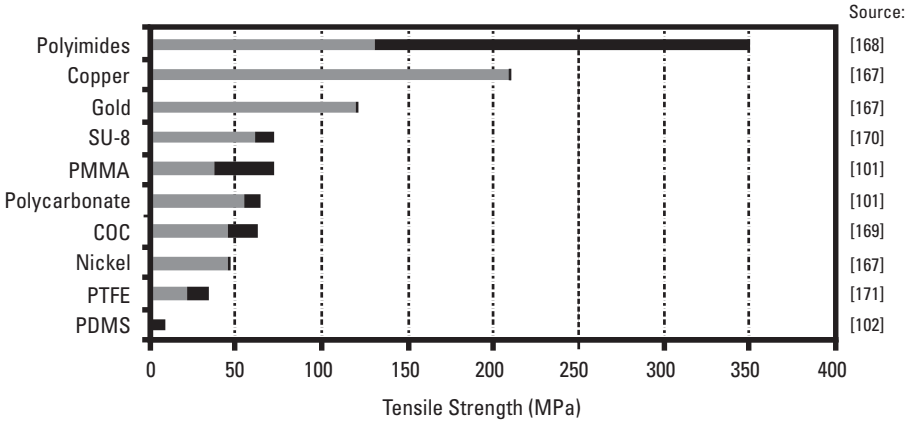

Figure 3.4 Comparison of tensile strength for selected materials.

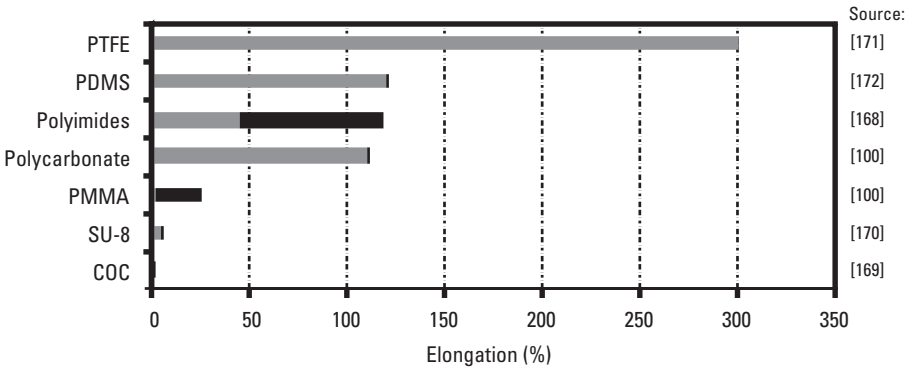

Figure 3.5 Comparison of total elongation before failure for selected polymers.

loading has been studied for a wide variety of bulk polymer materials including polymethyl methacrylate [108], polycarbonate [109], and polyvinylchloride [110]. However, such measurements have generally been applied to bulk specimens with crack dimensions on the order of millimeters.

For MEMS-scale components, performance lifetime in excess of one billion cycles has been reported for polysilicon, aluminum, silicon dioxide, and nickel [111, 112], but very little has been reported in the case of polymers. Polysilicon has excellent fatigue behavior [113–115] with endurance limits beyond 1 billion cycles. The fatigue life of metal thin films in the range from 100 nm to a few microns has been reported to exhibit thickness dependence

[116], and studies have been conducted on polyimide films as carrier substrates to evaluate the fatigue performance of submicron metal films [117].

3.2.2 Thermal Properties

The thermal properties of materials are important for several reasons in the context of microfluidic devices. If materials undergo significant thermal expansion, geometric design parameters such as microchannel cross-section and electrode spacing may be altered significantly. Some microvalves and micropumps are designed based on thermomechanical actuation. Microfluidic reactors often require the ability to set and control the temperature of reactants. Effective heat transfer is the fundamental objective for microchannel electronics cooling, and some gas sensors depend on monitoring sensitive changes in heat transfer. Flowing electric current through thin-film platinum wires, for example, is one way of rapidly increasing localized temperature. In electro-osmotic flow, Joule heating occurs as a result of the current flowing through resistive media. The thermal properties of microfluidic components are also very important because fundamental fluid properties such as viscosity are temperature dependent.

Even if there are no temperature-related issues for design functionality, thermal properties are also often critical from a manufacturing perspective. A very important case is the application of heat to thermoplastic materials for geometric shaping. For multistep fabrication processes, the complete sequence of thermal conditions must also be considered. For example, process steps that involve plasma exposure or heated chemical baths may subject substrates to temperatures near or above 100°C. This may present concern for dimensional integrity of many polymers and for thermal stresses occurring at the interfaces between dissimilar materials.

3.2.2.1 Melting Point

The melting point T_m of material is the temperature at which it changes from solid to liquid phase. Some materials, especially some polymers, degrade rather than melt at high temperature. Temperature is expressed in degrees kelvin (K) or degrees Celsius (°C). Figure 3.6 compares values of melting point for some materials used in microfluidic devices. From this set, silicon compounds and other inorganic compounds are observed have the highest melting points, followed by metals. Most polymers have substantially lower melting point generally below 300°C, and those that do not melt at substantially higher temperature (e.g., polyimide) decompose rather than melt. SU-8 is not characterized as having a melting point per se, but it loses dimensional stability above approximately 200°C.

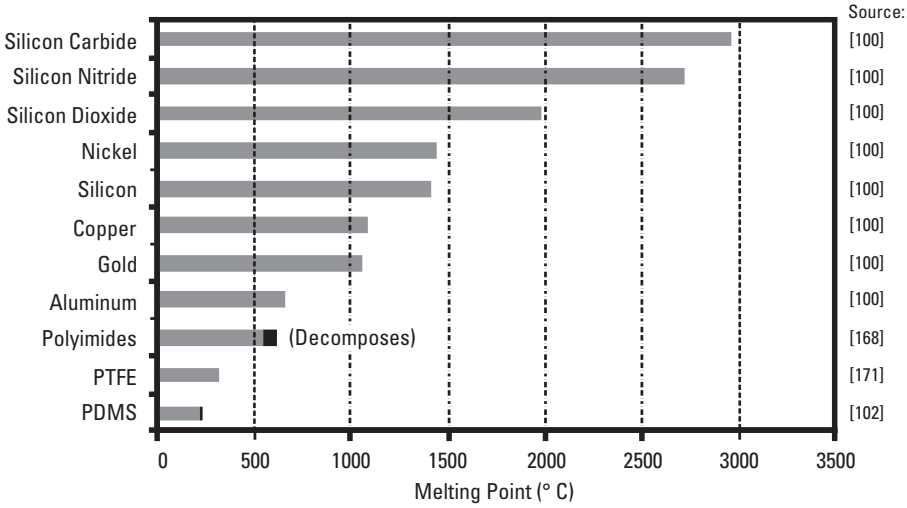

Figure 3.6 Comparison of melting point for selected materials.

3.2.2.2 Glass Transition Temperature

The definition of glass transition temperature T_g for a material can be confusing because there are subtle differences depending on the type of material being considered. For inorganic brittle materials like silica glass, the glass transition temperature is the temperature at which it experiences phase change (upon cooling) between liquid and amorphous glass phases. In the case of polymers, however, T_g represents a change in the degree of cross-linking. From an oversimplified yet practical standpoint, however, the glass transition temperature can be more loosely interpreted as a temperature (below melting) at which the thermomechanical behavior of a material exhibits an abrupt change. This change may be evidenced in such properties as heat capacity, coefficient of thermal expansion, viscosity, or even density. Therefore, reported values for glass transition temperature vary significantly based on measurement method. A very common method of determining glass transition temperature is differential scanning calorimeter (DSC), which ramps temperature at a prescribed rate and monitors any abrupt changes in heat capacity or enthalpy of fusion [118].

PMMA has a relatively low glass transition temperature of 105°C, making it a very favorable choice for imprint lithography (Chapter 5) and related fabrication techniques. Not all materials have a clearly defined threshold of glass transition, and some materials may have more than one glass transition temperature. Thermoplastics are sometimes characterized by a heat deflection temperature (HDT), pertaining to the temperature at which a material deforms by a

threshold magnitude when subjected to a specified load. HDT is clearly distinct from T_g because it is a mechanical performance parameter rather than a matter of phase change, but the two are similar in that materials with higher HDT have greater dimensional stability at elevated temperature.

3.2.2.3 Coefficient of Thermal Expansion

The coefficient of thermal expansion (CTE or α) quantifies the rate of linear dimensional change with respect to temperature. CTE relates the strain ε (change in length divided by original length) to a change in temperature ΔT by the equation $\varepsilon = \alpha \Delta T$. CTE is typically expressed in terms of microstrain (e.g., μm/m) per unit temperature. In data tables this is sometimes expressed in units of 10^{-6}/K or parts per million per degree kelvin (ppm/K). The coefficient of thermal expansion is temperature dependent, generally increasing with increasing temperature. Figure 3.7 compares CTE values for some materials commonly used in microfluidic devices.

Thermal expansion can be advantageous for devices that use thermomechanical actuation principles, but can also be detrimental for devices that cannot tolerate dimensional changes in service. During device fabrication, thermal expansion is an important factor any time there are dissimilar materials that share an interface at nonambient temperature. Upon returning to ambient conditions, the device will be subject to thermal stresses between the dissimilar materials, often resulting in distortion or failure.

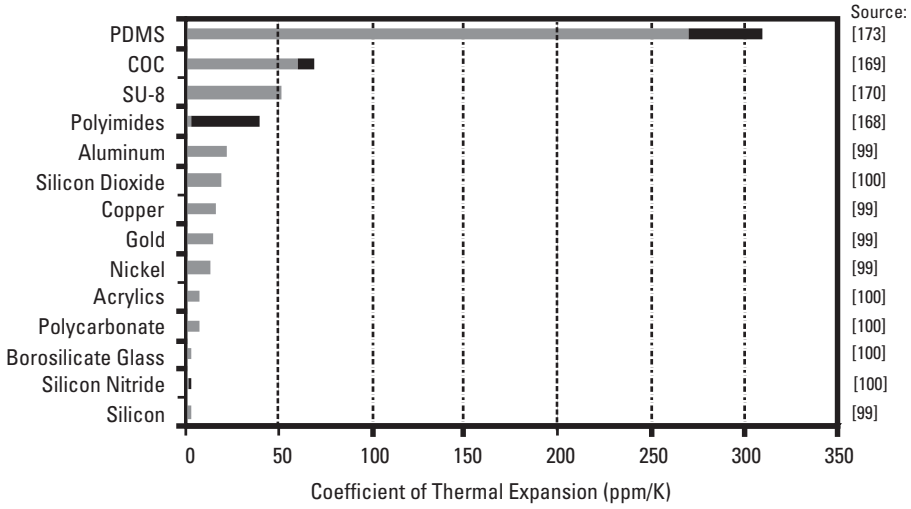

Figure 3.7 Comparison of coefficient of thermal expansion for selected materials.

3.2.2.4 Specific Heat Capacity

The specific heat capacity (C_p) at constant pressure is an expression of how much energy is required to increase the temperature of a material. Accordingly, a low value of C_p indicates greater ease of changing the temperature of a material. Metals have characteristically low heat capacity, while good thermal insulators like silicon dioxide have significantly higher heat capacity. In SI units the specific heat capacity is expressed in J/(kg·K), but C_p is also commonly tabulated in terms of J/(mol·K). Specific heat capacity is temperature dependent, generally increasing at higher temperature. For example, C_p for silicon dioxide can nearly double from 32.6 J/(mol·K) at 200K and 64.4 J/(mol·K) at 600K. Figure 3.8 compares values for specific heat capacity of some materials used in microfluidic devices. Most polymers fall in the range from 1,000 to 1,500 J/(kg·K), with some epoxies having substantially higher values. Common metals vary widely below 1,000 J/(kg·K). The very low specific heat capacity of platinum at 133 J/(kg·K), combined with its relatively high electrical resistivity and high thermal conductivity, motivates its favored use as a heating element.

3.2.2.5 Thermal Conductivity

Thermal conductivity k describes the ability of a material to conduct heat in response to a spatial temperature difference. Thermal conductivity is expressed

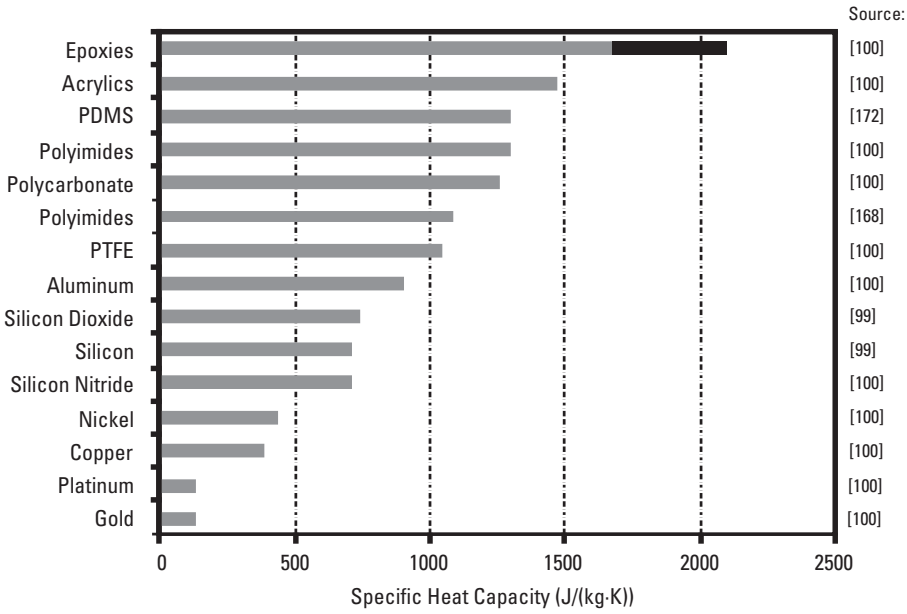

Figure 3.8 Comparison of specific heat capacity for selected metals.

in SI units as W/(m·K). Metals are generally good thermal conductors while polymers and inorganic compounds are relatively poor thermal conductors. Thermal conductivity varies over a wide range, and can vary significantly depending on factors such as impurities and processing conditions. Figure 3.9 compares values for materials with relatively low thermal conductivity, and Figure 3.10 compares values for materials with relatively high thermal conductivity.

As shown in Figure 3.11 for some common metals and silicon, thermal conductivity also varies with temperature, generally decreasing at higher temperature.

In some cases thermal conductivity depends significantly on orientation, and pyrolytic graphite (although not common in microfluidic applications) is an extreme-case example. At 300K, the thermal conductivity of pyrolytic graphite is 1,950 W/m·K parallel to the layer planes but only 5.70 W/m·K in the perpendicular direction.

3.2.3 Electrical Properties

The electrical properties of materials are important in microfluidics for functional purposes including electrostatic actuation, electrokinetic pumping, resistive heating, and capacitive sensing. Among the most basic properties are resistivity, relative permittivity (i.e., dielectric constant), and breakdown voltage (i.e., dielectric strength).

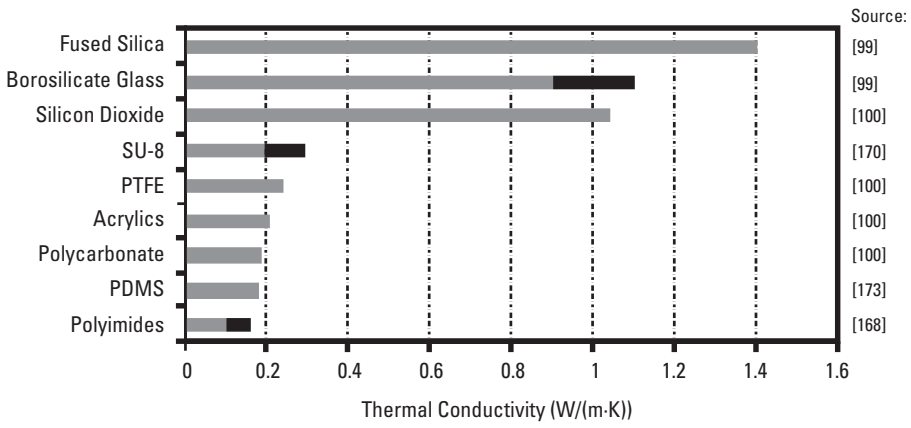

Figure 3.9 Comparison of values for materials with relatively low thermal conductivity.

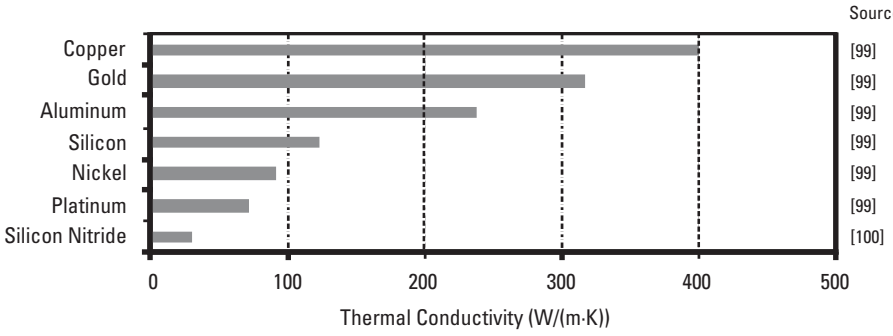

Figure 3.10 Comparison of values for materials with relatively high thermal conductivity.

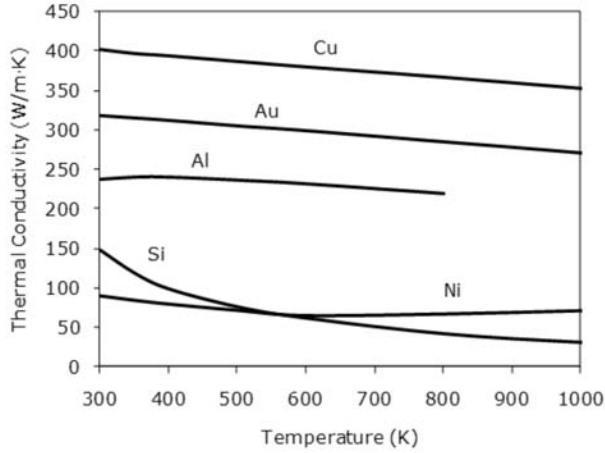

Figure 3.11 Temperature dependence of thermal conductivity. (Based on data from [99].)

3.2.3.1 Resistivity

The resistivity ρ of a material represents its tendency to oppose electric current, and is defined as the electric field (in volts per meter) divided by the current density (in amperes per square meter). The SI unit expression for resistivity is ohm·meter (Ω·m), although many data tables list conventionally in terms of Ω·cm. Resistivity of thin films is typically expressed two-dimensionally in terms of ohms per square, and a distinction is made between surface resistivity and volume resistivity ρ.

Notable about resistivity is that the different types of materials have drastically different ranges of values. For example, most metals have resistivity values

on the order of 10^{-7} or 10^{-8} Ω·m, whereas inorganic compounds like silicon nitride and silicon dioxide have resistivity values well exceeding 10^{10} Ω·m. Some polymers go several orders of magnitude higher, with PTFE, for example, exceeding 10^{16} Ω·m. Figure 3.12 compares resistivity values for selected metals.

Figure 3.13 compares values for dielectrics. Resistivity values of dielectrics are generally so high that they are shown here in terms of order of magnitude only. For silicon-based microfluidic devices, silicon dioxide and silicon nitride are often materials of choice for electrical insulation.

Resistivity of metals increases with temperature, while the resistivity of semiconductors decreases with increasing temperature. Figure 3.14 shows the temperature dependence of resistivity for come common pure metals, with most but not all exhibiting linear dependency.

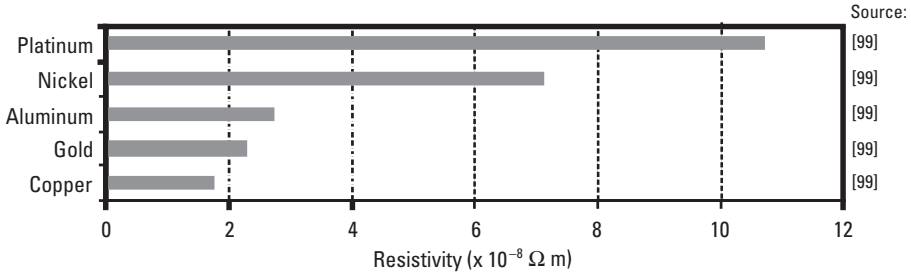

Figure 3.12 Comparison of resistivity for selected metals.

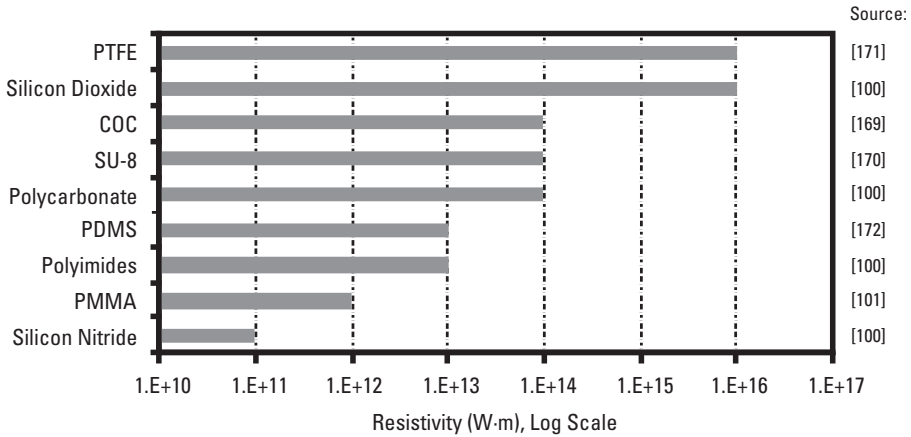

Figure 3.13 Comparison of resistivity for selected nonconducting materials.

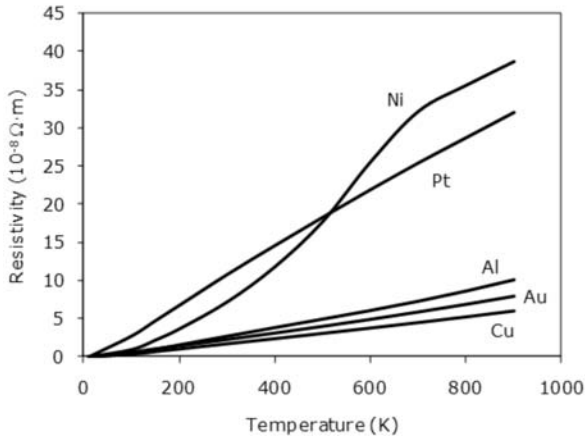

Figure 3.14 Temperature dependence of resistivity for selected metals. (Based on data from [99].)

Conductivity is the inverse of resistivity, defined by $\sigma = 1/\rho$. The SI unit expression for conductivity is siemens per meter (S/m). For the purposes of this book, however, resistivity will be used rather than conductivity.

3.2.3.2 Relative Permittivity

The relative permittivity ε_r of a material (also commonly called the *dielectric constant*) is an indicator of the extent to which a material stores electrical energy. The relative permittivity is dimensionless, because it is the permittivity of the material divided by the permittivity of free space, which is $\varepsilon_0 = 8.854 \times 10^{-12}$ farads per meter. In the case of capacitors, a high value of ε_r corresponds to more effective charge storage. Values for relative permittivity are compared in Figure 3.15.

Although materials with high resistivity tend to have high relative permittivity, the two properties should not be confused because resistivity addresses opposition to current flow while permittivity addresses polarization within the material. Measured values for ε_r depend not only on temperature, but also on the signal frequency used in measurement. Various types of glass have a wide range of values for ε_r depending on composition. Polymers may have different values for relative permittivity depending on molecular weight and degree of crystallinity.

3.2.3.3 Breakdown Voltage

The breakdown voltage V_B of an insulating material (also commonly called the *dielectric strength*) is the voltage at which it fails to continue performing as an electrical insulator. The units are typically expressed as volts per unit length,

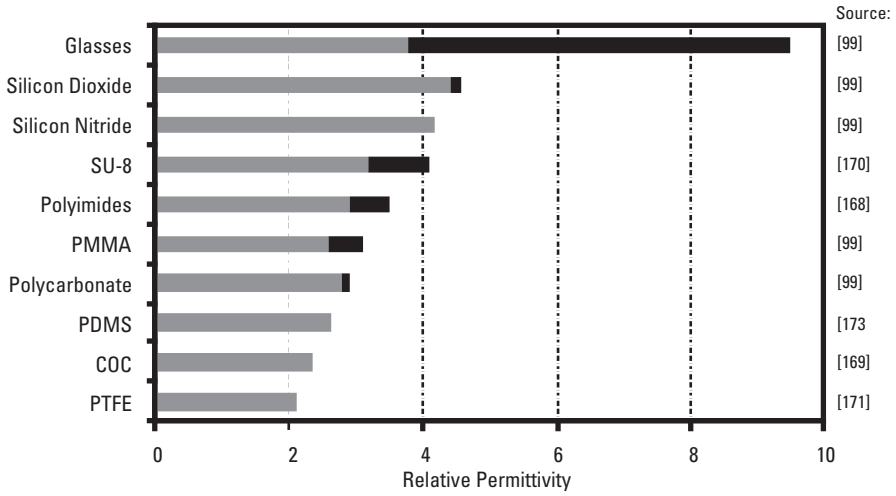

Figure 3.15 Comparison of relative permittivity for selected materials.

with respect to the thickness of the material within the electric field. Accordingly, thin films have higher breakdown voltage than thicker specimens of the same material.

Breakdown voltage is a particularly important parameter for microfluidic components that are subjected to large potential differences, as in the case of electro-osmotic flow for which raw potential difference may be in the range of a few tens of kilovolts. Many common materials have breakdown voltages in the range of a few million to a few hundred million V/m, so for convenience the units of kV/mm are often used, as is the case in Figure 3.16. Fused silica has exceptionally high dielectric strength (470 to 670 kV/mm), which is one of the merits that make it a material of choice for capillary electrophoresis.

3.2.4 Optical Properties

The transparency of glass and many polymers in the visible light region has straightforward benefits in terms of observing events such as fluid filling, gas bubble formation, and so on. A concise way of quantifying transparency is by reporting the percent transmission for the visible region of the spectrum (above 400 nm). Most glass and polymer materials that are considered transparent transmit 90% or more of incident light for thickness on the order of 1 mm.

In microfluidic applications, transparency over a wider range of the spectrum beyond visible light is particularly important for devices based on optical methods such as laser induced fluorescence (LIF) or UV absorption [119, 120]. Laser induced fluorescence is a highly sensitive detection method that excites

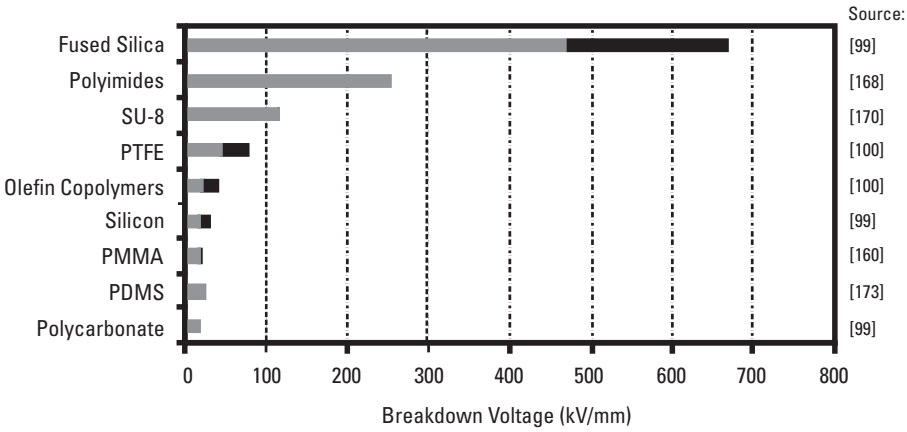

Figure 3.16 Comparison of breakdown voltage for selected materials.

targeted species based on tuned characteristic wavelength and detects the resulting fluorescence in response. With fast speed and fine resolution LIF can be used for applications beyond basic species detection, such as cytometry and three-dimensional flow visualization.

Different applications demand different UV and laser light sources, so the degree to which a material transmits light is typically plotted as a function of wavelength. As shown in Figure 3.17, common glass as used in conventional microscope slides is relatively limited in terms of transmitting lower wavelengths. The region of interest for ultraviolet transmission is below 400 nm, and depending on application it may be highly desirable to transmit for very low wavelength approaching 200 nm. Fused silica is exceptional, with at least 10% transmission for wavelength as low as 120 nm.

Light transmission performance is often reported for samples that are 1 to 3 mm thick, but the lack of uniformity on sample thickness makes it difficult to make head-to-head comparisons without having direct overlay plots of transmission across the spectrum. Furthermore, for most materials, light transmission especially at low wavelength becomes more attenuated with greater material thickness. One option is to specify the lowest wavelength that remains above an arbitrary significance threshold, for a fixed specimen thickness at a constant temperature.

Among optical properties, the index of refraction n is one of the most familiar parameters, and it is defined as the ratio of speed of light in a vacuum to the speed of light in the material. The index of refraction is not constant at all wavelengths, and the Abbe number is a parameter that quantifies the degree of dispersion (i.e., variability in refractive index as a function of wavelength) for transparent materials. A high value of Abbe number indicates low dispersion.

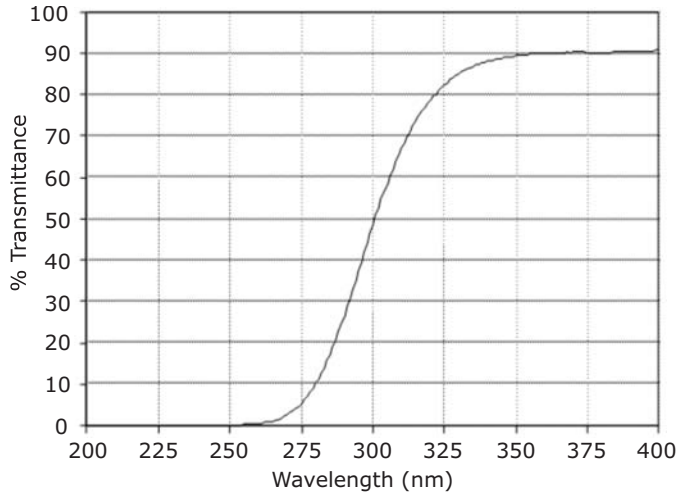

Figure 3.17 Light transmittance through a glass microscope slide, approximately 1 mm thick.

For microfluidic applications based on detecting species with fluorescent markers or stains, the autofluorescence of the chip material is an important factor. Whereas autofluorescence of cells or other targets of interest can be a desirable trait [121], autofluorescence of a particular glass or polymer chip impairs signal-to-noise ratio when imaging with fluorescence microscopy. Comparative study of autofluorescence has shown that a variety of optically clear polymers including PDMS, COC, PMMA, and polycarbonate have sufficiently low autofluorescence to be viable materials for microfluidic chips that are interfaced with fluorescent microscopy [122].

3.2.5 Magnetic Properties

Ferromagnetic materials are those that are significantly influenced by magnetic fields, evidenced in particular by force interaction. The most familiar expression to describe degree of ferromagnetism is magnetic permeability μ, which expresses the effectiveness of magnetic induction with respect to intensity of a magnetic field. In SI units, permeability is expressed in henrys per meter (H/m), and larger values of permeability correspond to greater ability to concentrate magnetic fields in engineering applications. Materials are sometimes characterized nondimensionally in terms of relative permeability, $\mu_r = \mu/\mu_0$, where μ_0 is the (constant) permeability of free space, $4\pi \times 10^{-7}$ H/m. Examples of common metals that exhibit ferromagnetism are nickel, cobalt, and iron. Nickel and nickel alloys are common microfabrication because of established processes such as physical vapor deposition and electroplating (Chapter 7).

3.2.6 Other Physical Properties and Characteristics

The *physical* properties of a material very broadly encompass the properties exhibited by a material without changing the molecules of which it is composed. This is distinguished from chemical properties such as electronegativity and enthalpy of formation, which have relevance only in the context of reactions that change molecular composition. So from a technical perspective, mechanical, thermal, electrical, optical, and magnetic properties can all be considered subsets of physical properties. Other physical properties include density, gas permeability, and water absorption. Hydrophobicity is not a material property per se because it is highly dependent on surface conditions. However, because of its great relevance to microfluidics (as mentioned in the discussion of surface forces in Chapter 1), hydrophobicity is also discussed in this section.

3.2.6.1 Density

Density ρ is defined as the mass per unit volume of a material. It is somewhat unique as a physical property because it does not clearly fall under one of the major categories (mechanical, electrical, optical, and so forth), although it is correlated to many of them (yield strength, resistivity, and transparency). The SI unit expression for density is kg/m^3, although it is common for materials to be described also in terms of g/cm^3 because many solids fall in the range between 1 and 20 g/cm^3. In macroscale engineering, density is often a primary concern because it determines the weight of a device. In microscale, however, weight is typically not a primary concern because of geometric scaling laws as discussed in Chapter 1. The densities of most solids and incompressible liquids are generally far less sensitive to changes in temperature and pressure than gases. However, even the densities of solids can vary as the volume of a fixed mass changes in response to temperature and pressure, and unless otherwise noted density is reported under room temperature conditions with no applied pressure. Figure 3.18 shows density values for some of the more common materials used in microfluidic devices.

Metals not only have the highest raw values for density, but also that they have the widest range of values as well. Considering metals not included in the Figure 3.18, this wide range is even more pronounced, for example with the density of magnesium (1.74 g/cm^3) less than 1/10 that of platinum (21.4 g/cm^3). Silicon (2.33 g/cm^3) and its compounds fall in a more narrow range between 2 and 3 g/cm^3. Most silica-based glasses also fall in a similar range between 2.0 and 2.5 g/cm^3, expectedly near the density of silicon dioxide (2.2 g/cm^3). Values for particular types of glass, however, can vary significantly depend on the fraction of other elements such as boron, sodium, and calcium, as tabulated in comprehensive references for glass properties [123, 124].

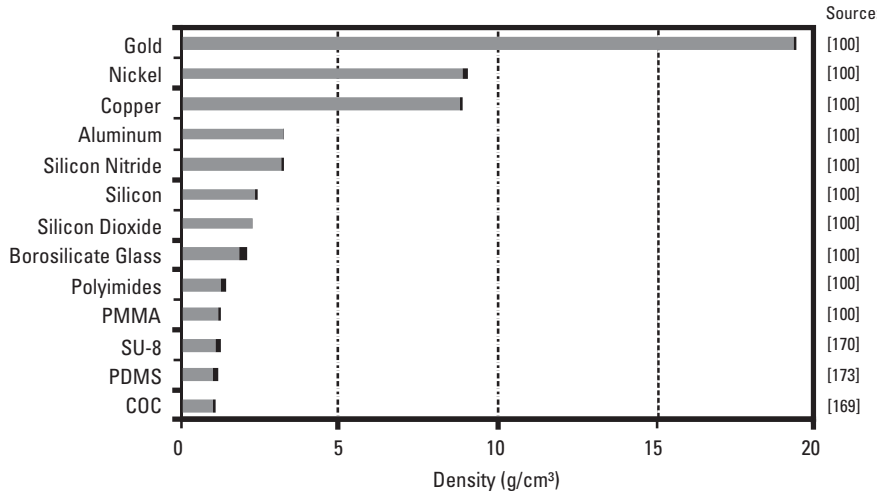

Figure 3.18 Comparison of density for selected materials.

Lead-containing glasses can have density even higher than 7.0 gm/cm^3 because of the high density of lead (11.34 gm/cm^3).

Polymers also have a relatively small range of values for density, generally between 1 and 2 g/cm^3. The density of a given polymer may have a range of values depending on not only composition but also processing state. For example, a dilute formulation of SU-8 in its liquid form can have density below 1.10 g/cm^3, but as carrier solvents evaporate during baking and curing the value can exceed 1.2 g/cm^3. By convention the densities of polymers are sometimes expressed in terms of *specific gravity*, which is the ratio of density of the polymer divided by the density of water (1.0 g/cm^3 at 4°C). ASTM D792 is a standard test method for quantifying the specific gravity of solid plastics [125].

An important quantity that is related to density for polymers is *molecular weight* (MW). Polymers are long chains of molecules, so expressing the molecular weight of polymers is not as simple as reporting the molecular mass of small molecules such as water (18 g/mol). The molecular mass of the repeating unit for a polymer may be straightforward, as in linear polyethylene–CH_2–CH_2–having molecular mass of 28 g/mol. However, a low-density polyethylene (LDPE) product may have average molecular weight near 50,000 g/mol, while high-density polyethylene can have well over 1 million g/mol [102]. Furthermore, the molecular weight for a quantity of polymer is not a single narrow value, but rather a distribution, sometimes scattered across a full order of magnitude. The various properties of polymers (mechanical, optical, chemical, and so forth) depend significantly on molecular weight as well as the

degree of branching. Molecular weight therefore is a factor that can contribute to significant variability in published values for physical and chemical properties.

3.2.6.2 Hydrophobicity

Hydrophobicity describes the lack of affinity toward liquid (typically water), and its converse, *hydophilicity* describes affinity to water. As mentioned previously, hydrophobicity is not a material property but rather a characteristic of a surface. The degree to which a surface is hydrophobic (i.e., nonwetting) or hydrophilic (i.e., wetting) depends on many factors including roughness, charge, and temperature. In some cases, modifications to wetting characteristics are temporary. Plasma treatment is one approach for improving wetting, although the effects may change as surfaces undergo hydrophobic recovery [126]. A quantitative parameter to express degree of hydrophobicity is contact angle (Chapter 1), often conveniently measured using a sessile drop technique [127]. Contact angle depends on all three material phases in contact, typically a solid surface, a liquid volume, and air. Deinonized water is a convenient benchmark for comparing different material surfaces.

3.2.6.3 Water Absorption

Water absorption is generally undesirable for microfluidic applications because it compromises deterministic control over liquid volume and fluid flow. It may also result in swelling and distortion of geometric features within the device structure. Water absorption is typically quantified by a percent absorbed over a fixed time, and the ISO 62 and ASTM D570 standards designate a 24-hour period. Polymers are generally subject to greatest concern, and some examples are compared in Figure 3.19.

Gas permeability may also be a concern in microfluidic applications [128]. Metals and glasses generally have negligible gas permeability, but all polymers are to some degree gas permeable. While low gas permeability may be in general desirable, in some cases microfluidic devices take advantage of permeability. For example, the relatively high gas permeability of PDMS makes it possible to use it for removing gas bubbles [129] or for flow control by taking advantage of gas diffusion through a thin membrane [130].

3.2.7 Chemical Resistance

Materials such as PDMS and COC are favorable for microfluidics because of good solvent compatibility [131]. Chemical resistance can roughly be categorized in terms of compatibility against acids, alkalis, and organic solvents. Many comparison tables offer only qualitative comparisons among materials, with ratings such as excellent, good, fair, and poor. Some manufacturers and

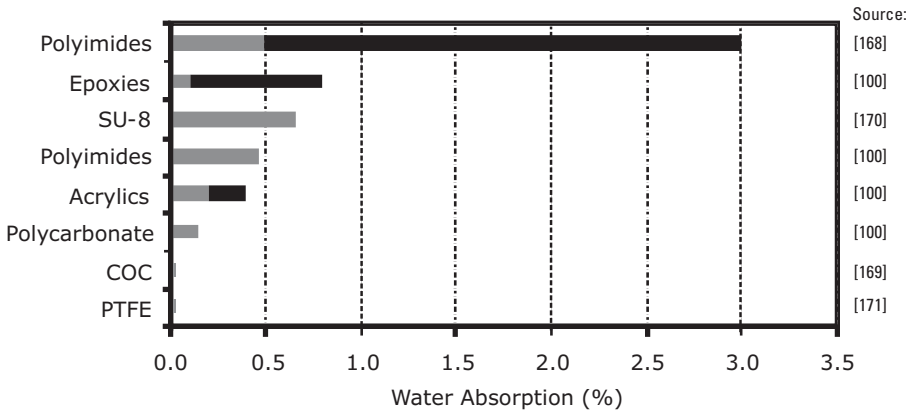

Figure 3.19 Comparison of water absorption for selected materials.

distributors of commercial fluidic components offer more extensive online references for chemical compatibility limitations and other properties [132, 133]. One quantitative but imperfect way to quantify chemical resistance of a material is to measure the change in mass when subjected to a particular chemical environment for a specified duration. Materials that exhibit insignificant mass change are assessed as being resilient to the corresponding chemical. The topic of chemical resistance presents a helpful transition into the next section that addresses not properties per se, but rather surface conditions that can —and often are—customized to meet various functional requirements in microfluidics.

3.3 Surface Conditions

Surface conditions are extremely relevant to almost all aspects of microfluidics. Plasma treatment is one of the most versatile approaches [134, 135], but other methods including chemical surface treatments [136] and laser irradiation are also used. As identified in the discussion of scaling phenomena in Chapter 1, surface forces and interactions become more influential than body forces and bulk interactions as dimensional scale decreases. Earlier sections of this chapter focused primarily on bulk properties such as melting point, elastic moduli, and electrical resistivity, but microfluidic functionality is often more heavily influenced by surface conditions. Examples of surface conditions are electrical charge density and hydrophobicity. A key point to emphasize is that these are not properties and are not constant with time. However, in many instances the surface conditions have more profound influence on microfluidic functionality

than material properties themselves. The particular selection of materials and fabrication processes will set a starting point for determining surface conditions, but often deliberate surface engineering is required to achieve intended functionality. The remaining discussion offers some of the reasons for altering surface conditions and cites some examples in which surfaces are modified to serve functional purposes.

In terms of liquid-solid interaction, wetting behavior in terms of either hydrophobic or hydrophilic nature is a dominant concern. There are several different ways in which wetting characteristics can be altered. The concept of electrowetting was introduced in Chapter 1. In microfabrication, two common ways of altering wetting characteristics are by plasma treatment (plasmas are discussed further in Chapter 6) or by liquid surfactants. Figure 3.20 [137] illustrates the effect of different surfactant concentrations on the contact angle of a liquid droplet.

For applications such as immobilization of biomolecules, it may be desirable to maintain a hydrophilic surface. Hydrophilicity also eases the filling of narrow channels, whereas hydrophobic surfaces can make operations such as filling more difficult. For microchannel filling, it is not unusual to begin with a priming liquid that fills channels more easily, followed by switching to the final liquid of interest once surface tension barriers have been reduced.

Although the hydrophobic/hydrophilic surface behavior or materials such as PDMS can be modified for various functional benefits such as improved performance in microchip electrophoresis [138], an important point to note is that wetting characteristics can often be dynamic and change with time. For example, surface-treated PDMS is known to exhibit what is called hydrophobic recovery over time [139, 140]. Introducing nanoscale roughness to the surface

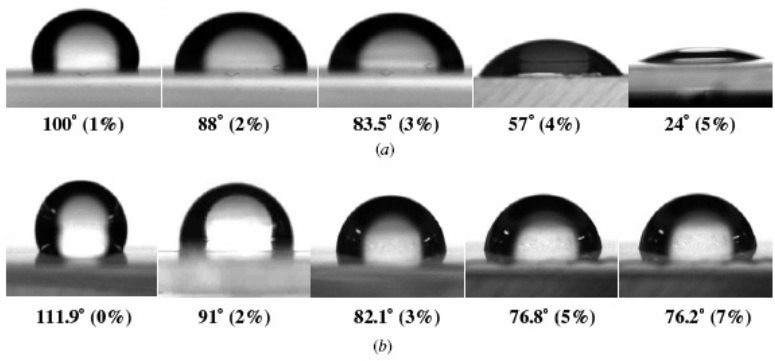

Figure 3.20 (a, b) Dependence of contact angle on the concentration of surfactant on an adhesive-coated surface. (Reprinted from [137], with permission from IOP Publishing.)

of PDMS by SF_6 plasma treatment has been shown to delay hydrophobic recovery, as the increased surface area promotes hydrophilic behavior [141]. Cyclic olefin polymers also must be oxidized to support electro-osmotic flow, and effects of the oxidation treatment also changes over time [142]. Although controlling the storage environment is one strategy for slowing hydrophobic recovery, plasma exposure conditions are reported to be more significant than subsequent storage conditions (e.g., air, water, or hexadecane) [143].

Studies on a variety of polymers including PTFE, PMMA, and polypropylene reveal that the relationship between surface roughness and contact angle can be related to the nature of equilibrium contact angle on smooth surfaces. Increasing roughness reduces contact angle for inherently hydrophilic surfaces but increases contact angle for inherently hydrophobic surfaces [144].

Flow behavior also depends on surface roughness. For example, molecular dynamics simulation suggests that when the roughness is comparable to the thickness of the electrical double-layer at the wall interface, even subnanometer changes in topography can reduce electro-osmotic flow significantly [145]. Wall roughness alters the friction characteristics of fluid flow. For very small channel dimensions (e.g., a few tens of microns in diameter) the relative magnitude of roughness features can be large compared to channel dimensions, leading to nonuniform cross-sections that may result in deviations from otherwise accurate predictive models for microchannel flow [146]. As discussed in Chapter 2, the degree of roughness is influenced by the method of fabrication (e.g., chemical etching versus laser ablation). In some cases the objective may be to smooth an otherwise rough surface. In the case of laser machined thermoplastics, roughness can be reduced by annealing [147].

In other cases it may be desirable to increase surface roughness, either to alter flow velocity or to provide more surface area for stationary-phase interactions with analytes in the fluid [148]. An example of altering surface topography by stress mechanisms is the wrinkling of PDMS upon oxidation. When the top surface of PDMS is oxidized by oxygen plasma treatment and subject to temperature differences, for example, the difference in thermomechanical response causes surface wrinkling to occur, as illustrated in Figure 3.21 [149].

Increasing the surface area may or may not enhance surface-to-surface adhesion between substrates, depending on the severity of deviation from flatness. Rougher surfaces tend to have larger surface area, but if roughness is severe the real contact area between surfaces can be reduced rather than enhanced. Although conventional perception may suggest that it is desirable to have large magnitude of real contact area, it has been shown that real contact perimeter is the more fundamental geometric parameter that affects adhesion [150].

Apart from engineering the surface roughness, there are other basic ways of improving adhesion or for preventing it. Plasma surface modification is one of the most versatile (and clean) methods of improving adhesion, especially for

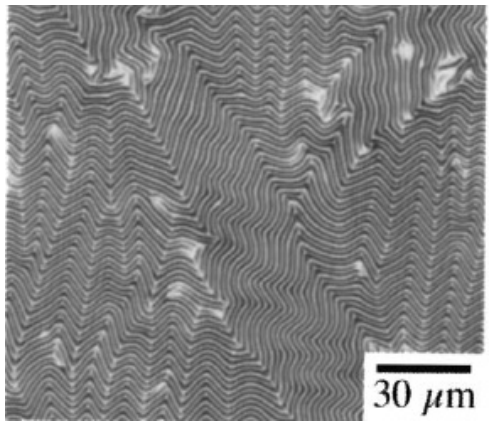

Figure 3.21 Wrinkled surface with ordered undulations caused by oxidation of an elastomeric polymer. (Reprinted with permission from [149]. Copyright 1999, American Institute of Physics.)

polymers [151], and some common reasons for enhancing adhesion would be to improve bond strength between plastic substrates [152] or to provide reliable adhesion of a deposited thin-film metal [153]. Surface-to-surface adhesion behavior differs depending on medium. For example, one type of surface coating might cause structures to exhibit greater adhesion in air than in water, yet have opposite effects if the surface condition is different. This has been the case observed for polysilicon beams in air and various liquids [154]. A reason for inhibiting adhesion would be to facilitate the release of microscale structures [155]. In soft lithography casting (Chapter 5), a release film is routinely needed to allow separation of the cast material from its mold [156].

In analytical chemistry applications, surface engineering can be an important tool for activating a surface to promote or catalyze chemical reactions, or for passivating the surface to prevent unwanted chemical reactions and analyte-wall interactions [157]. Stable coatings such as dimethylacrylamide have been used for achieving high separation efficiency for detection of proteins and peptides for capillary electrophoresis [158]. Polymers such as PDMS, however, are gas permeable and over time even liquids can diffuse into the material. One way to block such diffusion is by a glassy coating [159]. Surface treatments and coatings can also affect the interaction of channel materials and fluids in other ways, such as changing the *zeta potential*, which is a characteristic parameter that that dictates mobility in electro-osmotic flow [160, 161].

Surface engineering can serve biological applications by functionalizing a surface to promote biomolecule binding [162] or modifying it to assure prevention of unwanted adsorption [163, 164]. Surface modification plays an important role in addressing biocompatibility issues, in particular for devices that

must be physiologically integrated [165]. Surface coatings can also have a profound effect on flow velocity, and the effect can differ depending on type of fluid. For example, fluid velocity of water in silicon/glass microchannels was increased by a factor of 10 when coated with plasma polymerization of acrylic acid, yet decreased for a blood/water mixture. The decrease in flow velocity for the blood/water mixture suggests a possibility of cell interaction with the highly functionalized surfaces [166].

Surface engineering is so important to microfluidics that this discussion could continue indefinitely, and numerous books have been written on the subject of surface engineering for polymer science, analytical chemistry, biomedical devices, electrochemistry, and so on. The discussion above provides just a sampling of various ways in which surface engineering is relevant to microfluidics and—succumbing to an irresistible pun here—this discussion only begins to scratch the surface. With the importance of surface conditions conveyed and a few examples mentioned, the next set of chapters will proceed to focus on the methods that are actually used to fabricate three-dimensional geometric structures, without losing appreciation for the fact that the resulting surface conditions of those processes almost always have significant impact on microfluidic functionality.

References

[1] Becker, H., and C. Gartner, "Polymer Microfabrication Technologies for Microfluidic Systems," *Analytical and Bioanalytical Chemistry*, Vol. 390, No. 1, 2008, pp. 89–111.

[2] Ruprecht, R., et al., "Polymer Materials for Microsystem Technologies," *Microsystem Technologies*, Vol. 5, No. 1, 1998, pp. 44–48.

[3] Heckele, M., and W. K. Schomburg, "Review on Micro Molding of Thermoplastic Polymers," *Journal of Micromechanics and Microengineering*, Vol. 14, No. 3, 2004, pp. R1–R14.

[4] Kameoka, J., et al., "A Polymeric Microfluidic Chip for CE/MS Determination of Small Molecules," *Analytical Chemistry*, Vol. 73, No. 9, 2001, pp. 1935–1941.

[5] Nielsen, T., et al., "Nanoimprint Lithography in the Cyclic Olefin Copolymer, Topas, a Highly Ultraviolet-Transparent and Chemically Resistant Thermoplast," *Journal of Vacuum Science and Technology B: Microelectronics and Nanometer Structures*, Vol. 22, No. 4, 2004, pp. 1770–1775.

[6] Khanarian, G., and H. Celanese, "Optical Properties of Cyclic Olefin Copolymer," *Optical Engineering*, Vol. 40, No. 6, 2001, pp. 1024–1029.

[7] Sia, S. K., and G. M. Whitesides, "Microfluidic Devices Fabricated in Poly(Dimethylsiloxane) for Biological Studies," *Electrophoresis*, Vol. 24, No. 21, 2003, pp. 3563–3576.

[8] Gevers, L. E. M., I. F. J. Vankelecom, and P. A. Jacobs, "Solvent-Resistant Nanofiltration with Filled Polydimethylsiloxane (PDMS) Membranes," *Journal of Membrane Science*, Vol. 278, No. 1-2, 2006, pp. 199–204.

[9] Xia, Y., and G. M. Whitesides, "Soft Lithography," *Annual Review of Materials Science*, Vol. 28, No. 1, 1998, pp. 153–184.

[10] Yin, H. L., et al., "A Novel Electromagnetic Elastomer Membrane Actuator with a Semi-Embedded Coil," *Sensors and Actuators A: Physical*, Vol. 139, No. 1-2, 2007, pp. 194–202.

[11] Garra, J., et al., "Dry Etching of Polydimethylsiloxane for Microfluidic Systems," *Journal of Vacuum Science and Technology A*, Vol. 20, No. 3, 2002, pp. 975–982.

[12] Cong, H., and T. Pan, "Photopatternable Conductive PDMS Materials for Microfabrication," *Advanced Functional Materials*, Vol. 18, No. 13, 2008, pp. 1912–1921.

[13] Ng, J. M. K., et al., "Components for Integrated Poly(Dimethylsiloxane) Microfluidic Systems," *Electrophoresis*, Vol. 23, No. 20, 2002, pp. 3461–3473.

[14] Unger, M. A., et al., "Monolithic Microfabricated Valves and Pumps by Multilayer Soft Lithography," *Science*, Vol. 288, No. 5463, 2000, pp. 113–116.

[15] Lee, S. J., et al., "Characterization of Laterally Deformable Elastomer Membranes for Microfluidics," *Journal of Micromechanics and Microengineering*, Vol. 17, No. 5, 2007, pp. 843–851.

[16] Yu, Y. -S., and Y. -P. Zhao, "Deformation of PDMS Membrane and Microcantilever by a Water Droplet: Comparison Between Mooney–Rivlin and Linear Elastic Constitutive Models," *Journal of Colloid and Interface Science*, Vol. 332, No. 2, 2009, pp. 467–476.

[17] Lorenz, H., et al., "SU-8: A Low-Cost Negative Resist for MEMS," *Journal of Micromechanics and Microengineering*, Vol. 7, No. 3, 1997, pp. 121–124.

[18] Zhang, J., M. B. Chan-Park, and S. R. Conner, "Effect of Exposure Dose on the Replication Fidelity and Profile of Very High Aspect Ratio Microchannels in SU-8," *Lab on a Chip*, Vol. 4, No. 6, 2004, pp. 646–653.

[19] Sato, H., et al., "An All SU-8 Microfluidic Chip with Built-In 3D Fine Microstructures," *Journal of Micromechanics and Microengineering*, Vol. 16, No. 11, 2006, pp. 2318–2322.

[20] Ezkerra, A., et al., "Fabrication of SU-8 Free-Standing Structures Embedded in Microchannels for Microfluidic Control," *Journal of Micromechanics and Microengineering*, Vol. 17, No. 11, 2007, pp. 2264–2271.

[21] Chung, C., and M. Allen, "Uncrosslinked SU-8 as a Sacrificial Material," *Journal of Micromechanics and Microengineering*, Vol. 15, No. 1, 2005, pp. 1–5.

[22] Kim, S. -J., et al., "Study of SU-8 to Make a Ni Master-Mold: Adhesion, Sidewall Profile, and Removal," *Electrophoresis*, Vol. 27, No. 16, 2006, pp. 3284–3296.

[23] Chen, H., and C. Fu., "An Investigation into the Characteristics of Deep Reactive Ion Etching of Quartz Using SU-8 as a Mask," *Journal of Micromechanics and Microengineering*, Vol. 18, No. 10, 2008, p. 105001.

[24] Saragih, A. S., and T. J. Ko, "A Thick SU-8 Mask for Microabrasive Jet Machining on Glass," *International Journal of Advanced Manufacturing Technology*, Vol. 41, No. 7-8, 2009, pp. 734–740.

[25] Duffy, D. C., et al., "Rapid Prototyping of Microfluidic Switches in Poly(Dimethyl Siloxane) and Their Actuation by Electro-Osmotic Flow," *Journal of Micromechanics and Microengineering*, Vol. 9, No. 3, 1999, pp. 211–217.

[26] Sikanen, T., et al., "Characterization of SU-8 for Electrokinetic Microfluidic Applications," *Lab on a Chip*, Vol. 5, No. 8, 2005, pp. 888–896.

[27] Cheng, J. -Y., et al., "Direct-Write Laser Micromachining and Universal Surface Modification of PMMA for Device Development," *Sensors and Actuators, B: Chemical*, Vol. 99, No. 1, 2004, pp. 186–196.

[28] Chen, R., et al., "Determination of EOF of PMMA Microfluidic Chip by Indirect Laser-Induced Fluorescence Detection," *Sensors and Actuators B: Chemical*, Vol. 114, No. 2, 2006, pp. 1100–1107.

[29] Nugen, S. R., et al., "PMMA Biosensor for Nucleic Acids with Integrated Mixer and Electrochemical Detection," *Biosensors and Bioelectronics*, Vol. 24, No. 8, 2009, pp. 2428–2433.

[30] Shiu, P. P., et al., "Rapid Fabrication of Tooling for Microfluidic Devices Via Laser Micromachining and Hot Embossing," *Journal of Micromechanics and Microengineering*, Vol. 18, No. 2, 2008, p. 025012.

[31] Bilenberg, B., et al., "PMMA to SU-8 Bonding for Polymer Based Lab-on-a-Chip Systems with Integrated Optics," *Journal of Micromechanics and Microengineering*, Vol. 14, No. 6, 2004, pp. 814–818.

[32] Dukkipati, V. R., and S. W. Pang, "Integration of Electrodes in Si Channels Using Low Temperature Polymethylmethacrylate Bonding," *Journal of Vacuum Science and Technology B: Microelectronics and Nanometer Structures*, Vol. 25, No. 2, 2007, pp. 368–372.

[33] Wilson, D., H. D. Stenzenberger, and P. M. Hergenrother, *Polyimides*, New York: Chapman and Hall, 1990.

[34] Xiao, S. Y., et al., "A Novel Fabrication Process of MEMS Devices on Polyimide Flexible Substrates," *Microelectronic Engineering*, Vol. 85, No. 2, 2008, pp. 452–457.

[35] Moss, E. D., A. Han, and A. B. Frazier, "A Fabrication Technology for Multi-Layer Polymer-Based Microsystems with Integrated Fluidic and Electrical Functionality," *Sensors and Actuators B: Chemical*, Vol. 121, No. 2, 2007, pp. 689–697.

[36] Buder, U., J. P. von Klitzing, and E. Obermeier. "Reactive Ion Etching for Bulk Structuring of Polyimide," *Sensors and Actuators A: Physical*, Vol. 132, No. 1, 2006, pp. 393–399.

[37] Nguyen, L. T. T., H. N. Nguyen, and T. H. T. La, "Synthesis and Characterization of a Photosensitive Polyimide Precursor and Its Photocuring Behavior for Lithography Applications," *Optical Materials*, Vol. 29, No. 6, 2007, pp. 610–618.

[38] Yin, H., et al., "Compilation and Indexing Terms, Microfluidic Chip for Peptide Analysis with an Integrated HPLC Column, Sample Enrichment Column, and Nanoelectrospray Tip," *Analytical Chemistry*, Vol. 77, No. 2, 2005, pp. 527–533.

[39] Bhansali, S., et al., "Resolving Chemical/Bio-Compatibility Issues in Microfluidic MEMS Systems," *Proceedings of the SPIE*, Vol. 3877, 1999.

[40] Steigert, J., et al., "Rapid Prototyping of Microfluidic Chips in COC," *Journal of Micromechanics and Microengineering*, Vol. 17, No. 2, 2007, pp. 333–341.

[41] Chang, W. Y., C. -H. Chu, and Y. -C. Lin, "A Flexible Piezoelectric Sensor for Microfluidic Applications Using Polyvinylidene Fluoride," *IEEE Sensors Journal*, Vol. 8, No. 5, 2008, pp. 495–500.

[42] Xia, F., S. Tadigadapa, and Q. M. Zhang, "Electroactive Polymer Based Microfluidic Pump," *Sensors and Actuators A: Physical*, Vol. 125, No. 2, 2006, pp. 346–352.

[43] Dae, S. Y., et al., "A Microfluidic Gel Valve Device Using Reversible Sol-Gel Transition of Methyl Cellulose for Biomedical Application," *Microsystem Technologies*, Vol. 12, No. 3, 2006, pp. 238–246.

[44] Selvaganapathy, P., E. T. Carlen, and C. H. Mastrangelo, "Electrothermally Actuated Inline Microfluidic Valve," *Sensors and Actuators, A: Physical*, Vol. 104, No. 3, 2003, pp. 275–282.

[45] Boden, R., et al., "A Polymeric Paraffin Actuated High-Pressure Micropump," *Sensors and Actuators A: Physical*, Vol. 127, No. 1, 2006, pp. 88–93.

[46] Lee, S. J., et al., "Polymethylhydrosiloxane (PMHS) as a Functional Material for Microfluidic Chips," *Journal of Micromechanics and Microengineering*, Vol. 18, No. 2, 2008, p. 025026.

[47] Armani, D. K., and C. Liu, "Microfabrication Technology for Polycaprolactone, a Biodegradable Polymer," *Journal of Micromechanics and Microengineering*, Vol. 10, No. 1, 2000, pp. 80–84.

[48] Campbell, S. A., *Fabrication Engineering at the Micro- and Nanoscale*, 3rd ed., New York: Oxford University Press, 2008.

[49] Ho, C. -M., and Y. -C. Tai, "Review: MEMS and Its Applications for Flow Control," *Journal of Fluids Engineering, Transactions of the ASME*, Vol. 118, No. 3, 1996, pp. 437–446.

[50] Petersen, K. E., "Silicon as a Mechanical Material," *Proceedings of the IEEE*, Vol. 70, No. 5, 1982, pp. 420–457.

[51] Kovacs, G. T. A., *Micromachined Transducers Sourcebook*, New York: McGraw-Hill, 1998.

[52] Smith, W. F., *Foundations of Materials Science and Engineering*, 2nd ed., New York: McGraw-Hill, 1993.

[53] Won, I. J., et al., "Surface Micromachined Electrostatic Diaphragm Micropump," *Proceedings of the SPIE*, Vol. 3891, 1999.

[54] Jang, W. I., et al., "Surface Micromachined Thermally Driven Micropump," *Sensors and Actuators, A: Physical*, Vol. 115, No. 1, 2004, pp. 151–158.

[55] Sathaye, A., and A. Lal, "An Ultrasonic Micromachined Integrated Capacitive Sensor for Biological Sample Preparation on a Microfluidic Platform," *Proceedings of the IEEE Ultrasonics Symposium*, Vol. 1, 2003, pp. 1062–1065.

[56] Tuantranont, A., et al., "Symmetrical polyMUMPs-Based Piezoresistive Microcantilever Sensors with On-Chip Temperature Compensation for Microfluidics Applications," *IEEE Sensors Journal*, Vol. 8, No. 5, 2008, pp. 543–547.

[57] Barret, S., et al., "Porous Silicon as a Material in Microsensor Technology," *Sensors and Actuators A: Physical*, Vol. 33, No. 1-2, 1992, pp. 19–24.

[58] Camara, E. H. M., et al., "Microfluidic Channels in Porous Silicon Filled with a Carbon Absorbent for Gas Preconcentration," *TRANSDUCERS and EUROSENSORS '07, 4th International Conference on Solid-State Sensors, Actuators and Microsystems*, Lyon, France, 2007.

[59] Low, S. P., et al., "Evaluation of Mammalian Cell Adhesion on Surface-Modified Porous Silicon," *Biomaterials*, Vol. 27, No. 26, 2006, pp. 4538–4546.

[60] Coffer, J. L., et al., "Porous Silicon-Based Scaffolds for Tissue Engineering and Other Biomedical Applications," *4th International Conference on Porous Semiconductors-Science and Technology*, Vol. 202, 2005.

[61] http://www.micralyne.com/.

[62] http://www.micronit.com/.

[63] Pollack, M. G., A. D. Shenderov, and R. B. Fair, "Electrowetting-Based Actuation of Droplets for Integrated Microfluidics," *Lab on a Chip*, Vol. 2, No. 2, 2002, pp. 96–101.

[64] Vulto, P., et al., "A Full-Wafer Fabrication Process for Glass Microfluidic Chips with Integrated Electroplated Electrodes by Direct Bonding of Dry Film Resist," *Journal of Micromechanics and Microengineering*, Vol. 19, No. 7, 2009, p. 077001.

[65] Cozma, A., and B. Puers, "Characterization of the Electrostatic Bonding of Silicon and Pyrex Glass," *Journal of Micromechanics and Microengineering*, Vol. 5, No. 2, 1995, pp. 98–102.

[66] Zhang, J., and T. H. Gong, "Micromachining Technologies for Capillary Electrophoresis Utilizing Pyrex Glass Etching and Bonding," *Proceedings of the SPIE—The International Society for Optical Engineering*, Vol. 4174, 2000.

[67] Park, J. H., et al., "Deep Dry Etching of Borosilicate Glass Using SF6 and SF6/Ar Inductively Coupled Plasmas," *Microelectronic Engineering*, Vol. 82, No. 2, 2005, pp. 119–128.

[68] Malek, C. K., et al., "Deep Microstructuring in Glass for Microfluidic Applications," *Microsystem Technologies*, Vol. 13, No. 5-6, 2007, pp. 447–453.

[69] Chen, H., and C. Fu, "An Investigation into the Characteristics of Deep Reactive Ion Etching of Quartz Using SU-8 as a Mask," *Journal of Micromechanics and Microengineering*, Vol. 18, No. 10, 2008, p. 105001.

[70] Diepold, T., and E. Obermeier, "Smoothing of Ultrasonically Drilled Holes in Borosilicate Glass by Wet Chemical Etching," *Journal of Micromechanics and Microengineering*, Vol. 6, No. 1, 1996, pp. 29–32.

[71] Ben-Yakar, A., and R. L. Byer, "Femtosecond Laser Machining of Fluidic Microchannels for Miniaturized Bioanalytical Systems," *SPIE-Int. Soc. Opt. Eng.*, Vol. 4637, 2002.

[72] Dietrich, T. R., et al., "Fabrication Technologies for Microsystems Utilizing Photoetchable Glass," *Microelectronic Engineering*, Vol. 30, No. 1-4, 1996, pp. 497–504.

[73] Moyer, P. J., et al., "Applications of Spin-on-Glass for Waveguide and Micro-Optical Systems," *Proceedings of SPIE—The International Society for Optical Engineering*, Vol. 4984, San Jose, CA, 2003.

[74] Krishnaswamy, M., et al., "Formation of Hollow Glass Microcylinders of Silica," *Proceedings of SPIE—The International Society for Optical Engineering*, Vol. 3211, Madras, India, 1998.

[75] Lee, H., A. M. Purdon, and R. M. Westervelt, "Manipulation of Biological Cells Using a Microelectromagnet Matrix," *Applied Physics Letters*, Vol. 85, No. 6, 2004, pp. 1063–1065.

[76] Kang, S. -W., S. -H. Tsai, and M. -H. Ko, "Metallic Micro Heat Pipe Heat Spreader Fabrication," *Applied Thermal Engineering*, Vol. 24, No. 2-3, 2004, pp. 299–309.

[77] Boden, R., et al., "A Metallic Micropump for High-Pressure Microfluidics," *Journal of Micromechanics and Microengineering*, Vol. 18, No. 11, 2008, p. 115009.

[78] Lu, L. -H., K. S. Ryu, and C. Liu, "A Magnetic Microstirrer and Array for Microfluidic Mixing," *Journal of Microelectromechanical Systems*, Vol. 11, No. 5, 2002, pp. 462–469.

[79] Pan, T., et al., "A Magnetically Driven PDMS Micropump with Ball Check-Valves," *Journal of Micromechanics and Microengineering*, Vol. 15, No. 5, 2005, pp. 1021–1026.

[80] Fu, C., Z. Rummler, and W. Schomburg, "Magnetically Driven Micro Ball Valves Fabricated by Multilayer Adhesive Film Bonding," *Journal of Micromechanics and Microengineering*, Vol. 13, No. 4, 2003, pp. 96–102.

[81] Gaspar, A., et al., "Magnetically Controlled Valve for Flow Manipulation in Polymer Microfluidic Devices," *Microfluidics and Nanofluidics*, Vol. 4, No. 6, 2008, pp. 525–531.

[82] Benard, W. L., et al., "Thin-Film Shape-Memory Alloy Actuated Micropumps," *Journal of Microelectromechanical Systems*, Vol. 7, No. 2, 1998, pp. 245–251.

[83] Vyawahare, S., et al., "Electronic Control of Elastomeric Microfluidic Circuits with Shape Memory Actuators," *Lab on a Chip*, Vol. 8, No. 9, 2008, pp. 1530–1535.

[84] Schneider, M., H. Mohwald, and S. Akari, "Quantitative Measurement of Chromium's Ability to Promote Adhesion," *Journal of Adhesion*, Vol. 79, No. 6, 2003, pp. 597–607.

[85] Siewell, G. L., W. R. Boucher, and P. H. McClelland, "The ThinkJet Orifice Plate: A Part with Many Functions," *Hewlett-Packard Journal*, Vol. 36, No. 5, 1985, pp. 33–37.

[86] Papautsky, I., et al., "A Low-Temperature IC-Compatible Process for Fabricating Surface-Micromachined Metallic Microchannels," *Journal of Microelectromechanical Systems*, Vol. 7, No. 2, 1998, pp. 267–273.

[87] Hakamada, M., et al., "Microfluidic Flows in Metallic Microchannels Fabricated by the Spacer Method," *Journal of Micromechanics and Microengineering*, Vol. 18, No. 7, 2008, p. 075029.

[88] Shiu, P. P., et al., "Rapid Fabrication of Tooling for Microfluidic Devices Via Laser Micromachining and Hot Embossing," *Journal of Micromechanics and Microengineering*, Vol. 18, No. 2, 2008, p. 025012.

[89] Hamblin, M. N., et al., "Electroosmotic Flow in Vapor Deposited Silicon Dioxide and Nitride Microchannels," *Biomicrofluidics*, Vol. 1, No. 3, 2007, p. 034101-1.

[90] Galambos, P., et al., "Silicon Nitride Membranes for Filtration and Separation," *Proceedings of the SPIE*, Vol. 3877, 1999.

[91] Hamblin, M. N., et al., "Electroosmotic Flow in Vapor Deposited Silicon Dioxide and Nitride Microchannels," *Biomicrofluidics*, Vol. 1, No. 3, 2007, p. 034101-1.

[92] Gallis, S., et al., "Thermal Chemical Vapor Deposition of Silicon Carbide Films as Protective Coatings for Microfluidic Structures," *Materials Research Society Symposium*, Warrendale, PA, 2003.

[93] Aura, S., et al., "Novel Hybrid Material for Microfluidic Devices," *Sensors and Actuators B: Chemical*, Vol. 132, No. 2, 2008, pp. 397–403.

[94] Schindler, K., and A. Roosen, "Manufacture of 3D Structures by Cold Low Pressure Lamination of Ceramic Green Tapes," *Journal of the European Ceramic Society*, Vol. 29, No. 5, 2009, pp. 899–904.

[95] Kuo, C.-W., et al., "Monolithic Integration of Well-Ordered Nanoporous Structures in the Microfluidic Channels for Bioseparation," *Journal of Chromatography A*, Vol. 1162, No. 2, 2007, pp. 175–179.

[96] Doll, A., et al., "Characterization of Active Silicon Microvalves with Piezoelectric Membrane Actuators," *Microelectronic Engineering*, Vol. 84, No. 5-8, 2007, pp. 1202–1206.

[97] Chen, S. C., C. H. Cheng, and Y. C. Lin, "Analysis and Experiment of a Novel Actuating Design with a Shear Mode PZT Actuator for Microfluidic Application," *Sensors and Actuators, A: Physical*, Vol. 135, No. 1, 2007, pp. 1–9.

[98] Richter, A., et al., "Electronically Controllable Microvalves Based on Smart Hydrogels: Magnitudes and Potential Applications," *Journal of Microelectromechanical Systems*, Vol. 12, No. 5, 2003, pp. 748–753.

[99] Lide, D. R., *CRC Handbook of Chemistry and Physics*, 90th ed., Boca Raton, FL: CRC Press, 2009.

[100] Shackelford, J. F., and A. William, (eds.), *CRC Materials Science and Engineering Handbook*, 3rd ed., Boca Raton, FL: CRC Press, 2001.

[101] Kreith, F., and D. Y. Goswami, (eds.), *CRC Handbook of Mechanical Engineering*, 2nd ed., Boca Raton, FL: CRC Press, 2005.

[102] Mark, J. E., (ed.), *Polymer Data Handbook*, New York: Oxford University Press, 1999.

[103] Gervais, T., et al., "Flow-Induced Deformation of Shallow Microfluidic Channels," *Lab on a Chip*, Vol. 6, No. 4, 2006, pp. 500–507.

[104] Choi, S., and J.-K. Park, "Tuneable Hydrophoretic Separation Using Elastic Deformation of Poly(Dimethylsiloxane)," *Lab on a Chip*, Vol. 9, 2009, pp. 1962–1965.

[105] Magonov, S. N., "Probing Mechanical Properties of Polymers with AFM," *Proceedings of the American Chemical Society, Polymer Preprints, Division of Polymer Chemistry*, Vol. 37, 1996, pp. 597–598.

[106] Al-Halhouli, A. T., et al., "Nanoindentation Testing of SU-8 Photoresist Mechanical Properties," *Microelectronic Engineering*, Vol. 85, No. 5-6, 2008, pp. 942–944.

[107] Riddell, M. N., "Guide to Better Testing of Plastics," *Plastics Engineering*, Vol. 30, 1974, pp. 71–78.

[108] Imai, Y., and I. M. Ward, "A Study of Craze Deformation in the Fatigue Fracture of Polymethylmethacrylate," *J. Mater. Sci.*, Vol. 20, November 1985, pp. 3842–3852.

[109] Mackay, M. E., T. Teng, and J. M. Schultz, "Craze Roles in the Fatigue of Polycarbonate," *J. Mater. Sci.*, Vol. 14, January 1979, pp. 221–227.

[110] Mandell, J. F., and J. -F. Chevaillier, "Craze Initiation, Crack Growth, and Lifetime Trends in Fatigue of Poly(Vinylchloride)," *Polym. Eng. Sci.*, Vol. 25, February 1985, pp. 170–177.

[111] Srikar, V. T., and S. M. Spearing, "Materials Selection for Microfabricated Electrostatic Actuators," *Sens Actuators A Phys*, Vol. 102, 2003, pp. 279–285.

[112] Sparks, D. R., M. I. Chia, and G. Q. Jiang, "Cyclic Fatigue and Creep of Electroformed Micromachines," *Sensors and Actuators A: Physical*, Vol. 95, 2001, pp. 61–68.

[113] Muhlstein, C. L., S. B. Brown, and R. O. Ritchie, "High-Cycle Fatigue and Durability of Polycrystalline Silicon Thin Films in Ambient Air," *Sensors and Actuators A: Physical*, Vol. 94, 2001, pp. 177–188.

[114] Ye, X. Y., et al., "Determination of the Mechanical Properties of Microstructures," *Sensors and Actuators A: Physical*, Vol. 54, 1996, pp. 750–754.

[115] Bagdahn, J., and W. N. Sharpe, "Fatigue of Polycrystalline Silicon Under Long-Term Cyclic Loading," *Sensors and Actuators A: Physical*, Vol. 103, 2003, pp. 9–15.

[116] Sun, X. J., "Thickness Dependent Fatigue Life at Microcrack Nucleation for Metal Thin Films on Flexible Substrates," *J. Phys. D*, Vol. 41, 2008, p. 195404.

[117] Alaca, B. E., et al., "Biaxial Testing of Nanoscale Films on Compliant Substrates: Fatigue and Fracture," *Rev. Sci. Instrum.*, Vol. 73, August 2002, pp. 2963–2970.

[118] Soutzidou, M., A. Panas, and K. Viras, "Differential Scanning Calorimetry (DSC) and Raman Spectroscopy Study of Poly(Dimethylsiloxane)," *Journal of Polymer Science, Part B: Polymer Physics*, Vol. 36, No. 15, 1998, pp. 2805–2810.

[119] Gotz, S., and U. Karst, "Recent Developments in Optical Detection Methods for Microchip Separations," *Analytical and Bioanalytical Chemistry*, Vol. 387, No. 1, 2007, pp. 183–192.

[120] Khanarian, G., and H. Celanese, "Optical Properties of Cyclic Olefin Copolymers," *Optical Engineering*, Vol. 40, No. 6, 2001, pp. 1024–1029.

[121] Emmelkamp, J., et al., "The Potential if Autofluorescence for the Detection of Single Living Cells for Label-Free Cell Sorting in Microfluidic Systems," *Electrophoresis*, Vol. 25, No. 21-22, 2004, pp. 3740–3745.

[122] Piruska, A., et al., "The Autofluorescence of Plastic Materials and Chips Measured Under Laser Irradiation," *Lab on a Chip*, Vol. 5, No. 12, 2005, pp. 1348–1354.

[123] Bansal, N. P., and R. H. Doremus, *Handbook of Glass Properties*, Orlando, FL: Academic Press, 1986.

[124] Mazurin, O. V., M. V. Streltsina, and T. P. Shvaiko-Shvaikovskaya, *Handbook of Glass Data*, New York: Elsevier, 1983.

[125] ASTM Standard D792, 2008, "Standard Test Methods for Density and Specific Gravity (Relative Density) of Plastics by Displacement," ASTM International, West Conshohocken, PA, 2008, DOI: 10.1520/D0792-08, www.astm.org.

[126] Bhattacharya, S., et al., "Studies on Surface Wettability of Poly(Dimethyl) Siloxane (PDMS) and Glass Under Oxygen-Plasma Treatment and Correlation with Bond Strength," *Journal of Microelectromechanical Systems*, Vol. 14, No. 3, 2005, pp. 590–597.

[127] Kumar, G., and K. N. Prabhu, "Review of Non-Reactive and Reactive Wetting of Liquids on Surfaces," *Advances in Colloid and Interface Science*, Vol. 133, No. 2, 2007, pp. 61–89.

[128] Mescher, M. J., et al., "Fabrication Methods and Performance of Low-Permeability Microfluidic Components for a Miniaturized Wearable Drug Delivery System," *Journal of Microelectromechanical Systems*, Vol. 18, No. 3, 2009, pp. 501–510.

[129] Kang, J. H., Y. C. Kim, and J. -K. Park, "Analysis of Pressure-Driven Air Bubble Elimination in a Microfluidic Device," *Lab on a Chip*, Vol. 8, 2008, pp. 176–178.

[130] Eddings, M. A., and B. K. Gale, "A PDMS-Based Gas Permeation Pump for On-Chip Fluid Handling in Microfluidic Devices," *Journal of Micromechanics and Microengineering*, Vol. 16, No. 11, 2006, pp. 2396–2402.

[131] Lee, J. N., C. Park, and G. M. Whitesides, "Solvent Compatibility of Poly(dimethylsiloxane)-Based Microfluidic Devices," *Analytical Chemistry*, Vol. 75, No. 23, 2003, pp. 6544–6554.

[132] http://www.upchurch.com/.

[133] http://www.coleparmer.com/.

[134] Chu, P. K., et al., "Plasma-Surface Modification of Biomaterials," *Materials Science and Engineering: R: Reports*, Vol. 36, No. 5-6, 2002, p. 64.

[135] Chan, C. M., T. M. Ko, and H. Hiraoka, "Polymer Surface Modification by Plasmas and Photons," *Surface Science Reports*, Vol. 24, No. 1-2, 1996, pp. 1–54.

[136] Penn, L. S., and H. Wang, "Chemical Modification of Polymer Surfaces: A Review," *Polymers for Advanced Technologies*, Vol. 5, No. 12, 1994, pp. 809–817.

[137] Lim, Y. T., et al., "Controlling the Hydrophilicity of Microchannels with Bonding Adhesives Containing Surfactants," *Journal of Micromechanics and Microengineering*, Vol. 16, No. 7, 2006, pp. N9–N16.

[138] Vickers, J. A., M. M. Caulum, and C. S. Henry, "Generation of Hydrophilic Poly(Dimethylsiloxane) for High-Performance Microchip Electrophoresis," *Analytical Chemistry*, Vol. 78, No. 21, 2006, pp. 7446–7452.

[139] Bodas, D., and C. Khan-Malek, "Hydrophilization and Hydrophobic Recovery of PDMS by Oxygen Plasma and Chemical Treatment—An SEM Investigation," *Sensors and Actuators, B: Chemical*, Vol. 123, No. 1, 2007, pp. 368–373.

[140] Kim, B., E. T. K. Peterson, and I. Papautsky, "Long-Term Stability of Plasma Oxidized PDMS Surfaces," *Proceedings of the 26th Annual International Conference of the IEEE Engineering in Medicine and Biology Society*, Vol. 2, 2004.

[141] Vlachopoulou, M. E., et al., "Effect of Surface Nanostructuring of PDMS on Wetting Properties, Hydrophobic Recovery and Protein Adsorption," *Microelectronic Engineering*, Vol. 86, No. 4-6, 2009, pp. 1321–1324.

[142] Gaudioso, J., and H. G. Craighead, "Characterizing Electroosmotic Flow in Microfluidic Devices," *Journal of Chromatography A*, Vol. 971, No. 1-2, 2002, pp. 249–253.

[143] Lawton, R. A., et al., "Air Plasma Treatment of Submicron Thick PDMS Polymer Films: Effect of Oxidation Time and Storage Conditions," *Colloids and Surfaces A: Physicochemical and Engineering Aspects*, Vol. 253, No. 1-3, 2005, pp. 213–215.

[144] Busscher, H. J., et al., "The Effect of Surface Roughening of Polymers on Measured Contact Angles of Liquids," *Colloids and Surfaces*, Vol. 9, No. 4, 1984, pp. 319–331.

[145] Qiao, R., "Effects of Molecular Level Surface Roughness on Electroosmotic Flow," *Microfluidics and Nanofluidics*, Vol. 3, No. 1, 2007, pp. 33–38.

[146] Celata, G. P., et al., "Characterization of Fluid Dynamic Behaviour and Channel Wall Effects in Microtube," *International Journal of Heat and Fluid Flow*, Vol. 27, No. 1, 2006, pp. 135–143.

[147] Cheng, J. -Y., et al., "Direct-Write Laser Micromachining and Universal Surface Modification of PMMA for Device Development," *Sensors and Actuators, B: Chemical*, Vol. 99, No. 1, 2004, pp. 186–196.

[148] Pullen, P. E., et al., "Characterization by Atomic Force Microscopy of Fused-Silica Capillaries Chemically Modified for Capillary Electrokinetic Chromatography," *Analytical Chemistry*, Vol. 72, No. 13, 2000, pp. 2751–2757.

[149] Bowden, N., et al., "The Controlled Formation of Ordered, Sinusoidal Structures by Plasma Oxidation of an Elastomeric Polymer," *Applied Physics Letters*, Vol. 75, No. 17, 1999, pp. 2557–2559.

[150] Varenberg, M., et al., "Effect of Real Contact Geometry on Adhesion," *Applied Physics Letters*, Vol. 89, No. 12, 2006, p. 121905.

[151] Liston, E. M., L. Martinu, and M. R. Wertheimer, "Plasma Surface Modification of Polymers for Improved Adhesion: A Critical Review," *Journal of Adhesion Science and Technology*, Vol. 7, No. 10, 1993, pp. 1091–1127.

[152] Vlachopoulou, M. E., et al., "A Low Temperature Surface Modification Assisted Method for Bonding Plastic Substrates," *Journal of Micromechanics and Microengineering*, Vol. 19, No. 1, 2009, p. 015007.

[153] Lee, K. W., and A. Viehbeck, "Wet-Process Surface Modification of Dielectric Polymers: Adhesion Enhancement and Metallization," *IBM Journal of Research and Development*, Vol. 38, No. 4, 1994, pp. 457–474.

[154] Parker, E. E., et al., "Adhesion Characteristics of MEMS in Microfluidic Environments," *Journal of Microelectromechanical Systems*, Vol. 14, No. 5, 2005, pp. 947–953.

[155] Cheng, M. C., et al., "Dry Release of Polymer Structures with Anti-Sticking Layer," *Journal of Vacuum Science & Technology A: Vacuum, Surfaces, and Films*, Vol. 22, No. 3, 2004, pp. 837–841.

[156] Chiang, Y. M., et al., "Characterizing the Process of Cast Molding Microfluidic Systems," *Proceedings of the SPIE*, Santa Clara, CA, Vol. 3877, 1999.

[157] Belder, D., and M. Ludwig, "Surface Modification in Microchip Electrophoresis," *Electrophoresis*, Vol. 24, No. 21, 2003, pp. 3595–3606.

[158] Wan, H., M. Ohman, and L. G. Blomberg, "Bonded Dimethylacrylamide as a Permanent Coating for Capillary Electrophoresis," *Journal of Chromatography A*, Vol. 924, No. 1-2, 2001, pp. 59–70.

[159] Abate, A. R., et al., "Glass Coating for PDMS Microfluidic Channels by Sol-Gel Methods," *Lab on a Chip*, Vol. 8, No. 4, pp. 516–518.

[160] Wu, Q., H. Claessens, and C. Cramers, "The Influence of Surface Treatments on the Electroosmotic Flow in Micellar Electrokinetic Capillary Chromatography," *Chromatographia*, Vol. 33, No. 7, 1992, pp. 303–308.

[161] Johnson, T. J., et al., "Laser Modification of Preformed Polymer Microchannels: Application to Reduce Band Broadening Around Turns Subject to Electrokinetic Flow," *Analytical Chemistry*, Vol. 73, No. 15, 2001 pp. 3656–3661.

[162] Cretich, M., et al., "Functionalization of Poly(Dimethylsiloxane) by Chemisorption of Copolymers: DNA Microarrays for Pathogen Detection," *Sensors and Actuators B: Chemical*, Vol. 132, No. 1, 2008, pp. 258–264.

[163] Cheng, J. -Y., et al., "Direct-Write Laser Micromachining and Universal Surface Modification of PMMA for Device Development," *Sensors and Actuators, B: Chemical*, Vol. 99, No. 1, 2004, pp. 186–196.

[164] Kingshott, P., and H. J. Griesser, "Surfaces That Resist Bioadhesion," *Current Opinion in Solid State and Materials Science*, Vol. 4, No. 4, 1999, pp. 403–412.

[165] Grayson, A. C. R., et al., "A BioMEMS Review: MEMS Technology for Physiologically Integrated Devices," *Proceedings of the IEEE*, Vol. 92, No. 1, 2004, pp. 6–21.

[166] Dhayal, M., J. S. Choi, and C. H. So, "Biological Fluid Interaction with Controlled Surface Properties of Organic Micro-Fluidic Devices," *Vacuum*, Vol. 80, No. 8, 2006, pp. 876–879.

[167] http://www.matweb.com.

[168] http://www.hdmicrosystems.com.

[169] http://www.topas.com.

[170] http://www.microchem.com.

[171] http://www.dupont.com.

[172] http://www.momentive.com.

[173] http://www.dowcorning.com.

4

Photolithography

4.1 Introduction

Photolithography is the process of defining a prescribed latent image in a photosensitive material by selective exposure to radiation. As the principal method of defining geometric features and shaped boundaries between materials, photolithography is often the most important process step in microfabrication. This chapter provides a concise overview in order to provide a basic understanding for the next few chapters on various fabrication methods, and it defers to more comprehensive resources for greater detail on photolithography and related lithography technologies [1, 2].

Most commonly, *photolithography* is understood to mean optical photolithography with UV light (approximately 400 to 300 nm wavelength) as the radiation source. This is the primary type of lithography discussed throughout this chapter. More broadly, however, lithography in a more general sense encompasses not only alternative radiation sources, but also other patterning methods not based on radiation at all. Interestingly, both nanoimprint lithography and soft lithography (discussed in Chapter 5) are capable of achieving resolution on the order of 10 nm, significantly finer than conventional optical lithography.

Photolithography is used one or more times in the fabrication process sequences of a vast majority of microfluidic devices. The particular role of photo-patterning differs depending not only on the type of material that is meant to be patterned (silicon, glass, metals, and polymers), but also on dimensional requirements such as depth, thickness, resolution, and aspect ratio.

Historically the most common purpose of patterned photoresist has been to serve as a mask for etch processes, as discussed in Chapter 6. Particularly for

microfluidic devices, however, several fabrication methods depend on patterned photoresist in intermediate role for masters or molds in casting and molding processes, discussed in Chapter 5. Some photosensitive materials can be used directly as end-use structural components rather than as an intermediate material in support of other fabrication processes. For additive processes such as thin-film metal deposition and electroplating (Chapter 7), photoresist can serve as a blocking material to expose only the specific regions where material is to be added. Still other ways of using photopatterned films include sacrificial layer support (Chapter 8) and substrate bonding (Chapter 9). Given the ubiquitous and vital role of photolithography in so many process steps, some of the basic principles are first introduced in this chapter before discussing the other fabrication processes in the remaining chapters.

4.1.1 Photoresist

Photoresist materials (often abbreviated simply as resists) consist of a polymer resin, a UV-sensitive initiator, and solvent. The solvent is important for achieving proper viscosity during dispensing and coating, but also must be sufficiently removable by baking for dimensional stability during exposure. Advances in materials engineering of photoresists enhance the capabilities of photolithography in terms of resolution, high aspect ratio, topography coverage, and etch resistance. Other important criteria to consider for comparing photoresists include adhesion quality, ease of removal, method of coating, and (side) profile [3]. The most fundamental distinction among photoresist materials is whether they are positive tone or negative tone. A positive resist produces a latent image that corresponds to the opaque regions of the photomask because exposed regions are made soluble and removed during developing. A negative resist produces a latent image that is opposite from the photomask, because only the exposed regions are cured while other regions are removed during developing. The distinction between positive resists and negative resists is illustrated in Figure 4.1.

4.1.2 Photomasks

Photomasks for optical lithography are conventionally made of transparent substrates coated with an opaque metal film, most commonly chromium. Fused silica or quartz is a material of choice for photolithography masks because of excellent transmission characteristics even in the low UV range. The metal is patterned by etching through a photoresist coating, routinely patterned with excellent submicron resolution by electron beam lithography. Laser patterning of chromium-on-glass masks is also effective for features approximately 1 micron or larger. For coarse features approximately 10 microns or larger, other

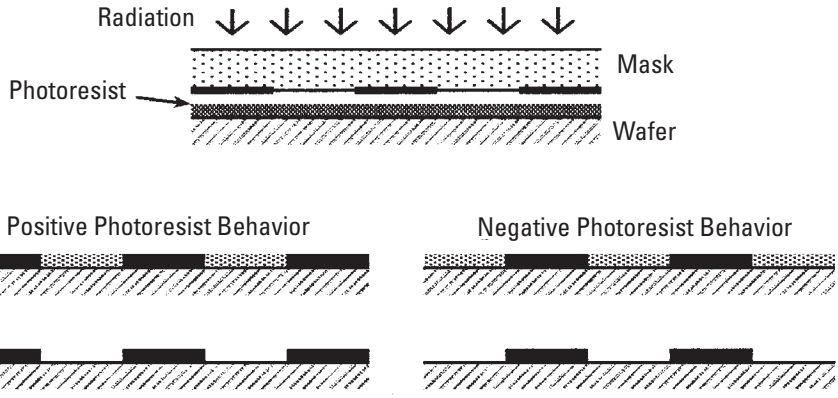

Figure 4.1 Distinction between positive photoresist and negative photoresist.

options such as laser photoplotting are favorable for low-cost, rapid prototyping. In principle, even images produced by conventional office laser printers and overhead transparency paper can be used, although resolution and opaque contrast are significantly compromised. In a broader sense, any material combination that has distinctly different transmission versus blocking characteristics can be used as a patterning method for photolithography. One very novel example of nontraditional masking is dynamic microfluidic masking, in which a fluid streams actively participate in focusing light in selective spatial regions [4].

4.2 Process Basics

The most basic steps in photolithography are: (1) *coating* photoresist onto a substrate, (2) selectively *exposing* regions to UV radiation through a photomask, and (3) removing the regions that remain soluble by *developing*. Intermixed among the fundamental steps of coating, exposing, and developing are baking treatments to evaporate solvent and to assist curing. The flow of process steps is shown in Figure 4.2.

A pre-expose bake, sometimes called a soft bake, is used to remove some solvent from liquid photoresist such that the photoresist is no longer fluid and can be placed in contact with a photomask. A post-expose bake is applied after UV exposure so that the curing process can be completed before developing. In some cases, an additional hard bake is applied after developing to increase resistance to subsequent processes, such as etching.

Particle contamination and poor adhesion are two common flaws encountered during photolithography, so in addition to providing a sufficiently clean environment the substrates must be cleaned. For bare silicon wafers, standard

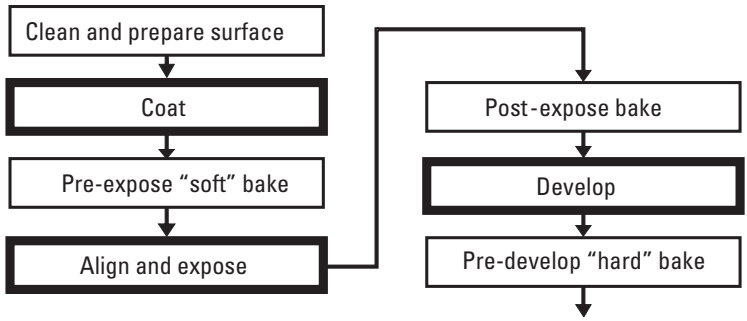

Figure 4.2 Basic photolithography process steps.

cleaning sequences are established from precedence in microelectronics fabrication. Sulfuric acid (H_2SO_4) with hydrogen peroxide (H_2O_2), known as *piranha* clean, is used to remove organic contaminants, dilute hydrofluoric acid (HF) is used to remove native oxide that naturally forms on the surface of silicon in air, and hydrochloric acid (HCl) with hydrogen peroxide is used to remove metal ion contaminants. For glass substrates, only the piranha clean is typically used, because HF begins to etch silica glass. HCl is usually not frequently necessary for glass because metal ion contaminants are primarily a concern only for semiconductor substrates. Wafers are rinsed with deionized water and normally dried by spin-drying at high speed. Cleaning with an ultrasonic jet of deionized water is also occasionally used as a method of removing larger particles.

4.2.1 Coating

Photoresist is most commonly distributed as a uniform, thin layer on a flat substrate by spin coating. Before coating, wafers are normally subjected to either a dehydration bake in an oven or a singe on a hotplate to drive off moisture and any other volatile residue. Temperatures may vary from as low as 125°C for a singe or up to 200°C and higher for dehydration in an oven. Faster spin speed results in thinner films, and photoresists are conveniently characterized on a plot of film thickness versus spin speed. Depending on application, the photoresist layer may be less than 1 μm or more than 100 microns thick. Often an adhesion promoter such as hexamethyldisilazane (HMDS) is either vapor coated or spun onto a heated wafer to prime the surface for better photoresist adhesion. For relatively coarse features, dry-film photoresists can be applied by lamination instead of the more traditional spin-coating method. Dry-film photoresist processing is common in printed circuit board manufacturing, for which critical dimensions are typically larger than MEMS-scale devices. Spray

coating [5] and electrodeposition [6] of photoresist are alternatives to spin coating that are particularly useful for substrates that have relatively extreme changes in three-dimensional topography.

4.2.2 Baking

As mentioned previously, bake steps are used at multiple stages of photolithography processing. They are typically performed either on a hotplate or in an oven, with soft bakes and post-exposure bakes for most resists generally near 100°C. For thick resists, however, a gentler post exposure bake temperature is helpful for improving resolution and for reducing thermal stresses and for avoiding corresponding process failures such as cracking and delamination [7, 8]. Baking on a hotplate is much faster than doing so in an oven, but the latter option has the benefit of batch processing large numbers of wafers simultaneously. Soft bakes for a 1-μm positive resist for example, may take on the order of 1 minute on a hotplate but close to a half-hour or longer in an oven. In many cases hotplates are outfitted with vacuum ports to assure good thermal contact and better process repeatability. Even factors such as pre-bake time can have a major influence on resolution and achievable aspect ratio, especially for thick resists such as SU-8 [9]. Infrared (IR) radiation is an alternative to hotplate or oven baking, and has been shown to be effective particularly for both positive and negative resists [10]. For very thick resists, IR baking provides important benefits of fast cycle time, low stress, and high aspect ratio. Since a major function of soft baking is to evaporate solvents and photoresists routinely have compounds that are toxic to humans, proper ventilated exhaust is essential regardless of whatever particular method is used to perform bake steps.

High-volume production photolithography systems often integrate several process steps onto a single platform. For example, a cassette of wafers can be loaded onto a single system on which a track or robotic transfer mechanism takes each wafer through singe, prime, coat, and soft bake. The wafers may be taken for exposure on an aligner by robotic or manual transfer, and then returned to a similar automated station for post-exposure bake and developing. In a less automated facility, the entire process would be run on separate stations, which may include a single-wafer spin coater, manual transfer to hotplates, and immersion developing in glassware.

4.2.3 Alignment

UV exposure is most routinely performed on an *aligner*, with the most common radiation sources being mercury-based lamps. Lamp intensity is typically

measured in terms of power per unit area (e.g., mW/cm^2), and the exposure is timed to deliver a target energy per unit area (e.g., mJ/cm^2). For predictable and repeatable results, the light is filtered to a very narrow and specific spectral peak. In conventional photolithography, the g-line at 436 nm and the i-line at 365 nm are the most common, and a given photoresist material can be characterized and optimized for a specific spectral line.

In photolithography, aligning refers to the important task of positioning existing features on a wafer with respect to features on a photomask, after which the exposure step is performed. This alignment is what allows features on multiple layers to be positioned correctly with respect to each other. Simple devices with only one photolithography step or the very first mask in a multilayer set may not need alignment because there are no underlying features that need to be aligned. However, in some cases (as in anisotropic wet etching of silicon discussed in Chapter 6) it may still be necessary to perform alignment of the first photopatterned layer even with respect to the otherwise bare wafer. When geometric features on more than one photolithography layer must be aligned, it is necessary for each mask in the set to have fiducial marks that facilitate alignment. Alignment targets may be as simple as lines, rectangles, or simple cross patterns positioned on far ends of the wafer. Most aligners are equipped with two microscope cameras to view a pair of alignment targets, one left and one right. Assuming a stationary mask, a wafer can be positioned and rotated on a manual or automated stage until targets on the mask align with corresponding features on the wafer. Figure 4.3 shows an example of an alignment scheme that includes a simple *cross-in-box* arrangement as well as vernier patterns for finer alignment.

Some device designs may involve aligned features on opposite sides of a wafer, in which case *backside alignment* is required [11, 12]. Front-side alignment is relatively straightforward, as long as the wafer has visible features and the mask has sufficiently broad clear regions in the vicinity of the alignment marks to facilitate ease of locating them. Aligning the target on the mask to features on the (opposite) backside of wafers is less straight forward, especially if the wafers are opaque. One way to perform backside alignment is to mount microscopes on the underside of an aligner. A stored image of targets on the mask is captured (e.g., by digital image on a computer), and subsequently the wafer is moved into place between the mask and the backside optics. The wafer is aligned to images that have been stored and redisplayed for alignment, rather than to real-time features on the mask. Figure 4.4 illustrates the difference between front-side and backside alignment. An alternative way to perform backside alignment is to use infrared illumination from beneath the wafer. With infrared illumination, features can be imaged using front-side optics as long as infrared contrast through the wafer is sufficient.

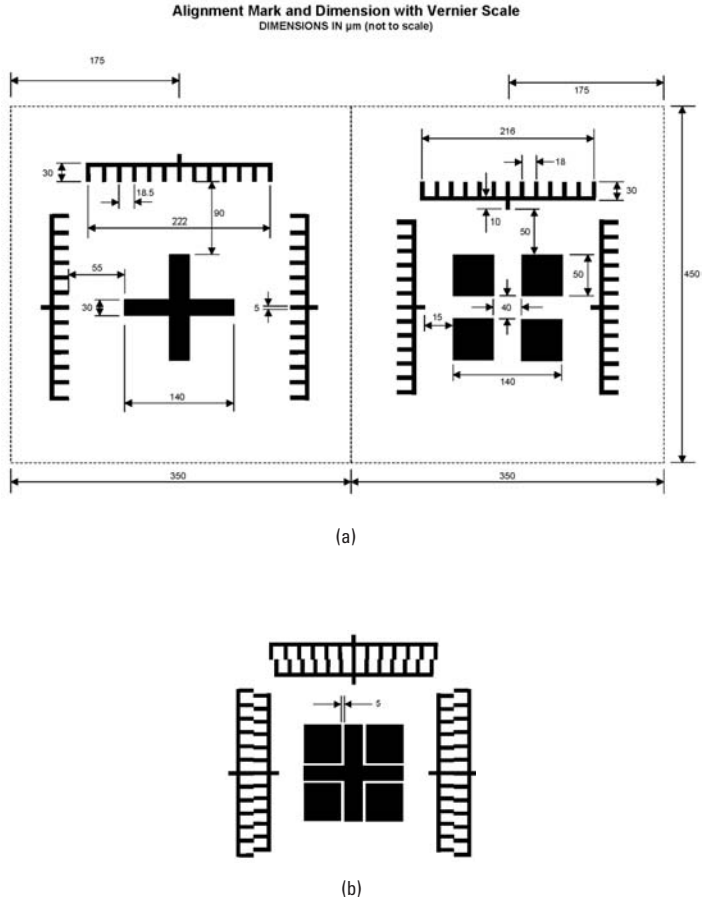

Figure 4.3 (a, b) Photolithography alignment targets with vernier scales, with first layer pattern, second layer pattern and superimposed alignment. Dimensions shown are in micron units. (Image courtesy of SUSS MicroTec.)

4.2.4 Exposure

A very useful quantitative tool for determining the optimal exposure dose for a given photoresist is the *contrast curve*. The contrast curve is determined experimentally by subjecting wafers to different exposure dose levels and measuring the corresponding resist thickness after developing. The resist thickness is plotted versus exposure dose (in log scale), and the results reveal three useful pieces of information: (1) the minimum energy dose that in needed to effect any photo-initiated change, (2) the minimum energy dose needed to remove all of

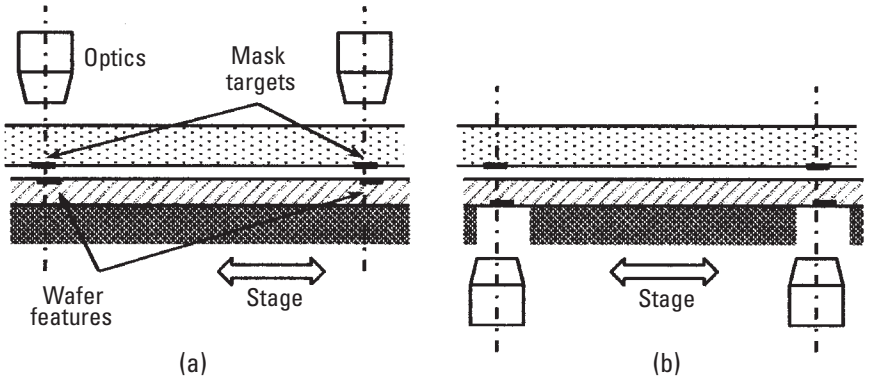

Figure 4.4 Wafer alignment for photolithography, comparing (a) front-side alignment to (b) backside alignment.

the resist, and (3) the sharpness of contrast. At very low dose, developing has almost no distinguishing effect, but after a minimum threshold is exceeded there is a difference in solubility that continues to magnify with increasing dose. Figure 4.5 shows hypothetical contrast curves for both positive and negative resists. Contrast performance depends on several factors including not only resist material and exposure dose, but also other factors such as bake temperatures and developer concentration.

When exposing, there are different approaches for interfacing a wafer with respect to a photomask. In *contact printing*, as the name suggests, a wafer is pressed into direct physical contact with the mask to maximize fidelity. *Proximity printing* maintains a narrow gap between surfaces to avoid any contact-related degradation, but compromises some loss of resolution because of diffraction. On the other hand, *vacuum contact printing* eliminates air between wafer and mask for improved optical resolution at the risk of minor surface damage. *Projection printing* uses optics to demagnify images (5×, for example), so that the feature resolution on the imaged wafer can be even finer than the resolution on the reticle. The word reticle is often used interchangeably with mask, although reticles are more commonly associated with projection lithography. The term stepper is used to refer to an exposure system that incrementally moves a reticle with respect to the wafer to produce multiple copies of the same image. A stepper and an aligner both perform the essential task of UV exposure, but the term aligner more typically refers to a system that uses a mask imaging at 1:1 scale rather than incrementing a reticle along multiple grid positions.

More advanced radiation-based lithography methods generally use shorter wavelength with the primary goal being finer feature resolution. Other ranges include deep ultraviolet (DUV, less than ~300 nm), extreme ultraviolet (EUV,

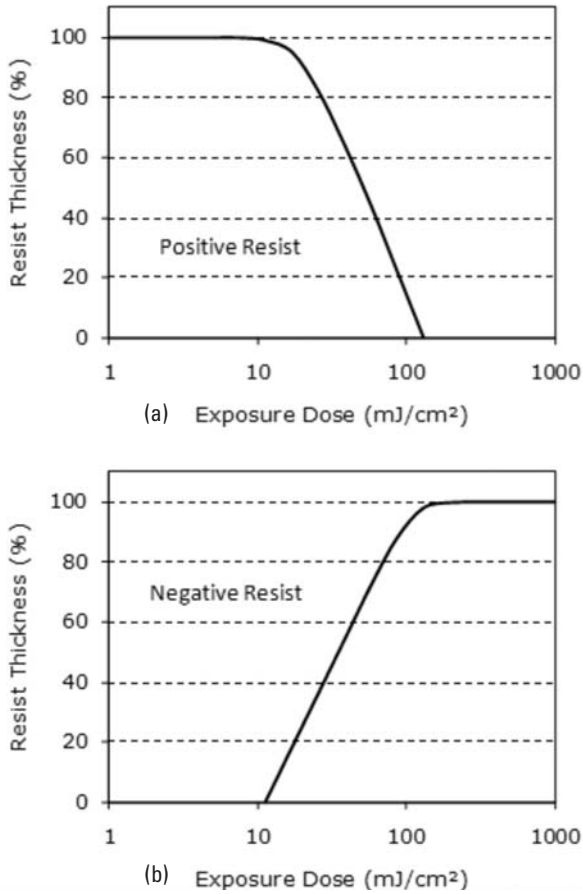

Figure 4.5 Examples of contrast curves for (a) positive and (b) negative photoresists.

less than ~100 nm), and X-rays (10 to 0.01 nm). X-ray lithography is capable of achieving feature resolution below 100 nm. However, particularly with X-ray lithography the equipment set becomes less accessible and often prohibitive in terms of cost, limiting use to only the largest commercial entities and advanced research facilities. Electron beam lithography (EBL) is a serial process in which an electron beam is steered over the surface with very fine resolution. EBL is routinely used to pattern photomasks for subsequent use in optical lithography, but its high cost and slow rate otherwise limit its use to niche research applications and low-volume prototyping. Feature sizes for most microfluidic devices, however, typically demand relatively coarse resolution, on the order of a few microns or larger, which is routinely achieved by conventional UV photolithography.

4.2.5 Developing

Developing is the step in which the uncured regions of photoresist are removed. Dilute solutions of tetramethyl ammonium hydroxide (TMAH) are effective for a wide variety of positive photoresists, and they are preferred in many facilities over alkaline chemicals such as potassium hydroxide (KOH) because the latter may introduce ions that can contaminate semiconductor devices. Developers for negative photoresists are less universal, and are typically based on organic solvents. For less common photoresist materials, resist manufacturers typically have an associated developer recommended for a given photoresist product. Wafers may be entirely immersed in developer solution for fabrication in low quantities. For reduced waste and cross-contamination, however, it is preferred to puddle develop by dispensing limited measured volumes of developer onto a wafer. Spray developing makes even more efficient use of chemicals by uniformly distributing the minimum quantity of solution needed for proper developing. Removal of uncured resist is a difficult challenge for features with high aspect ratio, such as deep holes or narrow channels. In such cases agitation or ultrasonic excitation is sometimes used to assist material displacement. Especially for thick resist, ultrasonic agitation as well as its directionality with respect to patterned features, affects resist profile, surface roughness, and developing time [13].

References

[1] Levinson, H. J., *Principles of Lithography*, 2nd ed., Bellingham, WA: SPIE—The International Society for Optical Engineering, 2005.

[2] Rai-Choudhury, P., (ed.), *Handbook of Microlithography, Micromachining, and Microfabrication, Volume 1: Microlithography*, Bellingham, WA: SPIE Optical Engineering Press, 1997.

[3] O'Brien, J., et al., "Advanced Photoresist Technologies for Microsystems," *Journal of Micromechanics and Microengineering*, Vol. 11, No. 4, 2000, pp. 353–358.

[4] McKechnie, J., and D. Sinton, "Dynamic Microfluidic Photomasking," *Journal of Microelectromechanical Systems*, Vol. 16, No. 5, 2007, pp. 1145–1151.

[5] Pham, N. P., et al., "Direct Spray Coating of Photoresist for MEMS Applications," *SPIE-Int. Soc. Opt. Eng.*, Vol. 4557, 2001.

[6] Kersten, P., S. Bouwstra, and J. W. Petersen, "Photolithography on Micromachined 3D Surfaces Using Electrodeposited Photoresists," *Sensors and Actuators A: Physical*, Vol. 51, No. 1, 1995, pp. 51–54.

[7] Anhoj, T. A., et al., "The Effect of Soft Bake Temperature on the Polymerization of SU-8 Photoresist," *Journal of Micromechanics and Microengineering*, Vol. 16, No. 9, 2006, pp. 1819–1824.

[8] Hong, S. J., et al., "Characterization of Low-Temperature SU-8 Photoresist Processing for MEMS Applications," *Proc. IEEE Conference and Workshop on Advanced Semiconductor Manufacturing*, 2004, pp. 404–408.

[9] Zhang, J., K. L. Tan, and H. Q. Gong, "Characterization of the Polymerization of SU-8 Photoresist and Its Applications in Micro-Electro-Mechanical Systems (MEMS)," *Polymer Testing*, Vol. 20, No. 6, 2001, pp. 693–701.

[10] Kubenz, M., et al., "Effective Baking of Thick and Ultra-Thick Photoresist Layers by Infrared Radiation," *Microelectronic Engineering*, Vol. 67-68, 2003, pp. 495–501.

[11] Pal, P., Y. -J. Kim, and S. Chandra, "Front-to-Back Alignment Techniques in Microelectronics/MEMS Fabrication: A Review," *Sensor Letters*, Vol. 4, No. 1, 2006, pp. 1–10.

[12] Kim, E. S., R. S. Muller, and R. S. Hijab, "Front-to-Backside Alignment Using Resist-Patterned Etch Control and One Etching Step," *Journal of Microelectromechanical Systems*, Vol. 1, No. 2, 1992, pp. 95–99.

[13] Tseng, F. G., and C. S. Yu, "Angle Effect of Ultrasonic Agitation on the Development of Thick JSR THB-430N Negative UV Photoresist," *Microsystem Technologies*, Vol. 8, No. 6, 2002, pp. 363–367.

5

Solidification Processes and Soft Lithography

The processes featured in this chapter focus on producing geometric features in materials by a phase change from a fluid or semifluid state to a solid. This general heading of *solidification processes* includes processes such as photopolymerization of UV-curable materials, casting, molding, and related phase-change processes. In some processes such as embossing, the material may already be solid, but subject to prescribed deformation with the addition of heat and pressure. In such reshaping of material, it may be more appropriate to describe the process as *resolidification*, but for simplicity reshaping processes and liquid-to-solid solidification processes will be grouped together in this chapter. Most solidification processes that are used in microfabrication apply to polymers rather than metals or inorganic materials. A few exceptions have been investigated to provide greater thermal stability or chemical resistance compared to polymers. For example, microchannel devices have been demonstrated using organically modified ceramics [1].

Soft lithography is a name used to encompass a broad suite of processes for fabricating microscale and nanoscale features. Although intermediate steps of photopatterning may certainly be involved, soft lithography is distinct from photolithography in that an elastomeric master is the key shape-defining tool rather than a photolithography mask. This master is also described by several other names depending on application, and common terms include such names as mold, stamp, pattern, and template. There is often some interchangeability, confusion, and even debate among proper use of terminology. A mold or stamp that is cast from a primary master, for example, may serve as a secondary master for subsequent processes. Regardless of the particular name, the fundamental

idea is that a patterned soft material plays a central role in the definition of fabricated structures, and the descriptions in this book will focus on describing functional role rather than attempting to enforce rigorous distinction among particular names. Soft lithography is best viewed as a suite of processes rather than a single, narrow process. There are several variations on soft lithography, and the subset described as *replica molding* is discussed with greatest attention in this section. Another important variation called *micro contact printing* is discussed in more detail as an additive process later in this chapter. Soft lithography review papers [2–4] provide more comprehensive discussion of other variants.

Polydimethylsiloxane (PDMS) is by far the most common material used in soft lithography [5]. As introduced in Chapter 3, PDMS has a unique combination of favorable properties for microfabrication. Uncured PDMS flows very freely at room temperature, and once cured it produces a mechanically resilient and optically transparent material. PDMS is not only very common as a final device material [6, 7], but also is frequently used as a material for molds and stamps to produce features in other materials. PDMS stamps are capable of reproducing features with characteristic dimensions as small as ~25 nm. The very pliable nature of PDMS, however, can lead to flaws such as structural collapse of thin or tall structures. Other materials may be advantageous if there is a need to satisfy different material constraints such as mechanical stiffness, thermal stability, and chemical resistance. Furthermore, the properties of PDMS can also be chemically modified for more favorable properties such as higher stiffness or toughness for soft lithography tooling [8].

The remainder of this chapter will be organized in three broad categories: radiation-selective polymerization (Section 5.1), casting and molding (Section 5.2), and thermoplastic reshaping (Section 5.3). The distinguishing characteristics among these categories will be explained at the beginning of each section. Indeed, there are many cases in which the distinctions among categories are not absolute, and processes are not mutually exclusive. Even if imperfect, it is the intent of the authors that grouping related fabrication processes in this way will help highlight fundamental similarities, capabilities, and limitations.

5.1 Radiation-Selective Polymerization

The basic process of photolithography has already been discussed in Chapter 4, but that discussion was focused on photolithography as a patterning step for downstream processes such as etching or metal film lift-off. In this section, the context shifts to the fabrication of microfluidic components in a more direct way, in general with the polymerized material remaining as a permanent part of the final device. A specific example of a functional component that can be fabricated by radiation-curing is a check valve. Radiation-cured check

valve components have taken a variety of design manifestations including out-of-plane [9] or in-plane [10] concepts.

UV-initiated polymerization is most commonly associated with accelerated curing, but it can also be used to define regions that are to be removed, as is the case for removing unexposed of polyethylene terephthalate in a dimethylformamide solution [11]. Accordingly, the heading of this section is more broadly described as *radiation-selective polymerization*. This choice of words is meant to encompass both positive and negative photosensitive materials. As explained previously, a negative-acting photoresist, for example, is one for which the regions exposed to UV light are the ones that undergo cross-linking and remain. In contrast, UV light affects positive-acting photoresists by making exposed regions soluble. It is the unexposed regions that are polymerized (typically by thermally accelerated curing). The subsections below divide radiation-selective polymerization into three topics. Presented first is curing with a UV lamp through a photomask. This is almost identical to routine photolithography, and is the most common method of curing photosensitive polymers.

5.1.1 Ultraviolet Polymerization

A tremendously wide variety of materials can be patterned by UV polymerization. The most widely investigated photoresist that has been used as a structural material in lab-on-chip systems is SU-8 [12], with examples of geometric features shown in Chapter 2 and material properties discussed in Chapter 3. Several other photosensitive polymers have also been explored for microfluidic devices. Photopatternable polyimide has been used as the sealing component of a thin-film titanium membrane [13]. A UV-curable perfluoropolyether (PFPE) has been demonstrated as a highly robust membrane in microfluidic devices proposed for the environmental stresses of interplanetary missions [14]. Novel use of sequential UV polymerization can be used to fabricate more complex devices. For example, stimuli-responsive materials such as pH-sensitive hydrogels can be patterned locally inside an existing microchannel structure by UV curing through a photomask that is aligned over previously defined geometric features [15].

Spin coating is the most common method of distributing a photosensitive polymer layer. Highly viscous photoresist materials such as SU-8 can be coated with thickness even beyond 100 μm in a single step. Alternatively, multiple coating steps can be performed to produce thicker layers, even if viscosity or uniformity constraints require thinner distribution per coating. For more extreme thickness on the order of 1 mm, an alternative approach would be to use filling of a predetermined volume of the photosensitive material into a fixed gap between rigid substrates [16].

It is even possible to achieve polymerization of a material in situ within a fluidic channel, as long as the appropriate monomers and photoinitiators can be distributed properly. For example, novel fabrication of a micron-thin vertical membrane within a PDMS microchannel has been demonstrated using polymerization of a hydrodynamically focused stream of polyacrylamide [17].

Most frequently, collimated light from the lamp of a standard photolithography aligner is used as the UV source, but other sources can be used as well. Some reasons for considering sources other than standard photolithography aligners might include factors such as cost, clean room compatibility, substrate dimensions, and feature size. For coarse features a UV flood lamp may be used to initiate the curing. For fine features without a photolithography aligner, conventional laboratory microscopes can be modified to photopattern structures with approximately 1-μm lateral resolution [18].

There are multiple trade-offs on processing conditions for achieving desirable characteristics such as fine resolution, high aspect ratio, and robust adhesion [19]. For SU-8, high aspect ratio and resolution can be improved by lowering exposure dose, with some compromise in hardness [20]. Limitations to high aspect ratio are not solely attributed to the penetration radiation energy, but important factors also include mechanical stability and redeposition of partially dissolved resist [21].

5.1.2 Alternative Radiation Sources

Examples of radiation sources that involve a directed beam include laser [22], electron beams [23], and proton beams [24]. Electron-beam lithography (EBL) can be used to pattern SU-8 in a direct-write mode with submicron resolution [25]. In addition to having exceptionally fine resolution both laterally and in the depth direction, e-beam and proton-beam methods can produce three-dimensional structures with overhangs and undercuts by varying energy level.

The various methods of irradiation with a directed beam are generally much slower than conventional photolithography through a mask because the irradiation paths must be traversed in spatially serial fashion. To manage trade-offs among speed, resolution, and flexible spatial control, combining UV lamp exposure and directed-beam irradiation is a viable strategy for achieving a productivity compromise while still being able to create a combination of nanoscale and microscale features. For example, e-beam lithography in combination with UV lithography has been demonstrated in fabricating 100-nm-wide lines and much larger micron-scale features on the same layer of SU-8 [26].

With the multitude of directed-beam processes that have been developed and the corresponding variety of coined phrases that have been associated with them, there is understandably confusion regarding what constitutes a writing process versus a lithography process. For example, *proton beam writing* (PBW) is

one basic form of *ion beam lithography* [27]. PBW is distinguished from a focused ion beam (FIB) by virtue of using faster, lighter ions than FIB. The word lithography usually carries some implication that the substrate is a photoresist material. However, that does not exclude writing processes from working with photoresists, and in fact PBW is most often associated with patterning PMMA-based photoresists. As discussed in context of subtractive processes later in this chapter, FIB can very well be used on many substrates that are not photoresists, and yet FIB is still considered a type of ion beam lithography. Furthermore, in addition to the radiation-selective solidification discussed in this chapter, directed-beam processes can be used for subtractive as well additive processes too. Given the inexactness of distinctions among such processes, for the purposes of this book there will be no firm delineation between beam writing and beam lithography. Instead, any directed-beam process will be appreciated more in terms of how it is distinct from broad-area processes such as UV lamp exposure through a glass photomask.

5.1.3 Multilevel Features and 3D Profiles

Research and development for silicon-based MEMS transducers has generated much innovation in microfabrication processes, particularly with respect to surface micromachining of functional three-dimensional structures. Much of the innovation has been enabled by novel use of sacrificial materials such as those based on silicon dioxide [28] and other materials. Unlike some of the more complex structures used in such devices as polysilicon-based MEMS devices (e.g., accelerometers and gyroscopes), a large portion of very useful polymer microfluidic devices are geometrically very simple (e.g., wells and channels). However, an area in which microfluidics activity has contributed significant innovation is three-dimensional microfabrication based on photocurable polymers. Not all the novel concepts are necessarily practical, and other processes may often be more practical or economical. However, special attention is given here to some of the creative strategies for multilevel and 3D structures because they may be enablers toward new concepts and future innovations in microfluidic device design.

There is a wide variety of novel process sequences for producing multilevel features. One basic way of forming simple multilevel structures is by postponing the developing step until after two or more exposure steps are completed. Figure 5.1 shows an example multilevel structure that includes a small nozzle, long connecting channel, and large reservoir intended for reagent dispensing in pharmaceutical research. The structure is fabricated in SU-8 by simultaneous development of multiple layers.

Figure 5.2 explains illustrates the basic process for a negative-acting photoresist. An inverse process is conceivable for positive-acting resists, but

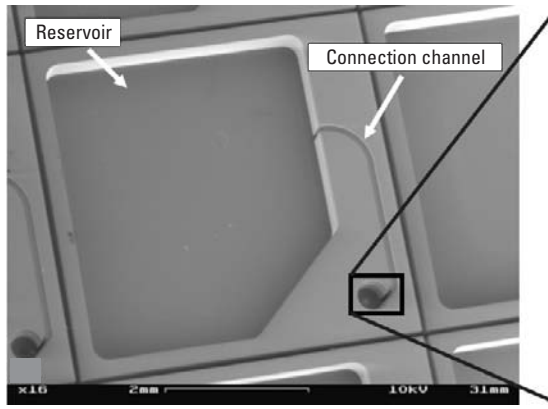

(a)

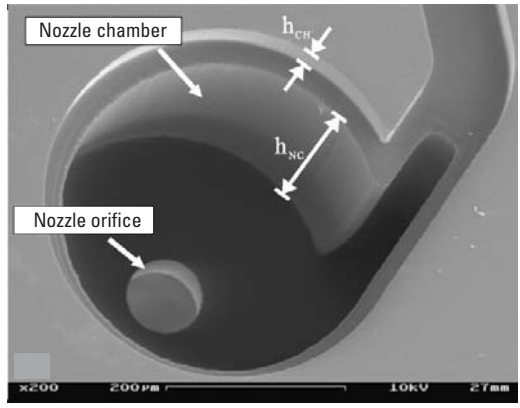

(b)

Figure 5.1 (a, b) Multilevel structure with reservoir, channel, and nozzle fabricated by simultaneous development of multiple SU-8 layers. (Reprinted from [29], with permission from IOP Publishing.)

tends to be more problematic because exposure to UV light is what destroys structural integrity rather than establishing solidified features. So in practice, this strategy is almost exclusively based on negative resists, with SU-8 being the most widely investigated material. The sequence is illustrated for just two layers, but the same basic approach can be used for several layers. Although not explicitly stated in the figure, baking steps also play an important role in providing proper conditions for multilayer coatings and assuring complete curing of the final structure.

The strategy of delaying development until after all layers are sequentially exposed is generally limited to structures that are always supported from the bottom. Forming solid structures above vacant cavities is significantly more

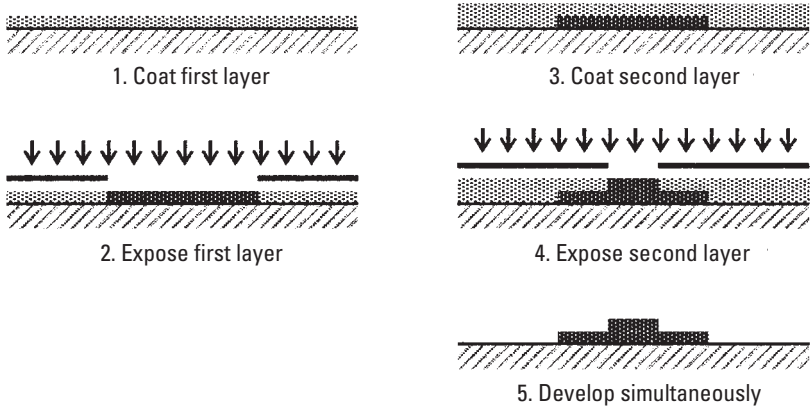

Figure 5.2 Fabrication of multilevel features by simultaneous developing of multiple exposure layers.

challenging than producing step features that simply have smaller features stacked upon larger ones. One basic way to fabricate multilevel structures with embedded cavities, overhangs, and undercuts, is by controlling the local dose and depth of radiation exposure. Figure 5.3 illustrates the basic concept of producing a multilevel structure by partial-depth curing. In this figure the source of radiation is shown generically as a focused beam that scans across the surface with controllable position and intensity. The exposure dose that is delivered to the photosensitive material can be altered not only by modulating power input, but also by varying scan speed.

A specific way of achieving depth control is by altering both the focus and the intensity of a UV laser [30]. In principle, partial-depth curing should also be possible by reducing the power intensity or otherwise attenuating the power of a UV lamp, but in practice such depth control is difficult to achieve consistently. One problem with lamp-based UV curing, is light reflection off the substrate surface. The novel use of an antireflection coating beneath an SU-8 layer, has produced well-defined boundaries of embedded micro-channels by limiting the UV exposure to a finite depth. Figure 5.4 shows a well-defined embedded microchannel using such implementation.

A very deterministic way to limit depth of exposure is to use the concept of a *buried mask* [32]. If an opaque thin film is coated upon a first patterned layer, a second layer can be exposed subsequently with a different pattern because the buried mask protects the first layer from further change. This principle is illustrated in Figure 5.5. The thin film is generally weak enough that it is easily removed during the developing step. However, unlike fabrication by partial-depth curing, the metal film remains in between portions of the patterned

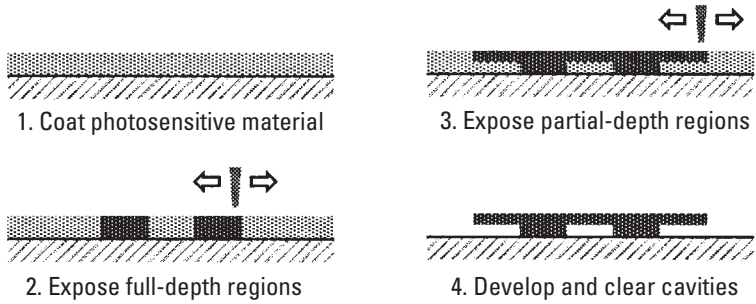

Figure 5.3 Fabrication of multilevel features by partial-depth curing.

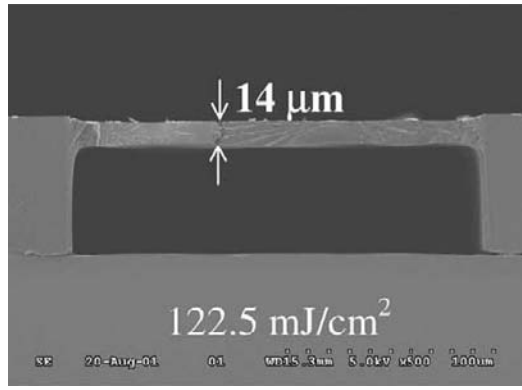

Figure 5.4 Embedded microchannel fabricated by partial-depth UV curing with antireflection coating. (Reprinted from [31]. Copyright 2003, with permission from Elsevier.)

layers, so this must be tolerable in the functional design requirements if a buried mask approach is used.

The main functional requirement for the buried mask material is that it must be opaque to the type of radiation that is used. Common thin-film metal film materials such as chromium and aluminum are generally adequate for blocking UV light. The particular method of film coating, however, must be chosen such that incidental exposure to UV light is minimized during thin-film deposition. Depending on the particular materials used and the conditions under which the metal film is deposited, wrinkling may be another problem that can occur. Wrinkling may be caused by significant differences in thermal expansion coefficient and/or accelerated solvent evaporation during high vacuum steps that may be part of the thin-film deposition process. For some applications this wrinkling phenomenon can be used to an advantage to engineer

nanotextured surfaces [33], but flat films are generally preferred for buried masks.

The examples discussed above were based on developing (i.e., removal of the unwanted material) in a single step. Using sufficiently thick photosensitive materials, however, makes it possible to perform a coat-and-expose sequence upon features that have already been completely developed in a prior sequence. Figure 5.6 shows this 3D fabrication strategy based on embedding existing features with a second layer that is thicker than the first. This strategy is uniquely empowering because the two layers do not have to be based on the same material. The final structure could consist of two adjacent materials that have different mechanical, chemical, electrical, or optical properties. As shown in the figure, the second material can wholly embed the first, or leave designated portions of the first material open to the surroundings.

An important factor to consider for strategies based on nonhomogeneous materials, however, is whether or not surface wetting is adequate. If the material interfaces are nonwetting, it becomes difficult or impossible to combine different materials unless surface treatments are applied to alter the wetting behavior. Solvent compatibility is another practical concern with many photoresists. All photoresists contain a significant fraction of liquid solvent, so whenever attempting to photopattern nonhomogenous structures it is important to assure that the solvent in one photoresist will not inadvertently compromise the chemical stability of the other photoresist.

Yet another relatively straightforward way of producing suspended structures over vacant cavities is to use dry films of photosensitive material [34]. Dry films are typically coated on a backing layer to facilitate handling and ease of lamination. A dry film can be aligned over complex cavities and subsequently patterned by UV exposure. Multilevel structures and cavities with embedded

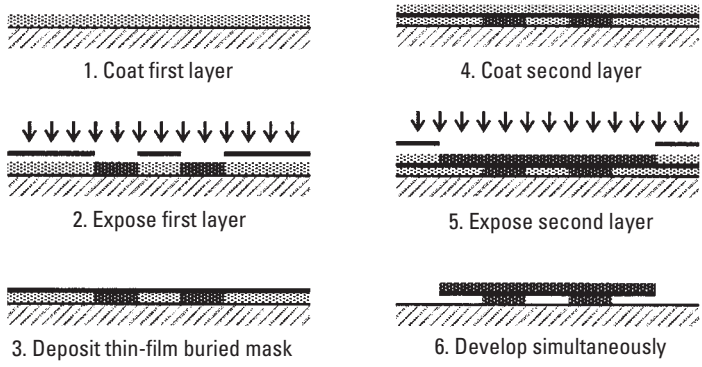

Figure 5.5 Fabrication of multilevel features using a buried mask between layers.

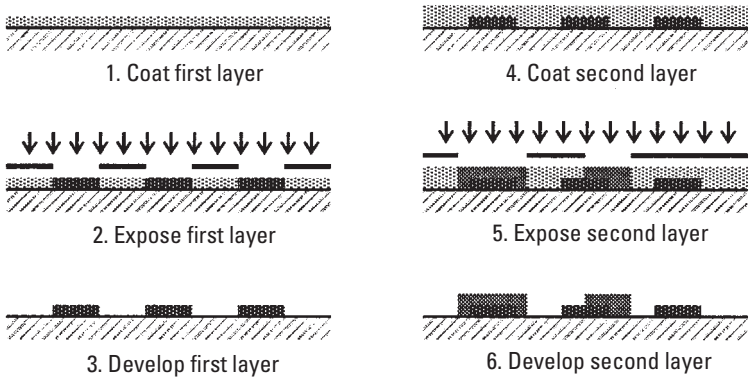

Figure 5.6 Fabrication of multilevel features by embedding prior features with a second photolithography step.

metal electrodes have been demonstrated using a polyethylene terephthalate (PET) carrier sheet for SU-8 [35]. Figure 5.7 shows a single channel fabricated by this dry-film method and a five-layer stack showing part of a 3D microchannel network. As opposed to lamination of prepatterned layers, performing UV exposure to define features after lamination provides better accuracy because photolithography generally has finer control over alignment than physical alignment of material sheets.

Flat inclined surfaces can be fabricated by coating thick photoresist materials on tilted substrates and allowing them to flow under gravitational forces [36] before curing. Finer inclined features can be patterned by altering the angle between substrate and light source, and it has been possible to pattern complex micromesh structures inside microchannels (as featured in Chapter 2) for applications such as microchannel filtering [37]. The size and shape of cavities throughout the mesh are more deterministic than other strategies for filtering, such as the use of packed particles.

Grayscale lithography methods, either with semiopaque masks or variable energy dose, can be used to fabricate gradient slopes and even rounded profiles [38, 39]. If the focal depth can be sufficiently controlled, complex shapes like the bent pipe shown in Figure 5.8 [40] can be fabricated by directing the path of a laser beam within a volume of photosensitive liquid polymer.

There are still other approaches to fabricating three-dimensional structures by novel sequences of photopatterning, but the examples above cover many of the fundamental concepts. These sequences become even more enabling when the photopatterned structure is not the final result, but rather used as a 3D tool for making replica components in another material. The replication step makes it possible to design locally shallow cavities, patterns on top of plateaus and mesas, and other innovative features [41]. The transfer of geometric features

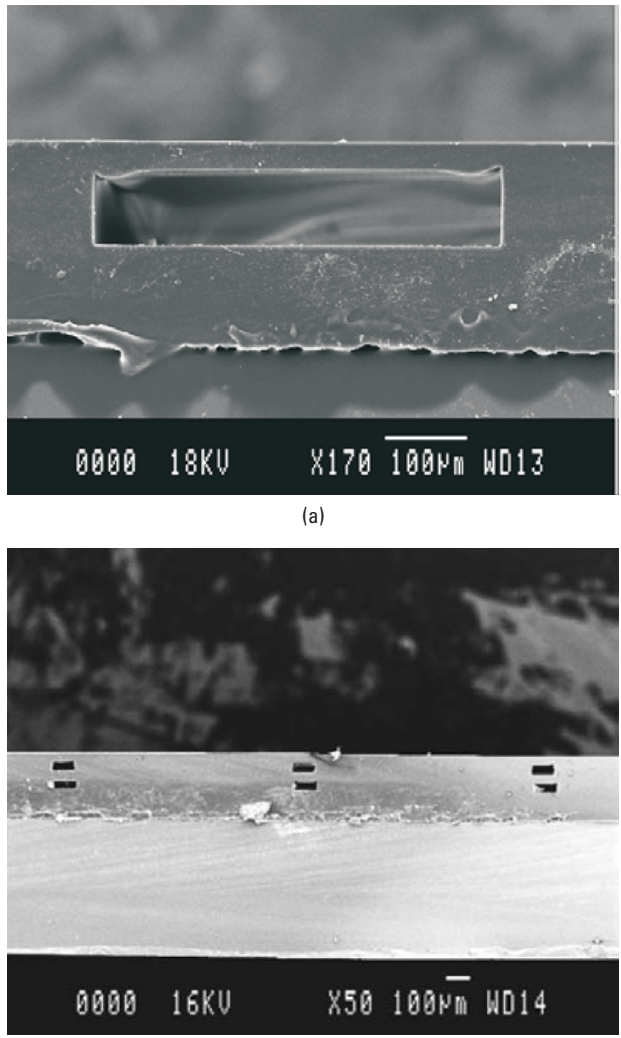

Figure 5.7 Fabrication of moltlithic 3D microfluidic structures based on photocurable dry films. (a) A single channel fabricated by a dry-film method. (b) A five-layer stack showing part of a 3D microchannel network. (Reprinted from [35], with permission from IOP Publishing.)

from a master to another material not only has the benefits of shape transfer, but perhaps more importantly opens the door to a tremendous variety of other materials and corresponding material properties. Discussed next are several fabrication processes that, like photopolymerization, are based on material solidification, but do so by achieving phase change in other ways.

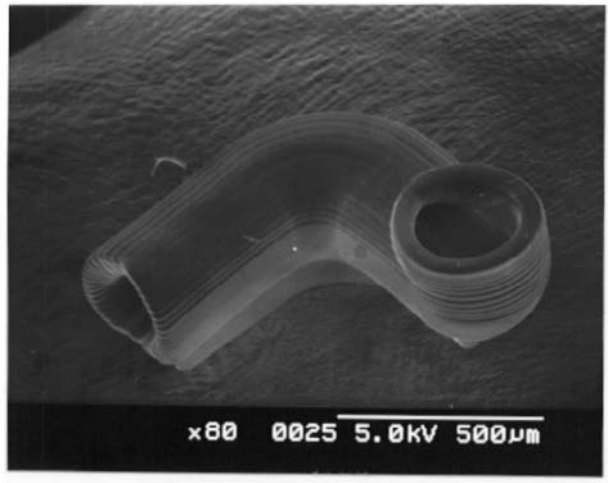

Figure 5.8 Three-dimensional micropipe fabricated by UV laser induced polymerization. (Reprinted from [40], with permission from IOP publishing.)

5.2 Casting and Molding

Like the radiation-selective solidification processes discussed above, casting and molding are processes that convert a material in a relatively fluid state into a more permanent solid form. Casting and UV curing are not mutually exclusive because UV activation of a photoinitiator can be an important mechanism that allows a material to change from liquid to solid phase. However, a distinction between this section of the chapter and the radiation-selective polymerization processes discussed earlier is that casting and molding depend primarily on the physical shape of molds to define geometric features. In contrast, the radiation-selective polymerization processes described above define geometric features based on the patterns in photomasks or the paths traversed by focused energy beams.

Common to either casting or molding is the need to pattern a shape-defining master. Quality metrics such as resolution and aspect ratio for cast and molded structures are ultimately limited by the master [42]. SU-8 masters fabricated by conventional photolithography can typically achieve features as small as ~1 μm. Finer features on the order of 100 nm can be patterned by other methods such as a lift-off process for evaporated titanium onto e-beam patterned PMMA [43]. Relatively coarse patterns with line widths of approximately 100 μm can even be produced quickly and inexpensively by less common methods such as the use of laser printing onto printed circuit board (PCB) substrates [44].

A natural question that comes to mind when discussing casting and molding is: What is the difference between a casting process and a molding process? Indeed, both processes result in similar net-shape changes of material. The names have in some ways have been inherited from analogous macroscale manufacturing processes like sand casting of metals and injection molding of plastics. One functional distinction that can be applied is to describe casting as a process that does not involve active pressurization or positive driving forces. So a process in which an uncured polymer is poured over a master relief pattern would be described as casting. In contrast, molding would more appropriately describe if a plate were used to press the uncured polymer onto the same master under a controlled load. Injection molding fits well into this distinction because clearly the flowing material is driven into a shaped cavity under significantly high pressure. Related macroscale processes that align with this distinction include compression molding and transfer molding [45]. However, die casting of metal is fundamentally almost identical to injection molding of plastic, and replica molding is arguably better described as secondary casting. So a distinction based on the presence of absence of particular driving forces is clearly imperfect. Accordingly, in this book there will not be any rigorous attempt to draw firm lines between what is named casting versus molding, and in general nomenclature will be propagated simply as encountered in published literature, even if imperfectly categorized.

A very important practical consideration for casting and molding is mold release. The same issue is also vitally important for embossing and imprinting as well. With potentially strong surface adhesion and geometrically delicate features, high aspect ratio and fine resolution are not useful if the cast material cannot be removed from the master without damage. A relatively drastic solution to releasing fragile objects is to destroy the master by completely etching it away. It is often more preferable to preserve the master for reuse by applying an appropriate surface treatment to facilitate mold release. Silanization by exposure to triridecafluorooctyl trichlorosilane vapor is an effective method for releasing complex PDMS structures after casting upon SU-8 features on silicon [46]. Other examples of release agents that have been used include fluouropolymers by spin coating [47] and plasma processing [48], as well as self-assembled monolayers (SAMs) coated by immersion in organo-silicon solution [49]. Still other chemicals such as the heptanes-based Sigmacote offer some limited enhancement to ease of mold release, but the difficulty of separating a rigid cast material from a rigid master is one of the major motivating factors for using an intermediate mold in a secondary casting process, rather than casting the final material directly onto the primary master [50]. The basic process of casting will be discussed next, followed by replica molding and other molding processes.

5.2.1 Primary Casting

Casting is such a flexible process because it applies to any material that can be solidified in a shaped cavity. The basic process is relatively straightforward as illustrated in Figure 5.9. A master is fabricated by some prior method of patterning, with some options discussed further below. As discussed previously, a release agent may be necessary to facilitate mold separation. A material in liquid form (typically an uncured polymer resin) is poured onto the master and allowed to cure. After curing, the newly shaped solid material is separated from the master. Cast materials may exhibit significant shrinkage, but proper characterization of the magnitude and corresponding adjustment in the design of the master may be used to compensate [51].

The word primary is used in front of the word casting to convey that the final product is made in one step from its original master. This would be distinct from secondary casting, in which the first casting from a master is used as the mold for another material that will eventually be used in the final microfluidic device. Secondary casting will be discussed in the next section under the name replica molding. The distinction can just as well be made with the words direct and indirect casting [52] with the same understanding.

A common example of primary casting is the fabrication of a PDMS microfluidic chip made by curing from a two-part mixture over photopatterned SU-8 features on a silicon wafer [53]. PDMS is favorable for casting because it flows very freely prior to curing, reproduces fine features with high fidelity, and attains high mechanical resiliency after curing. SU-8 is often chosen as a rapid and convenient method of producing required topographical features. The relative merits of SU-8 are based on its conveniently fast processing with near vertical wall and high aspect ratio, rather than exceptionally fine lateral resolution. Other methods of fabricating a master include etching silicon or electroplating metal.

In cases for which very fine lateral dimensions are required, other methods of establishing relief patterns may be preferable. For example, titanium lines by physical vapor deposition and lift-off has been used to cast PDMS channels with

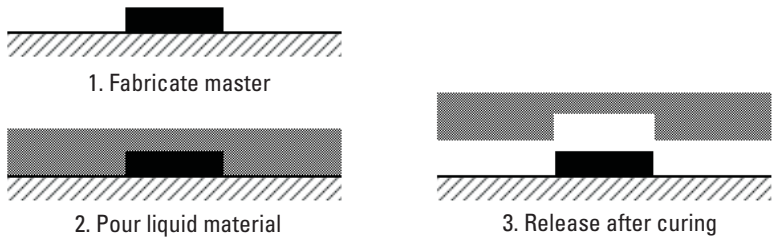

Figure 5.9 Primary casting process steps.

less than 500 nm wide and less than 100 nm deep [54]. Metal lines can be patterned in submicron dimensions with relative ease using e-beam lithography and high-resolution resists based on PMMA.

If the master is patterned using a thermoplastic material, reflow of patterned features under heated conditions can be used as a way to produce rounded cavities in the mold. The basic concept of producing smooth rounded features is shown in Figure 5.10. Such a method has been used to produce cavities for stimulation and lysis of epithelial cells under more uniformly loaded membrane compression that would otherwise not be achievable using rectangular cavities [55].

Casting facilitates the incorporation of a wide variety of functional components within a microfluidic device [56]. Unlike spin-coating, casting can be used quite easily over relatively tall existing structures, and this ability is useful for embedding functional components such as plated metal coils for electromagnetic actuation [57]. As another example, casting makes it readily possible to fabricate devices with embedded shape memory alloy wire for electronic control of microfluidic valve arrays [58].

Viscosity and removal of trapped gas constrain the aspect ratio of features that can be cast. Many polymers require degassing under vacuum to remove gaseous byproducts of the reactions during curing. The other important role of vacuum is to overcome surface forces while filling narrow cavities. In macroscale manufacturing, the name vacuum casting is sometimes necessary to state explicitly that the process is being assisted by vacuum. For microfluidic dimensions, however, it is almost an implicit assumption that vacuum is involved because forces related to viscosity and surface tension are always very significant in

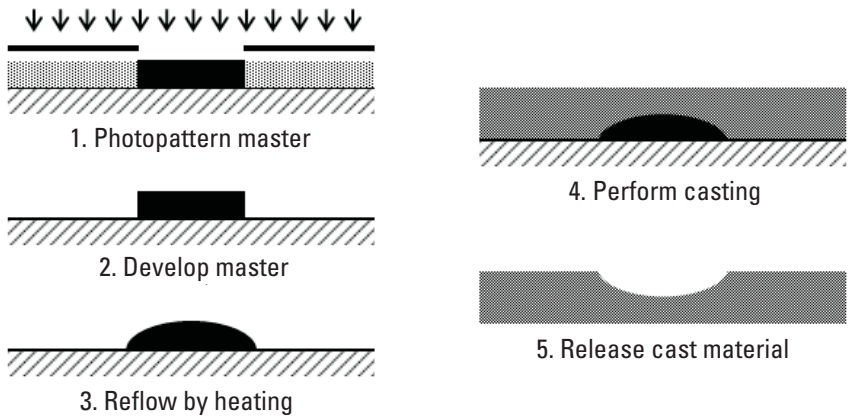

Figure 5.10 Casting of concave rounded features by thermoplastic reflow of features in the master.

microscale (as emphasized in Chapter 1). With proper combinations of thinning solvent, curing conditions, and vacuum degassing, however, it has been shown that PDMS can be cast into narrow trenches 12 μm deep and 0.5 μm wide for an impressive aspect ratio of 24:1 [59]. Especially for long, narrow structures, vacuum can play an important role for filling cavities with high fidelity [60].

A unique advantage of casting in small confined regions is that meniscus effects of liquid in confined cavities can be used to fabricate self-rounding shapes. If an inverted trough is placed in contact with a liquid layer material and wetting characteristics are compatible, surface tension will cause the liquid to move upward into the trough cavity and form a rounded meniscus. Allowing the liquid to cure in place will result in a half-rounded cavity. Extending this principle to draw liquid into a narrow cavity simultaneously from two opposing sides can produce fully rounded cavity. Examples of this innovative approach are shown in Figure 5.11.

5.2.2 Replica Molding

In contrast to primary casting discussed above, in this book *replica molding* will refer more narrowly to reproducing geometric features on a master by first casting a mold of an intermediate material, followed by a secondary casting step in that mold to produce the final component(s). Some instances in the published

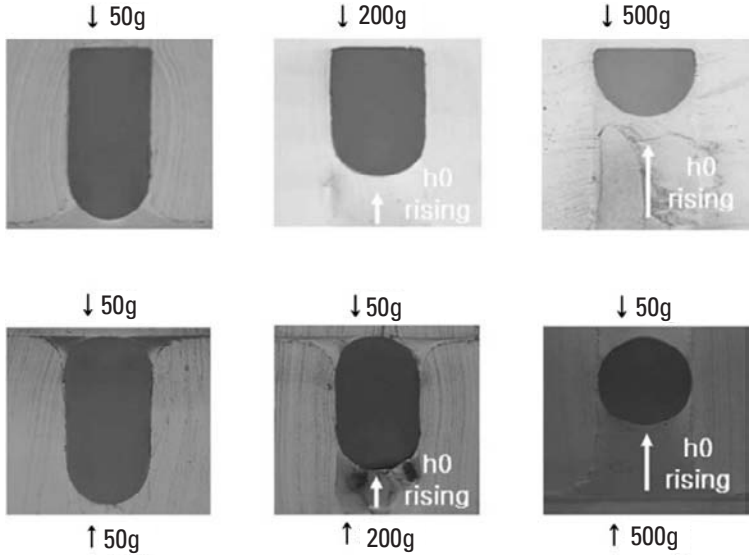

Figure 5.11 Rounded cavities formed by drawing liquid polymer into confined regions under surface tension before curing. (Reprinted from [61], with permission from IOP Publishing.)

literature refer more broadly to replica molding as inclusive of primary casting, but here replica molding will more descriptively be limited to reproduction of a positive image with the aid of an intermediate mold.

Replica molding, illustrated in Figure 5.12, is one of the most common variants of soft lithography, and PDMS is the predominant material used for the intermediate mold. PDMS is favorable for use as the intermediate mold because of its flexibility, mechanical resilience, a chemical stability. As is the case for primary casting discussed previously, the original master may be defined using any of a wide variety of processes including photolithography, etching, electroplating, and so on.

The primary master almost always represents the most time intensive and expensive part of the overall process. It may require specialized upstream processes such as electron-beam writing and/or multistep sequences such as metal film vapor deposition and lift-off. However, once a high-quality master is produced, several intermediate molds can be cast and from those several molds many more replicas can be fabricated. Facility requirements for the latter steps are also much less demanding, because clean room conditions are generally not required. Accordingly, the productivity and cost benefits of replica molding are very significant.

In addition to manufacturing cost, another major advantage of replica molding is the freedom to replicate a pattern with almost any material that can be readily changed from liquid to solid. Materials such as polyurethane-methacrylate (PUMA) can readily be cast in PDMS molds, and such a material is favorable not only for its mechanical and optical properties but also other important considerations such as compliance with regulatory standards for medical devices [62]. Ceramics, metals, and virtually any material that is available in

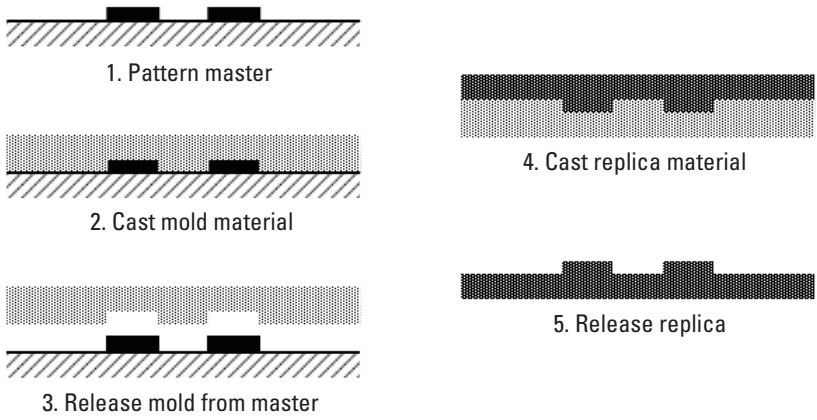

Figure 5.12 Replica molding process steps.

fine powder can be patterned into structures by mixing into suspensions and casting in soft molds. For example, micron-scale aluminum oxide has been demonstrated using PDMS molds [63]. After drying out the carrier liquid and removing from the soft mold, a sintering step would typically be used to eliminate porosity and achieve full density. Glass paste and bismuth alloys are other examples of less common materials that have been made by replica molding [64]. In such cases it is especially favorable to have the mold be made of a flexible material to facilitate ease of removing the material that has been cast in it. The analogous process for macroscopic part fabrication is typically described as soft tooling.

The concept of using thermoplastic reflow to produce rounded cavities was introduced previously in the discussion of casting. In replica molding, another way to produce similar cavities with rounded profiles is to take special advantage of the very high compliance that is characteristic of materials like PDMS. If the intermediate mold for replica molding is elastomeric, novel molds with air cavities underneath the exposes surfaces can be pressurized to cause membrane deformation and thereby attain shapes with rounded surface contours, and the curvature can be tuned by the level of pressurization [65, 66]. The kinds of shapes that can be produced by membrane pressurization are roughly similar to those that can be fabricated by thermoplastic reflow, but in principle they can be customized with negative pressure as well as positive pressure behind the membrane.

5.2.3 Microinjection Molding

Injection molding is a process used for a wide variety of microfluidic devices [67]. Injection molding can handle a diverse set of polymer materials, including conductive polyimide that can provide both electrical and mechanical functionality in microfluidic valves [68]. Like casting and replica molding, injection molding requires a master to determine the geometric features that are to be defined. The word injection, however, implies that the material is introduced from a compartment that is distinct from the mold cavity. The material is forced by a hydraulic ram into a cavity that is held closed during the injection step.

In the published literature, the coined phrase microinjection molding is often used to distinguish it from conventional macro injection molding. Although this distinction in wording is not emphasized in this book, what must be clearly acknowledged is that process considerations are not limited to just scale-down of equipment and tooling. In particular, scaling laws associated with such factors as viscosity dependence and heat transfer make microinjection molding significantly more challenging [69].

5.2.4 Compression Molding

Compression molding is a process very similar to injection molding, differing primarily on how the material is introduced into the mold cavity. In compression molding the material may be placed between compression die by any suitable method, and the die surfaces may move from a separation position to a tightly mated closed position. This positioning of die facilitates various options for multilevel planar alignment as well as the control over the thickness of membrane structures between die [70].

Compression molding shares similarities with other process such as hot embossing and imprint lithography, discussed in the next section. The main functional distinction is that the latter processes are generally used to describe thermoplastic reshaping, whereas traditionally compression molding is associated with thermoset polymers. A less fundamental distinction is that compression molding is most often associated with simultaneous shaping on opposing sides of a material (or even isostatically distributed pressure), whereas embossing and imprinting are more frequently associated with geometric reshaping applied to only one side. These distinctions in process naming are not absolute, however, because compression molding is sometimes used with thermoplastics as well as thermosets. Compression molding has been used to fabricate microfluidic chips in cyclic olefin copolymer (COC) with over 80 channels in close parallel arrangement for 2D protein separation [71], and the thermoplastic nature of COC materials is a merit that makes them attractive for high-volume manufacturing.

5.3 Thermoplastic Reshaping

This category of solidification processes focuses on processes that fundamentally involve reshaping from one dimensionally stable form to another. Processes such as hot embossing and imprint lithography are based on heating and plastic deformation of an otherwise dimensionally stable substance into a new shape. A broader set of thermoplastic molding processes [72] including injection molding and compression molding can very well be included in this category. However, as those processes can include thermoset resins, and were already discussed in a previous context above, the remainder of this section focuses primarily on the processes of hot embossing, imprint lithography, and thermoforming. A novel but less common method that is worth mentioning is the development of so-called shrink-dink microfluidics [73]. In this approach, sheets of polystyrene that are biaxially prestressed exhibit shrinkage upon heating. Geometric features such as scribe marks not only attain reduced dimensions laterally, but increase depth to form microchannels as the substrate sheet undergoes anisotropic shrinkage.

5.3.1 Hot Embossing

Hot embossing is a process in which a master, or stamp, uses mechanical pressure and heat to plastically deform a substrate material. The basic process is illustrated in Figure 5.13. A thermoplastic material is prepared (typically on a rigid substrate) and a patterned master is mated against it with heat and pressure to emboss features by plastic deformation. Spacers and other alignment features (not shown) are typically used to assure accurate positioning.

Hot embossing applies to almost any thermoplastic material and has been investigated for materials including polycarbonate (PC), polymethyl methacrylate (PMMA), and polyvinyl butyral (PVB) [74], as well as lower-temperature polymers such as poly(ethylene terephthalate) (PET) [75]. Although technically the process would not exactly be categorized as thermoplastic reshaping per se, PDMS can also be patterned by embossing techniques before complete curing occurs [76].

Hot embossing masters may be fabricated from a variety of materials including etched silicon, plated metal, and even some photoresists. Some of the many factors to consider for embossing material selection are thermal expansion compatibility, surface roughness, wear degradation, and ease of separation [77]. Most embossing masters tend to be flat, but using cylindrical rollers as an alternative offers the potential for higher manufacturing throughput and more consistent separation from the thermoplastic material [78].

Hot embossing is generally faster than casting because the process is readily automated and complete phase-change from liquid to solid is not required. In many case hot embossing may be able to fabricate features very similar to microinjection molding [79], although injection molding is recognized as having greater flexibility with complex geometric shapes.

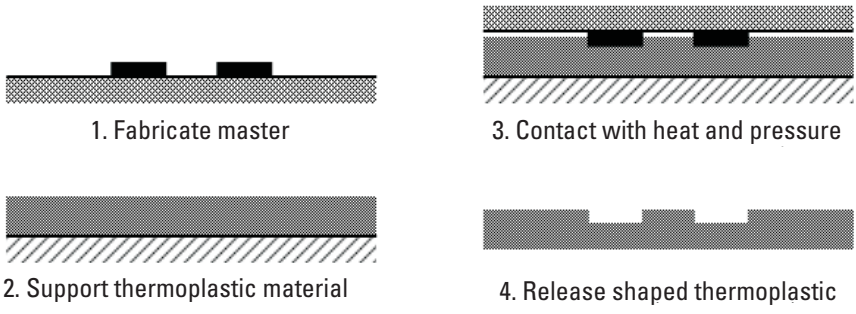

Figure 5.13 Hot embossing process steps.

5.3.2 Nanoimprint Lithography

Nanoimprint lithography (NIL) is a method of patterning a thermoplastic material with submicron resolution, even finer than 25 nm [80]. Although the characteristic dimensions are generally much smaller than those typically made by hot embossing, the deformation aspects of NIL are fundamentally no different. The more basic distinction between NIL is that the purpose if NIL is to define a pattern (hence the name lithography), whereas the purpose of embossing is to alter the geometry of a substrate. Accordingly, NIL typically implies that defined features penetrate the entire depth of a resist layer, whereas the depth of features for hot embossing is typically only a fraction of the material thickness. The process steps shown in Figure 5.14 are very similar to embossing, with the addition of a plasma etch step to clear the residual thinned regions to expose the substrate underneath. In a typical implementation of NIL, the master would be patterned in silicon dioxide by electron beam lithography, and then used to imprint features in a thermoplastic thin film of PMMA [81].

PMMA is well known for exhibiting fine feature resolution and is thus a popular choice of material for imprint lithography. Other materials such as COC have advantages in terms of being highly resistant to polar solvents, acids, and bases [82]. Still other options such as some commercial e-beam resists may be preferable for merits such as having lower glass transition temperature or higher etch resistance than PMMA [83].

The submicron dimensions produced by NIL are generally much smaller than characteristic dimensions of microfluidic chips features. However, NIL does provide complementary functionality. For example, for DNA electrophoresis, NIL has been use to superimpose a nanoscale pillar array with posts of 150

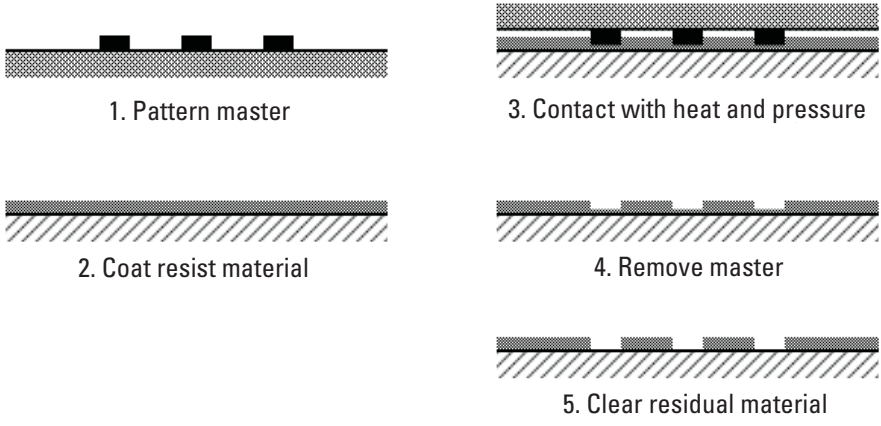

Figure 5.14 Process steps for nanoimprint lithography.

nm diameter and 200 nm depth on the surfaces of microchannels with a 50-μm width and a 10-μm depth [84].

The earliest masters (also called stamps) for NIL were based on patterned thin films on silicon substrates. However, some polymers including SU-8 are also viable, as long as the glass transition temperature and dimensional stability is sufficiently higher than the material to be imprinted. Furthermore, if the polymer to be used as the master is a fully cross-linked thermoset, the matter of softening under glass transition temperature is far less of a concern. The fine spatial control of e-beam exposure on negative-acting resist materials makes it possible to customize profiles of NIL masters [85]. Not only can polymers be patterned on rigid substrates directly, but by casting or molding, it is even possible to have NIL stamps be made entirely of a plastic material [86]. Cost-effective secondary masters in PDMS can be made by casting from an etched silicon master, and have been demonstrated with NIL resolution as fine as 50 nm [87].

As is the case for any molding or imprinting technique, separation of the master from the patterned thermoplastic is an important practical consideration. Some options for applying antisticking layers include plasma deposition of C_4F_8 fluorocarbon film and vapor phase deposition of long fluorocarbon films, with more durable performance observed using the latter [88].

5.3.3 Thermoforming

Thermoforming is another basic thermoplastic deformation process that begins with sheet material and deforms it into a shaped cavity or over a mold pattern [89]. In macroscale product manufacturing, thermoforming is commonly used for making shallow or hollow shapes used, for example, in simple enclosures and food packaging. The extent of material flow for the sheet material is generally less than hot embossing and much less than injection molding. One of the factors that limit the more widespread use of thermoforming for microfluidic devices is that features tend to have only mild aspect ratio and are more limited in shape complexity than injection molding, hot embossing, or imprint lithography. However, thermoforming is relatively fast and inexpensive, offering relative merits from a volume manufacturing viewpoint. It can even be produced on reels of thermoplastic sheets, and furthermore thin-film metal electrodes can be integrated into the process [90].

5.4 Tabulated Examples of Solidification Processes

Table 5.1 lists several examples of microfabrication processes that are based on solidification or reshaping of material. The contents are by no means comprehensive, but do attempt to sample a variety of processes that have been used for

microfluidic devices. A small number of table entries may be based on other microfabricated structures not specifically for fluidic devices per se, but are included to encompass the diversity of materials and processes that can potentially be used.

Table 5.1 lists the basic process by which material is solidified or reshaped, the particular materials used, and the general type of master that is used to define the geometry. Some attempt is made to group similar processes, although in some cases the distinctions are subject to interpretation. Furthermore, within each cluster of processes, the more conventional materials and individual processes are generally listed first, followed by less conventional or relatively novel alternatives.

Table 5.1
Examples of Microfabrication Solidification Processes

Solidification Process	Material	Master	Reference
UV polymerization	Polyurethane-methacrylate	PDMS mold from etched silicon	[91]
UV polymerization	Perfluoropolyether	Photomask upon glass	[14]
UV polymerization	Hydrogel	PDMS/glass cartridge	[15]
UV laser irradiation	SU-8	(direct-write)	[30]
Proton beam irradiation	SU-8	(direct-write)	[24]
E-beam irradiation	SU-8	(direct-write)	[25]
Casting	PDMS	Reflow photoresist	[55]
Casting	PDMS	Photopatterned SU-8	[42]
Casting	PDMS	Evaporated Ti patterned by lift-off	[43]
Casting	PDMS	Photopatterned SU-8 on Si	[63]
Replica molding + sintering	Aluminum oxide	PDMS	[92]
Reflow molding	Polycaprolactone	Etched silicon	[93]
Injection molding	PMMA	Electroformed nickel from SU-8 mold	[79]
Injection molding	PMMA	Electroformed nickel from SU-8 mold	[94]
Injection molding	COC	Etched silicon and sacrificial Al wire	[70]
Compression molding	PDMS	Photopatterned SU-8	[71]
Compression molding	COC	Electroformed metal from Si master	[78]
Hot embossing	PMMA	Electroplated nickel roller	[95]

Table 5.1 (continued)

Solidification Process	Material	Master	Reference
Hot embossing	Polyurethane	Machined brass	[79]
Hot embossing	PMMA	Electroformed nickel from SU-8 mold	[74]
Hot embossing	Polycarbonate, polyvinyl butyral	Machined steel	[96]
Nanoimprint lithography	COC	RIE silicon	[77]
Nanoimprint lithography	COC	RIE silicon or photopatterned SU-8	[81]
Nanoimprint lithography	PMMA	Silicon dioxide on Si	[89]
Thermoforming	PET	PVD metal or machined metal	[90]
Thermoforming	Polystyrene	Machined brass	[73]
Thermoplastic shrinkage	Polystyrene	Mechanical scribing	[97]

References

[1] Aura, S., et al., "Novel Hybrid Material for Microfluidic Devices," *Sensors and Actuators B: Chemical*, Vol. 132, No. 2, 2008, pp. 397–403.

[2] Xia, Y., and G. M. Whitesides, "Soft Lithography," *Annual Review of Materials Science*, Vol. 28, No. 1, 1998, pp. 153–184.

[3] Love, J. C., J. R. Anderson, and G. M. Whitesides, "Fabrication of Three-Dimensional Microfluidic Systems by Soft Lithography," *MRS Bulletin*, Vol. 26, No. 7, 2001, pp. 523–528.

[4] Rogers, J. A., and R. G. Nuzzo, "Recent Progress in Soft Lithography," *Materials Today*, Vol. 8, No. 2, 2005, pp. 50–56.

[5] McDonald, J. C., et al., "Fabrication of Microfluidic Systems in Poly(Dimethylsiloxane)," *Electrophoresis*, Vol. 21, No. 1, 2000, pp. 27–40.

[6] Sia, S. K., and G. M. Whitesides, "Microfluidic Devices Fabricated in Poly(Dimethylsiloxane) for Biological Studies," *Electrophoresis*, Vol. 24, No. 21, 2003, pp. 3563–3576.

[7] Unger, M. A., et al., "Monolithic Microfabricated Valves and Pumps by Multilayer Soft Lithography," *Science*, Vol. 288, No. 5463, 2000, pp. 113–116.

[8] Choi, K. M., and J. A. Rogers, "Novel Chemical Approach to Achieve Advanced Soft Lithography by Developing New Stiffer, Photocurable PDMS Stamp Materials," *Materials Research Society*, Vol. 820, 2004.

[9] Nguyen, N. -T., et al., "Micro Check Valves for Integration into Polymeric Microfluidic Devices," *Journal of Micromechanics and Microengineering*, Vol. 14, No. 1, 2004, pp. 69–75.

[10] Seidemann, V., S. Butefisch, and S. Buttgenbach, "Fabrication and Investigation of In-Plane Compliant SU8 Structures for MEMS and Their Application to Micro Valves and Micro Grippers," *Sensors and Actuators, A: Physical*, Vol. 97-98, 2002, pp. 457–461.

[11] Jahanshahi, A., et al., "Enhanced UV-Assisted Vertical Etching of Polyethylene Terephthalate for Fabrication of Microsystems," *Journal of Micromechanics and Microengineering*, Vol. 19, No. 7, 2009, p. 074016.

[12] Abgrall, P., et al., "SU-8 as a Structural Material for Labs-on-Chips and Microelectromechanical Systems," *Electrophoresis*, Vol. 28, No. 24, 2007, pp. 4539–4551.

[13] Schomburg, W. K., and B. Scherrer, "3.5 μm Thin Valves in Titanium Membranes," *Journal of Micromechanics and Microengineering*, Vol. 2, No. 3, 1992, pp. 184–186.

[14] Willis, P. A., et al., "Monolithic Photolithographically Patterned Fluorocur PFPE Membrane Valves and Pumps for In Situ Planetary Exploration," *Lab on a Chip*, Vol. 8, No. 8, 2008, pp. 1024–1026.

[15] Beebe, D. J., et al., "Functional Hydrogel Structures for Autonomous Flow Control Inside Microfluidic Channels," *Nature*, Vol. 404, No. 6778, 2000, pp. 588–590.

[16] Lin, C. -H., et al., "A New Fabrication Process for Ultra-Thick Microfluidic Microstructures Utilizing SU-8 Photoresist," *Journal of Micromechanics and Microengineering*, Vol. 12, No. 5, 2002, pp. 590–597.

[17] Orhan, J. B., et al., "In Situ Fabrication of a Poly-Acrylamide Membrane in a Microfluidic Channel," *Microelectronic Engineering*, Vol. 85, No. 5-6, 2008, pp. 1083–1085.

[18] Love, J. C., et al., "Microscope Projection Photolithography for Rapid Prototyping of Masters with Micron-Scale Features for Use in Soft Lithography," *Langmuir*, Vol. 17, No. 19, 2001, pp. 6005–6012.

[19] Zhang, J., et al., "Polymerization Optimization of SU-8 Photoresist and Its Applications in Microfluidic Systems and MEMS," *Journal of Micromechanics and Microengineering*, Vol. 11, No. 1, 2001, pp. 20–26.

[20] Chan-Park, M. B., et al., "Fabrication of Large SU-8 Mold with High Aspect Ratio Microchannels by UV Exposure Dose Reduction," *Sensors and Actuators, B: Chemical*, Vol. 101, No. 1-2, 2004, pp. 175–182.

[21] Dentinger, P. M., et al., "High Aspect Ratio Patterning with a Proximity Ultraviolet Source," *Microelectronic Engineering*, Vol. 61-62, 2002, pp. 1001–1007.

[22] Yu, H., et al., "Fabrication of Three-Dimensional Microstructures Based on Single-Layered SU-8 for Lab-on-Chip Applications," *Sensors and Actuators, A: Physical*, Vol. 127, No. 2, 2006, pp. 228–234.

[23] Chen, K.-S., I.-K. Lin, and F.-H. Ko, "Fabrication of 3D Polymer Microstructures Using Electron Beam Lithography and Nanoimprinting Technologies," *Journal of Micromechanics and Microengineering*, Vol. 15, No. 10, 2005, pp. 1894–1903.

[24] Tay, F. E. H., et al., "Novel Micro-Machining Method for the Fabrication of Thick-Film SU-8 Embedded Micro-Channels," *Journal of Micromechanics and Microengineering*, Vol. 11, No. 1, 2001, pp. 27–32.

[25] Koller, D. M., et al., "Three-Dimensional SU-8 Sub-Micrometer Structuring by Electron Beam Lithography," *Microelectronic Engineering*, Vol. 85, No. 7, 2008, pp. 1639–1641.

[26] Gersborg-Hansen, M., et al., "Combined Electron Beam and UV Lithography in SU-8," *Microelectronic Engineering*, Vol. 84, No. 5-8, 2007, pp. 1058–1061.

[27] Watt, F., et al., "Ion Beam Lithography and Nanofabrication: A Review," *International Journal of Nanoscience*, Vol. 4, No. 3, 2005, pp. 269–286.

[28] Monk, D. J., D. S. Soane, and R. T. Howe, "Hydrofluoric Acid Etching of Silicon Dioxide Sacrificial Layers. I. Experimental Observations," *J. of the Electrochem. Soc.*, Vol. 141, No. 1, 1994, pp. 264–269.

[29] Bohl, B., et al., "Multi-Layer SU-8 Lift-Off Technology for Microfluidic Devices," *J. of Micromechanics and Microengineering*, Vol. 15, No. 6, 2005, pp. 1125–1130.

[30] Yu, H., et al., "Building Embedded Microchannels Using a Single Layered SU-8, and Determining Young's Modulus Using a Laser Acoustic Technique," *Journal of Micromechanics and Microengineering*, Vol. 14, No. 11, 2004, pp. 1576–1584.

[31] Chuang, Y. -J., et al., "A Novel Fabrication Method of Embedded Micro-Channels by Using SU-8 Thick-Film Photoresists," *Sensors and Actuators A: Physical*, Vol. 103, No. 1-2, 2003, pp. 64–69.

[32] Ceyssens, F., and R. Puers, "Creating Multi-Layered Structures with Freestanding Parts in SU-8," *Journal of Micromechanics and Microengineering*, Vol. 16, No. 6, 2006, pp. S19–S23.

[33] Zhao, X. L., et al., "Modulated Wrinkle Patterns in a Gold Thin Film Deposited onto an Elastomeric Polymer," *Proceedings of SPIE—The International Society for Optical Engineering,* Harbin, China, Vol. 6423, 2007.

[34] Tsai, Y. -C., et al., "Fabrication of Microfluidic Devices Using Dry Film Photoresist for Microchip Capillary Electrophoresis," *Journal of Chromatography A*, Vol. 1111, No. 2, 2006, pp. 267–271.

[35] Abgrall, P., et al., "A Novel Fabrication Method of Flexible and Monolithic 3D Microfluidic Structures Using Lamination of SU-8 Films," *Journal of Micromechanics and Microengineering*, Vol. 16, No. 1, 2006, pp. 113–121.

[36] Choi, Y., K. Kim, and M. G. Allen, "Continuously-Varying, Three-Dimensional SU-8 Structures: Fabrication of Inclined Magnetic Actuators," *15th IEEE International Conference on Micro Electro Mechanical Systems*, 2002.

[37] Sato, H., et al., "A Novel Fabrication of In-Channel 3-D Micromesh Structure Using Maskless Multi-Angle Exposure and Its Microfilter Application," *IEEE 16th Annual International Conference on Micro Electro Mechanical Systems*, Kyoto, Japan, 2003.

[38] Totsu, K., et al., "Fabrication of Three-Dimensional Microstructure Using Maskless Gray-Scale Lithography," *Sensors and Actuators A: Physical*, Vol. 130-131, 2006, pp. 387–392.

[39] Kudryashov, V., et al., "Grey Scale Structures Formation in SU-8 with E-Beam and UV," *Microelectronic Engineering*, Vol. 67-68, 2003, pp. 306–311.

[40] Nakamoto, T., et al., "Manufacturing of Three-Dimensional Micro-Parts by UV Laser Induced Polymerization," *Journal of Micromechanics and Microengineering*, Vol. 6, No. 2, 1996, pp. 240–253.

[41] Chung, S., et al., "Multi-Height Micro Structures in Poly(Dimethyl Siloxane) Lab-on-a-Chip," *Microsystem Technologies*, Vol. 10, No. 2, 2004, pp. 81–88.

[42] Natarajan, S., D. A. Chang-Yen, and B. K. Gale, "Large-Area, High-Aspect-Ratio SU-8 Molds for the Fabrication of PDMS Microfluidic Devices," *Journal of Micromechanics and Microengineering*, Vol. 18, No. 4, 2008, p. 045021.

[43] Rust, M. J., S. Subramaniam, and C. H. Ahn, "Fabrication of Nanochannels with Microfluidic Interface Using PDMS Casting on Ti/Si Nanomold," *Nanotech 2005 Technical Proceedings*, 2005.

[44] Abdelgawad, M., et al., "Soft Lithography: Masters on Demand," *Lab on a Chip*, Vol. 8, No. 8, 2008, pp. 1379–1385.

[45] Kalpakjian, S., and S. Schmid, *Manufacturing Engineering and Technology*, 5th ed., Upper Saddle River, NJ: Prentice-Hall, 2005.

[46] Anderson, J. R., et al., "Fabrication of Topologically Complex Three-Dimensional Microfluidic Systems in PDMS by Rapid Prototyping," *Analytical Chemistry*, Vol. 72, No. 14, 2000, pp. 3158–3164.

[47] Cheng, M. C., et al., "Dry Release of Polymer Structures with Anti-Sticking Layer," *Journal of Vacuum Science and Technology A: Vacuum, Surfaces and Films*, Vol. 22, No. 3, 2004, pp. 837–841.

[48] Haefliger, D., et al., "Dry Release of All-Polymer Structures," *Microelectronic Engineering*, Vol. 78-79, 2005, pp. 88–92.

[49] Kim, B. J., et al., "A self-Assembled Monolayer-Assisted Surface Microfabrication and Release Technique," *Micro-and Nano- Engineering 2000 (MNE 2000)*, Vol. 57-58, Jena, Germany, 2001.

[50] Chiang, Y. M., et al., "Characterizing the Process of Cast Molding Microfluidic Systems," *Proceedings of the SPIE*, Santa Clara, CA, Vol. 3877, 1999.

[51] Lee, S., and S. Lee, "Shrinkage Ratio of PDMS and Its Alignment Method for the Wafer Level Process," *Microsystem Technologies*, Vol. 14, No. 2, 2008, pp. 205–208.

[52] Thian, S. C. H., et al., "Fabrication of Microfluidic Channel Utilizing Silicone Rubber with Vacuum Casting," *Microsystem Technologies*, Vol. 14, No. 8, 2008, pp. 1125–1135.

[53] Duffy, D. C., et al., "Rapid Prototyping of Microfluidic Systems in Poly(dimethylsiloxane)," *Analytical Chemistry*, Vol. 70, No. 23, 1998, pp. 4974–4984.

[54] Rust, M. J., S. Subramaniam, and C. H. Ahn, "Fabrication of Nanochannels with Microfluidic Interface Using PDMS Casting on Ti/Si Nanomold," *NSTI Nanotech 2005 Technical Proceedings*, Anaheim, CA, 2005.

[55] Kim, Y. C., et al., "Microfluidic Biomechanical Device for Compressive Cell Stimulation and Lysis," *Sensors and Actuators B: Chemical*, Vol. 128, No. 1, 2007, pp. 108–116.

[56] Ng, J. M. K., et al., "Components for Integrated Poly(Dimethylsiloxane) Microfluidic Systems," *Electrophoresis*, Vol. 23, No. 20, 2002, pp. 3461-3473.

[57] Yin, H. -L., et al., "A Novel Electromagnetic Elastomer Membrane Actuator with a Semi-Embedded Coil," *Sensors and Actuators A: Physical*, Vol. 139, No. 1-2, 2007, pp. 194–202.

[58] Vyawahare, S., et al., "Electronic Control of Elastomeric Microfluidic Circuits with Shape Memory Actuators," *Lab on a Chip*, Vol. 8, No. 9, 2008, pp. 1530–1535.

[59] Lau, G. K., et al., "Actuated Elastomers with Rigid Vertical Electrodes," *Journal of Micromechanics and Microengineering*, Vol. 16, No. 6, 2006, pp. S35–S44.

[60] Zhao, Y., and H. Zeng, "Fabricating Non-Photodefinable Polymer Microstructures for Micro-Total-Analysis," *Sensors and Actuators, B: Chemical*, Vol. 139, No. 2, 2009, pp. 673–681.

[61] Lee, K., et al., "Fabrication of Round Channels Using the Surface Tension of PDMS and Its Application to a 3D Serpentine Mixer," *J. of Micromechanics and Microengineering*, Vol. 17, No. 8, 2007, pp. 1533–1541.

[62] Kuo, J. S., et al., "A New USP Class Vl-Compliant Substrate for Manufacturing Disposable Microfluidic Devices," *Lab on a Chip*, Vol. 9, No. 7, 2009, pp. 870–876.

[63] Zhu, Z., X. Wei, and K. Jiang, "A Net-Shape Fabrication Process of Alumina Micro-Components Using a Soft Lithography Technique," *Journal of Micromechanics and Microengineering*, Vol. 17, No. 2, 2007, pp. 193–198.

[64] Chung, S., et al., "Microreplication Techniques Using Soft Lithography," *Microelectronic Engineering*, Vol. 75, No. 2, 2004, pp. 194–200.

[65] Hongbin, Y., et al., "Novel Polydimethylsiloxane (PDMS) Based Microchannel Fabrication Method for Lab-on-a-Chip Application," *Sensors and Actuators B: Chemical*, Vol. 137, No. 2, 2009, pp. 754–761.

[66] Go, J. S., and S. Shoji, "A Disposable, Dead Volume-Free and Leak-Free In-Plane PDMS Microvalve," *Sensors and Actuators, A: Physical*, Vol. 114, No. 2-3, 2004, pp. 438–444.

[67] Attia, U., S. Marson, and J. Alcock, "Micro-Injection Moulding of Polymer Microfluidic Devices," *Microfluidics and Nanofluidics*, Vol. 7, No. 1, 2009, pp. 1–28.

[68] Goll, C., et al., "An Electrostatically Actuated Polymer Microvalve Equipped with a Movable Membrane Electrode," *Journal of Micromechanics and Microengineering*, Vol. 7, No. 3, 1997, pp. 224–226.

[69] Giboz, J., T. Copponnex, and P. Mélé Patrice, "Microinjection Molding of Thermoplastic Polymers: A Review," *Journal of Micromechanics and Microengineering*, Vol. 17, No. 6, 2007, pp. R96–R109.

[70] Lucas, N., et al., "An Improved Method for Double-Sided Moulding of PDMS," *Journal of Micromechanics and Microengineering*, Vol. 18, No. 7, 2008, p. 075037.

[71] Fredrickson, C. K., et al., "Effects of Fabrication Process Parameters on the Properties of Cyclic Olefin Copolymer Microfluidic Devices," *Journal of Microelectromechanical Systems*, Vol. 15, No. 5, 2006, pp. 1060–1068.

[72] Heckele, M., and W. K. Schomburg, "Review on Micro Molding of Thermoplastic Polymers," *Journal of Micromechanics and Microengineering*, Vol. 14, No. 3, 2004, pp. R1–R14.

[73] Chen, C. -S., et al., "Shrinky-Dink Microfluidics: 3D Polystyrene Chips," *Lab on a Chip*, Vol. 8, No. 4, pp. 622–624.

[74] Juang, Y. -J., L. L. James, and K. W. Koelling, "Hot Embossing in Microfabrication. Part I: Experimental," *Polymer Engineering and Science*, Vol. 42, No. 3, 2002, pp. 539–550.

[75] Li, J. M., et al., "Hot Embossing/Bonding of a Poly(Ethylene Terephthalate) (PET) Microfluidic Chip," *Journal of Micromechanics and Microengineering*, Vol. 18, No. 1, 2008, p. 015008.

[76] Kloter, U., et al., "High-Resolution Patterning and Transfer of Thin PDMS Films: Fabrication of Hybrid Self-Sealing 3D Microfluidic Systems," *17th IEEE International Conference on Micro Electro Mechanical Systems*, Piscataway, NJ, 2004.

[77] Esch, M. B., et al., "Influence of Master Fabrication Techniques on the Characteristics of Embossed Microfluidic Channels," *Lab on a Chip*, Vol. 3, No. 2, 2003, pp. 121–127.

[78] Yeo, L. P., et al., "Micro-Fabrication of Polymeric Devices Using Hot Roller Embossing," *Microelectronic Engineering*, Vol. 86, No. 4-6, 2009, pp. 933–936.

[79] Chien, R. -D., "Micromolding of Biochip Devices Designed with Microchannels," *Sensors and Actuators A: Physical*, Vol. 128, No. 2, 2006, pp. 238–247.

[80] Chou, S. Y., P. R. Krauss, and P. J. Renstrom, "Imprint of Sub-25 nm Vias and Trenches in Polymers," *Applied Physics Letters*, Vol. 67, No. 21, 1995, pp. 3114–3116.

[81] Chou, S. Y., P. R. Krauss, and P. J. Renstrom, "Nanoimprint Lithography," *Journal of Vacuum Science & Technology B: Microelectronics and Nanometer Structures*, Vol. 14, No. 6, 1996, pp. 4129–4133.

[82] Nielsen, T., et al., "Nanoimprint Lithography in the Cyclic Olefin Copolymer, Topas, a Highly Ultraviolet-Transparent and Chemically Resistant Thermoplast," *Journal of Vacuum Science and Technology B: Microelectronics and Nanometer Structures*, Vol. 22, No. 4, 2004, pp. 1770–1775.

[83] Gourgon, C., C. Perret, and G. Micouin, "Electron Beam Photoresists for Nanoimprint Lithography," *Microelectronic Engineering*, Vol. 61-62, 2002, pp. 385–392.

[84] Pepin, A., et al., "Nanoimprint Lithography for the Fabrication of DNA Electrophoresis Chips," *Microelectronic Engineering*, Vol. 61-62, 2002, pp. 927–932.

[85] Chen, K. -S., I. -K. Lin, and F. -H. Ko, "Fabrication of 3D Polymer Microstructures Using Electron Beam Lithography and Nanoimprinting Technologies," *Journal of Micromechanics and Microengineering*, Vol. 15, No. 10, 2005, pp. 1894–1903.

[86] Pfeiffer, K., et al., "Polymer Stamps for Nanoimprinting," *Microelectronic Engineering*, Vol. 61-62, 2002, pp. 393–398.

[87] Koo, N., et al., "Improved Mold Fabrication for the Definition of High Quality Nanopatterns by Soft UV-Nanoimprint Lithography Using Diluted PDMS Material," *Microelectronic Engineering*, Vol. 84, No. 5-8, 2007, pp. 904–908.

[88] Bilenberg, B., et al., "Topas-Based Lab-on-a-Chip Microsystems Fabricated by Thermal Nanoimprint Lithography," *Journal of Vacuum Science and Technology B: Microelectronics and Nanometer Structures*, Vol. 23, No. 6, 2005, pp. 2944–2949.

[89] Dreuth, H., and C. Heiden, "Thermoplastic Structuring of Thin Polymer Films," *Sensors and Actuators, A: Physical*, Vol. 78, No. 2, 1999, pp. 198–204.

[90] Truckenmuller, R., et al., "Low-Cost Thermoforming of Micro Fluidic Analysis Chips," *Journal of Micromechanics and Microengineering*, Vol. 12, No. 4, 2002, pp. 375–379.

[91] Kuo, J. S., et al., "Microfabricating High-Aspect-Ratio Structures in Polyurethane-Methacrylate (PUMA) Disposable Microfluidic Devices," *Lab on a Chip*, Vol. 9, 2009, pp. 1951–1956.

[92] Armani, D. K., and C. Liu, "Microfabrication Technology for Polycaprolactone, a Biodegradable Polymer," *Journal of Micromechanics and Microengineering*, Vol. 10, No. 1, 2000, pp. 80–84.

[93] McCormick, R. M., et al., "Microchannel Electrophoretic Separations of DNA in Injection-Molded Plastic Substrates," *Analytical Chemistry*, Vol. 69, No. 14, 1997, pp. 2626–2630.

[94] Lippmann, J. M., E. J. Geiger, and A. P. Pisano, "Polymer Investment Molding: Method for Fabricating Hollow, Microscale Parts," *Sensors and Actuators A: Physical*, Vol. 134, No. 1, 2007, pp. 2–10.

[95] Stoyanov, I., et al., "Microfluidic Devices with Integrated Active Valves Based on Thermoplastic Elastomers," *Microelectronic Engineering*, Vol. 83, No. 4-9, 2006, pp. 1681–1683.

[96] Hansen, M., et al., "A Nanoimprinted Polymer Lab-on-a-Chip with Integrated Optics," *SPIE: The International Society for Optical Engineering*, Vol. 5872, 2005.

[97] Leech, P. W., "Hot Embossing of Cyclic Olefin Copolymers," *Journal of Micromechanics and Microengineering*, Vol. 19, No. 5, 2009, p. 055008.

6

Subtractive Processes

Subtractive processes (or equivalently, material removal processes) are perhaps the most intuitive among fabrication strategies, microscale or otherwise. For fabrication of microfluidic devices, subtractive processes are used frequently for defining a variety of cavities such as microchannels, wells, orifices, and plenums. Subtractive processes are also an essential part of patterning masks, defining master patterns, and shaping molds. Inheriting a wide variety of techniques from fabrication of silicon-based MEMS transducers, subtractive processes benefit from an extensive history of process knowledge. Especially as microfluidic applications have drawn increasing attention toward polymers, a wide variety of methods have been developed for selective removal of polymer materials as well.

Photoresists are engineered not only for high resolution in patterning, but also for resistance in etch environments. For example, most positive photoresists can withstand hydrofluoric acid, which is the most commonly used wet etchant for silicon dioxide films. Some photoresists exhibit adequate resistance against plasma chemistries, such as sulfur hexafluoride (SF_6) used to dry etch silicon. Figure 6.1 illustrates the use of patterned photoresist as a direct etch mask.

In many cases, photoresist is not the primary mask, but instead is used to pattern a thin layer of another material that may be even more effective. For example, while photoresist is capable of withstanding relatively short, mild etches of silicon and glass substrates, silicon nitride is superior for extended SF_6 plasma etching of silicon and gold is superior for HF wet etching of glass. Figure 6.2 illustrates the use of photolithography as an intermediate step for patterning a secondary mask in a thin film of another material.

The introductory section of this chapter draws a distinction between spatially serial and spatially parallel processes. Etching exposed regions of a wafer by

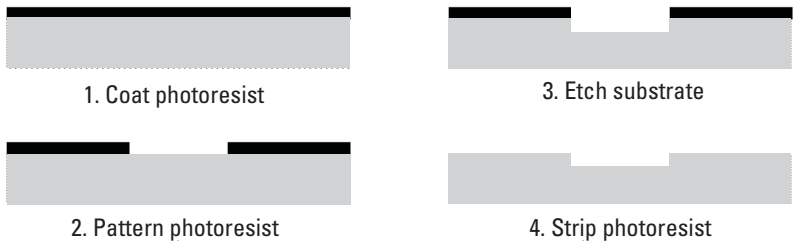

Figure 6.1 Patterned photoresist as a direct mask for etching a substrate.

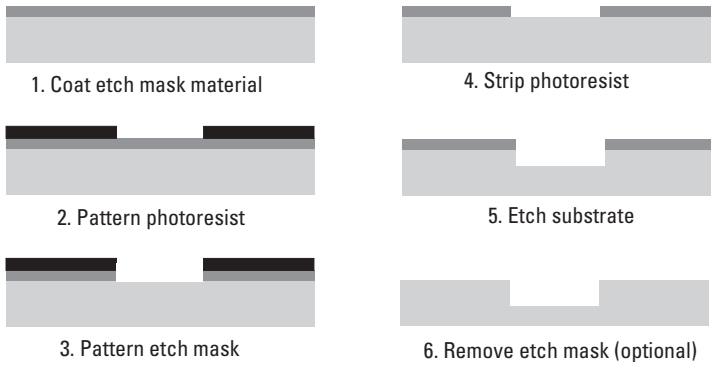

Figure 6.2 Using photolithography to pattern a thin-film etch mask.

wet chemical etching is an example of a spatially parallel process, while cutting grooves by laser ablation is an example of a spatially serial process. Even with just these two examples, there are a few other fundamental distinctions that can be drawn among subtractive processes for effectively understanding their relative merits and limitations.

A fundamental distinction among subtractive processes is the actual mechanism of material removal, whether physical or chemical. An erosion process such as abrasive jet cutting is a clear example of a physical removal mechanism. In contrast, wet etching in a caustic solution is chemically driven. Some processes such as reactive ion etching (RIE) often use a combination of both mechanisms. Whether a subtractive process is physical or chemical is an important factor that influences what combinations of materials are appropriate for achieving the required *selectivity* during the process. Selectivity for subtractive processes can be quantified as the ratio of material removal rates between two materials, as defined below. It is common in microfabrication to use the term etch selectivity, but in this book selectivity will be treated in the more general sense to include nonetch processes such as abrasive jet milling.

$$\text{Selectivity Ratio} = \frac{\text{Removal Rate for Material A}}{\text{Removal Rate for Material B}} \tag{6.1}$$

High selectivity is desirable for removing only the targeted material while preserving other device materials and maintaining the integrity of any mask layers. Figure 6.3 shows a few cases concerning selectivity issues. Ideally a subtractive process affects only a specific target material and does not deteriorate mask layers or remove other materials. However, with insufficient selectivity either the mask may deteriorate before the intended process is complete, or the subtractive process may continue too far into other materials. Extensive compilations of etch rates for a variety of materials and etch conditions are reported in [1, 2].

The term etch stop is used to describe an interface at which material removal terminates at a material boundary because of substantial selectivity between materials. The boundary may be two nonhomogeneous materials or more subtle changes such as a significant difference in dopant concentration. For some devices, a very convenient and deterministic way of setting an etch stop is to take advantage of the buried oxide layer in a silicon-on-insulator wafer [3]. One way of producing a buried oxide layer at a deterministic depth below the surface is to bond two silicon wafers with an oxide layer in between, then to etch away one of the wafers until only a designated thickness remains [4]. The remaining thickness can be a few microns or several tens of microns, depending on the application need. With appropriate masking, either the upper or lower wafer can be etched using a variety of methods as discussed below, and if the process is selective in a way that etches silicon much faster than oxide, the oxide serves as an effective etch stop.

Directionality is another very fundamental distinction for comparing subtractive processes, and it is often closely related to whether the removal mechanism is physical or chemical. The directionality of removal may be categorized as either *isotropic* (uniform in all directions) or *anisotropic* (preferential

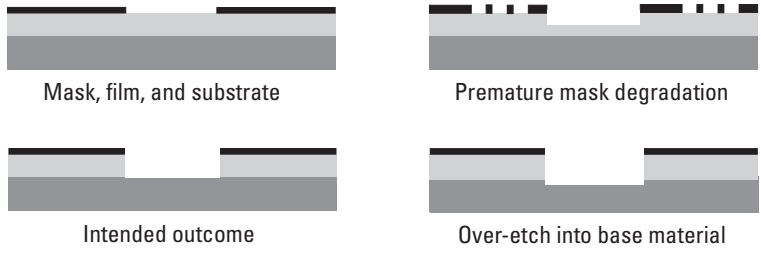

Figure 6.3 Selectivity issues for a material subtractive process, showing potential problems of premature mask degradation and over-etch into the base material.

in one direction over others). Physical subtractive processes depend on either momentum (e.g., heavy ion bombardment) or focused incident energy (e.g., laser ablation), and therefore tend to be anisotropic with fastest removal in the direction of highest momentum or energy density. Anisotropic profiles with very high aspect ratio have been very desirable for many MEMS devices, particularly those requiring tight clearance gaps or broad surface area between electrodes. In contrast, chemical subtractive processes depend on the thermodynamics and kinetics of reactions, and are typically isotropic unless material composition and/or crystallography dictate preferentially anisotropic results. In Chapter 2, some geometric profiles were illustrated based on their general shape (e.g., rectangular, rounded, or trapezoidal). The shapes of these profiles are consequences of directional control, and they are discussed further in the following sections on wet and dry etching.

In addition to the distinction between physical versus chemical mechanisms and anisotropic versus isotropic profiles, another helpful distinction is the environment in which material removal occurs. In some cases the substrates are immersed in a *wet* environment (i.e., a liquid bath). In others, the process may remain *dry*, conducted in ambient air, in a low-pressure vapor chamber, or in plasma (highly ionized gaseous state of matter). The relevance to feature geometry will be discussed later, but regardless of the features produced, the wet versus dry distinction has a very significant impact on factors such as production rate and chemical consumption. An advantage of wet immersion processes is that many units can be processed simultaneously (e.g., 100 wafers or more in a large etch bath), whereas the vacuum chambers needed for plasma etching are usually limited to either single wafers or small batches. Dry processing in vapor or plasma has the advantage of using significantly smaller quantities of chemicals that wet etching, and in general is less prone to contamination than processing in liquid baths.

The first two sections that follow describe wet etching and dry etching processes. Both types of etching are typically parallel in terms of spatial coverage because the entire substrate is subjected to the etch environment. Selectivity is normally achieved by using some form of masking that is patterned by photoresist or a hard mask with prescribed openings. Next, spatially serial subtractive processes based on the path of a focused energy beam are discussed, followed by a few methods of mechanical material removal based on abrasion or shearing of material.

6.1 Wet Etching

When a material is attacked by a liquid chemical etchant, in most cases material removal occurs in an isotropic fashion, uniformly in all directions. Material

removal rates for wet etching are often faster than rates for many dry etching processes, and these can be readily increased by elevated temperature or higher concentration of active species. There are two very notable exceptions to this generalization about isotropic profiles, anisotropic wet etching of silicon based on selectivity among crystal planes and anisotropic wet etching of photosensitive glass. In the subsections below, the more general case of isotropic wet etching is presented first, followed by the special circumstances under which wet etching can produce highly anisotropic profiles.

A variant on basic wet chemical etching discussed only briefly here is *electrochemical machining*, in which a metal is selectively patterned through exposed regions of a protective photoresist by an electrochemical removal process [5]. Copper, stainless steel, and many other metals can be patterned by electrochemical machining. Examples in which such an approach is used are the fabrication of nozzle arrays [5] and chemical reaction microchannels [6].

6.1.1 Isotropic Wet Etching

In terms of bulk fabrication of microfluidic devices, etching channels and other cavities in glass is perhaps the most common scenario that involves isotropic wet etching. Gold is sufficiently resistant to concentrated hydrofluoric acid (HF) that it serves as an effective etch mask for glass microfluidic chips. A thin chromium layer is typically used between the gold and glass to facilitate good film adhesion. Photoresist is sufficient for short duration etching in HF, although for finer edge definition and longer etches gold is superior. A thin film of amorphous silicon has been proven to provide good selectivity to allow very deep etching of glass substrates up to 1 mm in thickness [7]. In the case of silicon, a mixture of hydrofluoric acid, nitric acid, and acetic acid is the most common isotropic etchant used, known by the abbreviation HNA. The proportions of each component affect factors such as etch rate and the tendency to round corners. Silicon nitride is the most common thin-film etch mask against HNA, although silicon dioxide is a viable alternative with lower selectivity.

As an etch front progresses in isotropic wet etching, material is removed laterally at a rate similar to the speed of etching downward. The same situation occurs for any kind of isotropic etching in general, including vapor phase etching described later in this chapter as a form of dry etching. What results from this significant rate of lateral etching is a situation of mask undercutting. If the etch front were perfectly isotropic with no material redeposition, then a pinhole opening would result in a hemispherical etch cavity. Wider openings result in rounded trough features, as approximated by Figure 6.4. Accordingly, dimensions of the openings in the mask must be designed to account for the lateral etching that occurs.

When thin films are used as the mask for wet etching, particle contamination is one common concern which can result in pinhole defects. Pinholes in the film allow etchant to attack the substrate in unintended regions. In Figure 6.4 the cavity beneath the pinhole may be exaggerated relative to the larger opening because differences in ease of mass transport would likely cause the two cases to differ in terms of net removal rate. However, the effects can still result in sizable flaws. Enforcing strict clean room requirements is an obvious method of minimizing particle contamination for thin-film etch masks. A novel approach to overcoming the problem is to use multilayer thin films with random redistribution of particle contamination through the corresponding venting and high vacuum steps [8].

The poor aspect ratio of lateral etching makes it unfavorable to incorporate deep cavities in substrates if lateral dimensions need to be kept relatively small. For example, if the aspect ratio of a wet etched process were roughly 1:2, then a through-hole etched through a glass wafer that is 500 μm thick could be no smaller than 1 mm in diameter. A partial solution would be to perform etching simultaneously from both sides of the wafer, using appropriately aligned etch masks. Etching from both sides simultaneously not only benefits aspect ratio but also reduces the overall time to approximately half the time needed for one-sided etching.

For relatively coarse features, or for features that are less concerned with aspect ratio, isotropic wet etching is a convenient option for material removal. The copper layer commonly used in printed circuit boards is typically tens of microns thick, and can be etched to form fluid passages in PCB microfluidic devices [9]. Such an approach has been used for devices such as micropumps [10] and for reactant flow channels used in miniature fuel cells [11].

The issues of shallow aspect ratio, rounded etch profile, and mask undercutting are important factors for determining whether or not isotropic wet etching is suitable for meeting geometric design requirements. In some cases a rounded profile may be desirable to avoid sudden slope discontinuity at sharp corners. However, if mask undercutting is unacceptable or if high aspect ratio is required, either anisotropic wet etching (discussed next) or anisotropic dry

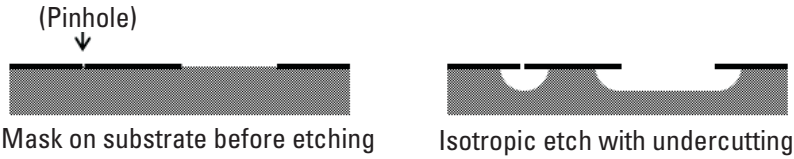

Figure 6.4 Mask undercutting as a result of lateral material removal during isotropic etching.

etching (discussed thereafter) are alternative types of etching that may provide a solution.

6.1.2 Anisotropic Wet Etching

A very diverse range of microengineered devices has been developed based on bulk micromachining of silicon [12]. A significant fraction of these has included microvalves, micropumps, and other microfluidic devices based specifically on anisotropic wet etching of silicon. Single-crystal silicon has what is described as a diamond cubic crystal structure. The bonds among silicon atoms are covalently bonded, and the (111) planes are the ones that have the highest atomic packing density.

In some etchants such as HNA mentioned above, the etching of silicon is isotropic. However, particularly against some alkaline substances such as tetramethyl ammonium hydroxide (TMAH), there is a large directional difference in the etch rates depending on silicon crystal planes. Specifically, (111) planes are relatively impervious to etching compared to other crystal planes. For silicon wafers that are sliced and polished along (100) planes, etch cavities can be made entirely through the thickness of a wafer with virtually no penetration through the (111) planes. This provides the opportunity to design with atomically flat surfaces that are deterministically at a 54.74° angle to the top and bottom surfaces of the (100) wafer. Furthermore, the right-angle intersection of (111) planes along n vectors on the surface of a (100) wafer makes it possible to fabricate cavities with exact rectangular or square openings.

The precise angle between (111) planes and all crystal planes parallel to the top and bottom surface of a (100) wafer facilitates device design with deterministic outcome. Compared to the outcome of isotropic etching, anisotropic etching that takes advantage of (111) selectivity involves more straightforward mask design, because the width of a mask opening and the depth of etch are all that are needed to determine the width of the etched plane that is parallel to the surface. This is illustrated in Figure 6.5.

The sloping walls can be used to design directional features with very consistent profiles. If an etched cavity is used for a mold, the surface smoothness and inherently generous draft angle facilitate ease of mold separation. For example, counterdirectional pyramid cavities can be used to design a micropump with one-way flow dictated simply by differences in directional flow resistance [13].

Novel design with an understanding of crystallographic dependencies can be used to produce very consistent and sometimes very complex three-dimensional features by anisotropic wet etching, including microvalves based on thin plates oriented along {111} planes [14]. Figure 6.6 [15] shows an example of using anisotropic etch characteristics of silicon to geometrically constrain etch

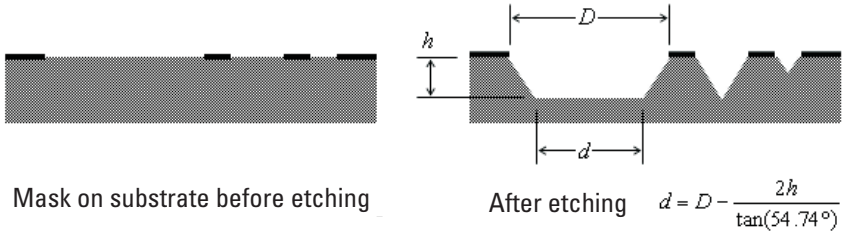

Figure 6.5 Examples of etch profiles in anisotropic etching of (100) silicon and the relationship among mask dimensions, etch depth, and floor width.

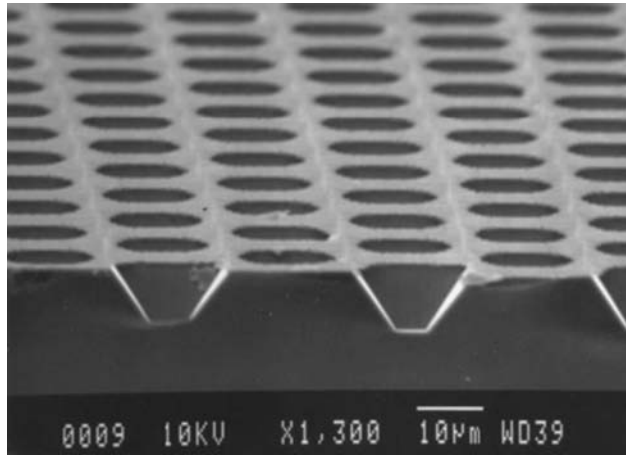

Figure 6.6 Etched cavities formed by taking advantage of geometric constraints in single-crystal silicon. (Reprinted from [15], with permission from IOP Publishing.)

cavities, the principle of which has been demonstrated in the microfabrication of hot-wire anemometer.

A unique advantage of the predictable angle among silicon crystal planes is that is that V-grooves can be used as geometric indicators of etch depth. Knowing only the width of a mask opening is sufficient for knowing the precise depth at which the etch sidewalls will converge at a line. This feature can be used to set an etch stop based on geometry alone. For more automated precision, however, it is preferable not to rely on careful timing or inspection-based monitoring. Instead, it is preferable to use etch selectivity among materials. For example, TMAH etches silicon much faster than silicon nitride or silicon dioxide, so it becomes possible to etch all the way through a wafer to leave only a thin silicon nitride membrane at the far side, or to etch only as far as the buried oxide layer

in a silicon-on-insulator wafer [16]. Another effective way to set an etch-stop is to have boron implanted to a designated depth, because the etch rate will slow dramatically when TMAH, for example, reaches a boundary of high boron concentration [17].

TMAH is a highly favored anisotropic silicon etchant. Under some conditions potassium hydroxide (KOH) can exhibit superior performance along various metrics including etch rate, selectivity, and surface roughness [18]. However, KOH is problematic in some clean room settings because the alkali metal content makes it a contaminant in CMOS processing. KOH is also known to damage aluminum. Modifications to TMAH, such as doping with silicic acid and ammonium peroxodisulphate can improve roughness while providing other benefits such as passivation of aluminum [19]. Another relatively well-known anisotropic silicon etchant is ethylenediamine pyrocatechol (EDP), but management of its toxic health hazards is more demanding than either TMAH or KOH.

Unlike the results obtained from isotropic etching, anisotropic wet etching can be performed through a properly aligned rectangular opening such that there is no undercutting of the mask. This was the assumption for openings illustrated in Figure 6.5. The presence of mask features with convex features, however, presents an ability for etchant to act behind and around (111) planes that are otherwise relatively impervious [20]. Therefore, convex corners require special attention when designing masks. In some cases, the undercutting can be used to an advantage, especially if material beneath a structural component needs to be entirely removed to fabricate a bridge or cantilever diving board over an otherwise etched cavity. In many cases, however, the irregular shapes formed by the undercutting are undesirable, and there have been several strategies to compensate for undercutting in both KOH [21, 22] and TMAH [23] based on modified mask design.

Anisotropic wet etching is not restricted to crystal-plane selectivity in silicon. Photosensitive glass is uniquely capable of facilitating anisotropic etch profiles by selective exposure to UV light. In the case of FOTURAN glass, exposure to UV light, followed by a heat treatment step, can alter the etch rate of exposed areas such that in hydrofluoric acid they are removed 20 times faster than unexposed regions [24]. While in most cases wet etching of glass is isotropic, high aspect ratio has been demonstrated for photosensitive glass. The general principle is explained in Figure 6.7 and an example is shown in Figure 6.8 [25].

This novel method of etching glass produces vertical walls and aspect ratios not achievable by the other type of wet etching described previously. In general, most wet etch processes produce isotropic profiles, and the set of materials that respond with anisotropic selectivity is relatively limited. The next section of this chapter discusses dry etching. Some types of dry etching have been developed specifically to produce highly anisotropic profiles with fine

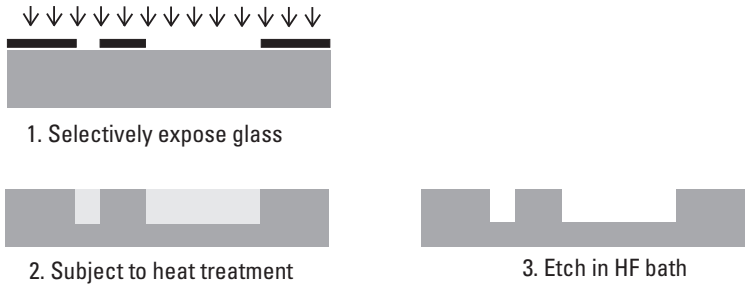

Figure 6.7 Process for anisotropic wet etching of photosensitive glass.

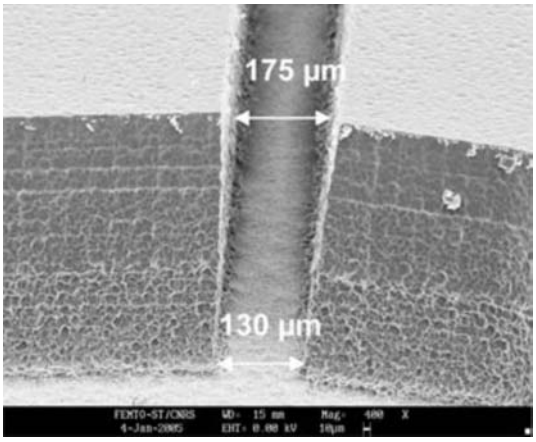

Figure 6.8 Example of anisotropically wet-etched photosensitve glass. (*Source:* [5].)

resolution, vertical sidewalls, and high aspect ratio in a much wider variety of materials.

6.2 Dry Etching

Dry etching is distinguished from wet etching in that the substrate is not immersed in liquid. Dry etching is extremely versatile and dry etch processes have been developed for nearly all materials common to microfabrication. Processes for silicon, inorganic compounds (e.g., silicon nitride), photoresist, and metals are the most mature, in large part thanks to the long history of development for microelectronics. However, motivated largely by microfluidic applications, dry etch processes for materials including borosilicate glass [26, 27], PDMS [28, 29], and polyimide [30] have also gained interest. Previously discussed methods

such as casting, replica molding, and hot embossing remain more common for polymer materials, but dry etching methods provide an even wider choice of options.

Dry etch processes are not categorically anisotropic. The etch profiles from dry etching may be either isotropic or anisotropic, depending on etchant chemistry, processing conditions, and substrate materials. Anisotropic dry etching simply receives greater attention because of the ability to etch with finer resolution and higher aspect ratio than isotropic etching, whether wet or dry. Furthermore, the directional nature of anisotropic dry etching significantly lessens the severity of problems related to mask undercutting and pinholes compared to isotropic etch processes.

The most common types of dry etching occur in a *plasma*, which is a state of matter consisting of high-energy ions and electrons in addition to neutral particles. The use of plasma in microfabrication [31] most routinely assumes that a substrate is placed in a vacuum chamber in which the plasma is sustained. Low pressure inside the vacuum chamber, typically operating in the millitorr range, facilitates high-energy collisions that would otherwise be impossible in a denser environment. The plasma etch systems used in microfabrication are commonly characterized by a *glow discharge*, in which bright light is emitted as electrons and ions recombine. Plasma jets can very well be produced for processes such as plasma cutting and plasma spraying, but such processes are normally associated with macroscopic applications and methods rather than microfluidic applications and microfabrication techniques.

Two major types of plasmas are direct current (dc) plasma and radio frequency (RF) plasma. Both cases are dependent on electrical breakdown of an inert gas such as argon, and an ability to sustain collisions to maintain a sufficiently constant balance of excitation versus recombination. dc plasmas rely on a continual resupply of electrons emitted from the cathode. RF plasmas differ from dc plasmas in that they use an oscillatory electromagnetic field to initiate and sustain the plasma. One of the most unique benefits of RF plasmas from a fabrication perspective is that nonconductive materials can be etched. In terms of equipment, inductively coupled plasma (ICP) systems with circumferential RF coils rather than a pair of planar electrodes provide better control over plasma uniformity and ion flux density. Using microwave energy is another basic approach that has been less frequently explored, but microwave plasmas have the relative merit of providing higher density plasma that can be orders of magnitude higher than RF plasma [32].

Pressure is a very significant factor in plasma etching, and it affects both the etch profile as well as surface roughness. At lower pressure, physical mechanisms play a relatively greater role. Momentum is less impeded, which corresponds to having fewer lateral collisions among species in the plasma, typically resulting in more vertical sidewalls and smoother walls. At higher pressure,

molecular interactions occur at a higher rate, so chemical mechanisms tend to play a relatively greater role and etch profiles tend to be more isotropic.

Discussed next are some different types of plasma etching and the distinctions among them. In particular, the discussion will be organized under the headings of ion etching, reactive ion etching (RIE), and deep reactive ion etching (DRIE). The categories are not mutually exclusive because sputter etching can very well occur in RIE, and DRIE is an extension of RIE. However, the topics will be presented to highlight the main concepts and a few functional distinctions. Another basic type of etching in a dry environment is vapor phase etching, which does not involve the use of plasma.

6.2.1 Ion Etching

In the introductory discussion of subtractive processes above, a distinction was made between physical and chemical mechanisms. Ion etching is a basic type of plasma etching that is based specifically on the physical mechanism of having high-energy ions impinge upon a substrate to remove material from it. The interactions of ions, electrons, and target atoms are essentially the same as those that occur during sputtering [33]. However, the name sputtering is frequently associated with a process in which the purpose is not only to erode material from a target but also to deposit that material as a film on another substrate in the same vacuum chamber. In cases of potential ambiguity, the words sputter etching or sputter deposition can be used accordingly to make clear distinction.

Some confusion also often arises among closely related terms such as ion milling, ion beam etching (IBE), and ion beam milling. All cases share core similarity in that they are subtractive processes based on impingement of ions. There is some convergence toward distinguishing beam processes as those that are external to the plasma, by allowing the ions to exit through openings in the negative electrode to impinge upon a substrate in a separate chamber. The word milling would seem to imply removal along a spatially serial path, but in microfabrication this distinction is not emphasized and milling still routinely applies to spatially parallel etching of a wafer through a patterned mask. The core principle of physical impingement of accelerated ions is the same throughout, so the remainder of this section will focus on ion etching in a general sense, with the understanding that there are many similarities with the other related processes. The special case of a focused ion beam (FIB), however, is specifically directed along a spatially serial path, and discussion of FIB is deferred until the next section on directed beam subtractive processes.

Ion etching is characterized by good directionality. The direction of highest incoming ion momentum (perpendicular to the target surface) dictates the direction of fastest etching. These processes are generally run at very low pressure, less than ~100 millitorr, to facilitate high-energy bombardment. However,

this condition simultaneously results in relatively poor material selectivity, especially compared to etch processes driven by chemical reactions.

Argon is the conventionally favored choice for ion etching because as a noble gas it is more inert than other viable alternatives such as nitrogen. Argon is also favorable because it has relatively large atomic mass (18 g/mol) compared to other inert substances, and argon is far more readily available than heavier gases such as krypton.

Even with heavy atoms and relatively high input energy, the material removal rate for ion etching is inherently slow, on the order of 100 angstroms per minute. Accordingly, the use of a magnetron to help confine secondary electrons is now almost universal in all ion etching and sputtering systems. The magnetic field generated by the magnetron confines secondary electrons near the target, so that they can contribute to additional ionization and thus provide more dense plasma. Various innovations such as geometric design, rotating, and pulsing have been developed to improve both rate and uniformity [34].

Successful removal of material requires enough kinetic energy to eject material from the substrate cleanly with minimal redeposition. However, the kinetic energy of impinging ions must not be so high as to drive ions entirely into the substrate (i.e., ion implantation). For faster rate and better selectivity, physical mechanisms alone can be insufficient, which motivates the use of chemical etch mechanisms, and more often a combination of physical and chemical etch mechanisms.

6.2.2 Vapor Phase Etching

In microfabrication, reactive ion etching (described in the next section) is more widely used than either sputter etching or vapor phase etching. Vapor phase etching is described briefly here to make distinction between physical mechanisms and chemical mechanisms. Vapor phase etching occurs at low pressure but without plasma. Unlike in sputtering, there is no directional impingement of high-energy ions, and the mechanism of material removal is therefore chemical, not physical.

Fluorine is the most chemically reactive element and has the highest electronegativity of all elements, so there is little wonder that it would be a favored candidate for chemical etching. Hydrofluoric acid is a liquid at room temperature and is the standard wet etchant for silicon dioxide. For dry etching, fluorine is available in gaseous form in compounds such as carbon tetrafluoride (CF_4) and sulfur hexafluoride (SF_6). For these compounds, however, plasma is generally needed to free the fluorine atoms.

Xenon difluoride is the favored etchant for vapor phase etching of silicon. In ambient conditions it is a solid, but has a vapor pressure slightly less than ~5 torr, which is easily achieved by vacuum pump. XeF2 vapor can etch silicon at

rates of thousands of angstroms per minute, with good selectivity to silicon nitride, silicon carbide, and silicon dioxide masks [35]. If moisture is present, however, there is a concern of forming hydrofluoric acid, which would destroy the silicon dioxide mask. Chlorine is another reactive element that can serve as the basis of vapor phase etching, but its use has been directed primarily to compound semiconductor applications [36] rather than microfluidic systems per se.

Although material selectivity is good and etch rates are relatively high, the two major limitations of vapor phase etching are that it is isotropic and not very diverse in terms of the types of materials that can be etched. A combination of chemical and physical removal mechanisms is desirable to achieve anisotropic profiles with good selectivity in a wider variety of materials. This motivates combining the merits of plasma etching with chemically reactive species in reactive ion etching, discussed next.

6.2.3 Reactive Ion Etching

Reactive ion etching (RIE) is one of the most diverse and most widely used processes in microfabrication. RIE involves a combination of physical and chemical mechanisms, and combines the attributes of both to achieve fine resolution, controlled anisotropy, and fast etch rate. RIE is so prevalent in microfabrication that when speaking of plasma etching without specifying one of the other types of plasma-based subtractive processes, RIE is often assumed by default.

The name reactive ion etching is acknowledged to be a misnomer because in general the ions have little or no direct role in chemical reactions per se. Instead, accelerated particles play important supporting roles to enable chemical reactions and to make them more effective. For example, the high-energy collisions from ionization help to dissociate etchant molecules such as CF_4 into more reactive CF_3 and F species. Physical impingement of energetic ions on the substrate helps to make its surface less chemically stable and more susceptible to reaction with chemical species. Although an expression such as ion-assisted chemical plasma etching might be more accurately descriptive, RIE remains the accepted name for this type of physical-chemical etching combination.

RIE technology has traditionally been most highly developed for silicon. A variety of different materials have been used for masking, including photoresists, silicon dioxide, and silicon nitride, although metals such as aluminum can be superior for well-defined etch profiles and deep cavities [37]. A significant impact that microfluidics has contributed with respect to RIE processes has been greater attention to other materials, especially glasses and polymers. RIE for silicon is a relatively mature technology and has been extensively documented elsewhere [38], so the examples below will focus on glass and polymers.

Both PYREX glass and quartz can be plasma etched using CF_4/Ar or CF_4/O_2 [39]. Thin-film nickel serves adequately as an etch mask, although it is

subject to flaws related to having higher electric field density at edges. High etch rate of approximately 0.5 μm/min and higher can be achieved using SF_6/Ar plasma with electroplated nickel as the mask layer [27, 40]. Thick SU-8 can also be used as an alternative to metal masks, and using CF_4/Ar and CHF_3/Ar chemistries, microchannels over 50 μm deep with near vertical sidewalls have been successfully etched [41]. As shown in Figure 6.9 [42], deep cavities in the range of hundreds of microns can be etched in glass using a bonded silicon wafer as the etch mask.

PDMS is a material of great interest because of its widespread use in microfluidic devices. PDMS can be etched in oxygen, carbon tetrafluoride (CF_4), sulfur hexafluoride (SF_6) and mixtures thereof with varying results. Even oxygen plasma alone can etch PDMS, although in the absence of fluorine the mechanism differs significantly, attributed to a combination of ion sputtering and oxidation [43]. Figure 6.10 shows a cavity that results from plasma etching a PDMS-based substrate using a mixture of SF_6 and oxygen. Using microwave plasma with CF_4/O_2 can achieve very fast etch rate, on the order of a few microns per minute [44]. Another way to increase etch rates for PDMS is to combine plasma etching with wet etching [45].

Depending on process conditions, etched profiles can be made more isotropic with respect to a mask boundary, as seen in Figure 6.11. The example uses CF_4/O_2 and an evaporated thin-film aluminum mask. Notable is that plasma etching of PDMS tends to result in rough surface texture, as seen in the figures.

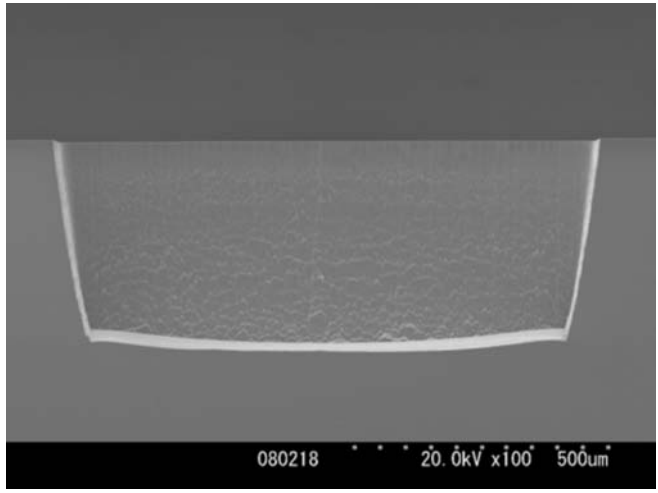

Figure 6.9 Deep cavity in borosilicate glass, etched using a bonded silicon wafer as the mask. (Reprinted from [42], with permission from IOP Publishing.)

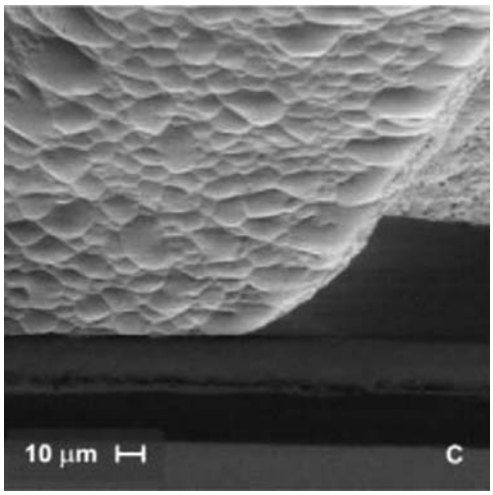

Figure 6.10 Plasma etched cavity in silicone elastomer. (Reprinted from [46]. Copyright 2006, with permission from Elsevier.)

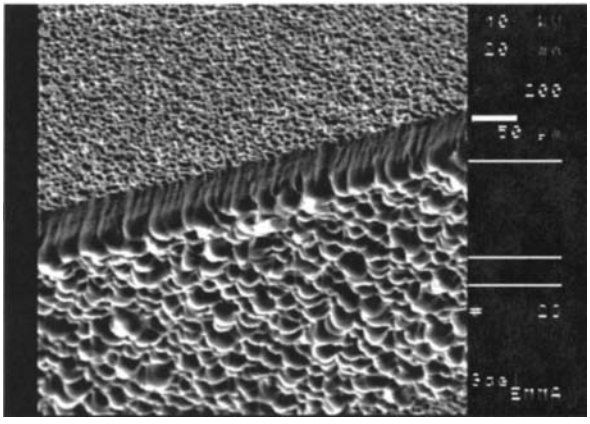

Figure 6.11 Anisotropic plasma etching of PDMS with CF_4/O_2 plasma and an aluminum film etch mask. (Reprinted with permission from [29]. Copyright 2002, American Institute of Physics.)

RIE can be used not only for removal per se, but also for altering surface morphology [47]. A unique phenomenon that occurs under some plasma etch conditions is the formation of a columnar layer. For example, Figure 6.12 shows results of plasma etching PDMS with a mixture of CF_4 and oxygen. The columnar structures are very fragile with narrow bases and do not remain after routine rinsing. The resulting surface after the columnar layer is removed shows a high degree of surface roughness.

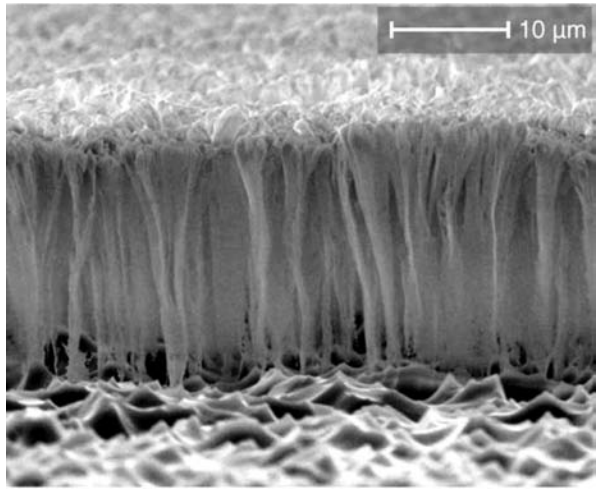

Figure 6.12 Columnar layer formed in PDMS etched by CF_4/O_2 plasma. (Reprinted from [48]. Copyright 2006, with permission from Elsevier.)

RIE processes are not always limited to the straightforward mechanisms of ion etching and chemical reactions between etchant atoms and the substrate surface. What has not yet been mentioned is the fact that some polymerization may occur when using hydrocarbon-containing plasmas (e.g., CHF_3, C_4F_8, and so forth). Polymerized films on the substrate may by design (or even serendipitously) improve selectivity, anisotropy, and aspect ratio. The best example of deliberately using intermediate passivation steps to improve directionality and aspect ratio is illustrated in deep reactive ion etching (DRIE), discussed next.

6.2.4 Deep Reactive Ion Etching

High aspect ratio is important for producing narrow gaps between components, as would be demanded by laterally sliding components such as microscale gate valves [49, 50]. Deep reactive ion etching (DRIE) is capable of etching very deep narrow holes with vertical sidewalls, and has been used for microvalves with fluid passages extending even through the entire thickness of a wafer [51].

The most significant apart about DRIE that distinguishes it from RIE in general is that DRIE includes a deliberate passivation steps in between etch steps. The primary manifestation of DRIE was innovated by Robert Bosch GmbH [52] and is well known in microfabrication as the *Bosch process* [53]. Although numerous variations have been explored, DRIE is most conventionally associated with silicon as the base material and SF_6 as the primary etchant. Figure 6.13 illustrates the basic principle, in which a fluorocarbon film is

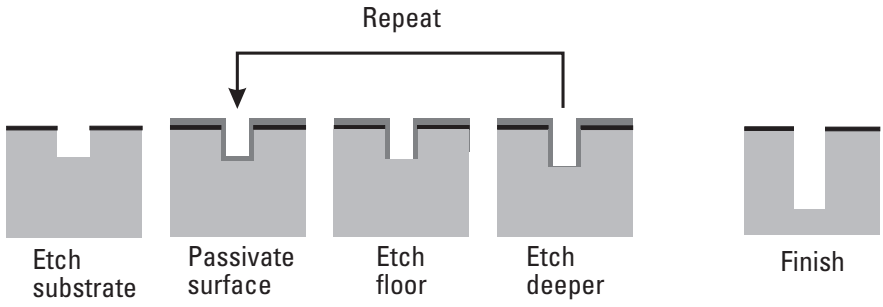

Figure 6.13 Deep reactive ion etching with a combination of etch and passivation steps.

deposited in plasma to make a thin conformal coating. The polymerization may be facilitated by gases such as trifluoromethane (CHF_3) or octofluorocyclobutane (C_4F_8). An SF_6 plasma performs the directional etching, assisted by a dc bias applied to the substrate. Some sidewall etching occurs, but the predominant removal of material occurs at the floor to expose the substrate at the bottom of trenches. Once exposed, the substrate is exposed to etching by fluorine free radicals. Even though the etching may be very locally isotropic, properly cycling the passivation and etching steps achieves very high aspect ratio with vertical sidewalls.

Another way of achieving extremely high aspect ratio is to perform plasma etching under cryogenic conditions [54]. The low temperature reduces chemical etching while not affecting the physical etching mechanism, thereby achieving high directionality. Cryogenic DRIE is less common than the Bosch approach, but it does offer some unique control over tapered profiles [55]. A practical challenge for cryogenic DRIE is management of thermal stresses for the substrate, masking layer, and any other films that may be present.

Although DRIE is a spatially parallel process, it takes advantage of intermediate sidewall passivation steps to achieve remarkably high aspect ratio. A different strategy for achieving high aspect ratio is to concentrate focused energy in a very narrow space, which is discussed next.

6.3 Directed Beam Subtractive Processes

The processes in this category are based on a focused beam that is directed along a prescribed path to remove material. As spatially serial processes, these are fundamentally slower than subtractive processes which can act on the entire surface of a substrate with much broader exposure. In most cases a mask is not needed at all, and feature quality instead becomes dependent on proper control and focusing of the beam. Compared to plasma etching, directed beam processes present

a trade-off between having greater flexibility versus having higher productivity with less variability.

6.3.1 Laser Ablation

Laser ablation (or laser machining) is a flexible method of material removal. There are several types of lasers, and the most common types used in micromachining are carbon dioxide (CO_2) lasers and excimer lasers. CO_2 lasers operate in the infrared part of the spectrum with power levels typically in tens of watts. Excimer lasers operate in the UV range (193 to 351 nm). Although more costly than CO_2 systems, UV lasers [56] and femtosecond lasers [57] have a key advantage over CO_2 lasers in that material is removed without a heat-affected-zone (HAZ) that may otherwise lead to thermal damage and distortion. Neodymium-yttrium aluminum garnet (Nd-YAG) is also used in laser machining, but more often for larger-scale features in metals that require hundreds of watts.

Profiles of materials cut by CO_2 laser ablation tend to have an inverted bell shape, consistent with the typical Gaussian distribution of irradiance [58]. The energy dose delivered to any given region can be altered by changing power intensity, scan speed, and/or number of passes. Figure 6.14 shows cross-section profiles of laser-cut profiles with various energy doses. Whereas in photolithography energy dose is typically expressed in energy per unit area (i.e., mJ/cm^2), in laser machining it is more intuitive to express in terms of energy per unit length (i.e., J/mm) along the path of the beam.

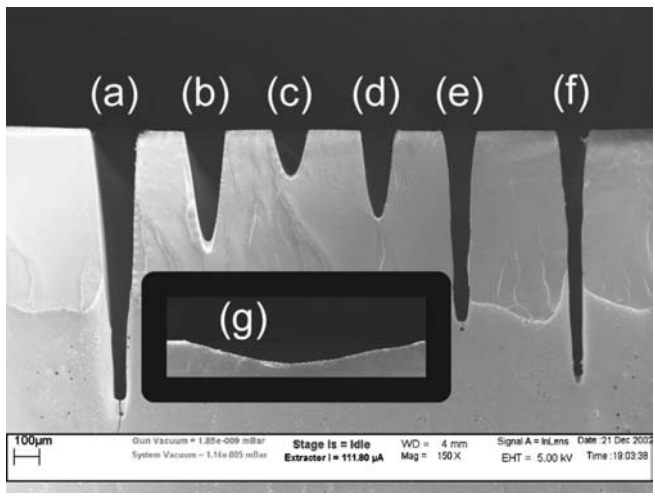

Figure 6.14 Profile control by CO_2 laser micromachining of PMMA. (Reprinted from [59]. Copyright 2004, with permission from Elsevier.)

Some of the materials of greatest relevance for microfluidic devices are PMMA and polyimide. PMMA is favorable for CO_2 laser ablation because it is relatively easy to control profile shapes, and PMMA is also compatible with a variety of subsequent bonding methods [60]. Instead of creating cavities in a material such as PMMA directly, laser ablation can also be used as a rapid and convenient way of defining relief features in a master, for subsequent casting of another material such as PDMS [61]. A major drawback of direct laser ablation on PDMS is that surface roughness tends to be very severe. Instead of using laser-cut cavities directly, one strategy that bypasses the problem is to etch completely through a PDMS layer, followed by transferring the patterned layer to another substrate, as shown in Figure 6.15. Subsequently, the structure can be bonded to PDMS or glass to form closed microchannels and cavities.

Excimer laser machining of microfluidic devices has been used effectively in a variety of materials including PMMA, polycarbonate, and polyimide [63, 64]. Excimer lasers not only avoid thermal damage but furthermore can be passed through UV-transparent masks (e.g., quartz) and focused by demagnification optics. Therefore, excimer laser features can be defined with finer resolution than those made by CO_2 laser ablation. Even if materials such as polyimide can be patterned with either, in some cases it may be favorable to select one or the other (or a combination of both) to achieve the best trade-off between rate and resolution [65].

Crater defects can be a concern as material is ejected from the trench onto the upper surface. One solution is to perform secondary removal of excess material under low power [66]. Instead of having the cavity geometry dictated by the diameter of the laser, ablation can be performed using opening in a mask. Using a metal foil mask is beneficial not only for increasing throughput but also for avoiding crater effects in a variety of polymers [67]. The ablation conditions can also change the extent to which the native surface chemistry is altered, and thereby affect performance in applications such as electro-osmotic flow [68].

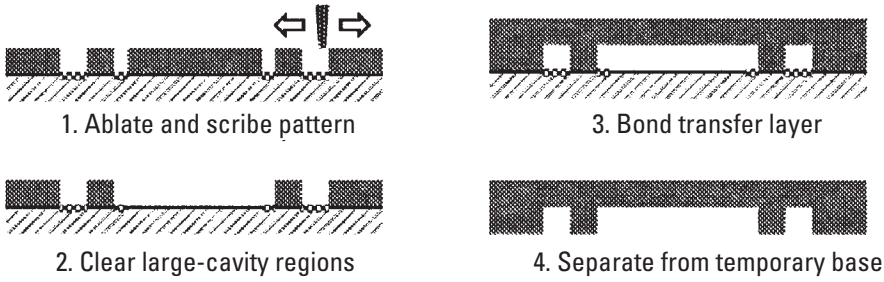

Figure 6.15 Through-layer laser ablation and transfer. (*After:* [62].)

6.3.2 Focused Ion Beam Milling

Focused ion beam (FIB) milling represents an exceptionally fine level of spatial control and can be applied to virtually any material. Ions are generated by strong electric field from a liquid metal source (typically gallium). The ions are accelerated through a focusing column and directed toward a substrate in a vacuum chamber. Upon impact, the ions remove material using the same physical principle of sputtering as previous discussed in the context of ion etching. Spot size of the ion beam is approximately 10 nm and aspect ratio can be as high as approximately 20:1 [69]. Advances in FIB milling include application of FIB to tapered walls, curved surfaces, and nonplanar substrates [70].

The dimensions of features defined by FIB are extremely small, typically on the order of tens of nanometers. Accordingly, the applications in microfluidics go beyond mere flow manipulation and tend to serve more specialized requirements than most other examples discussed throughout this book. Examples of the use of FIB in microfluidic/nanofluidic applications include patterning hole arrays smaller than nerve cell axons [71], forming molecular gates [72], and fabricating nanometer-scale channels for manipulation of DNA molecules [73].

FIB technology is not limited to subtractive processes. The impacting ions release secondary electrons from the substrate that can be used for imaging, using similar principles as scanning electron microscopy. Furthermore, if an appropriate chemical precursor is delivered during scanning, the local breaking of bonds can facilitate chemical reactions and thereby achieve spatially selective deposition.

Proton beam writing (PBW) is very similar in principle to FIB milling, but applies more narrowly to photoresist materials. The proton beam penetrates a photosensitive material with high aspect ratio, and the material is removed in a subsequent developing step. Material removal with proton beam writing has been used to fabricate channels in PMMA as narrow as 200 nm with straight and smooth sidewalls to a depth of 5 μm [74].

Proton beam writing shares similarities with electron beam lithography (EBL) [75], which is also primarily used for photoresist materials. EBL is capable of exceptional lateral resolution as fine as a few nanometers across, but it is not useful for high aspect ratio because electrons are subject to much scattering upon penetrating into a material.

6.4 Mechanical Subtractive Processes

The processes categorized here as mechanical share commonality in that they are based on shear and material fracture. Material removal for these processes occurs at a scale that is generally much larger than the molecular-scale momentum

transfer encountered in sputter etching. Three types of mechanical subtractive processes will be discussed: precision machining, abrasive jet machining, and polishing.

6.4.1 Precision Machining

Conventional machining using cutting tools can also be used to fabricate working fluidic devices with microscale dimensions, although typically limited to relatively coarse features on the order of 100 μm and larger. Although not always categorized as microfabrication in the same context as plasma etching and related processes, machining still finds utility for functional microfluidic devices. For example, a thin polyurethane membrane has been sandwiched between machined acrylic substrates to form a pneumatic micropump that has a stroke volume of approximately 1 μL [76]. Thin solid sheets are commercially available in very thin dimensions (e.g., 25-μm polyimide), and these have been used to fabricate microchannel devices by machining and lamination [77]. In general, minimum feature sizes and tolerances that are achievable by computer numerically controlled (CNC) machining are inadequate for feature sizes required by many microfluidic devices, but specialized calibration methods can be used for finer tolerance control [78].

A related process is direct cutting with a fine knife blade, under the coined name *xurography* [79]. Xurography offers benefits of low cost and rapid prototyping, and it is applicable to almost any polymer film that can be prepared in sheet form. Sheet thickness typically ranges from 25 μm to 1 mm, which can be effective for a variety of applications including shadow masks, electroplating masks, casting patterns, and laminated fluidic channels. Positive and negative features can be cut with resolution in the range of tens of microns with an aspect ratio better than 5:1.

6.4.2 Abrasive Jet Milling

Blasting with a high-velocity stream of abrasive particles from a pressurized nozzle is a relatively fast way of removing material. Accordingly, it is particularly favorable for bulk removal needs such as drilling port holes through glass substrates. Spatial control over a stream of particles is generally inadequate for direct-write patterning, but a protective mask can be used to designate narrow channels and other fine features. Aluminum oxide powder has been used to pattern glass microchannel devices with rates as high as 100 μm/min, using a laser-cut metal film as the patterning mask [80].

Since erosion is the primary mechanism of material removal, surfaces tend to be rough. However, less aggressive removal rates can produce smoother surfaces. Figure 6.16 shows differences in surface roughness between troughs

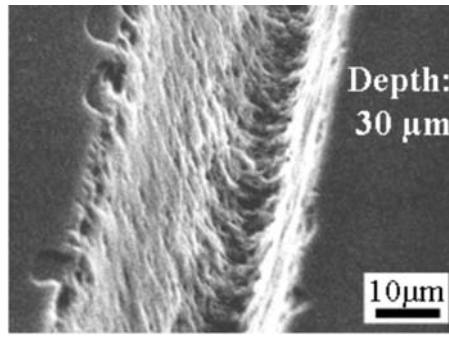

(a)

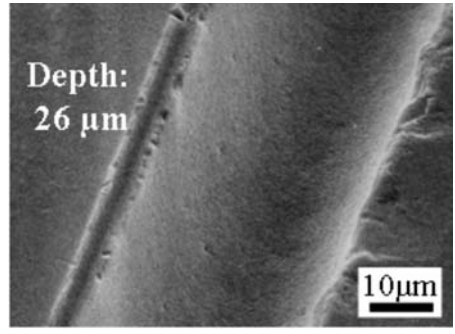

(b)

Figure 6.16 Contrast in abrasive jet milling of glass at (a) high pressure for a short duration versus (b) low pressure for a long duration. (Reprinted from [81], with permission from IOP Publishing.)

formed with higher pressure for a short duration (0.4 MPa for 3 minutes) versus lower pressure for a long duration (0.12 MPa for 180 minutes).

In terms of mask materials, resistance to fracture is fundamentally more important than hardness. For example, silicon carbide is a very hard material and as an abrasive powder it can erode stainless steel effectively. The mask however, must be resilient against fracture, so softer materials that have high erosion resistance such as PDMS turn out to be quite effective [82].

6.4.3 Chemical-Mechanical Polishing

Chemical-mechanical polishing (CMP) is a subtractive process that planarizes broad surfaces by mechanical abrasion assisted by chemical interaction [83]. A wafer is pressed by a polishing head against a polishing pad, and both the head and the pad are rotated as a fine slurry of particles is allowed to act on a wafer surface.

CMP is an invaluable asset for multilayer structures that require planarization. The most fundamental benefit of CMP that makes it effective for planarization is that the process is nondiscriminating in terms of the material that is removed. CMP was originally developed to serve the microelectronics industry since device complexity mandated an ability to provide flat surfaces as more and more conformal layers are stacked upon each other. Planarization facilitates not only better coating of photoresist but also more discrete control over material boundaries (i.e., dielectric material thickness between metal layers).

As is the case with RIE, microfluidics has motivated characterization and further development of CMP to address a wider variety of materials including polycarbonate and PMMA [84]. CMP is not presently of widespread use in microfluidic device fabrication, but the dimensional control is fine enough to produce channels 25 nm wide and 100 nm deep in amorphous silicon with thermally grown silicon dioxide as a sacrificial material [85].

6.5 Tabulated Examples of Subtractive Processes

Table 6.1 lists several examples of microfabrication processes that are based on removal of material. The contents are not comprehensive, but rather an attempt to sample a variety of processes that have been used for microfluidic devices. A small number of table entries may be based on other microfabricated structures not specifically for fluidic devices per se, but these are included in order to encompass the diversity of materials and processes that can potentially be used.

The table lists the basic process by which material is removed, the particular materials used, and the means by which selectivity is established. Within each cluster of processes, the more conventional materials and individual processes are generally listed first, followed by less conventional or relatively novel alternatives.

Table 6.1
Examples of Microfabrication Subtractive Processes

Subtractive Process	Material	Mask or Selective Boundary	Reference
Wet etching in HF	Glass	Au/Cr	[86]
Wet etching in KOH	Silicon	Silicon nitride	[87]
Wet etching in KOH	Porous silicon	Selectivity to nonporous Si	[88]
Wet etching in HF/NH_4F	Fused quartz	Sputtered Au/Cr	[89]
Wet etching in HF	Glass	Au/Cr/Au/Cr multilayer	[8]
Wet etching in TMAH	Silicon	TEOS	[90]

Table 6.1 (continued)

Subtractive Process	Material	Mask or Selective Boundary	Reference
Wet etching in EDP	Silicon	Crystallographic boundaries	[15]
Wet etching in iron chloride	Copper	Photoresist	[10]
Electrochemical machining	Copper, stainless steel	Photoresist	[5]
Plasma etching in CF_4/Ar or CF_4/O_2	Glass	Evaporated Ni	[39]
Plasma etching in C_4F_8 or CHF_3	Glass	Bonded silicon wafer	[42]
Plasma etching in SF_6/O_2 or CF_4/O_2	PDMS/PMHS	Sputtered Al	[91]
Plasma etching in SF_6/O_2	PDMS	SU-8	[28]
Plasma etching in CF_4/O_2	PDMS	Evaporated Al	[29]
Plasma etching in CF_4/Ar, CHF3/Ar	Quartz	SU-8	[41]
Plasma etching in O_2	Polyimide	PECVD silicon nitride	[30]
Plasma etching in O_2	Parylene	Photoresist	[92]
Plasma etching in SF_6/Ar	Glass	Electroplated nickel	[27]
Plasma etching	Polyimide	Copper	[93]
Plasma etching in microwave CF_4/O_2	PDMS	Nickel	[32]
Plasma etching in SF_6	Glass	Electroplated nickel	[94]
Plasma etching	Glass	Amporphous silicon	[26]
Deep reactive ion etching	Silicon	Thermally grown silicon dioxide	[95]
Vapor-phase etching in XeF2	Silicon dioxide	SiO_2, Si_3N_4, SiC	[35]
Laser ablation	Polyimide	(direct-write)	[96]
Laser ablation (CO_2)	PMMA	(direct-write)	[58]
Laser ablation (excimer)	Polycarbonate	(direct-write)	[97]
Laser ablation	PDMS	(direct-write)	[62]
Laser ablation (femtosecond)	PMMA, polyimide, glass	(direct-write)	[57]
Proton beam writing	PMMA	(direct-write)	[74]
Abrasive jet milling	Glass	Metal	[98]
Abrasive jet of Al_2O_3	Glass	PDMS	[99]
Abrasive jet of SiC	Stainless steel	PDMS	[82]

Table 6.1 (continued)

Subtractive Process	Material	Mask or Selective Boundary	Reference
Chemical-mechanical polishing	Polycarbonate, PMMA	(not applicable)	[84]
Razor cutting	Various polymer films	(direct-write)	[79]

References

[1] Williams, K. R., and R. S. Muller, "Etch Rates for Micromachining Processing," *Journal of Microelectromechanical Systems*, Vol. 5, No. 4, 1996, pp. 256–269.

[2] Williams, K. R., K. Gupta, and M. Wasilik, "Etch Rates for Micromachining Processing—Part II," *Journal of Microelectromechanical Systems*, Vol. 12, No. 6, 2003, pp. 761–778.

[3] Merlos, A., et al., "Optimized Technology for the Fabrication of Piezoresistive Pressure Sensors," *Journal of Micromechanics and Microengineering*, Vol. 10, No. 2, 2000, pp. 204–208.

[4] Lasky, J. B., "Wafer Bonding for Silicon-on-Insulator Technologies," *Applied Physics Letters*, Vol. 48, No. 1, 1986, pp. 78–80.

[5] Datta, M., "Fabrication of an Array of Precision Nozzles by Through-Mask Electrochemical Micromachining," *Journal of the Electrochemical Society*, Vol. 142, No. 11, 1995, pp. 3801–3805.

[6] Matson, D. W., et al., "Fabrication of a Stainless Steel Microchannel Microcombustor Using a Lamination Process," *SPIE*, Vol. 3514, Santa Clara, CA, 1998.

[7] Iliescu, C., B. Chen, and J. Miao, "Deep Wet Etching-Through 1mm Pyrex Glass Wafer for Microfluidic Applications," *20th IEEE International Conference on Micro Electro Mechanical Systems*, Kobe, Japan, 2007.

[8] Bu, M., et al., "A New Masking Technology for Deep Glass Etching and Its Microfluidic Application," *Sensors and Actuators, A: Physical*, Vol. 115, No. 2-3, 2004, pp. 476–482.

[9] Merkel, T., M. Graeber, and L. Pagel, "New Technology for Fluidic Microsystems Based on PCB Technology," *Sensors and Actuators, A: Physical*, Vol. 77, No. 2, 1999, pp. 98–105.

[10] Nguyen, N. -T., and X. Huang, "Miniature Valveless Pumps Based on Printed Circuit Board Technique," *Sensors and Actuators, A: Physical*, Vol. 88, No. 2, 2001, pp. 104–111.

[11] O'Hayre, R., et al., "Development of Portable Fuel Cell Arrays with Printed-Circuit Technology," *Journal of Power Sources*, Vol. 124, No. 2, 2003, pp. 459–472.

[12] Kovacs, G. T. A., N. I. Maluf, and K. E. Petersen, "Bulk Micromachining of Silicon," *Proceedings of the IEEE*, Vol. 86, No. 8, 1998, pp. 1536–1551.

[13] Gerlach, T., M. Schuenemann, and H. Wurmus, "New Micropump Principle of the Reciprocating Type Using Pyramidic Micro Flowchannels as Passive Valves," *Journal of Micromechanics and Microengineering*, Vol. 5, No. 2, 1995, pp. 199–201.

[14] Oosterbroek, R. E., et al., "Designing, Simulation and Realization of In-Plane Operating Micro Valves, Using New Etching Techniques," *Journal of Micromechanics and Microengineering*, Vol. 9, No. 2, 1999, pp. 194–198.

[15] Parviz, B. A., and K. Najafi, "A Geometric Etch-Stop Technology for Bulk Micromachining," *Journal of Micromechanics and Microengineering*, Vol. 11, No. 3, 2001, pp. 277–282.

[16] Sharma, S., et al., "Silicon-on-Insulator Microfluidic Device with Monolithic Sensor Integration for μTAS Applications," *Journal of Microelectromechanical Systems*, Vol. 15, No. 2, 2006, pp. 308–313.

[17] Steinsland, E., et al., "Boron Etch-Stop in TMAH Solutions," *Sensors and Actuators, A: Physical*, Vol. 54, No. 1-3, 1996, pp. 728–732.

[18] Tokoro, K., et al., "Anisotropic Etching Properties of Silicon in KOH and TMAH Solutions," *Proceedings of the 1998 International Symposium on Micromechatronics and Human Science*, 1998, pp. 65–70.

[19] Biswas, K., and S. Kal, "Etch Characteristics of KOH, TMAH and Dual Doped TMAH for Bulk Micromachining of Silicon," *Microelectronics Journal*, Vol. 37, No. 6, 2006, pp. 519–525.

[20] Biswas, K., S. Das, and S. Kal, "Analysis and Prevention of Convex Corner Undercutting in Bulk Micromachined Silicon Microstructures," *Microelectronics Journal*, Vol. 37, No. 8, 2006, pp. 765–769.

[21] Sandmaier, H., et al., "Corner Compensation Techniques in Anisotropic Etching of (100)-Silicon Using Aqueous KOH," *TRANSDUCERS '91 International Conference on Solid-State Sensors and Actuators*, San Francisco, CA, 1991.

[22] Fan, W., and D. Zhang, "A Simple Approach to Convex Corner Compensation in Anisotropic KOH Etching on a (1 0 0) Silicon Wafer," *Journal of Micromechanics and Microengineering*, Vol. 16, No. 10, 2006, pp. 1951–1957.

[23] Pal, P., et al., "Study of Corner Compensating Structures and Fabrication of Various Shapes of MEMS Structures in Pure and Surfactant Added TMAH," *Sensors and Actuators, A: Physical*, Vol. 154, No. 2, 2009, pp. 192–203.

[24] Dietrich, T. R., et al., "Fabrication Technologies for Microsystems Utilizing Photoetchable Glass," *Microelectronic Engineering*, Vol. 30, No. 1-4, 1996, pp. 497–504.

[25] Malek, C. K., et al., "Deep Microstructuring in Glass for Microfluidic Applications," *Microsystem Technologies*, Vol. 13, No. 5-6, 2007, pp. 447–453.

[26] Kutchoukov, V. G., et al., "Fabrication of Nanofluidic Devices Using Glass-to-Glass Anodic Bonding," *Sensors and Actuators, A: Physical*, Vol. 114, No. 2-3, 2004, pp. 521–527.

[27] Park, J. H., et al., "Deep Dry Etching of Borosilicate Glass Using SF6 and SF6/Ar Inductively Coupled Plasmas," *Microelectronic Engineering*, Vol. 82, No. 2, 2005, pp. 119–128.

[28] Plecis, A., and Y. Chen, "Improved Glass-PDMS-Glass Device Technology for Accurate Measurements of Electro-Osmotic Mobilities," *Microelectronic Engineering*, Vol. 85, No. 5-6, 2008, pp. 1334–1336.

[29] Garra, J., et al., "Dry Etching of Polydimethylsiloxane for Microfluidic Systems," *Journal of Vacuum Science and Technology A*, Vol. 20, No. 3, 2002, pp. 975–982.

[30] Agarwal, N., et al., "Optimized Oxygen Plasma Etching of Polyimide Films for Low Loss Optical Waveguides," *Journal of Vacuum Science and Technology A: Vacuum, Surfaces and Films*, Vol. 20, 2002, No. 5, pp. 1587–1591.

[31] Coburn, J. W., and H. F. Winters, "Plasma-Assisted Etching in Microfabrication," *Annual Review of Materials Science*, Vol. 13, 1983, pp. 91–116.

[32] Sung, J. H., et al., "Dry Etching of Polydimethylsiloxane Using Microwave Plasma," *Journal of Micromechanics and Microengineering*, Vol. 19, No. 9, 2009, p. 095010.

[33] Behrisch, R., (ed.), *Sputtering by Particle Bombardment I, Volume 47*, Berlin/Heidelberg: Springer, 1997.

[34] Kelly, P. J., and R. D. Arnell, "Magnetron Sputtering: A Review of Recent Developments and Applications," *Vacuum*, Vol. 56, No. 3, 2000, pp. 159–172.

[35] Winters, H. F., and J. W. Coburn, "The Etching of Silicon with XeF2 Vapor," *Applied Physics Letters*, Vol. 34, No. 1, 1979, pp. 70–73.

[36] Heyen, M., and P. Balk, "Vapor Phase Etching of GaAs in a Chlorine System," *Journal of Crystal Growth*, Vol. 53, No. 3, 1981, pp. 558–562.

[37] Wang, W. -C., J. N. Ho, and P. Reinhall, "Deep Reactive Ion Etching of Silicon Using an Aluminum Etching Mask," *SPIE-Int. Soc. Opt. Eng.*, Vol. 4876, 2003.

[38] Jansen, H., et al., "Survey on the Reactive Ion Etching of Silicon in Microtechnology," *Journal of Micromechanics and Microengineering*, Vol. 6, No. 1, 1996, pp. 14–28.

[39] Zeze, D. A., et al., "Reactive Ion Etching of Quartz and Pyrex for Microelectronic Applications," *Journal of Applied Physics*, Vol. 92, No. 7, 2002, pp. 3624–3629.

[40] Goyal, A., V. Hood, and S. Tadigadapa, "High Speed Anisotropic Etching of Pyrex(R) for Microsystems Applications," *Journal of Non-Crystalline Solids*, Vol. 352, No. 6-7, 2006, pp. 657–663.

[41] Chen, H., and C. Fu, "An Investigation into the Characteristics of Deep Reactive Ion Etching of Quartz Using SU-8 as a Mask," *Journal of Micromechanics and Microengineering*, Vol. 18, No. 10, 2008, p. 105001.

[42] Akashi, T., and Y. Yoshimura, "Deep Reactive Ion Etching of Borosilicate Glass Using an Anodically Bonded Silicon Wafer as an Etching Mask," *Journal of Micromechanics and Microengineering*, Vol. 16, No. 5, 2006, pp. 1051–1056.

[43] Chou, N. J., et al., "Mechanism of Oxygen Plasma Etching of Polydimethyl Siloxane Films," *Applied Physics Letters*, Vol. 46, No. 1, 1985, pp. 31–33.

[44] Sung, J. H., et al., "Dry Etching of Polydimethylsiloxane Using Microwave Plasma," *Journal of Micromechanics and Microengineering*, Vol. 19, No. 9, 2009, p. 095010.

[45] Balakrisnan, B., S. Patil, and E. Smela, "Patterning PDMS Using a Combination of Wet and Dry Etching," *Journal of Micromechanics and Microengineering*, Vol. 19, No. 4, 2009, p. 047002.

[46] Szmigiel, D., et al., "Deep Etching of Biocompatible Silicone Rubber," *Microelectronic Engineering*, Vol. 83, No. 4-9, 2006, pp. 1178–1181.

[47] Nabesawa, H., et al., "Polymer Surface Morphology Control by Reactive Ion Etching for Microfluidic Devices," *Sensors and Actuators B: Chemical*, Vol. 132, No. 2, 2008, pp. 637–643.

[48] Szmigiel, D., et al., "The Effect of Fluorine-Based Plasma Treatment on Morphology and Chemical Surface Composition of Biocompatible Silicone Elastomer," *Applied Surface Science*, Vol. 253, 2006, No. 3, pp. 1506–1511.

[49] Papavasiliou, A. P., D. Liepmann, and A. P. Pisano, "Fabrication of a Free Floating Silicon Gate Valve," *Proceedings of ASME International Mechanical Engineering Congress and Exposition*, 1999.

[50] Frank, J. A., and A. P. Pisano, "Low-Leakage Micro Gate Valves," *TRANSDUCERS '03, 12th International Conference on Solid-State Sensors, Actuators and Microsystems*, Vol. 1, 2003.

[51] Luque, A., et al., "Integrable Silicon Microfluidic Valve with Pneumatic Actuation," *Sensors and Actuators, A: Physical*, Vol. 118, No. 1, 2005, pp. 144–151.

[52] Laermer, F., et al., "Method of Anisotropically Etching Silicon," U.S. Patent 5,501,893, 1996.

[53] Laermer, F., and A. Urban, "Challenges, Developments and Applications of Silicon Deep Reactive Ion Etching," *Microelectronic Engineering*, Vol. 67-68, 2003, pp. 349–355.

[54] Tachi, S., et al., "Low-Temperature Dry Etching," *Journal of Vacuum Science & Technology A (Vacuum, Surfaces, and Films)*, Vol. 9, No. 3, 1991, pp. 796–803.

[54] De Boer, M. J., et al., "Guidelines for Etching Silicon MEMS Structures Using Fluorine High-Density Plasmas at Cryogenic Temperatures," *Journal of Microelectromechanical Systems*, Vol. 11, No. 4, 2002, pp. 385–401.

[56] Srinivasan, R., and B. Braren, "Ultraviolet Laser Ablation of Organic Polymers," *Chemical Reviews*, Vol. 89, No. 6, 1989, pp. 1303–1316.

[57] Gomez, D., et al., "Femtosecond Laser Ablation for Microfluidics," *Optical Engineering*, Vol. 44, No. 5, 2005, p. 51105-1.

[58] Snakenborg, D., H. Klank, and J. P. Kutter, "Microstructure Fabrication with a CO_2 Laser System," *Journal of Micromechanics and Microengineering*, Vol. 14, No. 2, 2004, pp. 182–189.

[59] Cheng, J. -Y., et al., "Direct-Write Laser Micromachining and Universal Surface Modification of PMMA for Device Development," *Sensors and Actuators, B: Chemical*, Vol. 99, No. 1, 2004, pp. 186–196.

[60] Klank, H., J. P. Kutter, and O. Geschke, "CO_2-Laser Micromachining and Back-End Processing for Rapid Production of PMMA-Based Microfluidic Systems," *Lab on a Chip*, Vol. 2, No. 4, 2002, pp. 242–246.

[61] Luo, L. W., et al., "Rapid Prototyping of Microfluidic Systems Using a Laser-Patterned Tape," *Journal of Micromechanics and Microengineering*, Vol. 17, No. 12, 2007, pp. N107–N111.

[62] Liu, H. -B., and H. -Q. Gong, "Templateless Prototyping of Polydimethylsiloxane Microfluidic Structures Using a Pulsed CO_2 Laser," *Journal of Micromechanics and Microengineering*, Vol. 19, No. 3, 2009, p. 037002.

[63] Martin, P. M., et al., "Fabrication of Plastic Microfluidic Components," *Proceedings of the SPIE Conference on Microfluidic Devices and Systems*, Santa Clara, CA, Vol. 3515, 1998.

[64] Matson, D. W., et al., "Laser Machined Components for Microanalytical and Chemical Separation Devices," *SPIE*, Boston, MA, Vol. 3519, 1998.

[65] Moss, E. D., A. Han, and A. B. Frazier, "A Fabrication Technology for Multi-Layer Polymer-Based Microsystems with Integrated Fluidic and Electrical Functionality," *Sensors and Actuators B: Chemical*, Vol. 121, No. 2, 2007, pp. 689–697.

[66] Li, J. M., C. Liu, and L. Y. Zhu, "The Formation and Elimination of Polymer Bulges in CO_2 Laser Microfabrication," *Journal of Materials Processing Technology*, Vol. 209, No. 10, 2009, pp. 4814–4821.

[67] Roberts, M. A., et al., "UV Laser Machined Polymer Substrates for the Development of Microdiagnostic Systems," *Analytical Chemistry*, Vol. 69, No. 11, 1997, pp. 2035–2042.

[68] Pugmire, D. L., et al., "Surface Characterization of Laser-Ablated Polymers Used for Microfluidics," *Analytical Chemistry*, Vol. 74, No. 4, 2002, pp. 871–878.

[69] Reyntjens, S., and R. Puers, "A Review of Focused Ion Beam Applications in Microsystem Technology," *Journal of Micromechanics and Microengineering*, Vol. 11, No. 4, 2001, pp. 287–300.

[70] Tseng, A. A., "Recent Developments in Micromilling Using Focused Ion Beam Technology," *Journal of Micromechanics and Microengineering*, Vol. 14, No. 4, 2004, pp. 15–34.

[71] Yasuda, T., T. Higashi, and Y. Nakashima, "Fabrication of a Microfluidic Device for Axonal Growth Control," *IEEE International Solid-State Sensors and Actuators Conference*, Vol. 2, Piscataway, NJ, 2003.

[72] Cannon, D. M., et al., "Fabrication of Single Nanofluidic Channels in Poly(Methylmethacrylate) Films Via Focused-Ion Beam Milling for Use as Molecular Gates," *Applied Physics Letters*, Vol. 85, No. 7, 2004, pp. 1241–1243.

[73] Wang, K. -G., et al., "Manipulating DNA Molecules in Nanofluidic Channels," *Microfluidics and Nanofluidics*, Vol. 2, No. 1, 2006, pp. 85–88.

[74] Mahabadi, K. A., et al., "Fabrication of PMMA Micro- and Nanofluidic Channels by Proton Beam Writing: Electrokinetic and Morphological Characterization," *Journal of Micromechanics and Microengineering*, Vol. 16, No. 7, 2006, pp. 1170–1180.

[75] Broers, A. N., *A Review of Electron Beam Lithography Techniques*, Paris: Comite du Colloque Internat. Microlithographie, 1977.

[76] Inman, W., et al., "Design, Modeling and Fabrication of a Constant Flow Pneumatic Micropump," *Journal of Micromechanics and Microengineering*, Vol. 17, No. 5, 2007, pp. 891–899.

[77] Mescher, M. J., et al., "Fabrication Methods and Performance of Low-Permeability Microfluidic Components for a Miniaturized Wearable Drug Delivery System," *Journal of Microelectromechanical Systems*, Vol. 18, No. 3, 2009, pp. 501–510.

[78] Mecomber, J. S., D. Hurd, and P. A. Limbach, "Enhanced Machining of Micron-Scale Features in Microchip Molding Masters by CNC Milling," *International Journal of Machine Tools and Manufacture*, Vol. 45, No. 12-13, 2005, pp. 1542–1550.

[79] Bartholomeusz, D. A., R. W. Boutte, and J. D. Andrade, "Xurography: Rapid Prototyping of Microstructures Using a Cutting Plotter," *Journal of Microelectromechanical Systems*, Vol. 14, No. 6, 2005, pp. 1364–1374.

[80] Solignac, D., et al., "Powder Blasting for the Realisation of Microchips for Bio-Analytic Applications," *Sensors and Actuators, A: Physical*, Vol. 92, No. 1-3, 2001, pp. 388–393.

[81] Mineta, T., et al., "A Wet Abrasive Blasting Process for Smooth Micromachining of Glass by Ductile-Mode Removal," *Journal of Micromechanics and Microengineering*, Vol. 19, No. 1, 2009, p. 015031.

[82] Lomas, T., et al., "A Precision Hot Embossing Mold Fabricated by High-Resolution Powder Blasting with Polydimethylsiloxane and SU-8 Masking Technology," *Journal of Micromechanics and Microengineering*, Vol. 19, No. 3, 2009, p. 035002.

[83] Cook L. M., et al., "Theoretical and Practical Aspects of Dielectric and Metal CMP," *Semicond. Int.*, Vol. 18, 1995, pp. 141–144.

[84] Zhong, Z. W., Z. F. Wang, and B. M. P. Zirajutheen, "Chemical Mechanical Polishing of Polycarbonate and Poly Methyl Methacrylate Substrates," *Microelectronic Engineering*, Vol. 81, No. 1, 2005, pp. 117–124.

[85] Lee, C., et al., "A Nanochannel Fabrication Technique Using Chemical-Mechanical Polishing (CMP) and Thermal Oxidation," *IEEE Conference on Nanotechnology*, Vol. 2, Piscataway, NJ, 2003.

[86] Zhang, J., and T. H. Gong, "Micromachining Technologies for Capillary Electrophoresis Utilizing Pyrex Glass Etching and Bonding," *Proceedings of the SPIE—The International Society for Optical Engineering*, Vol. 4174, 2000.

[87] Feng, G. -H., and E. S. Kim, "Micropump Based on PZT Unimorph and One-Way Parylene Valves," *Journal of Micromechanics and Microengineering*, Vol. 14, No. 4, 2004, pp. 429–435.

[88] Steiner, P., A. Richter, and W. Lang, "Using Porous Silicon as a Sacrificial Layer," *Journal of Micromechanics and Microengineering*, Vol. 3, No. 1, 1993, pp. 32–36.

[89] Jacobson, S. C., A. W. Moore, and J. M. Ramsey, "Fused Quartz Substrates for Microchip Electrophoresis," *Analytical Chemistry*, Vol. 67, No. 13, 1995, pp. 2059–2063.

[90] Ko, H. S., C. W. Liu, and C. Gau, "Novel Fabrication of a Pressure Sensor with Polymer Material and Evaluation of Its Performance," *Journal of Micromechanics and Microengineering*, Vol. 17, No. 8, 2007, pp. 1640–1648.

[91] Szmigiel, D., et al., "Deep Etching of Biocompatible Silicone Rubber," *Microelectronic Engineering*, Vol. 83, No. 4-9, 2006, pp. 1178–1181.

[92] Meng, E., and Y. -C. Tai, *Parylene Etching Techniques for Microfluidics and BioMEMS*, Miami Beach, FL: Institute of Electrical and Electronics Engineers Inc., 2005.

[93] Rossier, J. S., et al., "Plasma Etched Polymer Microelectrochemical Systems," *Lab on a Chip*, Vol. 2, No. 3, 2002, pp. 145–150.

[94] Li, X., T. Abe, and M. Esashi, "Deep Reactive Ion Etching of Pyrex Glass Using SF6 Plasma," *Sensors and Actuators, A: Physical*, Vol. 87, No. 3, 2001, pp. 139–145.

[95] Olsson, A., et al., "Micromachined Flat-Walled Valveless Diffuser Pumps," *Journal of Microelectromechanical Systems*, Vol. 6, No. 2, 1997, pp. 161–166.

[96] Yin, H., et al., "Microfluidic Chip for Peptide Analysis with an Integrated HPLC Column, Sample Enrichment Column, and Nanoelectrospray Tip," *Analytical Chemistry*, Vol. 77, No. 2, 2005, pp. 527–533.

[97] Schluter, M., et al., "A Modular Structured, Planar Micro Pump with No Moving Part (NMP) Valve for Fluid Handling in Microanalysis Systems," *2nd Annual International IEEE-EMBS Special Topic Conference on Microtechnologies in Medicine and Biology*, 2002.

[98] Belloy, E., et al., "The Introduction of Powder Blasting for Sensor and Microsystem Applications," *Sensors and Actuators A: Physical*, Vol. 84, No. 3, 2000, pp. 330–337.

[99] Sayah, A., et al., "Fabrication of Microfluidic Mixers with Varying Topography in Glass Using the Powder-Blasting Process," *Journal of Micromechanics and Microengineering*, Vol. 19, No. 8, 2009, p. 085024.

7

Additive Processes

Solidification processes and subtractive processes alone are inadequate for producing the variety of material combinations needed in many microfluidic devices. Greater functionality almost always requires a combination of processes involving more than one type of material. Accordingly, additive microfabrication processes such as vapor deposition, plating, and printing are necessary for fabricating a wider variety of devices.

There are several ways in which additive processes may be categorized. As in the case of subtractive processes, one basic distinction is the kind of processing environment in which a process occurs. For example, sputter deposition occurs in a (dry) plasma chamber, whereas electroplating occurs in a (wet) liquid plating bath. Additive processes may also be distinguished based on whether the fundamental mechanism is physical or chemical in nature. The addition of material by chemical mechanism implies that chemical reactions occur, whereas the physical addition of material is accomplished by such mechanisms as impingement, electrostatic attraction, and surface wetting.

Methods of achieving spatial selectivity include parallel methods that add material broadly over an entire surface, and serial methods that add material with selectivity based on a prescribed path. Parallel additive processes use a variety of different approaches to designate where material should or should not be added. As illustrated in Figure 7.1, one common approach is to proceed with complete broad-area coverage first, followed by selectively removing material using one of the subtractive processes described in Chapter 6. There are other important strategies for spatially selective addition of material, and these will be described for each of the individual processes later in this section.

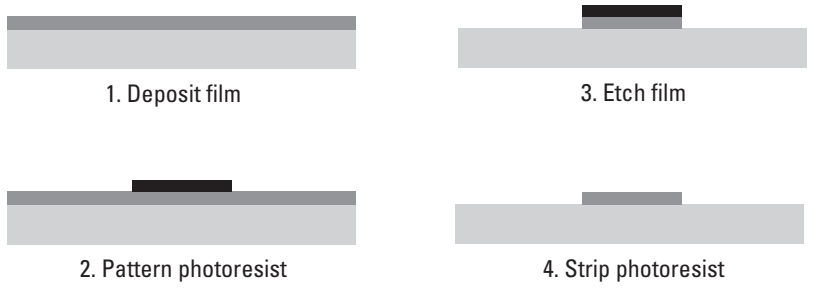

Figure 7.1 Selective addition of material by full-layer deposition and subsequent etching.

For subtractive processes, an important distinction among processes is whether they tend to produce profiles that are isotropic or anisotropic. For additive processes, a more common issue regarding directionality is whether the profile of added material is *conformal* or *nonconformal*. Figure 7.2 shows a film deposited over a trench, comparing a conformal profile with uniform thickness against cases that lack these characteristics. Nonconformal profiles are sometimes described as snowfall because they exhibit line-of-sight directionality, analogous to the accumulation of snow on building rooftops.

Conformal profiles are desirable especially when material continuity must be preserved. Precise control over continuity is particularly important for defining boundaries between electrically conducting and electrically insulating regions. Processes based on chemical reactions on surfaces are generally more conformal that processes based on physical mechanisms of material addition. The general assumption that conformal coating is preferable is not absolute, however. Nonconformal profiles can sometimes be used as a functional advantage. For example, tilting a substrate can allow sidewalls to be coated thicker than top surfaces and enable the fabrication of laterally deflecting bimorph actuators [1].

Another aspect that is related to conformal coverage is whether an added material is *self-planarizing* or not, as distinguished in Figure 7.3. In general, materials that exhibit highly conformal coverage are not self-planarizing unless

Figure 7.2 Conformal and uniform profile versus nonconformal and nonuniform profiles.

Figure 7.3 Self-planarizing layer compared to a conformal layer.

thickness becomes great enough that the underlying topography begins to be obscured. Additive processes that are self-planarizing are favorable for multilayer process integration because photolithography steps and other subsequent processes can avoid problems of step coverage. In cases for which a flat surface is required, chemical-mechanical polishing (CMP) is a common and effective way to achieve planarization.

For subtractive processes, the selectivity ratio between materials is one of the most fundamental considerations when planning the fabrication method. For additive processes, however, material *compatibility* often tends to be a dominant concern. Whenever new interfaces are created between dissimilar materials, compatibility must be ensured in several different ways. If any materials are processed in liquid state, wetting characteristics and/or miscibility must be compatible. Materials must be chemically compatible so that only the intended reactions occur and unwanted reactions do not. Electrical and electronic compatibility are important not only in terms of defining conductive and insulating boundaries, but also in terms of preventing interatomic diffusion that could compromise proper functionality of semiconductor devices. Materials must be thermally compatible so that the processing temperature for adding a new material does not exceed tolerable limits for any existing materials already present. Even if process temperatures remain well below glass transition, thermomechanical compatibility is still nontrivial because differences in coefficient of thermal expansion can result in distortion or stress-related failure at material interfaces. Residual stress is a fundamental concern for all thin-film fabrication methods [2, 3]. These examples are nonexhaustive, but they emphasize the wide range of compatibility issues for additive microfabrication processes. In the subsections that follow, some of the most common processes for material addition are presented, including a discussion of relative merits and examples of ways in which they are used in microfluidic device fabrication.

7.1 Physical Vapor Deposition

Physical vapor deposition (PVD) adds material to a surface by releasing material from a source or target and directing it toward the substrate to be coated. PVD is distinguished from chemical vapor deposition in that there are no chemical

reactions that fundamentally need to occur for the material to be deposited. The two most common types of physical vapor deposition in microfabrication are *evaporation* and *sputtering*. In evaporation, material is thermally vaporized from a source, whereas in sputtering the material is ejected by ion bombardment. Relative merits between evaporation and sputtering are discussed in the subsections below. Both evaporation and sputtering are routinely used to pattern metal on other substrates. Common purposes include electrical signal conduction, electrostatic actuation, electrochemical sensing, and resistive heating. For example, thin-film metal resistors can be used as integrated heaters for thermopneumatic peristaltic pumping [4]. PVD also often plays an important supporting role for electroplating (discussed in Section 7.4), because a metal seed layer is needed to initiate electroplating on nonconducting substrates.

In terms of spatial selectivity, the previously mentioned two-step process of depositing a full layer followed by selective etching is one possible approach. A faster approach used in PVD processes is simply to occlude incoming material, thus preventing it from ever making contact with the substrate surface. One basic way of occluding material is by using a *shadow mask*, as illustrated in Figure 7.4. A shadow mask in general can be any rigid or semirigid sheet of material with patterned openings. Some ways of fabricating shadow masks include electrochemical machining of metal foil, laser machining of plastic or metal shim stock, and through-wafer etching of silicon.

Shadow masks are not only convenient but in some cases they are also reusable. In terms of resolution and edge quality, however, shadow masks are limited for multiple reasons. One issue is that the size and proximity of openings in the mask must not compromise its basic structural integrity. This generally requires relatively thick material for the mask and thereby limits lateral resolution, especially if the profiles of the openings in the mask do not have vertical sidewalls. Another concern is the possibility of material being deposited underneath the corners of the shadow mask, where it is generally very difficult to

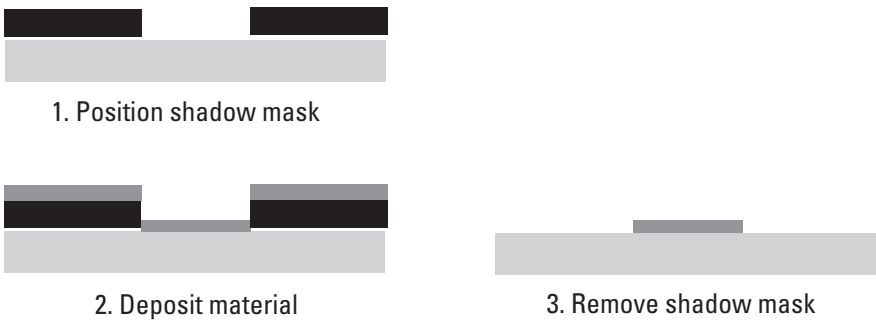

Figure 7.4 Selective addition of material by occlusion with a shadow mask.

ensure perfect contact. Although it is possible to improve contact by temporary bonding of the shadow mask to the substrate, such improvement in quality comes with some compromise in speed and convenience.

Along the same principles as a hard shadow mask, another approach for patterning is to use photoresist as a lift-off layer. A diagram for a basic lift-off process would be almost identical to the shadow mask process, with the mask layer typically being much thinner. While having a thin mask layer generally improves resolution over the same process using a hard mask, the lift-off method is still subject to irregularly defined edges because the deposited layer must be broken as the photoresist is removed. An effective way to avoid such damage is to include two different layers of photoresist such that the lower layer is undercut beneath the upper one. This ensures discontinuity between the deposited material and the material to be removed, as shown in Figure 7.5. The lift-off process may be more cumbersome for achieving well-defined features, but it has some advantages over depositing a full film and etching. For example, the substrate need not be subjected to chemical etchants, and it is generally much easier to locate alignment targets through photoresist than it is through a blanket metal film.

Adhesion is a fundamental concern for any additive process, but especially relevant for PVD because processes that are physical in nature do not have the benefit of forming strong chemical bonds at interfaces. Gold is one of the most common metals used in microfluidic and MEMS devices, but its advantage of being resistant to oxidation and corrosion coincidentally prevents it from having strong adhesion as a pure thin film. Therefore, it is quite common to use an intermediate adhesion layer when depositing PVD films. Chromium does form a metal oxide when deposited as a thin film on oxide glasses [5] and is a preferred material for use as an adhesion layer between gold and silicon dioxide [6].

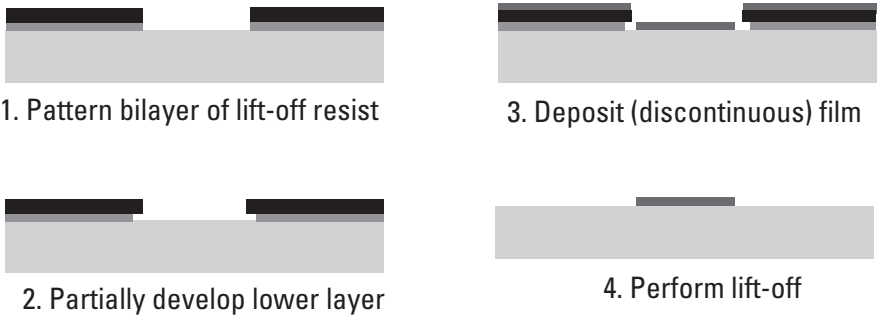

Figure 7.5 Lift-off procedure with two-layer resist and undercut for improved edge definition.

Similarly, titanium is known to be effective for improving the adhesion of platinum thin films [7].

PVD methods generally require high vacuum because of multiple factors, including maintaining vapor pressure and limiting contaminant concentration. In the case of sputtering, vacuum conditions are required for sustaining plasma with adequate particle momentum for ionization. Furthermore, long mean free paths between particle collisions facilitate more efficient, directional transport of material. Evaporation equipment tends to be less costly than sputtering systems because plasma is not required. Other relative merits are discussed in the subsections that follow.

7.1.1 Evaporation

Evaporation, as the name suggests, involves vaporizing a source material and allowing it to condense onto a substrate surface. Most conventionally the material to be evaporated is placed in a crucible, and energy is delivered by any variety of heat sources including electron beam, resistive heating, and inductive heating. E-beam evaporation is a preferred method because the energy density can be very high and narrowly targeted. Evaporation can also be achieved by placing discrete clips of material on a resistive filament wire. The rate can be increased by using higher input energy, and the deposition rate for evaporation is roughly an order of magnitude faster than sputtering. Faster rate, however, generally comes with a trade-off in thickness uniformity and greater likelihood of imperfections in film density.

Since evaporation is based on reaching a threshold of phase stability, in most cases evaporation is limited to pure elements. Pure metals have deterministic melting point, vapor pressure, specific heat of vaporization, and so on, whereas inorganic compounds and polymers generally do not. Although both vapor pressure and process temperature are the determining factors, melting point is often correlated to these factors and thus provides a rough indicator of suitability. Aluminum, with a low melting point of 660°C, is easily evaporated. Gold, with a melting point of 1,064°C, is also routinely evaporated, whereas refractory metals like tungsten (T_m = 3,370°C) are much more difficult.

7.1.2 Sputtering

Sputtering was introduced previously in Chapter 6 in the context of ion etching as a removal process. However, as mentioned, if a substrate is placed in the same plasma chamber as the target material while ion bombardment occurs, the substrate becomes coated with the sputtered material. As a purely physical process, sputtering applies to almost any material regardless of melting temperature or heat of vaporization. While evaporation is generally applicable only to pure

elements, sputtering is useful for a wider variety of materials, including nickel-iron alloys for magnetically actuated microvalves [8] and even more diverse materials such as SiO_2–LiO_2–BaO–TiO_2–La_2O_3 used in microfluidic pH sensing [9].

Deposition rates for sputtering are approximately an order of magnitude slower than evaporation, typically on the order of 100 Å/min. So a 1-micron film (10,000 Å) by sputtering is considered fairly thick, and may take more than an hour to complete. Accordingly, the deposition run may need to be divided into incremental segments to avoid problems from substrate heating.

Sputter deposition is a bidirectional process of ion flux toward the target and ejected atoms moving away from it. So, fundamentally, sputtering involves more lateral collisions than evaporation. This can be desirable in some cases such as achieving sidewall coverage over trenches and other topographical features. However, the same difference in behavior can be undesirable if shadow masking is used because there is a much greater tendency to deposit material under the edges of the shadow mask.

7.1.3 Pulsed Laser Deposition

Pulsed laser deposition (PLD) [10] is another physical deposition process that is capable of achieving relatively thick films. It shares commonality with evaporation and sputtering in that energy (a pulsed laser, in this case) is directed toward a target material and is vapor-deposited on another substrate. Like sputtering, it is applicable to a relatively wide variety of materials including metal oxides. An advantage of PLD over sputtering is that it does not require high-vacuum conditions or plasma. Perhaps more importantly, PLD is well suited for thicker films up to tens of microns, whereas sputtering is generally limited to films on the order of 1 micron. In microfluidics, PLD is not nearly as commonplace as evaporation or sputtering. However, PLD has unique advantages for niche requirements, such as the deposition of piezoelectric materials including zinc oxide and barium titanate [11].

7.2 Oxidation

Silicon dioxide plays a uniquely important role in microfabrication, and in many ways it has been just as vital as silicon itself with respect to success of the microelectronics industry. For microfabrication in a broader sense, some of the diverse ways in which silicon dioxide is used include functionality as an insulating film, etch mask, sacrificial layer, diffusion barrier, and field oxide (for field effect transistors).

Oxidation of silicon is a topographically conformal process, and a direct example of applying oxidation to microfluidics is the growth of oxide on etched silicon microchannels. The silicon dioxide layer makes channel surfaces electrically nonconducting and facilitates viability for electro-osmotic flow and sample detection by electrochemical means [12]. Oxide films on silicon are also used for other purposes such as patterned masters for a variety of casting, molding, and imprinting techniques, as introuduced in Chapter 5.

The most well-established way of creating a silicon dioxide film on a silicon substrate is by thermal oxidation at high temperature [13]. In the presence of oxygen, an oxide layer forms on the surface of silicon. Such oxidation on bare silicon occurs even in ordinary air at room temperature, with a subnanometer thin coating described as *native oxide*. Elevated temperature, however, is needed to enable adequate diffusion for greater film thickness. At sufficiently high temperature (typically near 1,000°C), oxygen atoms diffuse through the existing oxide layer to form silicon dioxide at the (buried) interface with silicon. Thermal oxidation is therefore actually a growth process at the oxide-silicon interface, not deposition onto the outer surface.

In thermal oxidation, some of the silicon is consumed in the process such that approximately 45% of the resulting oxide layer thickness is from the original silicon (i.e., a 1,000Å oxide film grown on a bare silicon surface adds a net thickness of only ~550Å). For flat layers, this simply requires compensation for planar offset when estimating film thickness and material boundaries. This partial consumption of silicon is also used as a technique to create sharp tips by oxidation of protruded features and subsequent etching of the oxide to leave a tip that is sharper than the original [14, 15].

Thermal oxidation can be conducted in dry oxygen or with water vapor (known as wet oxidation). Hydrochloric acid (HCl) is commonly added to help prevent metal contamination. Dry oxidation results in higher purity and fewer pinhole defects, whereas wet oxidation has the relative merit of faster growth rate. Other factors that affect growth rate include temperature, partial pressure, and crystal orientation. Over a wide range of conditions, oxide growth rate is observed to be linear with time for very thin oxides and parabolic for thicker oxides, with the most well-known predictive model based on the work of Deal and Grove [16]. A film of only 100-nm thickness can still take hours of processing time, so thermal oxidation is generally limited to film thickness no greater than ~2 microns.

7.3 Chemical Vapor Deposition

Thermal oxidation is an invaluable process in microfabrication, but with few exceptions it is limited to only silicon dioxide growth upon silicon. Evaporation,

sputtering, and other PVD methods provide a diverse set of processes to address requirements in terms of material type and deposition rate. As PVD processes are governed by line-of-sight arrival of material onto a substrate, however, conformal step coverage is limited and adhesion can sometimes be problematic. Although there are methods of reactive sputtering [17], in general, PVD methods are not well suited for producing films with precise stoichiometry. To answer some of these broader needs, chemical vapor deposition (CVD) methods provide a more comprehensive suite of vapor deposition alternatives. CVD is distinguished from PVD because species-altering chemical reactions occur, and CVD is distinguished from thermal oxidation because the material is deposited rather than grown.

In CVD, reactive species are introduced to a substrate, typically by flowing a dilute mixture in an inert carrier gas across its surface. Reactive species are adsorbed onto the surface where reactions occur, and any byproducts are removed by returning into the carrier stream. As the reactions continue to occur on the surface, nucleation sites eventually merge and form a continuous film. The formation of CVD films necessitates surface migration and diffusion of species, which is fundamentally very different from the line-of-sight type of transport that is characteristic of PVD processes. A direct consequence of this is that CVD films tend to have far better conformal step coverage than PVD films.

To promote favorable reaction kinetics, both the substrate and the gas stream are heated to elevated temperatures. These temperatures are generally above the melting or decomposition temperature of polymers (~300°C and higher), so CVD is far more commonly associated with silicon, glass, and inorganic compounds rather than polymers. CVD is an established method of depositing silicon dioxide films with significant dopant concentration (e.g., phosphosilicate glass PSG or borosilicate glass BSG). Phosphosilicate glass is a popular material choice for sacrificial processes because it exhibits fast etch rate with good selectivity with respect to materials such as silicon nitride and polysilicon. A limited set of metals (most notably tungsten) can be deposited by CVD, but applications for CVD metals are more relevant in microelectronics rather than microfluidics.

There are many variants of CVD, and one of the most common is low-pressure chemical vapor deposition (LPCVD). LPCVD operates at high temperature (typically near 1,000°C) and is known for having high purity and uniformity. It is useful not only for inorganic compounds like silicon nitride but also polysilicon. Silicon nitride is very effective as an insulator, an etch mask, a passivation layer, and in some cases even a mechanical structure. LPCVD of doped polysilicon is one established way of producing piezoresistive elements for strain-sensing purposes, such as needed for pressure sensors.

The characteristically high temperatures of LPCVD generally make it incompatible with polymer substrates. However, novel use of fabrication sequence can be implemented to combined LPCVD polysilicon with polymers such as SU-8 and PMMA, as long as the high temperature steps are conducted first, followed by subsequent processes involving polymers. For example, pressure sensors have been made with doped polysilicon piezoresistors on SU-8 membranes by beginning with the polysilicon film first, followed by SU-8 patterning [18].

Plasma-enhanced chemical vapor deposition (PECVD) is another type of CVD process that has the key advantage of operating at lower temperatures than LPCVD. The benefit of plasma is that it allows surface reactions to occur at substantial rate at lower temperatures than would otherwise be required by LPCVD. This not only facilitates a wider range of substrate materials but also subjects them to less severe thermal loading, which can be beneficial for managing film stress. The main drawback relative to LPCVD is that PECVD films tend to have inferior purity. The need for a plasma chamber can often mean lower productivity for PECVD as well, compared to LPCVD that can readily be manifested with batch processing in a tube furnace.

Atomic layer deposition (ALD) is essentially a CVD process with even finer compositional and dimensional control [19]. In ALD, reaction precursors are delivered to the substrate surface in pulses, with intermediate purging to remove excess. ALD reactions occur only on the surface and are self-limiting to the amount of precursor that is adsorbed onto the surface.

In microfluidics, CVD is more often encountered in supporting roles rather than being a primary part of fabricating geometric features directly. For example, the merits of silicon carbide in terms of high corrosion resistance and high temperature performance can be used by CVD coating SiC films onto silicon [20]. ALD-deposited aluminum oxide can be used to improve biocompatibility for cell adhesion and growth on glass [21]. There are also some other novel capabilities such as the fabrication of nanoporous LPCVD polysilicon thin films, which can be used to create permeable fluidic microchannels [22].

Another novel example of using LPCVD is the fabrication of three-dimensional pipettes as shown in Figure 7.6. Using the conformal nature of LPCVD, low-stress silicon nitride can be deposited onto the interior walls of DRIE silicon cavities with very high aspect ratio. Etching away much of the bulk silicon from the opposite side leaves a hollow tube-like structure. The pipettes can be fabricated with diameters ranging from 6 μm to as small as 250 nm. Thermal oxide growth and plasma RIE are also used as part of the integrated process.

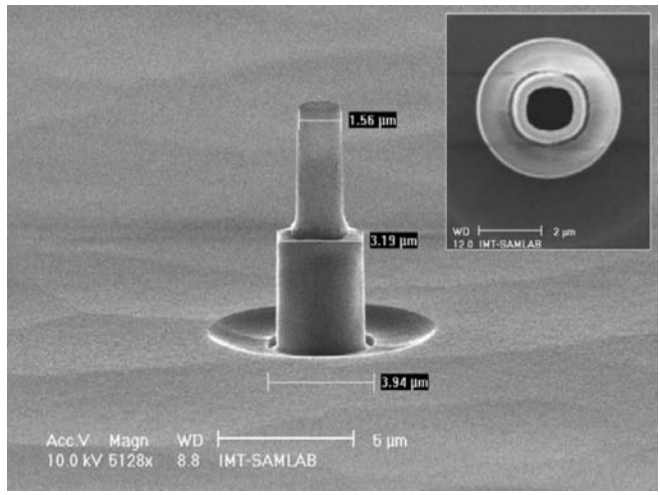

Figure 7.6 Hollow micro pipette from LPCVD silicon nitride coating of DRIE cavities. (Reprinted from [23], with permission from IOP Publishing.)

7.4 Electroplating

Thin-film vapor deposition and growth processes as described above are generally limited to thickness on the order of 1 μm. Thicker films are impractical using vapor deposition, so at least for metals electroplating is much more effective for thicker structures from several microns up to several hundreds of microns thick. Mechanically robust electrodes for use with plastic microfluidic chips can be made by electroplating [24]. Another major use for electroplated structures in microfluidics is the fabrication of durable masters for casting, molding, and imprinting techniques (Chapter 5).

Electroplating is a process in which metal ions in an electrolyte solution are deposited onto a surface. A dc power supply connected to two electrodes drives oxidation of metal atoms off one electrode into solution and also reduction of the ions from solution onto the other electrode. For microfabricated devices, using photopatterned masks to define the boundaries of electrodeposited material provides a very versatile fabrication method for a wide variety of metals and alloys [25].

There are three words with subtle differences that are sometimes used interchangeably in the context of microfabrication. *Electroplating* focuses on the outcome of producing a surface coating on a functional object for purposes such as corrosion resistance, abrasion resistance, and even visual appearance. *Electrodeposition* more closely addresses the fundamental electrochemical process of ion reduction at a surface. *Electroforming* describes the attainment of a

particular geometric shape by electrodeposition onto a (temporary) master pattern. In the manufacturing of macroscale products, the master pattern is called a mandrel, and common electroformed parts tend to be thin-walled shells. In microfabrication, the difference between electroplating and electroforming becomes less distinct as lateral dimensions of interest approach the same dimensional scale as plated film thickness. Accordingly, some liberties with interchangeability among the words electroplating, electrodeposition, and electroforming are taken throughout the published literature on microfabrication, as well as in this chapter.

Electroplating depends on an electrically conductive surface to allow the metal ions in solution to be reduced onto it. Under limited conditions, however, some metals can also be plated onto nonconductive surfaces if surface catalysis is sufficiently favorable. This so-called method of electroless plating is feasible with materials including nickel, copper, gold, and silver, but it is not common in microfabrication because rates are slow and the process is more difficult to control than conventional electroplating. The ease of adding a conductive seed layer by PVD obviates the need for electroless plating in most cases.

Ultrathick photoresist [26] and laminated dry-film photoresist [27] are popular options that serve as masks for defining the geometric boundaries of features made by electroplating. As illustrated in Figure 7.7, a patterned mask covers regions of the substrate that would otherwise allow plating to occur.

SU-8 is the most frequently cited negative resist for microfabrication by patterned electroplating. As a robust epoxy-based material, however, SU-8 can be very difficult to remove after plating [28]. A thin sacrificial layer can be used to facilitate ease of separation after plating [29]. Alternatives exist for thick negative resists that are more easily removed, such as THB-430N by JSR Corporation (Sunnyvale, California), which are also effective in achieving high aspect ratios of approximately 5:1 [30]. Positive resists such as AZ 4562 by AZ Electronic Materials (Branchburg, New Jersey) are also capable of high aspect

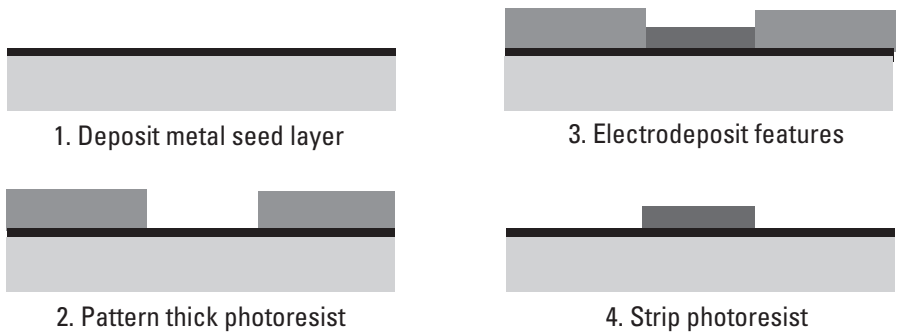

Figure 7.7 Electrodeposited features defined by thick photoresist mask.

ratio and are favorable in terms of compatibility with mainstream integrated circuit fabrication processes. While photopatternable polymers are most commonly used as the masking layer, in principle any material demonstrating proper selectivity may be used. For example, through-wafer patterns etched in silicon by DRIE have been used to fabricate electrodes with well-defined vertical sidewalls for submillimeter metal components by electrical discharge machining [31]. Having hydrophobic surfaces, however, is beneficial for enabling high aspect ratio features in masked electroplating. For example, argon plasma treatment of SU-8 makes it possible to electroform copper features with aspect ratio better than 15:1 [32].

Some of the most impressive microscale components in terms of aspect ratio are those fabricated by a process known as LIGA, which comes from the German acronym for "lithographie, galvanoformung, abformung." The main enabling factor is the use of X-ray lithography to produce very high aspect ratio features in thick PMMA layers. The PMMA layers are subsequently used as masks for electroplating metals such as nickel. Economically it is often favorable to use the first metal component as a parent molding tool to fabricate many more polymer masks, which in turn can be used to produce higher volumes of metal copies. Micro gear pumps have been fabricated by LIGA technology with meshed gear components approximately 500 μm tall and 600 μm in diameter [33]. In early years of demonstrating its unique capabilities, LIGA received much attention as a uniquely enabling MEMS fabrication process. However, the high investment in time and cost has drawn attention away from X-ray LIGA per se, with similar process combinations that can still achieve appreciably high aspect ratio without requiring a synchrotron source and X-ray masks. Processes using ultrathick UV resists (e.g., SU-8) as an electroplating mask are often described as UV-LIGA, to distinguish them from the original LIGA process based on X-ray lithography. SU-8 is the most common photoresist used in UV-LIGA, although alternatives including ultrathick positive resists such as methyl methacrylate (MMA) with tert-butyl methacrylate (TBMA) have been successfully demonstrated with aspect ratio near 10:1 [34].

An alternative approach to electroplating onto a flat substrate is to use a temporary substrate that has topographical features, as illustrated in Figure 7.8. This process produces a shaped electroform, and in some ways resembles casting because the final geometry represents the inverse image of the master from which it is patterned. If the surface is nonconductive, a metal seed layer can be deposited by PVD if necessary. If the master is made of a flexible material like PDMS, the electroform can be separated from it with much lower risk of damage than if the master were rigid [35].

The shape of the electroform reproduces features in the master with good fidelity. This is beneficial for cases in which it is important to achieve prescribed profiles. One example is the electroforming of a nickel-cobalt molding insert,

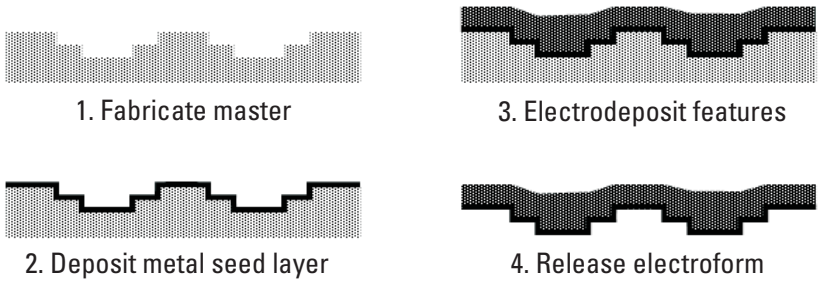

Figure 7.8 Electroforming onto topographical features of a master pattern.

shown in Figure 7.9. In this approach, an SU-8 pattern (not shown) is first defined with tapered profiles by excimer laser machining. A thin film of gold is deposited as a seed layer, and a Ni-Co mold is then electroformed onto the SU-8 master. Thereafter, the Ni-Co electroform is used as a molding insert to fabricate the final nozzle components in polyether sulfone.

In general, three-dimensional complexity can be achieved as long as there is an appropriate method of sequential masking. For example, (although not specifically for microfluidic applications) three-dimensional coils in nickel have been demonstrating by electroplating onto a wire with a UV-sensitive resin pattern that was shaped in a 3D PDMS mold [37].

Yet another alternative to defining the geometry of electroplated features is to abandon a mask altogether and use direct-write printing of a conductive seed layer on an otherwise nonconductive surface. The process is spatially selective because electroplating occurs only upon the printed regions [38]. Electroplating upon a direct-write seed layer offers some advantage over traditional mask-based approaches, particularly with respect to ease of rapid prototyping. However, lateral electrodeposition is not constrained, so resolution and aspect ratio tend to be limited.

7.5 Printing and Coating Techniques

This category describes a diverse range of additive processes apart from vapor phase and electrodeposition methods. The basis of commonality for processes in this category is that material is introduced in a liquid or other flowable material phase (e.g., inks and pastes), and is made permanent by a drying and/or curing mechanism. In this regard, some of these processes do qualify for being categorized under solidification processes (see Chapter 5). So there is no claim that these processes are entirely exclusive from that classification, but the grouping here is based on similarities in dispensing, leveling, or transferring material in liquid phase.

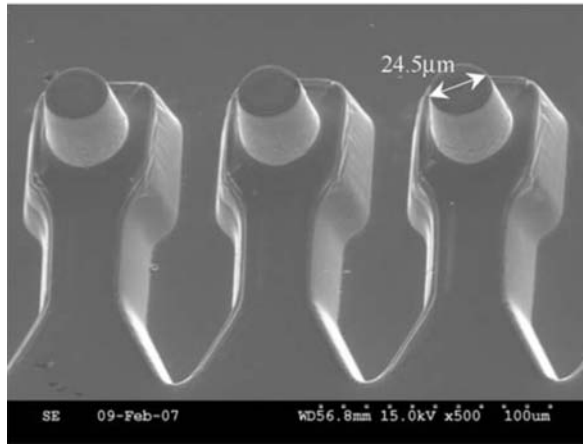

(a)

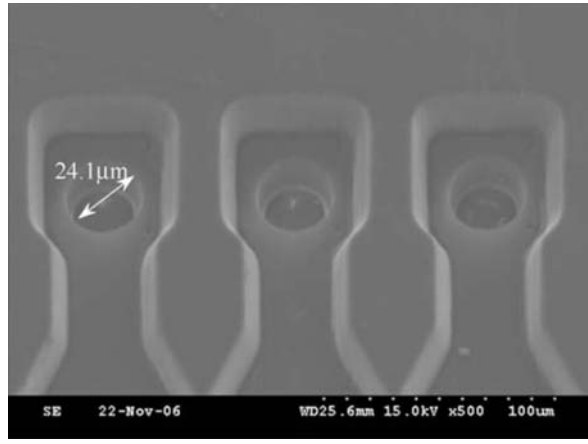

(b)

Figure 7.9 (a) Electroformed metal insert and (b) molded nozzles in polyether sulfone. (© 2009 IEEE. Reprinted with permission from [36].)

7.5.1 Spin-on-Glass

Spin coating has already been discussed in Chapter 4 as the primary method of distributing a layer of photoresist on a surface. In addition to photoresist, other materials may be dispensed and coated onto a surface by spin coating. The most notable example in microfabrication is spin-on-glass (SOG), which in microelectronics is often used for filling narrow gaps in dielectric planarization applications.

Spin-on-glass materials include inorganic silicate glasses and organic siloxanes. Silicate SOG liquids tend to have low viscosity and are generally limited to submicron thickness, whereas siloxanes can be coated appreciably thicker, even beyond several microns. Although coated in liquid form, SOG layers attain properties similar to CVD films after high-temperature curing, typically in the range of several hundreds of degrees Celsius. A functional advantage of SOG formulations is that they can be doped to form borosilicate or phosphosilicate glass.

Despite bearing the name "spin-on," SOG materials in a more general sense can be coated by capillary adhesion. An example of using organic SOG in microfluidics is the coating of etched glass microchannels by filling and capillary adhesion [39]. The SOG film provides benefits of smoothness and low refractive index, and it facilitates use in capillary electrophoresis with integrated optical waveguides for bioanalysis.

7.5.2 Screen Printing and Blade Leveling

Screen printing is a relatively coarse additive method for creating patterned material by forcing a solids-loaded ink or paste through a mesh. The mesh is prepatterned with regions that are completely blocked, forming a stencil such that material passes through only selected areas of the mesh. For micropumps, screen printing has been used effectively for fabricating piezoelectric actuators in materials such as lead zirconate titanate (PZT) [40, 41]. Although relatively coarse, screen printing can also be used to fabricate functional microchannel devices, such as has been demonstrated for isoelectric focusing with channels 100 μm tall and 1 mm wide [42].

In some cases blade-leveling methods without a mesh screen offer a functional alternative to spin coating, particularly for thicker films or films that need to fill deep cavities. Spin coating tends to excel for thinner films on completely flat substrates, but thicker films or membranes patterned within recesses can be made more uniformly with better repeatability by blade or squeegee methods [43]. Blade-leveling techniques have also been used for integrating soft sealing material such as PDMS with a more rigid material such as Parylene for more effective microvalve sealing [44].

7.5.3 Micro Contact Printing

At the opposite end of the spectrum from the relative coarseness of screen printing and blade-leveling methods is material pattern transfer at the monolayer scale. Micro contact printing (μCP) transfers a material by using an elastomeric stamp [45, 46]. The process is analogous to using a rubber stamp and ink pad, except for the fact that μCP use a single layer of molecules for exceptionally fine

resolution and consistency. The ability to form a *self-assembled monolayer* (SAM) of functionalized molecules such as alkanethiolates on compatible surfaces such as gold is a very important phenomenon that is exploited in μCP [47]. Thickness varies depending on the particular type of SAM, but the monolayer is typically no more than a few nanometers thick.

The stamps for micro contact printing are made of elastomer materials, and μCP is one of the core techniques in the suite of soft lithography processes. A primary reason for using an elastomeric stamp is that it provides good conformal contact. Some of the associated design concerns for micro contact printing stamps are pairing (i.e., mutual adhesion among adjacent features), buckling under load, and roof collapse [46]. PDMS is by far the predominant material used for μCP stamps, although alternative materials such as a composite based on vinyl and hydrosilane have been explored to improve fidelity [48]. Applications based on μCP and variants thereof include patterning of biomolecules, printing of catalysts for electroless deposition of metals, and fabrication of light-coupling masks [49].

An interesting combination of microchannel flow networks and μCP is the patterning of continuous gradients as well as discretely incremented samples by first using microchannel networks to achieve prescribed distribution of molecules on a surface [50]. Subsequent contact printing makes it possible to deposit proteins of numerous different types and proportions onto another substrate in a single transfer step.

7.5.4 Ink-Jet Printing and Direct-Write Material Deposition

Screen printing and micro contact printing are spatially parallel material addition processes because broad areas are patterned simultaneously (albeit at very different dimensional scales). In contrast, ink-jet printing and direct-write material deposition are spatially serial processes because material addition follows a prescribed path, based on how material is directed by some form of printhead or directed nozzle tip. For higher productivity it is beneficial to use an array of many nozzles, but the fundamental process is still spatially serial.

With typical orifice diameters in the range of tens of microns, ink-jet printing is a microfluidic application in its own right. However, in the context of this particular chapter section, ink-jet printing is also a tool for additive fabrication. Depending on the control scheme for steering the jet or stream of droplets, there may be important functional constraints related to factors such as surface tension and electrostatic charge. However, ink-jet printing is so versatile as an additive fabrication process because in general any material that can be suspended with adequate uniformity in liquid form can be printed. While ink-jet printing ejects material in the form of a train of droplets, material can also be deposited in direct-write mode using continuous pastes. Direct-write material

deposition techniques are also very versatile and can be applied to ceramic and metal pastes [51] as well as polymers such as polyimide [52].

Compared to the many other options for microchannel device fabrication, it often provides greater relative merit to use printed features as a sacrificial pattern rather than as bulk structures. Different materials can be cast or otherwise replicated over printed features to produce final devices. Wax-based inks, for example, can serve as effective sacrificial materials because they can be printed by direct-write methods and removed by melting and vacuum removal. The direct-write process is shown in Figure 7.10. Complex multilayer manifolds and even spiral passageways have been fabricated by such fugitive ink methods [53].

In the broader context of microfluidic technologies beyond structural device fabrication, ink-jet printing is also a powerfully enabling tool for microscale dispensing. Ink-jet methods can be used for diverse purposes including drug delivery, tissue engineering, and spot deposition of biomolecules [55]. In addition to having multiple jets working simultaneously, other innovations include colliding pairs of droplets to form microcapsules that form a polymer membrane film around an aqueous droplet [56].

7.5.5 Dip-Pen Nanolithography

Dip-pen nanolithography (DPN), illustrated in Figure 7.11, is a form of serial writing on a scale much finer than ink-jet printing. Like micro contact printing, DPN is a method that works with film thickness on the scale of a single molecular layer using SAMs. Line width can be as small as a few tens of nanometers, which is much finer than ink-jet printing, which normally produces typical line widths of a few tens of microns. In DPN, an atomic force microscope (AFM) tip uses capillary forces to control the deposition of molecules onto a surface by chemisorption.

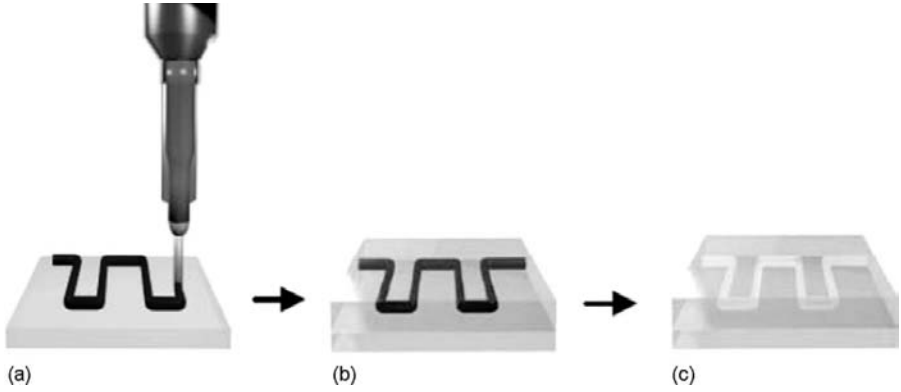

Figure 7.10 (a–c) Fabrication of microfluidic passageways using fugitive ink. (Reprinted from [54]. Copyright 2007, with permission from Elsevier.)

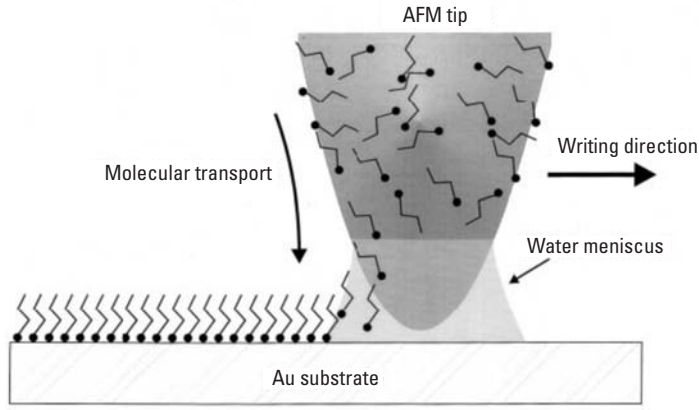

Figure 7.11 Operating principle of dip-pen nanolithography. (*From:* [57]. Reprinted with permission from AAAS.)

DPN is unique among other printing methods because it can also be used in a subtractive mode to selectively remove molecules along the traversed path, depending on relative affinity of the molecules for the tip versus the substrate. Some other key developments of the basic DPN principle include actuating with active bimorph probes [58], dipping into micromachined ink wells [59] and handling multiple ink species in large arrays [60]. Yet another extension of DPN technology is to use more tips with integrated microchannels connected to a reservoir, as illustrated in Figure 7.12, as a way of providing continuous writing capability.

A partial list of the integrated steps used to fabricate the microfluidic device in Figure 7.12 includes isotropic wet etching to form the protruding tip, oxide growth and etching to sharpen the tip, LPCVD deposition and RIE etching of silicon nitride to define the cantilever, anisotropic silicon etching to create the reservoir, wet etching of sacrificial silicon dioxide to clear the internal channels, and subsequent PVD deposition of a Cr/Au film for reflective laser sensing.

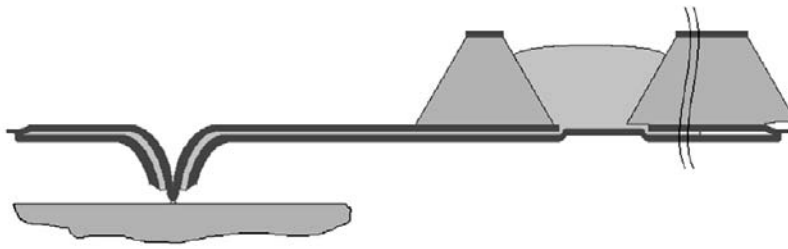

Figure 7.12 Dip-pen nanolithography tip with integrated microchannels connected to a reservoir. (©2006 IEEE. Reprinted with permission from [61].)

Also mentioned (but not shown in the figure) is a PDMS cap over the reservoir to prevent evaporation of the ink solvent. Such cap can very well be fabricated with precise dimensions by micro casting or molding. So this device provides a helpful review of many basic fabrication processes that have been discussed throughout this chapter.

7.6 Tabulated Examples of Additive Processes

Table 7.1 lists several examples of microfabrication processes that are based on prescribed addition of material. The contents are not comprehensive, but rather the table attempts to sample a variety of processes that have been used for microfluidic devices. A small number of table entries may be based on other microfabricated structures not specifically for fluidic devices per se, but these are included to encompass the diversity of materials and processes that can potentially be used.

Table 7.1 lists the basic process by which material is added, the particular materials used, and the means by which selectivity is established. Within each cluster of processes, the more conventional materials and individual processes are generally listed first.

Table 7.1
Examples of Additive Processes

Additive Process	Material	Base Material	Reference
Electroforming with Cu seed layer	Nickel	Shaped PDMS mold	[35]
RF sputtering	SiO_2–LiO_2–BaO–TiO_2–La_2O_3	Platinum	[9]
CVD	Parylene	Silicon	[62]
RF sputtering	Carbon	LPCVD Si_3N_4 on Si	[63]
e-beam evaporation	Platinum	PECVD Si_3N_4 on Si	[64]
Sputtering	Titanium	Polyimide	[65]
Sputtering	NiFe	Si or SiO_2	[8]
LPCVD	Silicon nitride	Si or SiO_2	[66]
Pulsed laser deposition	Barium titanate	Pt on Si	[67]
Pulsed laser deposition	Zinc oxide	Au or Pt films	[11]
LPCVD	Polysilicon, TEOS	Silicon	[18]
Multilayer spin coating	Polyimide	PDMS on Si	[68]
Screen printing	Lead zirconate titanate (PZT)	Cermet Au	[41]

References

[1] Sehr, H., et al., "Fabrication and Test of Thermal Vertical Bimorph Actuators for Movement in the Wafer Plane," *Journal of Micromechanics and Microengineering*, Vol. 11, No. 4, 2001, pp. 306–310.

[2] Malzbender, J., "Mechanical and Thermal Stresses in Multilayered Materials," *Journal of Applied Physics*, Vol. 95, No. 4, 2004, pp. 1780–1782.

[3] Fang, W., and J. A. Wickert, "Determining Mean and Gradient Residual Stresses in Thin Films Using Micromachined Cantilevers," *Journal of Micromechanics and Microengineering*, Vol. 6, No. 3, 1996, pp. 301–309.

[4] Yang, Y. -J., and H. -H. Liao, "Development and Characterization of Thermopneumatic Peristaltic Micropumps," *Journal of Micromechanics and Microengineering*, Vol. 19, No. 2, 2009, p. 025003.

[5] Jiang, N., and J. Silcox, "Observations of Reaction Zones at Chromium/Oxide Glass Interfaces," *Journal of Applied Physics*, Vol. 87, No. 8, 2000, pp. 3768–3776.

[6] Schneider, M., H. Mohwald, and S. Akari, "Quantitative Measurement of Chromium's Ability to Promote Adhesion," *Journal of Adhesion*, Vol. 79, No. 6, 2003, pp. 597–607.

[7] Mardare, C. C., et al., "Effects of Adhesion Layer (Ti or Zr) and Pt Deposition Temperature on the Properties of PZT Thin Films Deposited by RF Magnetron Sputtering," *Applied Surface Science*, Vol. 243, No. 1-4, 2005, pp. 113–124.

[8] Yanagisawa, K., H. Kuwano, and A. Tago, "Electromagetically Driven Microvalve," *Microsystem Technologies*, Vol. 2, No. 1, 1995, pp. 22–25.

[9] Lin, C. -F., et al., "Microfluidic pH-Sensing Chips Integrated with Pneumatic Fluid-Control Devices," *Biosensors and Bioelectronics*, Vol. 21, No. 8, 2006, pp. 1468–1475.

[10] Saenger, K. L., "Pulsed Laser Deposition. I. A Review of Process Characteristics and Capabilities," *Processing of Advanced Materials*, Vol. 3, No. 1, 1993, pp. 1–24.

[11] Kim, W. J., et al., "Pulsed Laser Deposition of Piezoelectric Films for Micro-Fluidic Applications," *Proceedings of the Materials Research Society Symposium*, Vol. 541, 1999, pp. 635–640.

[12] Virdi, G. S., et al., "Fabrication of Low Cost Integrated Micro-Capillary Electrophoresis Analytical Chip for Chemical Analysis," *Sensors and Actuators B: Chemical*, Vol. 128, No. 2, 2008, pp. 422–426.

[13] Law, J. T., "The High Temperature Oxidation of Silicon," *The Journal of Physical Chemistry*, Vol. 61, No. 9, 1957, pp. 1200–1205.

[14] Ravi, T. S., R. B. Marcus, and D. Liu, "Oxidation Sharpening of Silicon Tips," *Journal of Vacuum Science & Technology B (Microelectronics Processing and Phenomena)*, Vol. 9, No. 6, 1991, pp. 2733–2737.

[15] Zhang, Y., et al., "Formation of Single Tips of Oxidation-Sharpened Si," *Applied Physics Letters*, Vol. 69, No. 27, 1996, pp. 4260–4261.

[16] Deal, B. E., and A. S. Grove, "General Relationship for the Thermal Oxidation of Silicon," *Journal of Applied Physics*, Vol. 36, No. 12, 1965, pp. 3770–3778.

[17] Safi, I., "Recent Aspects Concerning DC Reactive Magnetron Sputtering of Thin Films: A Review," *Surface and Coatings Technology*, Vol. 127, No. 2, 2000, pp. 203–219.

[18] Ko, H. S., C. W. Liu, and C. Gau, "Novel Fabrication of a Pressure Sensor with Polymer Material and Evaluation of Its Performance," *Journal of Micromechanics and Microengineering*, Vol. 17, No. 8, 2007, pp. 1640–1648.

[19] Leskela, M., and M. Ritala, "Atomic Layer Deposition (ALD): From Precursors to Thin Film Structures," *Thin Solid Films*, Vol. 409, No. 1, 2002, pp. 138–146.

[20] Gallis, S., et al., "Thermal Chemical Vapor Deposition of Silicon Carbide Films as Protective Coatings for Microfluidic Structures," *Materials Research Society Symposium Proceedings*, Vol. 742, Boston, MA, 2002.

[21] Finch, D. S., et al., "Biocompatibility of Atomic Layer-Deposited Alumina Thin Films," *Journal of Biomedical Materials Research, Part A*, Vol. 87, No. 1, 2008, pp. 100–106.

[22] Dougherty, G. M., T. D. Sands, and A. P. Pisano, "Microfabrication Using One-Step LPCVD Porous Polysilicon Films," *Journal of Microelectromechanical Systems*, Vol. 12, No. 4, 2003, pp. 418–424.

[23] Guenat, O. T., et al., "Generic Technological Platform for Microfabricating Silicon Nitride Micro and Nanopipette Arrays," *Journal of Micromechanics and Microengineering*, Vol. 15, No. 12, 2005, pp. 2372–2378.

[24] Schrott, W., et al., "Metal Electrodes in Plastic Microfluidic Systems," *Microelectronic Engineering*, Vol. 86, No. 4-6, 2009, pp. 1340–1342.

[25] Gobet, J., et al., "Electrodeposition of 3D Microstructures on Silicon," *Journal of Micromechanics and Microengineering*, Vol. 3, No. 3, 1993, pp. 123–130.

[26] Ho, C. H., et al., "Ultrathick SU-8 Mold Formation and Removal, and Its Application to the Fabrication of LIGA-Like Micromotors with Embedded Roots," *Sensors and Actuators, A: Physical*, Vol. 102, No. 1-2, 2002, pp. 130–138.

[27] Kukharenka, E., et al., "Electroplating Moulds Using Dry Film Thick Negative Photoresist," *Journal of Micromechanics and Microengineering*, Vol. 13, No. 4, 2003, pp. 67–74.

[28] Dentinger, P. M., W. M. Clift, and S. H. Goods, "Removal of SU-8 Photoresist for Thick Film Applications," *Microelectronic Engineering*, Vol. 61-62, 2002, pp. 993–1000.

[29] Wang, P., et al., "Wet Releasing and Stripping SU-8 Structures with a Nanoscale Sacrificial Layer," *Microelectronic Engineering*, Vol. 86, No. 11, 2009, pp. 2232–2235.

[30] Tseng, F. -G., and C. -S. Yu, "High Aspect Ratio Ultrathick Micro-Stencil by JSR THB-430N Negative UV Photoresist," *Sensors and Actuators A: Physical*, Vol. 97-98, 2002, pp. 764–770.

[31] Stampfl, J., et al., "Electro-Discharge Machining of Mesoscopic Parts with Electroplated Copper and Hot-Pressed Silver Tungsten Electrodes," *Journal of Micromechanics and Microengineering*, Vol. 10, 2000, No. 1, pp. 1–6.

[32] Zhang, J., et al., "Argon Plasma Modification of SU-8 for Very High Aspect Ratio and Dense Copper Electroforming," *Journal of the Electrochemical Society*, Vol. 152, No. 10, 2005, pp. 716–721.

[33] Doepper, J., et al., "Micro Gear Pumps for Dosing of Viscous Fluids," *Journal of Micromechanics and Microengineering*, Vol. 7, No. 3, 1997, pp. 230–232.

[34] Yang, C. -R., et al., "Microstructuring Characteristics of a Chemically Amplified Photoresist Synthesized for Ultra-Thick UV-LIGA Applications," *Journal of Micromechanics and Microengineering*, Vol. 14, No. 8, 2004, pp. 1126–1134.

[35] Li, J., et al., "Indirect Removal of SU-8 Photoresist Using PDMS Technique," *Sensors and Actuators, A: Physical*, Vol. 125, No. 2, 2006, pp. 586–589.

[36] Shen, S. -C., M. -W. Wang, and C. -J. Lee, "Manufacture of an Integrated Three-Dimensional Structure Nozzle Plate Using Microinjection Molding for a 1200-dpi Inkjet Printhead," *Journal of Microelectromechanical Systems*, Vol. 18, No. 1, 2009, pp. 52–63.

[37] Lee, D., et al., "3D Replication Using PDMS Mold for Microcoil," *Microelectronic Engineering*, Vol. 86, No. 4-6, 2009, pp. 920–924.

[38] Konishi, S., et al., "Application of Direct Selective Metal Plating," *Proceedings of the IEEE Micro Electro Mechanical Systems*, 2002, pp. 396–399.

[39] Lin, C. H., et al., "Micro Capillary Electrophoresis Chips Integrated with Buried SU-8/SOG Optical Waveguides for Bio-Analytical Applications," *Sensors and Actuators, A: Physical*, Vol. 107, No. 2, 2003, pp. 125–131.

[40] Koch, M., A. G. R. Evans, and A. Brunnschweiler, "The Dynamic Micropump Driven with a Screen Printed PZT Actuator," *Journal of Micromechanics and Microengineering*, Vol. 8, No. 2, 1998, pp. 119–122.

[41] Koch, M., et al., "A Novel Micromachined Pump Based on Thick-Film Piezoelectric Actuation," *Sensors and Actuators, A: Physical*, Vol. 70, No. 1-2, 1998, pp. 98–103.

[42] Huang, T., et al., "Microfabrication of Microfluidic Cartridge for Isoelectric Focusing by Screen Printing," *Sensors and Materials*, Vol. 14, No. 3, 2002, pp. 141–149.

[43] Xing, Y., C. Grosjean, and T. Yu-Chong, "Design, Fabrication, and Testing of Micromachined Silicone Rubber Membrane Valves," *Journal of Microelectromechanical Systems*, Vol. 8, No. 4, 1999, pp. 393–402.

[44] Kee Suk, R., et al., "A Method for Precision Patterning of Silicone Elastomer and Its Applications," *Journal of Microelectromechanical Systems,* Vol. 13, No. 4, 2004, pp. 568–575.

[45] Biebuyck, H. A., et al., "Lithography Beyond Light: Microcontact Printing with Monolayer Resists," *IBM Journal of Research and Development*, Vol. 41, No. 1-2, 1997, pp. 159–170.

[46] Quist, A. P., E. Pavlovic, and S. Oscarsson, "Recent Advances in Microcontact Printing," *Analytical and Bioanalytical Chemistry*, Vol. 381, No. 3, 2005, pp. 591–600.

[47] Yan, L., W. T. S. Huck, and G.M. Whitesides, "Self-Assembled Monolayers (SAMs) and Synthesis of Planar Micro- and Nanostructures," *Journal of Macromolecular Science—Polymer Reviews*, Vol. 44, No. 2, 2004, pp. 175–206.

[48] Odom, T. W., et al., "Improved Pattern Transfer in Soft Lithography Using Composite Stamps," *Langmuir*, Vol. 18, No. 13, 2002, pp. 5314–5320.

[49] Michel, B., et al., "Printing Meets Lithography: Soft Approaches to High-Resolution Printing," *IBM Journal of Research and Development*, Vol. 45, No. 5, 2001, pp. 697–719.

[50] Crozatier, C., M. L. Berre, and Y. Chen, "Multi-Colour Micro-Contact Printing Based on Microfluidic Network Inking," *Microelectronic Engineering*, Vol. 83, No. 4-9, 2006, pp. 910–913.

[51] Dimos, D., B. H. King, and P. Yang, "Direct-Write Fabrication of Integrated, Multilayer Passive Components," *Proceedings International Symposium on Advanced Packaging Materials*, Reston, VA, 1999.

[52] Cao, Y., et al., "MicroPen Direct-Write Deposition of Polyimide," *Microelectronic Engineering*, Vol. 86, No. 10, 2009, pp. 1989–1993.

[53] Therriault, D., et al., "Fugitive Inks for Direct-Write Assembly of Three-Dimensional Microvascular Networks," *Advanced Materials*, Vol. 17, No. 4, 2005, pp. 395–399.

[54] Ghafar-Zadeh, E., M. Sawan, and D. Therriault, "Novel Direct-Write CMOS-Based Laboratory-on-Chip: Design, Assembly and Experimental Results," *Sensors and Actuators A: Physical*, Vol. 134, No. 1, 2007, pp. 27–36.

[55] Cooley, P., D. Wallace, and B. Antohe, "Applications of Ink-Jet Printing Technology to BioMEMS and Microfluidic Systems," *SPIE Proceedings—Microfluidics and BioMEMS*, Vol. 4560, San Francisco, CA, 2001.

[56] Yeo, Y., O. A. Basaran, and K. Park, "A New Process for Making Reservoir-Type Microcapsules Using Ink-Jet Technology and Interfacial Phase Separation," *Journal of Controlled Release*, Vol. 93, No. 2, 2003, pp. 161–173.

[57] Piner, R. D., et al., "Dip-Pen Nanolithography," *Science*, Vol. 283, No. 5402, 1999, pp. 661–663.

[58] Rosner, B., et al., "Active Probes and Microfluidic Ink Delivery for Dip Pen Nanolithography," *SPIE Proceedings*, Vol. 5275, Perth, WA, Australia, 2004.

[59] Banerjee, D., et al., "Optimizing Microfluidic Ink Delivery for Dip Pen Nanolithography," *Journal of Microlithography, Microfabrication and Microsystems*, Vol. 4, No. 2, 2005, pp. 1–8.

[60] Rivas-Cardona, J., and D. Banerjee, "Microfluidic Device for Delivery of Multiple Inks for Dip Pen Nanolithography," *Journal of Microlithography, Microfabrication, and Microsystems*, Vol. 6, No. 3, 2007, pp. 1–9.

[61] Moldovan, N., K. -H. Kim, and H. D. Espinosa, "Design and Fabrication of a Novel Microfluidic Nanoprobe," *Journal of Microelectromechanical Systems*, Vol. 15, No. 1, 2006, pp. 204–213.

[62] Tai, Y. -C., "Parylene BioMEMS," *2005 IEEE International Conference on Robotics and Biomimetics*, 2005.

[63] Fiaccabrino, G. C., et al., "Interdigitated Microelectrode Arrays Based on Sputtered Carbon Thin-Films," *Sensors and Actuators, B: Chemical*, Vol. B35, No. 3, 1996, pp. 247–254.

[64] Fiaccabrino, G. C., N. F. De Rooij, and M. Koudelka-Hep, "On-Chip Generation and Detection of Electrochemiluminescence," *Analytica Chimica Acta*, Vol. 359, No. 3, 1998, pp. 263–263.

[65] Fahrenberg, J., et al., "Microvalve System Fabricated by Thermoplastic Molding," *Journal of Micromechanics and Microengineering*, Vol. 5, No. 2, 1995, pp. 169–171.

[66] Hirano, M., et al., "Microvalve with Ultra-Low Leakage," *Proceedings of the 1997 10th Annual IEEE International Workshop on Micro Electro Mechanical Systems*, Nagoya, Japan, 1997.

[67] Rife, J. C., et al., "Miniature Valveless Ultrasonic Pumps and Mixers," *Sensors and Actuators A: Physical*, Vol. 86, No. 1-2, 2000, pp. 135–140.

[68] Xiao, S. Y., et al., "A Novel Fabrication Process of MEMS Devices on Polyimide Flexible Substrates," *Microelectronic Engineering*, Vol. 85, No. 2, 2008, pp. 452–457.

8

Fugitive and Sacrificial Release Processes

Fugitive and sacrificial release processes are those in which a material temporarily occupies prescribed space and is subsequently removed to complete fabrication. Such processes are fundamentally just a combination of the elementary processes already discussed in Chapters 6 and 7 (subtractive and additive processes), and in some cases Chapter 5 (solidification processes). The processes covered in this chapter are by no means any less important than those described in previous chapters. In fact, many of the examples given in previous chapters could not be fabricated if not for some use of fugitive and/or sacrificial release processes. However, to give more focused attention to the core principles of material solidification, subtraction, and addition, the dedicated discussion of fugitive and sacrificial steps has been postponed until this chapter.

Many sacrificial processes are indeed no different from what is called surface micromachining in MEMS. A counterexample that is more general than surface micromachining, however, is casting around a wire and later removing the wire to produce a microchannel. Surface micromachining is focused more traditionally on deposition and etching of films on wafers. It is helpful to address some semantics here, because microfabrication uses temporary materials so routinely and frequently that it may seem odd to have a dedicated chapter highlighting fugitive and sacrificial release processes separately. There is also much overlap with strategies used for casting and molding processes in particular. The discussion in this chapter will attempt to maintain a distinction among the operative words temporary material, fugitive process, and sacrificial release.

In other contexts, these words may be used somewhat interchangeably, but for a more deliberate treatment of fabrication processes they will be kept distinct in this chapter.

A *temporary* material is one that is used during intermediate fabrication steps but is not present in the final device. This is the most general case of the three concepts above. A photoresist layer that is used as an etch mask is a very common example, because the resist is typically stripped away as the very next step after etching is complete. Photoresist used as a lift-off layer is also removed after having served its purpose of facilitating spatially selective deposition. Electroplating masks in thick photoresists or dry-film resists are likewise used only temporarily. Molds used for casting, masters used for embossing, and stamps used for transfer patterning are all temporary because they are used to define features but do not remain as final products.

In this chapter, a process is considered *fugitive* if one material is enclosed from multiple sides by another, and the fugitive material is subsequently removed to create a prescribed cavity. The operative word fugitive conveys that one material is confined and must be removed to complete the fabrication process. The condition of being enclosed from multiple sides simply means that a whole layer of one material covered by another is not considered fugitive but rather simply buried. The terminology is inherited from macroscopic casting and molding, with one clear example being evaporative foam (or lost foam) casting, in which a fugitive polystyrene pattern is enclosed inside a gas permeable mold, and the fugitive pattern is disintegrated when molten metal is poured. A *fugitive insert* is sometimes used in injection molding and compression molding to define cavities as precured polymer flows around the insert and surrounds it before solidification. In macroscale casting, an outer mold may sometimes be described as fugitive to distinguish it from a permanent mold (as in die casting, for instance), but for microfabrication the word fugitive is used in a more narrow sense to refer only to internally confined materials.

The word sacrificial alone describes the fact that a material is destroyed or otherwise removed before completion of a fabrication process. In this sense, the word can be use interchangeably with fugitive in most cases because fugitive materials are also sacrificial. For more descriptive delineation among process strategies, however, this chapter uses the entire word pair *sacrificial release* to bring more attention to the fact that the purpose of removing the sacrificial material is to allow some other structure to have greater degree of freedom. A classic example from silicon MEMS is the release of a polysilicon cantilever beam by etching sacrificial oxide underneath it. So sacrificial release processes are distinguished from fugitive processes by purpose, as elaborated with examples in the next section.

8.1 Reasons for Fugitive and Sacrificial Release Processes

There are two major reasons for using fugitive and sacrificial release processes in the fabrication of microfluidic devices. Fugitive processes are used to create vacated cavities, with microchannels being the most straightforward example. Sacrificial release processes are used to make clearance for features that are intended to exhibit some freedom of motion. The released structures are generally meant to exhibit some freedom of motion, as in the case of membranes, flaps, and cantilevers. While this appears to be a clean separation in purpose between fugitive processes and sacrificial release processes, the purposes may overlap, as would be the case for pneumatic chambers that are not only enclosed but also intended to exhibit deflection upon clearing internal space. A few examples of each will be presented immediately below, and a summary of specific approaches to removing fugitive and sacrificial materials will be discussed in the following section.

Microchannels represent some of the most common features among all microfluidic devices. In Chapter 6, etching and laser ablation were discussed as straightforward options for fabricating troughs and grooves that could be used to form enclosed microchannels by sealing with another substrate. In Chapter 5, fabrication processes such as casting, replica molding, and hot embossing were presented as some basic ways of defining cavities, also requiring sealing with another substrate to form enclosed channels. A few novel approaches to photocuring in Chapter 5 showed possibilities for creating enclosed three-dimensional cavities by selective curing and removal of uncured liquid polymer. Liberally interpreted, the uncured polymer could be considered fugitive as well, although this chapter features examples for which the fugitive material and permanent material are heterogeneous.

Removing sacrificial material beneath a structure allows it to deform away from the substrate, as in the case of a microvalve that uses a planar flap to block an orifice. Sacrificial release processes depend heavily on material selectivity as discussed in Chapter 6, and problems such as over-etching because of poor selectivity are generally not tolerable. For released structures, the uniformity and surface roughness of clearance gaps are directly influenced by the type of sacrificial material used. Photoresists, silicon dioxide, and metals are among typical choices for sacrificial materials. Relative merits and specific processes used to remove them are identified using several examples in the next section.

8.2 Approaches to Fugitive and Sacrificial Release Processes

This section begins with some examples of fugitive processes to form cavities, followed by sacrificial release processes. Forming cavities tends to present greater

challenges in terms of material removal, especially if the aspect ratio of length versus thickness or width is severe. Access to sacrificial material between structural features that need to be released for motion tend to have better access for material removal, but designs may be more geometrically complex. In both cases, however, the fundamental commonality is that there is some material that must be selectively removed. Some of the various strategies for removing the fugitive or sacrificial material include dissolving, etching, melting, and vaporizing. Although the examples here are grouped into two categories based on devices demonstrated from published works, the basic strategies and material combinations are generally not restricted to one category or the other. The collective set of examples is intended to provide a broad understanding of the many options available.

8.2.1 Examples of Approaches to Fugitive Processes

The most straightforward scenario for using a fugitive process in the fabrication of microfluidic devices is perhaps clearing the hollow space within a microchannel. There are several different strategies for producing enclosed cavities using fugitive materials [1]. The general principle is that the fugitive material is first patterned onto a substrate, followed by deposition of the final device material as a conformal coating. If necessary for functional purposes such as electrical isolation or chemical resistance, the substrate can first be coated with a flat layer of material before the fugitive lines are patterned. The channel is cleared by selective removal of the fugitive material.

Figure 8.1 shows a microchannel produced by PECVD silicon dioxide using evaporated aluminum as the sacrificial material. The aluminum can be

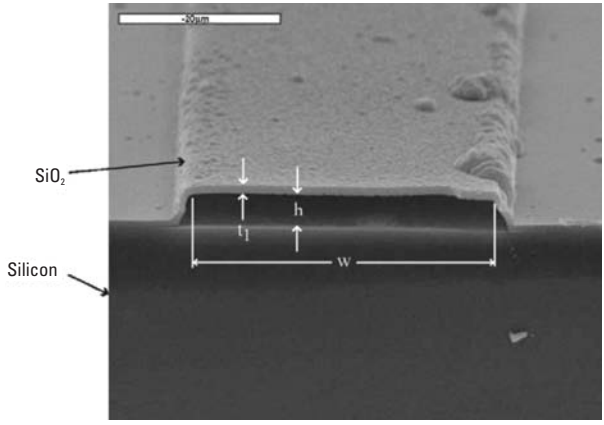

Figure 8.1 Silicon dioxide microchannel fabricated fugitive aluminum process. (Reprinted from [2], with permission from IOP Publishing.)

wet etched with good selectivity in a solution of hydrochloric acid and nitric acid, although the process is slow and can take several days. As mentioned in Chapter 7, PECVD is a good choice in this type of scenario not only because it is topographically conformal but also because the process can be conducted at relatively low temperature, even below 300°C.

The relatively low temperature of PECVD processing is not only advantageous for stress management, but it furthermore makes it possible to work with some photoresists as the fugitive material. With this added flexibility, the particular shape of the profile can be altered using reflow principles as previously described in Chapter 5. Figure 8.2 shows an example of shaped profiles under a PECVD silicon dioxide structure. Options for fugitive materials include a positive photoresist that is rounded by reflow as well as SU-8, which is well known for its ability to produce vertical sidewalls.

A subtle but important detail regarding the use of common photoresists under silicon dioxide or silicon nitride is that removal is a very slow process because inflow of etchant and outflow of the fugitive material is constrained to occur at the inlet and outlet of the channels. So a strategy used for the structures in Figure 8.2 is to include a submicron aluminum film underneath the photoresist. The aluminum film, albeit much thinner than the photoresist, can be etched faster and provides clearance for liquid stripping agent to more effectively act upon the photoresist.

A different approach for more efficient removal of fugitive material is to choose a material system that does not depend solely upon mass transport at the ends of a microchannel. One such material is polybutylnorborene, which has a unique advantage of having its thermal decomposition products permeate in gaseous form through dielectrics such as silicon dioxide [4]. Although thermal mismatch between polybutylnorborene and dielectrics can cause process challenges, the concept of fugitive material removal by permeation through the permanent material demonstrates a unique and faster approach than etching solely from the open ends.

Figure 8.3 illustrates a sequence based on electroforming for producing all-metal microchannels. A combination of seed layer deposition and photolithography is used to perform the required patterning. A thick positive photoresist (Hoechst AZ4620) is used as the sacrificial material, and it can be patterned with height ranging from 5 μm to as high as 100 μm. In this case, near vertical sidewalls of the resist result in channels with rectangular cross-section. Electroforming upon the seed layer builds the structural metal. Sidewall coverage is effective because the sputtered gold seed layer coats the sidewalls as well as the top surfaces of resist. Selective wet etching can be used to remove any intermediate seed layers and adhesion layers if necessary. The photoresist is dissolved in acetone. The entire process does not require high temperature and is compatible with integrated circuit processing.

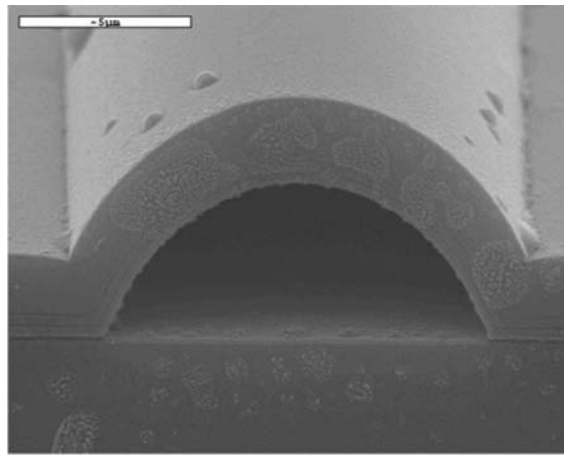

(a)

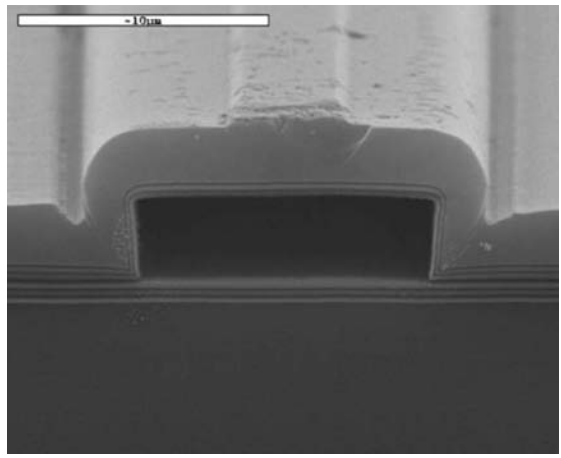

(b)

Figure 8.2 Shaped microchannels in silicon dioxide using (a) reflow positive resist and (b) SU-8. (*Source:* [3]. Reproduced by permission of The Royal Society of Chemistry.)

Also for metals, powder compaction is an alternative to electroplating for fabricating relatively larger structures with internal cavities. For example, fine metal powder can be compacted around a sacrificial wire. The process involves an initial compaction, etching of the sacrificial wire, and subsequent sintering of the powder to achieve full density. Microchannels have been fabricated using copper powder with average particle size of 1.5 μm around aluminum wire with

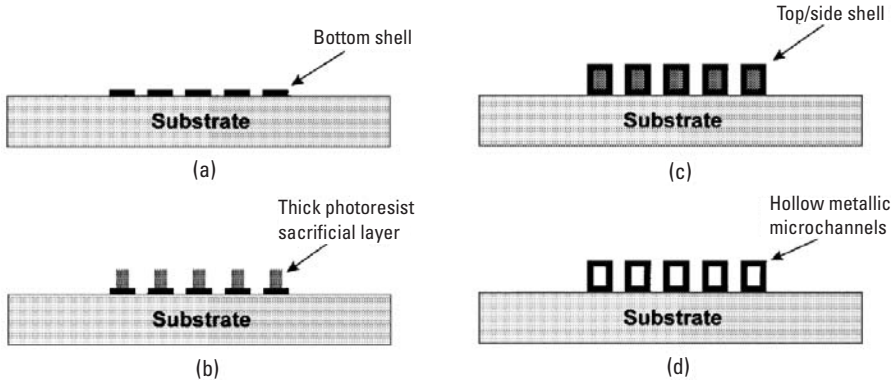

Figure 8.3 (a–d) Process sequence for fabricating hollow metal microchannels with thick photoresist as the fugitive material. (©1998 IEEE. Reprinted with permission from [5].)

diameter of 200 μm [6]. Larger particle sizes can be used at the expense of greater surface roughness. Although the process is more limited in geometric complexity and resolution than sacrificial materials patterned by photolithography, some complexity can still be introduced by using bent wires.

Dielectrics and metals are important and useful materials in microfabrication. As emphasized in Chapter 5, however, polymers have been commanding a greater proportion of attention, especially in recent years. Accordingly, fugitive methods to form cavities in polymer materials are also of interest. Analogous to the above example of packing metal around wire, fine hollow needles with smooth surfaces and narrow inner diameter of 35 μm have been fabricated by injection molding cyclic olefin copolymer around aluminum wire, followed by subsequent etching of the sacrificial wire [7]. A method of obtaining even smaller channels with width as small as 100 nm is to use silica nanowires, embedded by hot embossing in polycarbonate, followed by wet etching of the fugitive nanowires in HF [8].

One of the most common ways of fabricating PDMS chips is to cast over a temporary (but not fugitive) master and to bond with another flat substrate to enclose the channels. Alternatively, PDMS can be cast upon positive photoresist, and the photoresist can be dissolved as a fugitive material in acetone after PDMS curing [9]. This fugitive method has a valuable advantage in that metal electrodes can be integrated and aligned inside microchannels with the precision of photolithography. The steps of separating from a master pattern and bonding to another substrate are not required. Combining patterned SU-8 structures with the same general approach of PDMS upon sacrificial photoresist makes it possible to create more complex multilevel fluidic networks [10].

Other than using photolithography, direct-write methods (as introduced in Chapter 7) can also be used to print fugitive inks. An example is the use of a specially developed microcrystalline wax (engineered with a lower molecular weight organic phase) as the fugitive material for UV-curable epoxy structures [11]. After curing of the epoxy, the ink is melted and can be driven out of the cavities by pressurized air.

Porous silicon can be used as an effective fugitive material, and not only for plain vacant cavities. For example, a channel can be cleared around an integrated hot-wire probe for flow measurement [12]. Porous silicon has very large surface-to-volume ratio and can be removed even with dilute alkaline solutions, for example 0.1% KOH [13]. Another fugitive concept involving porous bodies is the partial clearing of channel interiors. Fugitive principles can be applied for producing uniform nanoporous structures inside microcavities, by using of colloidal silica particles inside a microchannel, followed by removal in a buffered oxide etch (BOE) solution [14].

8.2.2 Examples of Approaches to Sacrificial Release Processes

While the fugitive methods described above represent innovations in materials and processes, sacrificial release methods are in some ways more interesting because released structures demand added complexity in geometric design and mechanical behavior. As seen in Chapter 2, geometric features involving membranes, cantilevers, and other structures have much utility in microfluidics. Often the sacrificial material is a layer that is deposited or coated to cover a flat substrate, and removal of the sacrificial layer enables movement of a membrane, beam, of flap in a direction perpendicular to the substrate plane.

A good example of a sacrificial process is the release of a passive polysilicon microvalve as shown in Figure 8.4. The microvalve is fabricated on a silicon wafer with thermally grown silicon dioxide. After patterning the oxide by RIE, an LPCVD polysilicon layer is deposited. Silicon nitride is used as an etch mask for KOH etching of silicon from the back side, and it is subsequently removed by wet etching. The sacrificial silicon dioxide is removed by HF wet etching to release the valve plate. A similar approach is taken with silicon dioxide deposited over a patterned polysilicon layer (instead of being grown directly onto the silicon) to have the added advantage of electrostatic actuation [15].

The most common manifestation of sacrificial release processes in silicon-based surface micromachining is the removal of sacrificial silicon dioxide beneath structures in polysilicon, and Figure 8.4 represents just one of numerous examples from a wide variety of MEMS actuators. Hydrofluoric acid (HF) has excellent selectivity for removing the silicon dioxide while leaving the polysilicon intact. Some materials such as polyimide are viable as sacrificial

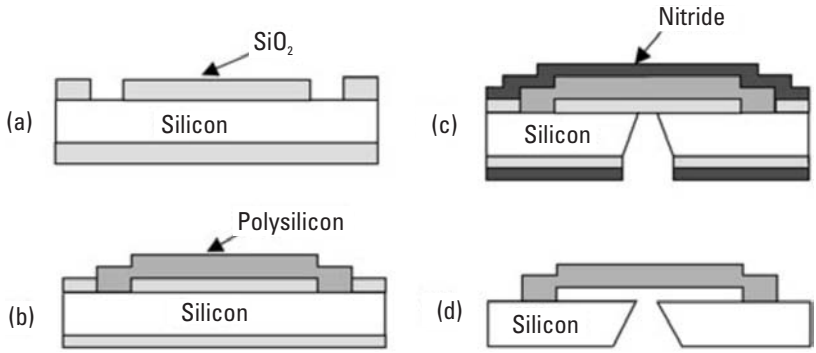

Figure 8.4 (a–d) Fabrication sequence for a polysilicon microvalve by removal of sacrificial silicon dioxide. (Reprinted from [16], with permission from IOP Publishing.)

layers beneath metal structures, and can be removed in the dry state by oxygen plasma [17].

An option that does not require any deposition processes is to use silicon-on-insulator (SOI) wafers, as illustrated by the check valve shown in Figure 8.5 [18]. SOI wafers can be purchased with specified thickness of oxide and top silicon layers, so an advantage of using SOI wafers is that fewer etch, deposition, and lithography steps are required. Another fundamental advantage of SOI wafers is that the top silicon layer is single-crystal silicon, thus offering very uniform mechanical behavior.

Removal of sacrificial layers with liquid etchants is often problematic because of *stiction*, which is a phenomenon that causes surfaces in close proximity to be mutually pulled into contact by attractive forces. The problem is often initiated by capillary forces during wet-etch and/or rinsing steps, but it can also be caused (or simply maintained) by such factors as electrostatic forces, van der Waals forces, and hydrogen bonding [19]. The stiction problem tends to be most severe for thin, broad surfaces in close proximity.

There have been various strategies used to address the problem of stiction in processes that require release of sacrificial layers, with the greatest attention given to polysilicon structures [20]. One option is to use vapor phase etching. HF vapor phase etching is a relatively well-established approach for performing dry release in surface micromachining of silicon upon sacrificial oxide [21]. *Critical point drying* with supercritical carbon dioxide has also been successfully used in MEMS release processes to avoid the stiction problem [22]. Yet another sacrificial release strategy is to use photoresist not only as a sacrificial material, but also as a patterned array of temporary support posts to prevent stiction [23]. This can be useful for a wide variety of microfluidic devices including

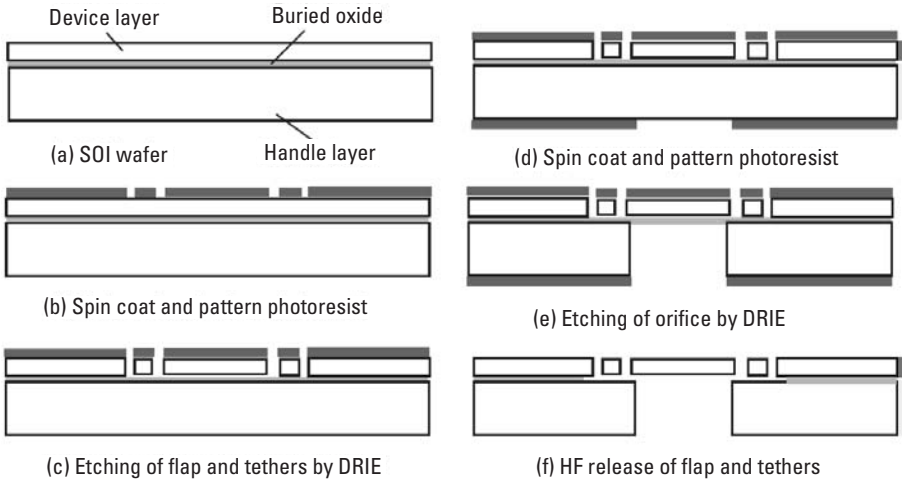

Figure 8.5 (a–f) Fabrication sequence for silicon-on-insulator check valve with sacrificial removal of buried oxide. (Reprinted from [16], with permission from IOP Publishing.)

diaphragm valves and peristaltic pumps that depend on suspended structures over broad but thin cavities.

Most cases of sacrificial release processes use flat, rigid substrates such as silicon wafers or glass slides. Other substrate materials such as metal foil, polymer sheet, or green ceramic sheets can also be used similarly. Flat, rigid substrates facilitate uniform layers, but the substrates can be only temporary. For example, flexible sheets with microvalves can be fabricated in parylene by releasing from a silicon base [24] after all key fabrication steps are complete.

Sacrificial methods can also be used to fabricate free-floating components without anchoring or tethering. For example, floating-disk concepts for pressure regulation have been manifested using parylene for the disk and retaining body, with photoresist as the sacrificial material [25]. A combination of copper and photoresist has been used to fabricate nickel-iron rotors that are free to spin around a hub [26].

Even though the sacrificial material may be a patterned film parallel to the substrate plane, it is worth noting that design options are not limited to motion perpendicular to the plane. Figure 8.6 shows two options for using patterned sacrificial layers to release a laterally acting cantilever beam for microfluidic flow control. The cantilever is fabricated with high aspect ratio using SU-8 photoresist, but without a sacrificial layer it would be anchored to the base substrate. Either photoresist or metals films are viable. Photoresist processing is convenient and requires fewer processing steps, but an advantage of using PVD metal (if needed) is that the thickness can be deposited uniformly in the range of

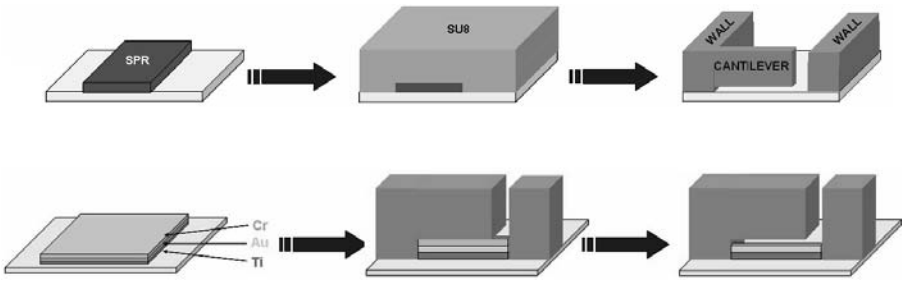

Figure 8.6 Use of sacrificial photoresist (top) or metal films (bottom) to release a laterally deflecting cantilever beam. (Reprinted from [27], with permission from IOP Publishing.)

tens of nanometers. Sacrificial photoresists tend to require coatings of 1 micron or thicker. Not shown in the figure is the need for aligned bonding of a cap substrate that has relief features to provide clearance above the cantilever as well. Substrate bonding is discussed in Chapter 9.

8.3 Tabulated Examples of Fugitive and Sacrificial Release Processes

Table 8.1 lists several examples of microfabrication processes that are based on fugitive or sacrificial release processes. The table does not place any emphasis on distinctions between fugitive processes and sacrificial release, because in principle most of the material combinations are interchangeable between these two categories. The table lists the fugitive or sacrificial material as the primary column of interest, the method by which it is removed, and the permanent material with its method of fabrication.

Table 8.1
Examples of Fugitive and Sacrificial Release Processes

Sacrificial Material	Removal Process	Permanent Material	Reference
Photoresist	Dissolving in acetone	PDMS	[9]
Photoresist	Dissolving in acetone	Electroformed nickel	[5]
Photoresist	Dissolving in acetone	Parylene	[25]
Photoresist	Dissolving in acetone	PECVD SiO_2	[3]
Photoresist	Dissolving in acetone	Photocured SU-8	[27]
Photoresist	Resist developing	Electroplated nickel	[28]

Table 8.1 (continued)

Sacrificial Material	Removal Process	Permanent Material	Reference
Silicon dioxide	Wet etching in HF	LPCVD polysilicon	[16]
Silicon dioxide	Wet etching in HF	Silicon-on-insulator wafer	[18]
Polyimide	Plasma etching in O_2	Sputtered aluminum	[17]
Wax-based ink	Melting	Photocured epoxy	[11]
Polybutylnorbornene	Thermal decomposition	PECVD SiO_2 or SiNx	[4]
Aluminum	Wet etching in HCl/HNO_3	PECVD SiO_2 or SiNx	[2]
Aluminum (wire)	Wet etching in NaOH	Compacted copper powder	[6]
Aluminum (wire)	Wet etching	Molded COC	[7]
Chromium	Wet etching	Photocured SU-8	[27]
Chromium	Wet etching	Photocured SU-8	[29]
Copper	Wet etching	Electroplated nickel	[30]
Copper	Wet etching	Electroplated nickel-iron	[26]

References

[1] Peeni, B. A., et al., "Sacrificial Layer Microfluidic Device Fabrication Methods," *Electrophoresis*, Vol. 27, No. 24, 2006, pp. 4888–4895.

[2] Hubbard, N. B., et al., "Structural Models and Design Rules for On-Chip Micro-Channels with Sacrificial Cores," *Journal of Micromechanics and Microengineering*, Vol. 15, No. 4, 2005, pp. 720–727.

[3] Peeni, B. A., et al., "Planar Thin Film Device for Capillary Electrophoresis," *Lab on a Chip*, Vol. 5, 2005, pp. 501–505.

[4] Bhusari, D., et al., "Fabrication of Air-Channel Structures for Microfluidic, Microelectromechanical, and Microelectronic Applications," *Journal of Microelectromechanical Systems*, Vol. 10, No. 3, 2001, pp. 400–408.

[5] Papautsky, I., et al., "A Low-Temperature IC-Compatible Process for Fabricating Surface-Micromachined Metallic Microchannels," *Journal of Microelectromechanical Systems*, Vol. 7, No. 2, 1998, pp. 267–273.

[6] Hakamada, M., et al., "Microfluidic Flows in Metallic Microchannels Fabricated by the Spacer Method," *Journal of Micromechanics and Microengineering*, Vol. 18, No. 7, 2008, p. 075029.

[7] Lippmann, J. M., E. J. Geiger, and A. P. Pisano, "Polymer Investment Molding: Method for Fabricating Hollow, Microscale Parts," *Sensors and Actuators A: Physical*, Vol. 134, No. 1, 2007, pp. 2–10.

[8] Zhang, L., et al., "Simple and Cost-Effective Fabrication of Two-Dimensional Plastic Nanochannels from Silica Nanowire Templates," *Microfluidics and Nanofluidics*, Vol. 5, No. 6, 2008, pp. 727–732.

[9] Subramani, B. G., and P. R. Selvaganapathy, "Surface Micromachined PDMS Microfluidic Devices Fabricated Using a Sacrificial Photoresist," *Journal of Micromechanics and Microengineering*, Vol. 19, No. 1, 2009, p. 015013.

[10] Yasukawa, T., et al., "Fabrication of Robust 2-D and 3-D Microfluidic Networks for Lab-on-a-Chip Bioassays," *Journal of Microelectromechanical Systems*, Vol. 14, No. 4, 2005, pp. 839–846.

[11] Therriault, D., et al., "Fugitive Inks for Direct-Write Assembly of Three-Dimensional Microvascular Networks," *Advanced Materials*, Vol. 17, No. 4, 2005, pp. 395–399.

[12] Lang, W., P. Steiner, and H. Sandmaier, "Applications of Porous Silicon Microstructuring," *Journal of Micromechanics and Microengineering*, Vol. 5, No. 2, 1995, pp. 175–176.

[13] Navarro, M., et al., "Electrochemical Etching of Porous Silicon Sacrificial Layers for Micromachining Applications," *Journal of Micromechanics and Microengineering*, Vol. 7, No. 3, 1997, pp. 131–132.

[14] Kuo, C. -W., et al., "Monolithic Integration of Well-Ordered Nanoporous Structures in the Microfluidic Channels for Bioseparation," *Journal of Chromatography A*, Vol. 1162, No. 2, 2007, pp. 175–179.

[15] Vandelli, N., et al., "Development of a MEMS Microvalve Array for Fluid Flow Control," *Journal of Microelectromechanical Systems*, Vol. 7, No. 4, 1998, pp. 395–403.

[16] Bien, D. C. S., S. J. N. Mitchell, and H. S. Gamble, "Fabrication and Characterization of a Micromachined Passive Valve," *Journal of Micromechanics and Microengineering*, Vol. 13, No. 5, 2003, pp. 557–562.

[17] Storment, C. W., et al., "Flexible, Dry-Released Process for Aluminum Electrostatic Actuators," *Journal of Microelectromechanical Systems*, Vol. 3, No. 3, 1994, pp. 90–96.

[18] Hu, M., et al., "A Silicon-on-Insulator Based Micro Check Valve," *Journal of Micromechanics and Microengineering*, Vol. 14, No. 3, 2004, pp. 382–387.

[19] Van Spengen, W. M., R. Puers, and I. De Wolf, "On the Physics of Stiction and Its Impact on the Reliability of Microstructures," *Journal of Adhesion Science and Technology*, Vol. 17, No. 4, 2003, pp. 563–582.

[20] Maboudian, R., and R. T. Howe, "Stiction Reduction Processes for Surface Micromachines," *Tribology Letters*, Vol. 3, No. 3, 1997, pp. 215–221.

[21] Lee, Y., et al., "Dry Release for Surface Micromachining with HF Vapor-Phase Etching," *Journal of Microelectromechanical Systems*, Vol. 6, No. 3, 1997, pp. 226–233.

[22] Jafri, I., H. Busta, and S. Walsh, "Critical Point Drying and Cleaning for MEMS Technology," *Proceedings of SPIE—The International Society for Optical Engineering*, Vol. 3880, 1999, pp. 51–58.

[23] Hwang, H. -S., and J. -T. Song, "An Effective Method to Prevent Stiction Problems Using a Photoresist Sacrificial Layer," *Journal of Micromechanics and Microengineering*, Vol. 17, No. 2, 2007, pp. 245–249.

[24] Pornsin-Sirirak, N., et al., "Flexible Parylene-Valved Skin for Adaptive Flow Control," *15th IEEE International Conference on Micro Electro Mechanical Systems*, Las Vegas, NV, 2002.

[25] Chen, P. -J., et al., "Floating-Disk Parylene Microvalves for Self-Pressure-Regulating Flow Controls," *Journal of Microelectromechanical Systems*, Vol. 17, No. 6, 2008, pp. 1352–1361.

[26] Lu, L. -H., K. S. Ryu, and C. Liu, "A Magnetic Microstirrer and Array for Microfluidic Mixing," *Journal of Microelectromechanical Systems*, Vol. 11, No. 5, 2002, pp. 462–469.

[27] Ezkerra, A., et al., "Fabrication of SU-8 Free-Standing Structures Embedded in Microchannels for Microfluidic Control," *Journal of Micromechanics and Microengineering*, Vol. 17, No. 11, 2007, pp. 2264–2271.

[28] Cui, Z., and R. A. Lawes, "New Sacrificial Layer Process for the Fabrication of Micromechanical Systems," *Journal of Micromechanics and Microengineering*, Vol. 7, No. 3, 1997, pp. 128–130.

[29] Nguyen, N. -T., et al., "Micro Check Valves for Integration into Polymeric Microfluidic Devices," *Journal of Micromechanics and Microengineering*, Vol. 14, No. 1, 2004, pp. 69–75.

[30] Jung, P. G., et al., "Nickel Microneedles Fabricated by Sequential Copper and Nickel Electroless Plating and Copper Chemical Wet Etching," *Sensors and Materials*, Vol. 20, No. 1, 2008, pp. 45–53.

9

Substrate Bonding and Fluidic Interfacing

This chapter covers the two broad topics of substrate bonding and fluidic interfacing. Both serve the more general need of fluidic packaging and very often must be engineered concurrently. The need for fluidic interfacing to the macro world is straightforward because the majority of microfluidic devices require some way of providing inflow and outflow generally provisioned by interfacing to external systems by tubing. There are several exceptions such as dispensing into open wells or ejecting from a nozzle, but some form of inlet and/or outlet connection is almost always needed. So the motivation for fluidic interfacing will be largely taken for granted, and the next section will discuss reasons for substrate bonding, which tend to be more diverse.

9.1 Reasons for Substrate Bonding

In the design and fabrication of microfluidic devices, the two dominant reasons for bonding substrates are to seal fluidic cavities and to interconnect three-dimensional flow. Sealing is foremost necessary to complement the many techniques of fabricating open cavities presented in Chapters 5 and 6. Many of the most useful and common processes such as casting, replica molding, etching, and laser ablation are generally limited to providing only one-sided open cavities that are then sealed by bonding with another substrate.

Substrate bonding is a way of directing more complex three-dimensional flows than can otherwise be achieved using single substrates, which can, for example, be beneficial for efficient microfluidic mixing [1]. In some cases design concepts are based on three-dimensional flow control using deformable structures such as membranes and flaps that have out-of-plane motion from one

substrate into cavities of another. For example, the deformation of a membrane, boss, or flap in one layer into the cavity of another layer can be used for a wide variety of microfluidic operations such as valve actuation [2], metering [3], and mixing [4]. Membranes can also be formed simply by bonding a thin layer of material over a cavity, as is done for some pneumatically driven peristaltic pumps [5].

The number of layers increases device complexity and as a general design principle it is preferable to use the minimum number of layers necessary to achieve required functionality. In some cases, however, the required functionality may motivate a stack of several layers. One example of a silicon-based microvalve that is capable of high-pressure, high-frequency actuation uses nine stacked layers with an embedded single-crystal piezo actuator [6].

Temporary bonding to a sheet of backing material can be useful for transferring relatively isolated and delicate structures from one substrate to another. For example, a polyester sheet can be used as a temporary backing to lift cast PDMS features and bond them onto a glass slide to form open reservoirs for controlled ejection of fluid samples [7].

A modular approach to bonding is the concept of *microfluidic assembly blocks*, which facilitates assembly of microfluidic systems by combining prefabricated units that include a variety of features including straight channels, 90° turns, inlet/outlet ports, T-channels, cross-channels, and chambers. The concept has been demonstrated with PDMS blocks that are bonded to glass slides but in principle can apply to a much wider variety of materials. Figure 9.1 illustrates the basic concept of device construction using microfluidic assembly blocks.

9.2 Process Issues and Selection Criteria for Substrate Bonding

This section surveys some of the various approaches used for bonding substrates, with primary attention focused on microfluidic devices in particular. Before proceeding with specific examples, however, it is helpful to first identify some of the important issues that help establish selection criteria. Some of the most common attributes of a substrate bonding method include the following:

- High bond strength;
- Low temperature processing;
- Robustness against flaws (e.g., contaminants, imperfect flatness, and so forth);
- Little or no long-term bond degradation;
- Manufacturing productivity.

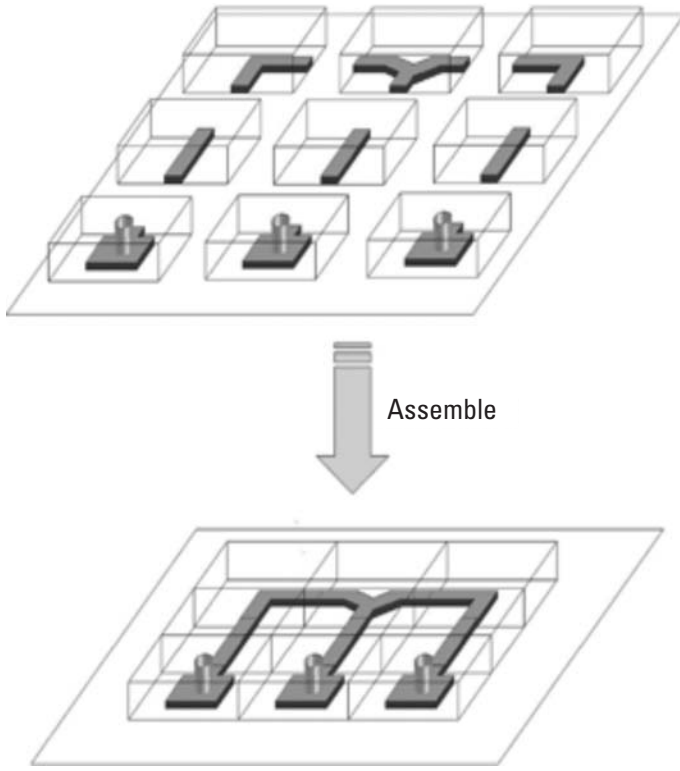

Figure 9.1 Modular construction of microfluidic devices using assembly blocks. (*Source:* [8]. Reproduced by permission of The Royal Society of Chemistry.)

The list above covers some of the more universal criteria but it is not comprehensive. Depending on application requirements, other desirable attributes may include such considerations as ease of lateral feature alignment, localized bond selectivity, or complete material homogeneity. There are also other important criteria that pertain more generally to materials and not specifically the bonding process itself. Examples of basic material issues include electrical insulation, optical transparency, chemical resistance, and biocompatibility.

Bond strength depends on inherent aspects of the substrate materials, such as the basic elemental composition at the surface and diffusion of species through the respective bulk material. It also depends on external factors such as surface roughness and particle contamination. Bond strength for rigid substrates generally require testing by cleaving methods or tensile fracture, whereas pliable materials such as PDMS are more effectively tested with pressurization using blister techniques [9–11].

Thermomechanical compatibility, specifically in terms of coefficient of thermal expansion, is important especially when bonding occurs at elevated

temperature. Some bonding processes reach the range of 1,000°C. Even after heating to a few hundred degrees, substrates can be subject to significant levels of thermal stress and thereby encounter distortion or bond failure. While most often it is problematic to have materials of different thermal expansion behavior, the mismatch can sometimes be used as a unique functional merit, as in the case of a bistable microvalve using adhesively bonded PMMA and polyimide [12].

Feature alignment is almost always required to some degree. A very simple and common case is the need to align inlet and outlet ports at the ends of microchannels. In other cases complex three-dimensional structures must be aligned very accurately to achieve proper layer-to-layer functional dependency. Aligned bonding is particularly challenging if substrates are opaque, but there are strategies such as infrared imaging that are capable of aligning even opaque substrates within a few microns of accuracy [13].

The size or form of substrates is an important consideration for productivity. In microfluidics, substrates are generally bonded either at the wafer level or at the chip level. Full wafer bonding is most common for silicon and glass wafers, whereas bonding of individual microfluidic chips tends to be more common for polymer substrates and smaller glass slides. Full wafer bonding lends itself to better automation and repeatability in commercial production, whereas individual chip bonding is very convenient and flexible for smaller-scale production and for research laboratories. Some polymers and green ceramics are commercially available in continuous rolls, which are favorable for high-volume manufacturing.

9.3 Approaches to Substrate Bonding

The most fundamental way to organize the many approaches to bonding processes would be based on the fundamental physical and/or chemical mechanisms that create the actual bonded interface. There are several forces that can act at the interface between two solid surfaces, and these include van der Waals forces, electrostatic forces, and capillary forces. Another very important mechanism is the rearrangement of chemical bonds across materials. Depending on factors such as surface composition, topography, intermediate species, diffusion rates, and environmental conditions (moisture, contaminants, and so forth), these various mechanisms play greater or lesser roles in substrate bonding. Details of specific force interactions and chemical reactions present a complexity beyond the scope of this book, so for a more thorough understanding the reader is referred to dedicated sources on the fundamentals of wafer bonding [14, 15].

A less fundamental yet still useful way to categorize bonding is based on applied process technology. For silicon-based microsystems, silicon fusion

bonding [16] and anodic bonding [17] are two of the most well-known methods. Many examples of polymer microfluidic devices are based on plasma activation, thermal lamination, or solvent-assisted bonding. Adhesive bonding is a very versatile option especially for mixed material types. There are still other bonding principles such as glass frit bonding [18] and gold thermocompression bonding [19, 20] that are advantageous for hermetic sealing of MEMS inertial sensors and RF-MEMS devices.

Regardless of fundamental surface mechanisms or process technologies, the choice of materials for a microfluidic application is often the most practical factor that influences selection of any given fabrication process. Accordingly, the subsections below group examples based on major categories of materials. These subsections are grouped similar to those in Chapter 3, although here there will be many instances of overlap as examples of mixed material types are presented (e.g., PDMS-glass). The discussion begins with polymers, which represent the most contemporary area of interest for microfluidics. The special mixed combination of glass and silicon by anodic bonding will be discussed in the context of glass bonding, and a section on adhesive bonding for arbitrary substrates will be described last.

9.3.1 Polymer Substrate Bonding

There are numerous approaches for bonding polymer substrates to each other and to other types of materials. Some of the major principles are based on thermal lamination, plasma surface activation, intermediate liquid curing, and solvent interaction. Thermoplastics in particular are very advantageous for manufacturability and are compatible with a wide variety of bonding methods [21].

The most straightforward approach for thermoplastic microfluidic chips is to use elevated temperature and pressure to achieve local flow at the interface between substrates. An advantage of thermoplastic bonding in this way is that homogenous chips can be fabricated with no intermediate species. Heated lamination is also effective for bonding dry polymer films onto rigid substrates such as glass or rigid plastic. The process is convenient for lamination-based processes such as xerography [22] and fabrication strategies based on dry-film photoresist [23]. Ultrasonic energy provides an alternative to direct heating [24]. For even greater spatial selectivity, UV irradiation [25] and laser welding provide additional versatility [26]. In the case of "shrinky-dink" microfluidics, patterned polystyrene layers can be bonded by stacking and allowing the layers to simultaneously undergo phase change and cross-linking [27] rather than the more conventional glass transition mechanism.

Plasma-activated bonding is especially common for bonding polymer microfluidic chips. A wide variety of devices have been fabricated using

plasma-activated PDMS bonding. Oxygen plasma provides strong irreversible bonds not only between PDMS and glass but also PDMS to PDMS. Just one of several examples fabricated by such bonding is a two-layer PDMS structure on glass to form a pneumatically actuated rotary device for pumping and mixing [28]. The basic principle of plasma-activated bonding is that the plasma catalyzes a surface to make it more reactive [29], and if compatible substrates are brought into contact with activated surfaces, strong permanent bonds (e.g., covalent) can be formed at the interface. The benefit of plasma activation is also relevant for silicon wafers and other substrates, but it is introduced here because of its frequent use with polymer substrates. Plasma-activated bonding has an advantage over thermal bonding because elevated temperature is not required. If substrates are sufficiently conformal, applied pressure is also not mandatory. In some cases, both plasma activation and thermal bonding can be used to optimize bond strength while maintaining low temperature. Plasma-activated bonding is effective not only for PDMS but other polymers as well, including PMMA [30] and COC [31]. An important benefit of maintaining a low temperature during the bonding process is limiting thermal expansion, which can cause problems for thin metal electrodes, fine alignment, interfacial stress, and so on.

Another basic way in which to bond polymer substrates is by using an intermediate fluid layer, which may be an uncured polymer film, an adhesive, or a solvent. In a comparative study of PDMS-to-PDMS bonding methods, bonding with partially cured and uncured PDMS were found to exhibit over twice the bond strength compared to oxygen plasma [32]. The method is applicable not only for PDMS-to-PDMS, but also PDMS-to-glass and PDMS-to-silicon [33]. PDMS films have likewise been used to bond PMMA-to-PMMA microfluidic chips [34]. Solvent-assisted bonding is similar in that a liquid is distributed between substrates, but the mechanism differs because the surfaces are locally dissolved to form the bond. Among the polymers that are frequently used in microfluidic devices, PMMA is a favorable material choice because it reacts with common organic solvents including methanol, ethanol, and isopropanol [35].

PDMS actually exhibits some degree of surface-to-surface affinity not only to itself but also to clean silicon and glass surfaces as well. At low pressure below 10 kPa, PDMS can be bonded to itself and still provide pneumatic functionality in microvalve arrays [36]. There are also a few bonding strategies based on mechanical principles. A reversible interface between two substrates can be made by using negative pressure in auxiliary cavities to pull surfaces together by active suction [37]. The adhesion of polymers to glass and silicon can also be improved by mechanical interlocking to bear some of the stresses that might otherwise cause delamination failure [38, 39].

9.3.2 Glass Substrate Bonding

All-glass microfluidic chips can be bonded with high strength if pressed in tight contact and subjected to temperatures above 500°C [40]. However, the high temperature makes this process incompatible for integration with such features as metal electrodes and biocompatible polymer coatings. Low-temperature alternatives have been pursued for all-glass microfluidic chips below 100°C and even at room temperature [41]. The threshold for what is considered low-temperature depends subjectively on application, but in the case of wafer bonding temperatures below ~300°C are generally accepted as qualifying. As discussed in Chapter 3, this is near the survivability limit for even high-performance polymers, and enters a region in which differences in thermal expansion among materials can become quite severe.

A straightforward way to avoid high temperatures altogether is to use an intermediate polymer film, which in most cases never requires processing with temperature beyond 100°C. PDMS can readily be coated as a thin liquid film to join pairs of glass slides or silicon substrates [42] prior to curing. Upon curing, the substrates become bonded together. PDMS can also be spin-coated, completely cured, and then plasma-treated before bonding [43]. Benzocyclobutene (BCB) is another material that can be used to bond glass to glass [44]. BCB has a functional merit of being effective as a patternable etch mask for better process integration not only with glass substrates but also with silicon. BCB bonding performance has been compared to other polymers including positive photoresist, negative photoresist, and polyimide [45], and has been found to be superior especially in terms of having void-free bonds.

Despite the benefit of low-temperature processing, an obvious drawback of using a polymer intermediate layer is that it sacrifices homogeneity. A more subtle concern is the possibility of outgassing, and a long-term concern is degradation by aging. Anodic bonding provides an option that falls between the clean, high-strength benefits of fusion bonding and the low-temperature benefits of adhesive or liquid-film bonding.

Anodic bonding most commonly bonds glass to silicon, and no intermediate material is needed. The process takes advantage of the mobility of ions (typically sodium) in some types of glass to create a depleted charge region at the interface between glass and silicon. Under a strong electric field with voltage levels on the order of several hundreds of volts, surfaces are attracted to each other with strong electrostatic force, creating opportunity to form covalent bonds across the interface. Consequently, anodically bonded interfaces are very strong and generally suffer no degradation over time. To achieve sufficient ion mobility and to promote permanent bonding, moderately high temperature with typical range between 300°C and 400°C is needed.

Although anodic bonding is most traditionally applied to one silicon wafer and one glass wafer, the process is actually much more versatile. Glass can be anodically bonded to glass with a dielectric film in between [46], and more than two substrates can be anodically bonded either simultaneously or sequentially, as long as the substrates and electrodes can be arranged appropriately [47]. Using sputtered amorphous silicon in between glass wafers, the required temperature for strong anodic bonds can be as low as 200°C [48]. If the intermediate layer is furthermore patterned by etching, it is possible to have nanoscale channels in the bonding layer itself. Such an approach has been used to fabricate channels with depth of only a few tens of nanometers by etching into an LPCVD amorphous silicon layer before anodic bonding [49].

Silicon-to-silicon bonds can be made with the anodic process occurring at two interfaces using a glass intermediate layer [50]. There is some evidence of the possibility of reversing an anodic bond between silicon and glass with a reverse (cathodic) process, but such a reverse process is subject to multiple defects and is sensitive to the quality of the original bond [51]. Beyond silicon, other material combinations such as titanium and nickel alloys can also be anodically bonded to glass [52].

9.3.3 Silicon Substrate Bonding

For practical purposes, this section will describe some of the bonding approaches that are applied primarily to silicon and oxide-coated silicon wafers under the collective heading of *silicon direct bonding*. The more restrictive name, *silicon fusion bonding*, is sometimes used too liberally because fusion per se is not always the primary mechanism of bonding. In addition to the physical forces listed above, hydrogen bonding (even at room temperature) and annealing play very important roles in many instances of silicon direct bonding.

Bare silicon wafers used in semiconductor processing are generally flat enough such that when cleaned properly even van der Waals forces are sufficient to form a relatively strong bond once trapped air is sufficiently removed. To form permanent chemical bonds, however, high temperature annealing is typically required. Silicon has a high melting point of 1,410°C. So literally melting surface regions into liquid phase is generally not a direct objective, but early approaches still used high temperature treatment near 1,000°C to produce high-strength permanent bonds.

Maintaining low processing temperature is very often an important concern for microelectronics, MEMS, and microfluidic devices. Rarely is a device comprised solely of bare silicon. Oxide layers are very common, and depending on device complexity, nitride layers and other materials may also be present. Although dielectrics can withstand higher temperature, thermal mismatch tends to be a more critical problem. Dopant migration is another serious concern for

semiconductor devices. High temperatures up to a few hundred degrees Celsius become extremely problematic for metals and polymers, and above that threshold integration with metals and polymers becomes essentially impossible. Accordingly, many of the advancements in silicon direct bonding have focused on low-temperature silicon direct bonding [53–55].

9.3.4 Other Substrate Materials and Bonding Methods

Adhesives provide one of the most versatile ways of bonding arbitrary substrates. SU-8 is an especially favorable choice as the adhesive layer between substrates not only because it is an epoxy but also because it is directly photopatternable [56]. If SU-8 is used as the intermediate layer and is also selectively patterned with channels and cavities, then the bonding of even plain, flat substrates can be used to produce complete microfluidic devices with one or more SU-8 layers forming the cavity geometry [57]. For example, as shown in Figure 9.2, SU-8 can be used as a bonding layer between glass and silicon not only to form channels, but multilevel cavities as well. A similar approach with surfactant-added SU-8 improves hydrophilic behavior for even wider material applicability, including bonding with PDMS substrates [58].

A drawback of using flowable adhesives is that alignment during bonding can be nontrivial because liquid between substrates generally promotes slip. One approach to reducing such slip is the patterning of selected metal films with relatively high coefficients of friction to increase stability [60]. Another basic problem with an intermediate substance for bonding two layers is that the intermediate material may leak into microchannels and other cavities. One solution

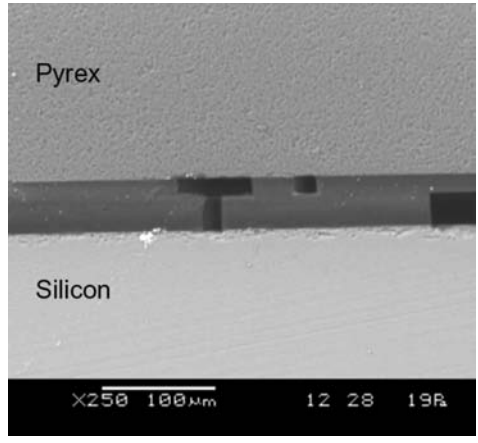

Figure 9.2 Multilevel embedded microchannels in SU-8, acting also as a bonding layer between silicon and glass. (Reprinted from [59], with permission from IOP Publishing.)

to this problem is to use a contact printing or stamping approach such that the bonding agent or glue adheres only to raised surfaces [61]. Rollers have also been used as a method of selectively transferring thin adhesive layers [62].

For relatively thick layers, solid adhesive films rather than liquids can be used to bond other substrates. One example is the use of double-sided acrylate adhesive film to bond a stack of metal and polysulfone layers to form magnetically driven ball valves [63]. The adhesive film can be patterned with appropriate holes and other cavities by processes such as laser cutting or mechanical punching.

Copper microfluidic structures based on printed circuit board (PCB) technology can be coated with thinly coated epoxy [64]. Metals can also be bonded with no foreign intermediate material as well in some cases. In particular, diffusion bonding or cold welding is applicable to metals, provided that the surfaces are adequately clean and flat, in order to promote metallic bonding across the interface. In the context of microfluidic applications, diffusion bonding has been used to fabricate microchannel combustors in stainless steel [65] and micro heat pipe spreaders in copper [66]. Thin films of gold can be made to bond at ambient conditions with the help of an elastomer under-layer. Compliance of the PDMS elastomer layer allows the gold surfaces to conform with excellent surface contact such that the process is effective at room temperature with low bonding pressure [67, 68].

Compression between heated platens can be used to laminate patterned green ceramic tapes [69] as a preliminary bonding step before binder burn-out and high-temperature sintering. An advantage of using low-temperature cofired ceramics (LTCC) beyond the high-productivity benefit of stamped cavities is that LTCC technology is compatible with metal interconnects. This can be beneficial for having integrated electrodes in capillary electrophoresis [70], and is beneficial beyond microfluidics for other MEMS packaging applications as well [71].

9.4 Tabulated Examples of Bonding Processes

This section cites several examples of processes for bonding substrates. The contents are divided into tables based on material categories, with polymers in Table 9.1, silicon and glass in Table 9.2, and metals and ceramics in Table 9.3. Some processes may be applicable to combinations of substrates across different material categories, and these are listed in Table 9.4. Each table lists the substrate material(s) with a coarse description of the bonding process.

The selected examples attempt to cover representative examples from a variety of different approaches. Some attempt has been made to limit redundancies, although a few table entries may be very similar in materials and

Table 9.1
Examples of Bonding Processes with Polymer Substrates

Substrates	Bonding Process	Reference
Polyimide	Heat lamination	[22]
Dry film photoresist	Heat lamination	[24]
PDMS	Polymer interface curing	[1]
PDMS	Polymer interface curing	[5]
PDMS	Polymer interface curing	[33]
Polystyrene	Polymer interface curing	[28]
Polyester, PDMS	Polymer interface curing	[7]
PMMA	Polymer interface curing (using PDMS)	[35]
PMMA	Solvent assisted bonding	[36]
PMMA	Plasma-activated bonding	[31]
Cyclo-olefin polymer	Plasma-activated bonding	[32]
PMMA	UV irradiation welding	[26]
PMMA, COC	Laser welding	[27]
PDMS	Direct surface adhesion	[37]
PMMA, polyimide	Adhesive bonding	[12]
Polysulfone	Adhesive bonding	[65]
PMMA	Ultrasonic bonding	[25]
PDMS	Cold welding of gold films	[69]

fundamental bonding mechanisms. The naming of bonding processes may be inexact, particularly in cases where there are multiple mechanisms involved, such as hydrolization plus annealing or adhesive bonding plus thermal compression. Accordingly, cited sources are provided to facilitate more detailed and accurate descriptions of each case.

9.5 Practical Issues and Selection Criteria for Fluidic Interfacing

Fluidic interfacing is an important topic because there are a wide variety of methods used among researchers and developers, with no single best approach for all circumstances. This section complements existing reviews [72] by providing examples of approaches that have been taken. The collective familiarity with various options will enable the reader to choose a best approach based on

Table 9.2
Examples of Bonding Processes with Silicon and Glass Substrates

Substrates	Bonding Process	Reference
Silicon	Silicon direct bonding	[2]
Silicon	Silicon direct bonding	[13]
Silicon	Silicon direct bonding	[57]
Silicon, SiO_2	Silicon direct bonding	[55]
Silicon, glass	Silicon direct bonding, anodic bonding	[6]
Silicon, glass	Anodic bonding	[49]
Glass	Anodic bonding	[51]
Silicon	Anodic bonding with glass thin film	[52]
Glass	Anodic bonding (with CVD thin film)	[48]
Glass	Anodic bonding (with Si thin film)	[50]
Glass	Surface hydrolization	[43]
Glass	Surface hydrolization	[45]
Fused quartz	Surface hydrolization	[42]
Glass	Adhesive bonding	[63]
Silicon, glass	Adhesive bonding	[47]
Silicon, glass	Adhesive bonding (with BCB)	[46]
Silicon	Adhesive bonding (with SU-8)	[58]
Silicon, glass	Adhesive bonding (with SU-8)	[59]
Silicon, glass	Adhesive bonding (with SU-8)	[61]
Silicon (plus other materials)	Glass frit bonding	[18]
Silicon	Thermocompression bonding	[19]

Table 9.3
Examples of Bonding Processes with Metal and Ceramic Substrates

Substrates	Bonding Process	Reference
Copper	Adhesive bonding	[66]
Stainless steel	Diffusion bonding	[67]
Copper	Diffusion bonding	[68]
Ceramic tape	Heat lamination	[71]
LTCC	Heat lamination and sintering	[72]

Table 9.4
Examples of Bonding Processes with Mixed Material Substrates

Substrates	Bonding Process	Reference
PDMS, glass	Plasma-activated bonding	[29]
PDMS, glass	Polymer interface curing (using PDMS)	[44]
PDMS, silicon, glass	Polymer interface curing (using PDMS)	[34]
Glass, SU-8, PMMA, COC	Adhesive bonding	[64]
Silicon, glass, PDMS	Adhesive bonding (with SU-8)	[60]
PDMS, glass	Adhesive bonding (plus other methods)	[8]
Glass, Ti, Ni-Fe alloys	Anodic bonding	[54]
Silicon, LTCC	Thermocompression bonding	[20]
PDMS, glass	Vacuum pressure	[37]

context-specific design and performance criteria. Some of the most common criteria that are relevant when choosing an interfacing method are:

- High pressure rating;
- Low dead volume;
- Alignment accuracy;
- Robustness against flaws (e.g., contaminants and imperfect shape);
- Robustness against mechanical factors (e.g., strain, fatigue, wear);
- Little or no long-term seal degradation.

The list above covers some of the more universal criteria but it is not comprehensive. As previously discussed for substrate bonding, there are other important criteria that pertain more generally to materials and not specifically the interface itself. Depending on the materials that comprise the fluidic interface (including any sealants), examples of concerns may include issues such as electrical conductivity, chemical resistance, and biocompatibility. Further depending on application requirements, other desirable attributes may include considerations related to 3D orientation, parts reusability, or multiport complexity.

Chapter 1 explained that pressure-driven flow, in particular, faces very unfavorable scaling laws with respect to miniaturization of conduit flow, as fluidic resistance increase dramatically with decreasing channel size. This often places very high demand on pressure rating for fluidic interfaces, and surface

tension—also with profound scaling implications—further exacerbates the problem during initial filling operations. Despite various techniques to alleviate pressure requirements (e.g., vacuum pull, temporary priming liquids, and so forth), miniaturization scaling laws generally put significant burden on sealing integrity at fluidic interfaces.

In microfluidics, the type of interface used can have very significant effect on dead volume [73]. For simple fluid handling applications such as continuous pumping, significant dead volume may be tolerable. However, for chemical analysis or biosampling, even a few picoliters of dead volume can be critical and minimizing dead volume becomes paramount.

The issue of manufacturing productivity is different for fluidic interfacing compared to substrate bonding. For substrate bonding, productivity is objectively measured in terms of the number of bonded wafer pairs that can be produced per hour, for example. Evaluation of productivity does not easily mirror to fluidic interfaces, however, because typically there is still a set of connections that must be made at the user level. Often manufacturing of a microfluidic chip may stop after the point of producing inlet and outlet wells on a glass or polymer chip, leaving the interfacing task to the end user. So a more subjective criterion of user-friendliness may be more relevant than manufacturing productivity per se.

Robustness against mechanical factors is also a concern relatively unique to fluidic interface design. To insert a capillary tube perpendicularly into a planar microfluidic chip immediately creates the possibility of having very large torque at the mated interface. By macroscopic analogy, the situation is similar to supporting a very tall flagpole in the ground or even designing the foundation of a tall skyscraper building. Not all interfacing concepts have such perpendicular orientation, and some approaches have interconnection configured laterally in-plane [74]. In general, however, most fluidic interface concepts to a significant degree must take mechanical strain relief into account.

9.6 Approaches to Fluidic Interfacing

There are so many different approaches to fluidic interfacing that to categorize them neatly into exclusive branches presents a daunting task. This section merely attempts to identify some functional distinctions among various approaches, with the main intention of revealing relative merits among alternatives.

For substrate bonding methods discussed earlier in this chapter, the type of materials bonded provided a convenient way to subdivide the topic. Substrate material also affects what kinds of fluidic interfaces may or may not be suitable. For any sealed interface in general, conformal contact is a fundamental

requirement. So this typically means that any two materials in sealing contact should be clearly distinct in terms of rigidity, so that the more pliable material can conform against the more rigid one. In some cases, an integrated sealant [75] or other intermediate material (e.g., O-ring, gasket film) provides the required conformal contact. If adhesive sealing is involved, both the substrate and interfaced components (fittings, tubing) must be sufficiently compatible with the type of adhesive used.

Interfaces can be distinguished based on whether the interface is mechanically loaded or simply bound by material. An example of a mechanically loaded approach would be to compress an O-ring against a glass chip, whereas a mechanically passive example would be an epoxy-sealed joint. Mechanically loaded seals can further be distinguished based on whether the sealing interface is planar (i.e., face seal) or cylindrical (typically around the outer diameter). Figure 9.3 illustrates some of the generic possibilities, using a compliant substrate (such as PDMS) or a rigid substrate with O-ring.

The examples in Figure 9.3 represent only a few of several possible variants that might include shoulders to assist alignment and control insertion depth [76], bulkhead packaging design for reliable compression [77], alternative compliant materials [78], and integrated filling into DRIE cavities [79]. If adhesives are used, design of the interface must take their flow and risk of blockage into account. Some strategies may include cavities for overflow, careful viscosity management, or the use of temporary filling materials to assure that blockage cannot occur.

One of the many functional merits of PDMS is that its compliance can be used to an advantage for sealing interfaces. If the bore size of a port is slightly smaller than the outer diameter of inserted tubing, the scheme can be sufficient for rapid connections based solely on the compression of PDMS around the tubing. As illustrated in Figure 9.4, well-defined holes in PDMS can be made by coring with a modified stainless steel syringe tip, and the compression force can be set by the relative size of the cored hole compared to the outer diameter of

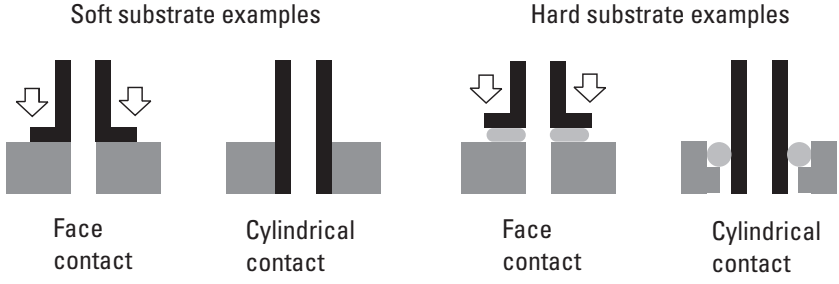

Figure 9.3 Examples of mechanically loaded interfaces for soft and hard materials.

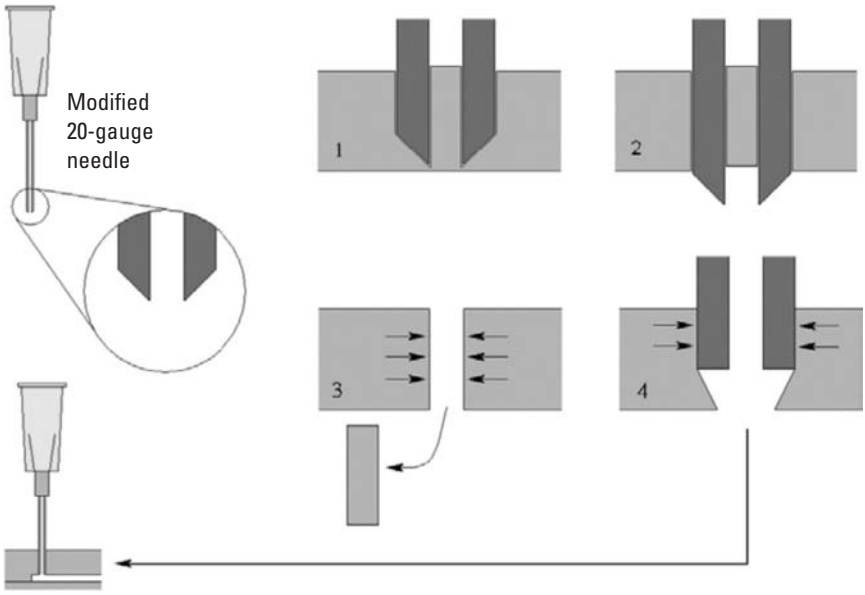

Figure 9.4 Fluidic interface in PDMS with syringe coring. (Reprinted from [81], with permission from IOP Publishing.)

another syringe tip after coring. This interference fit exhibits remarkably good resilience even when tested for fatigue with 1,000 insertion and removal cycles of low-density polyethylene (LPDE) tubing [80, 81].

Some approaches to fluidic interfacing are best suited to having a small number of individual ports. For more complex fluidic networks it becomes necessary to have multiport connection options with a more convenient plug-and-play interface and effective alignment of multiple ports [82], direct chip-to-chip interconnection [83], modular microfluidic breadboards [84], and interconnection blocks analogous to multipin electrical connectors [85].

This chapter began with a statement that in some cases substrate bonding and fluidic interfacing methods need to be engineered concurrently. A relatively obvious need is to assure that port locations and 3D geometric constraints are met. For example, it is often wisest to confirm success of cored holes in a substrate before bonding, to reduce likelihood of propagating defects and particle contamination into later stages of device fabrication. It is often preferable but not always essential to perform bonding on flat substrates before such things as fittings, tubing, and centering bases are attached. An integrated fabrication process plan for fluidic interfacing is necessary especially if the substrate bonding process involves heated platens, pressurized contact, high-voltage electrode plates, and or robotic handling. A good example of concurrently engineered

substrate bonding and fluidic interfacing is the use of anodic bonding to join Kovar (an alloy of nickel, iron, and cobalt) to glass, with stainless steel tubes either thread-fastened or laser soldered to the Kovar [86]. An extended need for concurrent engineering can go beyond the immediate chip itself interfacing with other substrates and test boards. This is illustrated in an example of interlocking fluidic connections shown in Figure 9.5.

Fluidic interfaces can also be distinguished based on whether the seals are permanent or separable, and mechanically loaded interfaces tend to be more readily separable. Separable interfaces have the advantage of working with very simple chip formats, often having just port holes in various locations on a planar surface. Relatively expensive components such as high voltage probes or optical lenses can be integrated into hardware components of the interface, while inexpensive and disposable chips can be inserted and removed with much lower risk of cross-contamination. Such an approach takes advantage of one of the chief merits of polymer microfluidic devices, which can be viable as single-use disposable devices in sensitive chemical analysis or biological sampling applications. From another perspective, it is desirable to have more permanent dependency among components with seamless integration of fluidic channels, sensor elements, and interconnections. An example of this strategy is the integration of a silicon-based magneto-resistive bioanalytical sensor in an integrated package with molded channel body, fluidic interconnections, and electrical contacts [88]. These issues related to electrical, optical, chemical, and biological factors are related to the next chapter, which addresses issues of multifunctional system integration.

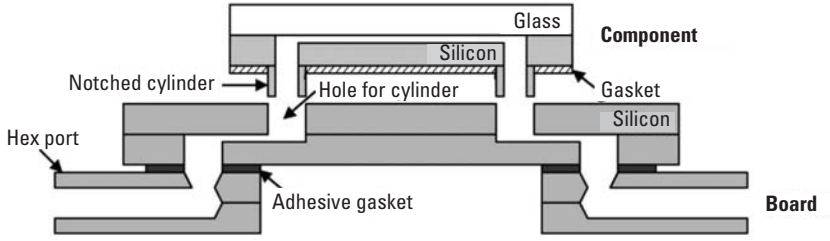

Figure 9.5 Interlocking fluidic connections between microfluidic component and test board. (Reprinted from [87]. Copyright 2004, with permission from Elsevier.)

References

[1] Cha, J., et al., "A Highly Efficient 3D Micromixer Using Soft PDMS Bonding," *Journal of Micromechanics and Microengineering*, Vol. 16, No. 9, 2006, pp. 1778–1782.

[2] Huff, M. A., and M. A. Schmidt, "Fabrication, Packaging, and Testing of a Wafer-Bonded Microvalve," *Proceedings of the 5th IEEE Solid-State Sensor and Actuator Workshop*, Hilton Head Island, SC, 1992.

[3] Lam, E. W., et al., "Microfluidic Circuits with Tunable Flow Resistances," *Applied Physics Letters*, Vol. 89, No. 16, 2006, p. 164105.

[4] Hsu, C. -H., and A. Folch, "Microfluidic Devices with Tunable Microtopographies," *Applied Physics Letters*, Vol. 86, No. 2, 2005, pp. 023508-1–023508-3.

[5] Jeong, O. C., and S. Konishi, "Fabrication and Drive Test of Pneumatic PDMS Micro Pump," *Sensors and Actuators A: Physical*, Vol. 135, No. 2, 2007, pp. 849–856.

[6] Li, H. Q., et al., "Fabrication of a Microvalve with Piezoelectric Actuation," *Proceedings of the IEEE Micro Electro Mechanical Systems*, 2003.

[7] Keenan, T. M., C. Hsu, and A. Folch, "Microfluidic 'Jets' for Generating Steady-State Gradients of Soluble Molecules on Open Surfaces," *Applied Physics Letters*, Vol. 89, No. 11, 2006, p. 114103-1.

[8] Rhee, M., "Microfluidic Assembly Blocks," *Lab on a Chip*, Vol. 8, No. 8, 2008, pp. 1365–1373.

[9] Chu, Y. Z., and C. J. Durning, "Application of the Blister Test to the Study of Polymer-Polymer Adhesion," *Journal of Applied Polymer Science*, Vol. 45, No. 7, 1992, pp. 1151–1164.

[10] Hohlfelder, R. J., et al., "Blister Test Analysis Methods," *Proceedings of the Materials Research Society Symposium*, Vol. 356, Boston, MA, 1995, pp. 585–590.

[11] Lu, Y. W., P. -T. Lin, and C. -S. Pai, "Polydimethylsiloxane (PDMS) Bonding Strength Characterization by a Line Force Model in Blister Tests," *Proceedings of the International Solid-State Sensors, Actuators and Microsystems Conference (TRANSDUCERS 2007)*, pp. 2095–2098.

[12] Goll, C., et al., "Microvalves with Bistable Buckled Polymer Diaphragms," *Journal of Micromechanics and Microengineering*, Vol. 6, No. 1, 1996, pp. 77–79.

[13] Bower, R. W., M. S. Ismail, and S. N. Farrens, "Aligned Wafer Bonding: A Key to Three Dimensional Microstructures," *Journal of Electronic Materials*, Vol. 20, No. 5, 1991, pp. 383–387.

[14] Tong, Q. Y., and U. Gosele, *Semiconductor Wafer Bonding: Science and Technology*, New York: John Wiley & Sons, 1999.

[15] Gosele, U., et al., "Fundamental Issues in Wafer Bonding," *Journal of Vacuum Science and Technology A*, Vol. 17, No. 4, 1999, pp. 1145–1152.

[16] Petersen, K., et al., "Surface Micromachined Structures Fabricated with Silicon Fusion Bonding," *IEEE International Conference on Solid-State Sensors and Actuators*, San Francisco, CA, 1991.

[17] Lapadatu, D., and H. Jakobsen, "Building of Silicon Mechanical Sensors by Bulk Micromachining and Anodic Bonding," *Proceedings of the 1998 IEEE International Semiconductor Conference*, Vol. 1, Sinaia, Romania, 1998.

[18] Knechtel, R., M. Wiemer, and J. Fromel, "Wafer Level Encapsulation of Microsystems Using Glass Frit Bonding," *Microsystem Technologies*, Vol. 12, No. 5, 2006, pp. 468–472.

[19] Tsau, C. H., S. M. Spearing, and M. A. Schmidt, "Fabrication of Wafer-Level Thermocompression Bonds," *Journal of Microelectromechanical Systems*, Vol. 11, No. 6, 2002, pp. 641–647.

[20] Heck, J. M., et al., "Ceramic Via Wafer-Level Packaging for MEMS," *ASME/Pacific Rim Technical Conference and Exhibition on Integration and Packaging of MEMS, NEMS, and Electronic Systems*, San Francisco, CA, 2005.

[21] Tsao, C. -W., and D. L. DeVoe, "Bonding of Thermoplastic Polymer Microfluidics," *Microfluidics and Nanofluidics*, Vol. 6, No. 1, 2009, pp. 1–16.

[22] Bartholomeusz, D. A., R. W. Boutte, and J. D. Andrade, "Xurography: Rapid Prototyping of Microstructures Using a Cutting Plotter," *Journal of Microelectromechanical Systems*, Vol. 14, No. 6, 2005, pp. 1364–1374.

[23] Heuschkel, M. O., et al., "Buried Microchannels in Photopolymer for Delivering of Solutions to Neurons in a Network," *Sensors and Actuators B: Chemical*, Vol. 48, No. 1-3, 1998, pp. 356–361.

[24] Li, S. W., et al., "Low-Temperature Bonding of Poly-(Methyl Methacrylate) Microfluidic Devices Under an Ultrasonic Field," *Journal of Micromechanics and Microengineering*, Vol. 19, No. 1, 2009, p. 015035.

[25] Truckenmuller, R., et al., "Bonding of Polymer Microstructures by UV Irradiation and Subsequent Welding at Low Temperatures," *Microsystem Technologies*, Vol. 10, No. 5, 2004, pp. 372–374.

[26] Pfleging, W., and O. Baldus, "Laser Patterning and Welding of Transparent Polymers for Microfluidic Device Fabrication," *SPIE Proceedings*, Vol. 6107, San Jose, CA, 2006.

[27] Chen, C. -S., et al., "Shrinky-Dink Microfluidics: 3D Polystyrene Chips," *Lab on a Chip*, Vol. 8, No. 4, pp. 622–624.

[28] Tseng, H. -Y., et al., "Membrane-Activated Microfluidic Rotary Devices for Pumping and Mixing," *Biomedical Microdevices*, Vol. 9, No. 4, 2007, pp. 545–554.

[29] Farrens, S., et al., "Plasma Bonding Replacement Methods for Traditional Bond Technologies," *Electrochemical Society Meeting Abstracts*, *207th Meeting of the Electrochemical Society*, Quebec, Canada, 2005.

[30] Liu, J., et al., "Plasma Assisted Thermal Bonding for PMMA Microfluidic Chips with Integrated Metal Microelectrodes," *Sensors and Actuators, B: Chemical*, Vol. 141, No. 2, 2009, pp. 646–651.

[31] Mizuno, J., et al., "Cyclo-Olefin Polymer Direct Bonding Using Low Temperature Plasma Activation Bonding," *Proceedings of the 2005 International Conference on MEMS, NANO and Smart Systems*, 2005.

[32] Eddings, M. A., M. A. Johnson, and B. K. Gale, "Determining the Optimal PDMS-PDMS Bonding Technique for Microfluidic Devices," *Journal of Micromechanics and Microengineering*, Vol. 18, No. 6, 2008, p. 067001.

[33] Samel, B., M. K. Chowdhury, and G. Stemme, "The Fabrication of Microfluidic Structures by Means of Full-Wafer Adhesive Bonding Using a Poly(Dimethylsiloxane) Catalyst," *Journal of Micromechanics and Microengineering*, Vol. 17, No. 8, 2007, pp. 1710–1714.

[34] Chow, W. W. Y., et al., "Microfluidic Channel Fabrication by PDMS-Interface Bonding," *Smart Materials and Structures*, Vol. 15, No. 1, 2006, pp. 112–116.

[35] Hsu, Y. -C., and T. -Y. Chen, "Applying Taguchi Methods for Solvent-Assisted PMMA Bonding Technique for Static and Dynamic TAS Devices," *Biomedical Microdevices*, Vol. 9, No. 4, 2007, pp. 513–522.

[36] Hosokawa, K., and R. Maeda, "Low-Cost Technology for High-Density Microvalve Arrays Using Polydimethylsiloxane (PDMS)," *Proceedings of the 14th IEEE International Conference on Micro Electro Mechanical Systems*, Interlaken, Switzerland, 2001.

[37] Bang, H., et al., "Active Sealing for Soft Polymer Microchips: Method and Practical Applications," *Journal of Micromechanics and Microengineering*, Vol. 16, No. 4, 2006, pp. 708–714.

[38] Larsson, M. P., R. R. A. Syms, and A. G. Wojcik, "Improved Adhesion in Hybrid Si-Polymer MEMS Via Micromechanical Interlocking," *Journal of Micromechanics and Microengineering*, Vol. 15, No. 11, 2005, pp. 2074–2082.

[39] Larsson, M. P., and M. M. Ahmad, "Improved Polymer-Glass Adhesion Through Micro-Mechanical Interlocking," *Journal of Micromechanics and Microengineering*, Vol. 16, No. 6, 2006, pp. S161–S168.

[40] Harrison, D. J., et al., "Capillary Electrophoresis and Sample Injection Systems Integrated on a Planar Glass Chip," *Analytical Chemistry*, Vol. 64, No. 17, 1992, p. 1926.

[41] Chen, L., et al., "Bonding of Glass-Based Microfluidic Chips at Low- or Room-Temperature in Routine Laboratory," *Sensors and Actuators B: Chemical*, Vol. 119, No. 1, 2006, pp. 335–344.

[42] Hongkai, W., H. Bo, and R. N. Zare, "Construction of Microfluidic Chips Using Polydimethylsiloxane for Adhesive Bonding," *Lab on a Chip*, Vol. 5, No. 12, 2005, pp. 1393–1398.

[43] McMahon, J. J., et al., "Bonding Characterization of Oxidized PDMS Thin Films," *Materials Research Society*, Vol. 795, 2003.

[44] Hwang, T., et al., "BCB Wafer Bonding for Microfluidics," *SPIE Proceedings*, Vol. 5342, 2004.

[45] Niklaus, F., et al., "Low-Temperature Full Wafer Adhesive Bonding," *Journal of Micromechanics and Microengineering*, Vol. 11, No. 2, 2001, pp. 100–107.

[46] Berthold, A., et al., "Glass-to-Glass Anodic Bonding with Standard IC Technology Thin Films as Intermediate Layers," *Sensors and Actuators, A: Physical*, Vol. 82, No. 1, 2000, pp. 224–228.

[47] Harz, M., "Anodic Bonding for the Third Dimension," *Journal of Micromechanics and Microengineering*, Vol. 2, No. 3, 1992, pp. 161–163.

[48] Wei, J., et al., "Low Temperature Glass-to-Glass Wafer Bonding," *IEEE Transactions on Advanced Packaging*, Vol. 26, No. 3, 2003, pp. 289–294.

[49] Kutchoukov, V. G., et al., "Fabrication of Nanofluidic Devices Using Glass-to-Glass Anodic Bonding," *Sensors and Actuators, A: Physical*, Vol. 114, No. 2-3, 2004, pp. 521–527.

[50] Hanneborg, A., M. Nese, and P. Ohlckers, "Silicon-to-Silicon Anodic Bonding with a Borosilicate Glass Layer," *Journal of Micromechanics and Microengineering*, Vol. 1, No. 3, 1991, pp. 139–144.

[51] Plaza, J. A., et al., "Cathodic Debond of Anodically Bonded Silicon to Glass Wafers," *Electrochemical and Solid-State Letters*, Vol. 3, No. 8, 2000, pp. 392–394.

[52] Briand, D., P. Weber, and N. F. De Rooij, "Bonding Properties of Metals Anodically Bonded to Glass," *Sensors and Actuators, A: Physical*, Vol. 114, No. 2-3, 2004, pp. 543–549.

[53] Tong, Q. -Y., et al., "Low Temperature Wafer Direct Bonding," *Journal of Microelectromechanical Systems*, Vol. 3, No. 1, 1994, pp. 29–35.

[54] Ayon, A. A., et al., "Low Temperature Silicon Wafer Bonding for MEMS Applications," *Proceedings of the 15th IEEE International Conference on Micro Electro Mechanical Systems*, Las Vegas, NV, 2002.

[55] Yu, W. B., et al., "Effect of Medium Vacuum on Low Temperature Wafer Bonding," *Journal of Micromechanics and Microengineering*, Vol. 15, No. 5, 2005, pp. 1001–1006.

[56] Pan, C. T., et al., "A Low-Temperature Wafer Bonding Technique Using Patternable Materials," *Journal of Micromechanics and Microengineering*, Vol. 12, No. 5, 2002, pp. 611–615.

[57] Li, S., et al., "Fabrication of Micronozzles Using Low-Temperature Wafer-Level Bonding with SU-8," *Journal of Micromechanics and Microengineering*, Vol. 13, No. 5, 2003, pp. 732–738.

[58] Chen, Y. -T., and D. Lee, "A Bonding Technique Using Hydrophilic SU-8," *Journal of Micromechanics and Microengineering*, Vol. 17, No. 10, 2007, pp. 1978–1984.

[59] Blanco, F. J., et al., "Novel Three-Dimensional Embedded SU-8 Microchannels Fabricated Using a Low Temperature Full Wafer Adhesive Bonding," *Journal of Micromechanics and Microengineering*, Vol. 14, No. 7, 2004, pp. 1047–1056.

[60] Niklaus, F., et al., "A Method to Maintain Wafer Alignment Precision During Adhesive Wafer Bonding," *Sensors and Actuators, A: Physical*, Vol. 107, No. 3, 2003, pp. 273–278.

[61] Schlautmann, S., et al., "Fabrication of a Microfluidic Chip by UV Bonding at Room Temperature for Integration of Temperature-Sensitive Layers," *Journal of Micromechanics and Microengineering*, Vol. 13, No. 4, 2003, pp. S81–S84.

[62] Kentsch, J., S. Breisch, and M. Stelzle, "Low Temperature Adhesion Bonding for BioMEMS," *Journal of Micromechanics and Microengineering*, Vol. 16, No. 4, 2006, pp. 802–807.

[63] Fu, C., Z. Rummler, and W. Schomburg, "Magnetically Driven Micro Ball Valves Fabricated by Multilayer Adhesive Film Bonding," *Journal of Micromechanics and Microengineering*, Vol. 13, No. 4, 2003, pp. 96–102.

[64] Merkel, T., M. Graeber, and L. Pagel, "New Technology for Fluidic Microsystems Based on PCB Technology," *Sensors and Actuators, A: Physical*, Vol. 77, No. 2, 1999, pp. 98–105.

[65] Matson, D. W., et al., "Fabrication of a Stainless Steel Microchannel Microcombustor Using a Lamination Process," *SPIE Proceedings*, Vol. 3514, Santa Clara, CA, 1998.

[66] Kang, S. -W., S. -H. Tsai, and M. -H. Ko, "Metallic Micro Heat Pipe Heat Spreader Fabrication," *Applied Thermal Engineering*, Vol. 24, No. 2-3, 2004, pp. 299–309.

[67] Ferguson, G. S., et al., "Contact Adhesion of Thin Gold Films on Elastomeric Supports: Cold Welding Under Ambient Conditions," *Science*, Vol. 253, No. 5021, 1991, pp. 776–778.

[68] Zhang, W. Y., G. S. Ferguson, and S. Tatic-Lucic, "Elastomer-Supported Cold Welding for Room Temperature Wafer-Level Bonding," *Proceedings of the IEEE International Conference on Micro Electro Mechanical Systems (MEMS)*, Maastricht, the Netherlands, 2004.

[69] Matson, D. W., et al., "Laminated Ceramic Components for Microfluidic Applications," *Proceedings of the SPIE*, Santa Clara, CA, Vol. 3877, 1999.

[70] Goldbach, M., H. Axthelm, and M. Keusgen, "LTCC-Based Microchips for the Electrochemical Detection of Phenolic Compounds," *Sensors and Actuators B: Chemical*, Vol. 120, No. 1, 2006, pp. 346–351.

[71] Dory, T. S., et al., "Wafer Level Bonding of MEMS Devices Using Ceramic Lids," *ASME Pacific Rim Technical Conference and Exhibition on Integration and Packaging of MEMS, NEMS, and Electronic Systems*, San Francisco, CA, 2005.

[72] Fredrickson, C. K., and Z. H. Fan, "Macro-to-Micro Interfaces for Microfluidic Devices," *Lab on a Chip*, Vol. 4, 2004, pp. 526–533.

[73] Chiou, C. -H., and G. -B. Lee, "Minimal Dead-Volume Connectors for Microfluidics Using PDMS Casting Techniques," *Journal of Micromechanics and Microengineering*, Vol. 14, No. 11, 2004, pp. 1484–1490.

[74] Lo, R., and E. Meng, "Integrated and Reusable In-Plane Microfluidic Interconnects," *Sensors and Actuators B: Chemical*, Vol. 132, No. 2, 2008, pp. 531–539.

[75] Tsai, J. -H., and L. Lin, "Micro-to-Macro Fluidic Interconnectors with an Integrated Polymer Sealant," *Journal of Micromechanics and Microengineering*, Vol. 11, No. 5, 2001, pp. 577–581.

[76] Westwood, S. M., S. Jaffer, and B. L. Gray, "Enclosed SU-8 and PDMS Microchannels with Integrated Interconnects for Chip-to-Chip and World-to-Chip Connections," *Journal of Micromechanics and Microengineering*, Vol. 18, No. 6, 2008, p. 064014.

[77] Friedrich, C. R., R. R. K. Avula, and S. Gugale, "A Fluid Microconnector Seal for Packaging Applications," *Journal of Micromechanics and Microengineering*, Vol. 15, No. 6, 2005, pp. 1115–1124.

[78] Perozziello, G., F. Bundgaard, and O. Geschke, "Fluidic Interconnections for Microfluidic Systems: A New Integrated Fluidic Interconnection Allowing Plug'n'Play Functionality," *Sensors and Actuators B: Chemical*, Vol. 130, No. 2, 2008, pp. 947–953.

[79] Tze-Jung, Y., et al., "Micromachined Rubber O-Ring Micro-Fluidic Couplers," *13th Annual International Conference on Micro Electro Mechanical Systems*, Miyazaki, Japan, 2000.

[80] Quaglio, M., et al., "Evaluation of Different PDMS Interconnection Solutions for Silicon, Pyrex and COC Microfluidic Chips," *Journal of Micromechanics and Microengineering*, Vol. 18, No. 5, 2008, p. 055012.

[81] Christensen, A. M., D. A. Chang-Yen, and B. K. Gale, "Characterization of Interconnects Used in PDMS Microfluidic Systems," *Journal of Micromechanics and Microengineering*, Vol. 15, No. 5, 2005, pp. 928–934.

[82] Han, K. -H., et al., "An Active Microfluidic System Packaging Technology," *Sensors and Actuators B: Chemical*, Vol. 122, No. 1, 2007, pp. 337–346.

[83] Pepper, M., et al., "Interconnecting Fluidic Packages and Interfaces for Micromachined Sensors," *Sensors and Actuators A: Physical*, Vol. 134, No. 1, 2007, pp. 278–285.

[84] Miserendino, S., and Y. C. Tai, "Modular Microfluidic Interconnects Using Photodefinable Silicone Microgaskets and MEMS O-Rings," *Sensors and Actuators A: Physical*, Vol. 143, No. 1, 2008, pp. 7–13.

[85] Sabourin, D., D. Snakenborg, and M. Dufva, "Interconnection Blocks: a Method for Providing Reusable, Rapid, Multiple, Aligned and Planar Microfluidic Interconnections," *Journal of Micromechanics and Microengineering*, Vol. 19, No. 3, 2009, p. 035021.

[86] Briand, D., P. Weber, and N. F. De Rooij, "Integration of Robust Fluidic Interconnects Using Metal to Glass Anodic Bonding," *Journal of Micromechanics and Microengineering*, Vol. 15, No. 9, 2005, pp. 1657–1663.

[87] Gray, B. L., S. D. Collins, and R. L. Smith, "Interlocking Mechanical and fluidic Interconnections for Microfluidic Circuit Boards," *Sensors and Actuators, A: Physical*, Vol. 112, No. 1, 2004, pp. 18–24.

[88] Wimberger-Friedl, R., et al., "Packaging of Silicon Sensors for Microfluidic Bio-Analytical Applications," *Journal of Micromechanics and Microengineering*, Vol. 19, No. 1, 2009, p. 015015.

10

Functional Domains and System Integration

10.1 Perspectives on Microfluidic Functionality

System integration is a broad term that can be loosely defined as developing an effective combination of interdependent functions, components, and subsystems to produce a required outcome. While much of this book has focused on the limited scope of fabricating geometric features, this chapter conveys ways in which system integration can and should influence design and fabrication decisions beyond individual functions and components.

Chapter 1 began with a simplified perspective of microfluidic functions being enabled by a collection of geometric features and appropriate materials. After an introductory overview of microscale phenomena and material properties, the central chapters of this book focused on various methods for fabricating geometric features such as channels, membranes, and fluidic ports. Figure 10.1 reviews the basic framework and highlights microfluidic functions as the result of combining geometric features, material properties, and microscale phenomena.

Figure 10.2 offers a modified look specifically at the relationship between microfluidic functions and end applications. Here microfluidic functionality is expressed more descriptively as a combination of actuation, sensing, and analysis functions. Depending on application, not all of these aspects are required. The figure clarifies that not all functions are necessarily on-chip, and in fact it is very rare not to have some off-chip subsystems that support on-chip functions.

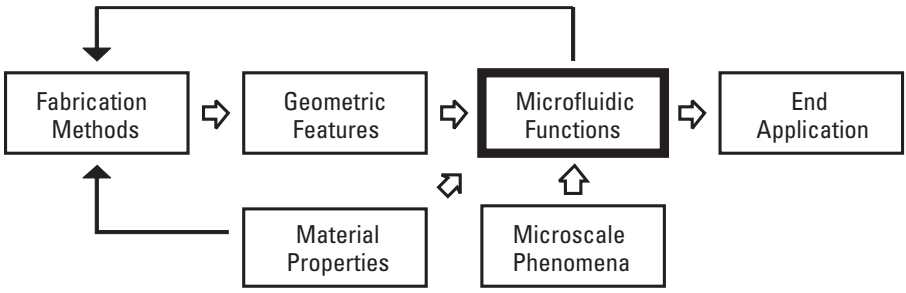

Figure 10.1 Relational map for microfluidics with emphasis on microfluidic functions.

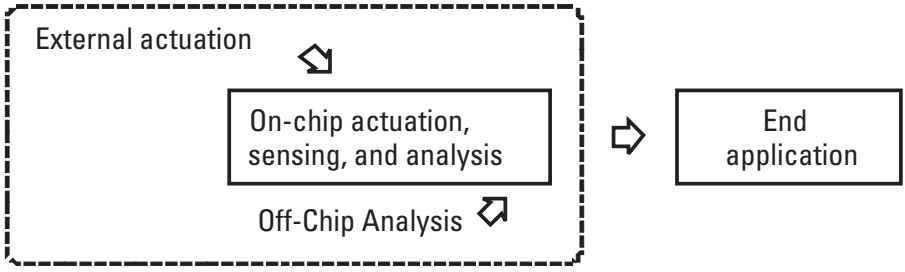

Figure 10.2 Relational map with emphasis on actuation, sensing, and analysis aspects of microfluidic functionality.

Actuation is most often initiated by electrical signals, but the nature of energy transduction may be based on principles that are electromechanical, thermopneumatic, electrokinetic, and so on. To drive fluid through a microfluidic device, for example, it is very common to use some external apparatus such as a programmable syringe pump or pressurized reservoir. Conversely, sensing is most often finalized with an electrical voltage or current signal that conveys some physical or chemical condition such as biomarker presence or ion concentration level. Many microfluidic devices perform some type of sensing, on-chip, but analysis and signal processing of the electrical signals are often performed using other instruments, auxiliary hardware, and computing resources. A microfluidic device is therefore only part of a more comprehensive solution to application requirements. Discussion over this broader perspective is continued in Section 10.3 with a few specific applications identified. To facilitate a more comprehensive understanding, however, Section 10.2 first elaborates on functionality in terms of energy transduction.

10.2 Energy Transduction

This section discusses component-level functionality with attention to various electrical, mechanical, thermal, optical, magnetic, chemical, and biological factors that have relevance to functional integration in microfluidic devices. *Transduction* pertains to converting energy from one domain to another, and Figure 10.3 provides visual mapping of some intersections between domains (or core disciplines) that have relevance to microfluidics.

	Fluidic	Electrical	Mechanical	Thermal
Fluidic		hydro-electric	pneumatic or hydraulic	
Electrical	Electro-kinetic		Electro-mechanical	Electro-thermal
Mechanical				
Thermal	Thermo-pneumatic	Thermo-electric	Thermo-mechanical	
Optical		Opto-electronic	Opto-mechanical	
Magnetic	Ferro-fluidic	Ferro-electric		
Chemical			Chemo-mechanical	
Biological		Bio-electronic	Bio-mechanical	

	Optical	Magnetic	Chemical	Biological
Fluidic				
Electrical		Electro-magnetic	Electro-chemical	Electro-physiological
Mechanical				
Thermal			Thermo-chemical	
Optical			Photo-chemical	
Magnetic				
Chemical				
Biological	Bio-optical		Bio-chemical	

Figure 10.3 Examples of cross-domain and cross-discipline functionality.

Words such as electrokinetic and thermopneumatic are commonplace in reference to microfluidic device design, and they often provide a basis for anticipating requirements for materials and geometric features. For example, electrical properties are undoubtedly relevant for devices based on electrokinetic principles, and sealed membrane cavities readily come to mind for devices based on pneumatic principles. Identifying the types of input energy and output energy offers better understanding of implications with respect to system integration requirements.

The entries in Figure 10.3 are not comprehensive, but they do illustrate ways in which different domains and disciplines can intersect. Fluidic, pneumatic, and hydraulic domains share commonality in that pressure and flow rate comprise the fundamental power variables for all three cases, and accordingly they are lumped into one category. The subsections that follow identify several examples of energy transduction across domains. The greatest variety is encountered with actuation rather than sensing, so the examples cited will be dominated by actuators, followed by a few examples of sensing elements.

As a disclaimer, in this chapter the word domain is not always meant in a rigorous physics sense. Some might reasonably argue that pressure-volume work of a fluid is still mechanical and should not be separated as fluidic, or that most biological interactions are more fundamentally chemical. However, the distinctions are presented in a more general sense for convenience of discussion and for recognition of the highly multidisciplinary nature of microfluidics.

10.2.1 Electrokinetic Transduction and Electrical Measurements

Electrokinetic transduction in the most general sense refers to using electric fields, currents, or charge distributions to affect motion. In microfluidics, the motion inherently applies to a fluid, and the word electrokinetic is sometimes used interchangeably with electrohydrodynamic (EHD). Specific examples of interactions between electric fields and fluids include droplet manipulation by electrowetting [1], fluid pumping by electro-osmotic pumping [2], separations by electrophoresis [3], particle manipulation by dielectrophoresis [4], and DNA stretching [5].

Integrated electrodes in microfluidic devices can be used to measure resistance or capacitance [6], and conductivity measurement across electrodes can be used to measure flow rate [7]. The word hydroelectric can be used to describe transduction in which fluid energy is converted into electrical signals. In macroscale engineering, the word hydroelectric is routinely encountered for turbines that are rotated by water power in order to generate electric power. The use of hydroelectric principles is not common for microfluidic devices, however. One fundamental reason can be gleaned from the poor scaling laws associated with inertial energy versus surface energy (Chapter 1). Conversely, surface forces

dictated by electrostatic charge and other phenomena [8] are very influential and versatile for microscale fluid mobilization.

10.2.2 Electromechanical, Electromagnetic, and Electroacoustic Transduction

Electromechanical actuators are among the most familiar transducers, and piezoelectric actuation is a common example. Piezo actuators are favorable for displacements needed by microvalves and micropumps because of the fine resolution, high repeatability, and low power consumption [9, 10]. Many electrostatic transducers are also designed to control mechanical displacements or to exhibit measurable changes in capacitance in response to displacements that alter gaps between electrodes.

Electric motors, often off-chip, are also important electromechanical sources of torque and angular displacement. Motor-driven syringe pumps are very common in microfluidics. Syringe pumps, however, are subject to pulsatile flow from discrete motor steps, motivating some investigations on flow stabilization and the dynamics of pulsatile flow [11–13]. A variety of functions including cell cultivation and lysis can be performed using rotational effects on a compact disc microfluidic device [14, 15]. As an external motor spins the disc, flow control is made possible by properly engineering imbalanced forces between centrifuge effects and surface capillary effects.

Electromagnetic actuators use electric current to create or alter magnetic fields. The transduction may be external, as in the case of off-the-shelf solenoid plungers to collapse cavities in PDMS [16]. One benefit of magnetic coupling is that is possible to put only part of the actuator (i.e., rotor) in the working fluid while having electrically wired components (i.e., stator) remain outside the fluid [17]. Magnetic coupling has been used to actuate a variety of pumps and valves by having a permanent magnet embedded or otherwise incorporated into the microfluidic device [18–20]. Magnetic fields can also be used to act on particles suspended in fluid if they are ferromagnetic [21]. Attaching magnetic beads provides a way of trapping, transporting, orienting, and sorting cells [22].

Electroacoustic actuation has been omitted from Figure 10.3 for the sake of brevity, but it does represent another form of transduction from electrical energy to acoustic energy, based on dynamic pressure waves. A surface acoustic wave (SAW) can be used in microfluidics including transport [23] and particle manipulation [24] and bubble generation [25]. Pulsing an electric field can also be used cell lysis by making cells structurally unstable [26].

10.2.3 Electrothermal, Thermopneumatic, and Thermomechanical Transduction

Electrothermal actuation refers to adding or removing heat by electric current or voltage. The most common use of electrothermal transduction in microfluidics

is the heating of a resistive element such as a platinum wire by electric current. The heating may in turn be used for other purposes such as volumetric expansion of a fluid. It is relatively common for electrical current to be used for electrothermal heating of elements for valves [27] and micropumps [28]. One way of taking advantage of electrical heating is the regulation of flow by temperature-driven gas expansion, used to constrict the passage of liquid flow [29].

If heating or cooling is ultimately intended to effect a mechanical change (as is often the case), a more comprehensive term could be electrothermomechanical, although as discussed later, simply using the word thermomechanical is more conventional. Rather than heating, thermoelectric cooling has also been used to provide valve actuation by freezing the working fluid [30].

Even if the end goal is not heating or cooling per se, understanding heat transfer in microfluidics is very important because chemical reactions in general are sensitive to temperature. An example of an often parasitic electrothermal effect in electro-osmotic flow is Joule heating as current flows through the fluid [31]. Accordingly, design of microfluidic devices involving chemical reactions must assure deterministic and uniform temperature [32]. Using Peltier junctions is one way of controlling temperature in both heating and cooling modes [33].

Thermopneumatic actuation refers to changing the temperature of a gas to change its volume. As mentioned for electrothermal actuation above, most implementations of thermopneumatic actuation involve resistive heating [34]. Technically, pneumatic implies a gas medium, whereas thermohydraulic would refer to liquid, but the word thermohydraulic is not common and in practice thermopneumatic can apply to liquids as well as gases. Peristaltic pumping is an example of taking advantage of thermopneumatic actuation [35].

Thermomechanical actuators use a change in temperature to effect dimensional change or other distortion of a mechanical solid. Shape memory alloys and bilayer film actuators are examples applying thermomechanical principles. PDMS microvalves actuated by shape memory alloy (SMA) wires have been incorporated into a biochemical assay system [36]. The wire is better described as a macroscale actuator, but it offers greater convenience, predictability, and reliability than attempting to integrate entirely in microscale. Thermal expansion of microspheres can be used for valve actuation or pumping [37].

10.2.4 Electrochemical and Chemomechanical Transduction

As mentioned previously, many implementations of on-chip sensing involve the use of electrode pairs or arrays. In addition to raw electrical measurements (i.e., resistance, voltage, capacitance), addressable electrodes provide the important ability to observe electrochemical reactions [38] or electrophysiological activity

[39], which are often more directly relevant to biological applications of microfluidics. Electrochemical principles are far more commonly used in sensing rather than transduction, but processes such as electrolysis can also be used to generate bubbles used in pumping [40].

Chemomechanical actuators produce mechanical response to chemical stimuli. An example of a chemomechanical process is the expansion of a hydrogel in response to a change in pH level in a working fluid [41]. An extension to the basic response would be to use electrical triggering, in which case the response would be chemoelectromechanical [42].

10.2.5 Optical Interfacing

While photosensitive chemical reactions are extremely common as the basis of photolithography (Chapter 4), photochemical transduction as an actuation principle in microfluidics is limited. One novel manifestation, however, is the mobilization of a liquid droplet based on surface isomer changes caused by irradiation of light [43].

With some exception, as noted, optical methods are used far more often in sensing applications rather than actuation [44–46]. Some variants include laser-induces fluorescence (LIF) using an external laser source acting on a capillary [47], or insertion of optical fibers into PDMS for more integrated fluorescence detection [48]. UV absorption is another alternative for species detection based on their characteristic absorption spectra. For any light-based detection methods, absorption characteristics of the substrate material must be considered. One strategy to overcome UV blocking characteristics of SU-8 is to incorporate quartz windows to take advantage of the UV transparency of quartz [49]. This is a good example of a case in which the system level solution (UV detection) has direct consequences on the materials and geometric features at the microfluidic component level.

Various methods of on-chip detection such as electrochemical measurements on cell activity often benefit greatly from simultaneous optical monitoring [50]. Optical methods are also often used for measuring flow velocity [51–53] as well as for imaging flow profiles. In some case, integration of functions involves embedding or otherwise positioning optical fibers [54, 55]. Alternatively, waveguides can also be patterned in the substrate material itself, as has been demonstrated using SU-8 [56].

A more subtle use of light energy is excitation and detection based on surface plasmon resonance (SPR). A microfluidic application of SPR is the study of protein adsorption based on sensitive changes in laterally propagating electromagnetic waves across gold-coated surfaces [57, 58].

At high optical magnification, a very practical problem that is often encountered is that the focal length for optical microscope objectives tends to

become very short. This is often quite problematic for multiple reasons. The use of probes is very common in electrophysiology studies on cell activity, and this would motivate the use of long-working-distance objectives, which can be in conflict with having very high magnification. Even for closed microchannels needing no external probes, a practical problem that is encountered is that desired focal distances from an optics standpoint can be shorter that the thickness of a microfluidic chip, making it difficult or impossible to image at arbitrary focal plane and magnification.

10.2.6 Biological Interfacing

The topic of biological interfacing is arguably more important to microfluidics than any particular transduction method. The scope, however, goes far beyond this book and the authors defer to other sources specifically dedicated to biological analysis and interfacing [59–61]. Only brief examples of interfacing with various domains will be mentioned here. An example of electrical interfacing is the measurement of cell impedance [62, 63]. Examples of mechanical interfacing are patch-clamp techniques to constrain cells, particularly for electrophysiological study [64]. A broader goal, however, is to provide a comprehensive platform for monitoring and altering electrical, mechanical, and biochemical interactions [65].

10.3 Microfluidic System Integration

Having presented several functionality issues from various domains and core disciplines, the issue of system integration is now revisited in terms of actuation, sensing, and analysis. A relatively high level of integration would entail functions across several domains, with an example shown in Figure 10.4. The chip includes fluid routing, electrothermal heating, thermoelectric temperature sensing, electrophoresis, and photoelectric detection.

Whether from an actuation perspective or in terms of sensing and analysis considerations, the most fundamental question for system integration is what should be integrated on-chip and what is best accomplished by interfacing a less complex microfluidic device to external subsystems. An idealized vision behind μTAS and LoC is to integrate as much as possible on-chip. However, the best approach is not always to put all functions on-chip simply in the name of integration. In some cases it may be more effective to divide by functional specialization.

Many biological and biomedical applications do present strong reasons for integrating multiple functions onto a single instrument [67]. Many of the transduction principles discussed above do not explicitly reveal the need for

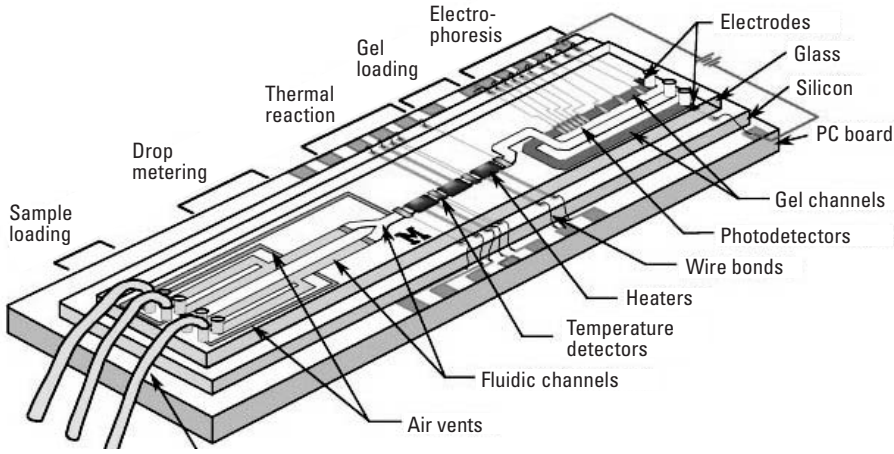

Figure 10.4 Microfluidic device with integrated components for fluid metering, heating, temperature sensing, electrophoresis, and photodetection. (*From:* [66]. Reprinted with permission from AAAS.)

extensive integration. However, implantable devices [68] and point-of-use health screening units with integrated control electronics and power [69] are good examples of motivation to perform analysis functions as locally as possible.

Functional integration in terms of actuation is relatively much simpler than sensing and analysis. An insulin delivery micropump or a thermal droplet generator may have basic mobilization of fluid as the essential purpose. However, for other cases such as a passive microfluidic mixer or particle sorter, it may be more effective and more sensible to have supporting apparatus off-chip. In other devices, such as electrophoresis chips or thermopneumatic droplet generators, needs for supporting apparatus may simply entail appropriate power supplies and electronics control hardware. Decoupling the basic task of fluid delivery from other functions makes in possible to direct more attention to performance requirements and microscale phenomena that may be of greater interest.

From the perspective of sensing and analysis, the end application has even greater influence on system integration requirements. The question of how to integrate subsystems is often more complex than for actuators because of the greater level of sophistication in many analytical methods and instruments. Some of the diverse methods of sensing and analysis that have been integrated with microfluidic devices include fluorescence microscopy [70], capillary electrophoresis [71], isoelectric focusing [72], flow cytometry [73], particle image velocimetry (PIV) [74], electrospray mass spectrometry [75], Fourier-transform infrared (FTIR) spectroscopy [76], and nuclear magnetic resonance (NMR)

imaging [77]. In some cases one or more of the above examples are used in combination.

Thinking about system integration a little differently, a familiar example for comparative discussion is the hardware architecture of computer systems. Central processing units (CPUs), memory modules, video adapters, storage drives, and so on, are specialized separate entities, yet they work together as an integrated system through common bus interfaces and data exchange protocols. As seen in this chapter, however, microfluidic systems must be engineered over a much wider variety of domains and core disciplines than microelectronics and computing systems.

Some functions will continue to be incorporated with higher levels of integration on-chip, but the need for off-chip analysis with specialized instrumentation is likely to remain for many end applications. In the foreseeable future it is anticipated that microfluidic systems will continue to be diverse and responsive to unique requirements, rather than converging toward a universally common microfluidic system architecture. However, something that the field of microfluidics does share in common with microelectronics is that it is an undeniably powerful enabling technology. Accordingly the authors have every reason to believe that just as semiconductor fabrication processes and microelectronics applications pushed each other toward rapid advancement, microfluidics fabrication technology and diverse microfluidics applications will also drive innovation and growth for many years to come.

References

[1] Fouillet, Y., et al., "Digital Microfluidic Design and Optimization of Classic and New Fluidic Functions for Lab on a Chip Systems," *Microfluidics and Nanofluidics*, Vol. 4, No. 3, 2008, pp. 159–165.

[2] Wang, X., et al., "Electroosmotic Pumps and Their Applications in Microfluidic Systems," *Microfluidics and Nanofluidics*, Vol. 6, No. 2, 2009, pp. 145–162.

[3] Chan, Y. C., et al., "Design and Fabrication of an Integrated Microsystem for Microcapillary Electrophoresis," *Journal of Micromechanics and Microengineering*, Vol. 13, No. 6, 2003, pp. 914–921.

[4] Gascoyne, P. R. C., and J. Vykoukal, "Particle Separation by Dielectrophoresis," *Electrophoresis*, Vol. 23, No. 13, 2002, pp. 1973–1983.

[5] Dukkipati, V. R., and S. W. Pang, "Integration of Electrodes in Si Channels Using Low Temperature Polymethylmethacrylate Bonding," *Journal of Vacuum Science and Technology B: Microelectronics and Nanometer Structures*, Vol. 25, No. 2, 2007, pp. 368–372.

[6] Cole, M. C., and P. J. A. Kenis, "Multiplexed Electrical Sensor Arrays in Microfluidic Networks," *Sensors and Actuators B: Chemical*, Vol. 136, No. 2, 2009, pp. 350–358.

[7] Rainey, P. V., S. J. N. Mitchell, and H. S. Gamble, "Flow-Rate Measurement Via Conductivity Monitoring in Microfluidic Devices," *SPIE-Int. Soc. Opt. Eng.*, Vol. 4177, 2000.

[8] Darhuber, A. A., and S. M. Troian, "Principles of Microfluidic Actuation by Modulation of Surface Stresses," *Annual Review of Fluid Mechanics*, Vol. 37, pp. 425–455.

[9] Duggirala, R., and A. Lal, "A Hybrid PZT-Silicon Microvalve," *Journal of Microelectromechanical Systems*, Vol. 14, No. 3, 2005, pp. 488–497.

[10] Husband, B., et al., "Investigation for the Operation of an Integrated Peristaltic Micropump," *Journal of Micromechanics and Microengineering*, Vol. 14, No. 9, 2004, pp. 64–69.

[11] Yang, B., and Q. Lin, "A Compliance-Based Microflow Stabilizer," *Journal of Microelectromechanical Systems*, Vol. 18, No. 3, 2009, pp. 539–546.

[12] Goh, J. K., "Effects of Wall Compliance on Pulsatile Flow Attenuation in Microchannels," M.S. Thesis, Mechanical Engineering, San Jose State University, San Jose, California, 2009.

[13] Morris, P. J. "Equivalent Circuit Modeling and Analysis of Microflow Stabilization Using Compliant-Wall Microchannels," M.S. Thesis, Mechanical Engineering, San Jose State University, San Jose, CA, 2009.

[14] Madou, M. J., et al., "Automated Microfluidic Compact Disc (CD) Cultivation System of Caenorhabditis Elegans," *Sensors and Actuators B: Chemical*, Vol. 122, No. 2, 2007, pp. 511–518.

[15] Kim, J., et al., "Cell Lysis on a Microfluidic CD (Compact Disc)," *Lab on a Chip*, Vol. 4, No. 5, 2004, pp. 516–522.

[16] Vestad, T., D. W. M. Marr, and J. Oakey, "Flow Control for Capillary-Pumped Microfluidic Systems," *Journal of Micromechanics and Microengineering*, Vol. 14, No. 11, 2004, pp. 1503–1506.

[17] Barbic, M., et al., "Electromagnetic Micromotor for Microfluidics Applications," *Applied Physics Letters*, Vol. 79, No. 9, 2001, pp. 1399–1401.

[18] Pan, T., et al., "A Magnetically Driven PDMS Micropump with Ball Check-Valves," *Journal of Micromechanics and Microengineering*, Vol. 15, No. 5, 2005, pp. 1021–1026.

[19] Gaspar, A., et al., "Magnetically Controlled Valve for Flow Manipulation in Polymer Microfluidic Devices," *Microfluidics and Nanofluidics*, Vol. 4, No. 6, 2008, pp. 525–531.

[20] Yobas, L., et al., "A Disposable Planar Peristaltic Pump for Lab-on-a-Chip," *Lab on a Chip*, Vol. 8, No. 5, 2008, pp. 660–662.

[21] Wang, K., et al., "An Electromagnetic Chip for Microfluidic Manipulation of Ferromagnetic Microparticles," *IEEE International Conference on Biomedical Engineering and Informatics*, Vol. 2, Piscataway, NJ, 2008.

[22] Lee, H., A. M. Purdon, and R. M. Westervelt, "Manipulation of Biological Cells Using a Microelectromagnet Matrix," *Applied Physics Letters*, Vol. 85, No. 6, 2004, pp. 1063–1065.

[23] Yeo, L. Y., and J. R. Friend, "Ultrafast Microfluidics Using Surface Acoustic Waves," *Biomicrofluidics*, Vol. 3, No. 1, 2009, p. 012002.

[24] Wood, C. D., et al., "Formation and Manipulation of Two-Dimensional Arrays of Micron-Scale Particles in Microfluidic Systems by Surface Acoustic Waves," *Applied Physics Letters*, Vol. 94, No. 5, 2009, p. 054101.

[25] Wang, S. S., et al., "Acoustically Induced Bubbles in a Microfluidic Channel for Mixing Enhancement," *Microfluidics and Nanofluidics*, Vol. 6, No. 6, 2009, pp. 847–852.

[26] Lee, S. -W., and Y. -C. Tai, "Micro Cell Lysis Device," *Sensors and Actuators, A: Physical*, Vol. 73, No. 1-2, 1999, pp. 74–79.

[27] Selvaganapathy, P., E. T. Carlen, and C. H. Mastrangelo, "Electrothermally Actuated Inline Microfluidic Valve," *Sensors and Actuators, A: Physical*, Vol. 104, No. 3, 2003, pp. 275–282.

[28] Ha, S. -M., W. Cho, and Y. Ahn, "Disposable Thermo-Pneumatic Micropump for Bio Lab-on-a-Chip Application," *Microelectronic Engineering*, Vol. 86, No. 4-6, 2009, pp. 1337–1339.

[29] Xu, W., et al., "A Vapor Based Microfluidic Flow Regulator," *Sensors and Actuators B: Chemical*, Vol. 142, No. 1, 2009, pp. 355–361.

[30] Gui, L., and J. Liu, "Ice Valve for a Mini/Micro Flow Channel," *Journal of Micromechanics and Microengineering*, Vol. 14, No. 2, 2004, pp. 242–246.

[31] Hsieh, S. -S., and T. -K. Yang, "Electroosmotic Flow in Rectangular Microchannels with Joule Heating Effects," *Journal of Micromechanics and Microengineering*, Vol. 18, No. 2, 2008, p. 025025.

[32] Sammarco, T. S., and M. A. Burns, "Heat-Transfer Analysis of Microfabricated Thermocapillary Pumping and Reaction Devices," *Journal of Micromechanics and Microengineering*, Vol. 10, No. 1, 2000, pp. 42–55.

[33] Maltezos, G., M. Johnston, and A. Scherer, "Thermal Management in Microfluidics Using Micro-Peltier Junctions," *Applied Physics Letters*, Vol. 87, No. 15, 2005, pp. 1–3.

[34] Takao, H., et al., "A MEMS Microvalve with PDMS Diaphragm and Two-Chamber Configuration of Thermo-Pneumatic Actuator for Integrated Blood Test System on Silicon," *Sensors and Actuators, A: Physical*, Vol. 119, No. 2, 2005, pp. 468–475.

[35] Jeong, O. C., et al., "Fabrication of a Peristaltic PDMS Micropump," *Sensors and Actuators, A: Physical*, Vol. 123-124, 2005, pp. 453–458.

[36] Tamanaha, C. R., L. J. Whitman, and R. J. Colton, "Hybrid Macro-Micro Fluidics System for a Chip-Based Biosensor," *Journal of Micromechanics and Microengineering*, Vol. 12, No. 2, 2002, pp. N7–N17.

[37] Griss, P., H. Andersson, and G. Stemme, "Expandable Microspheres for the Handling of Liquids," *Lab on a Chip*, Vol. 2, No. 2, 2002, pp. 117–120.

[38] Goral, V. N., N. V. Zaytseva, and A. J. Baeumner, "Electrochemical Microfluidic Biosensor for the Detection of Nucleic Acid Sequences," *Lab on a Chip*, Vol. 6, No. 3, 2006, pp. 414–421.

[39] Moss, E. D., A. Han, and A. B. Frazier, "A Fabrication Technology for Multi-Layer Polymer-Based Microsystems with Integrated Fluidic and Electrical Functionality," *Sensors and Actuators B: Chemical*, Vol. 121, No. 2, 2007, pp. 689–697.

[40] Chiu, S. -H., and C. -H. Liu, "An Air-Bubble-Actuated Micropump for On-Chip Blood Transportation," *Lab on a Chip*, 2009.

[41] Yu, Q., et al., "Responsive Biomimetic Hydrogel Valve for Microfluidics," *Applied Physics Letters*, Vol. 78, No. 17, 2001, pp. 2589–2591.

[42] Bassetti, M. J., et al., "Development and Modeling of Electrically Triggered Hydrogels for Microfluidic Applications," *Journal of Microelectromechanical Systems*, Vol. 14, No. 5, 2005, pp. 1198–1207.

[43] Oh, S., M. Nakagawa, and K. Ichimura, "Light-Guided Movement of a Liquid Droplet," *Molecular Crystals and Liquid Crystals Science and Technology Section A: Molecular Crystals and Liquid Crystals*, Vol. 345, 2000, pp. 635/311–640/316.

[44] Kuswandi, B., J. H. Nuriman, and W. Verboom, "Optical Sensing Systems for Microfluidic Devices: A Review," *Analytica Chimica Acta*, Vol. 601, No. 2, 2007, pp. 141–155.

[45] Uchiyama, K., H. Nakajima, and T. Hobo, "Detection Methods for Microchip Separations," *Analytical and Bioanalytical Chemistry*, Vol. 379, No. 3, 2004, pp. 375–382.

[46] Gotz, S., and U. Karst, "Recent Developments in Optical Detection Methods for Microchip Separations," *Analytical and Bioanalytical Chemistry*, Vol. 387, No. 1, 2007, pp. 183–192.

[47] Lin, Y.-W., T.-C. Chiu, and H.-T. Chang, "Laser-Induced Fluorescence Technique for DNA and Proteins Separated by Capillary Electrophoresis," *Journal of Chromatography B: Analytical Technologies in the Biomedical and Life Sciences*, Vol. 793, No. 1, 2003, pp. 37–48.

[48] Chabinyc, M. L., et al., "An Integrated Fluorescence Detection System in Poly(Dimethylsiloxane) for Microfluidic Applications," *Analytical Chemistry*, Vol. 73, No. 18, 2001, pp. 4491–4498.

[49] Jackman, R. J., et al., "Microfluidic Systems with On-Line UV Detection Fabricated in Photodefinable Epoxy," *Journal of Micromechanics and Microengineering*, Vol. 11, No. 3, 2001, pp. 263–269.

[50] Yi, C., et al., "Optical and Electrochemical Detection Techniques for Cell-Based Microfluidic Systems," *Analytical and Bioanalytical Chemistry*, Vol. 384, No. 6, 2006, pp. 1259–1268.

[51] McMullin, J. N., et al., "Integrated Optical Measurement of Microfluid Velocity," *Journal of Micromechanics and Microengineering*, Vol. 15, No. 10, 2005, pp. 1810–1816.

[52] Sinton, D., et al., "Direct and Indirect Electroosmotic Flow Velocity Measurements in Microchannels," *Journal of Colloid and Interface Science*, Vol. 254, No. 1, 2002, pp. 184–189.

[53] Chen, R., et al., "Determination of EOF of PMMA Microfluidic Chip by Indirect Laser-Induced Fluorescence Detection," *Sensors and Actuators B: Chemical*, Vol. 114, No. 2, 2006, pp. 1100–1107.

[54] Hartmann, D. M., et al., "A Low-Cost, Manufacturable Method for Fabricating Capillary and Optical Fiber Interconnects for Microfluidic Devices," *Lab on a Chip*, Vol. 8, No. 4, pp. 609–616.

[55] Bargiel, S., et al., "Nanoliter Detectors for Flow Systems," *Sensors and Actuators A: Physical*, Vol. A115, No. 2-3, 2004, pp. 245–251.

[56] Leeds, A. R., et al., "Integration of Microfluidic and Microoptical Elements Using a Single-Mask Photolithographic Step," *Sensors and Actuators, A: Physical*, Vol. 115, No. 2-3, 2004, pp. 571–580.

[57] Furuki, M., et al., "Surface Plasmon Resonance Sensors Utilizing Microfabricated Channels," *Sensors and Actuators, B: Chemical*, Vol. 79, No. 1, 2001, pp. 63–69.

[58] Abrantes, M., et al., "Adaptation of a Surface Plasmon Resonance Biosensor with Microfluidics for Use with Small Sample Volumes and Long Contact Times," *Analytical Chemistry*, Vol. 73, No. 13, 2001, pp. 2828–2835.

[59] Gomez, F. A., *Biological Applications of Microfluidics*, New York: Wiley-Interscience, 2008.

[60] Sia, S. K., and G. M. Whitesides, "Microfluidic Devices Fabricated in Poly(Dimethylsiloxane) for Biological Studies," *Electrophoresis*, Vol. 24, No. 21, 2003, pp. 3563–3576.

[61] Yi, C., et al., "Microfluidics Technology for Manipulation and Analysis of Biological Cells," *Analytica Chimica Acta*, Vol. 560, No. 1-2, 2006, pp. 1–23.

[62] Cho, Y. H., et al., "Development of Microfluidic Device for Electrical/Physical Characterization of Single Cell," *Journal of Microelectromechanical Systems*, Vol. 15, No. 2, 2006, pp. 287–295.

[63] Helmke, B. P., and A. R. Minerick, "Designing a Nano-Interface in a Microfluidic Chip to Probe Living Cells: Challenges and Perspectives," *Proceedings of the National Academy of Sciences*, Vol. 103, No. 17, 2006, pp. 6419–6424.

[64] Matthews, B., and J. W. Judy, "Design and Fabrication of a Micromachined Planar Patch-Clamp Substrate with Integrated Microfluidics for Single-Cell Measurements," *Journal of Microelectromechanical Systems*, Vol. 15, No. 1, 2006, pp. 214–222.

[65] Helmke, B. P., and A. R. Minerick, "Designing a Nano-Interface in a Microfluidic Chip to Probe Living Cells: Challenges and Perspectives," *Proceedings of the National Academy of Sciences*, Vol. 103, No. 17, 2006, pp. 6419–6424.

[66] Burns, M. A., et al., "Integrated Nanoliter DNA Analysis Device," *Science*, Vol. 282, No. 5388, 1998, pp. 484–487.

[67] Dario, P., et al., "Micro-Systems in Biomedical Applications," *Journal of Micromechanics and Microengineering*, Vol. 10, No. 2, 2000, pp. 235–244.

[68] Receveur, R. A. M., F. W. Lindemans, and N. F. D. Rooij, "Microsystem Technologies for Implantable Applications," *Journal of Micromechanics and Microengineering*, Vol. 17, No. 5, 2007, pp. R50–R80.

[69] Wang, C. -H., and G. -B. Lee, "Automatic Bio-Sampling Chips Integrated with Micro-Pumps and Micro-Valves for Disease Detection," *Biosensors and Bioelectronics*, Vol. 21, No. 3, 2005, pp. 419–425.

[70] Shen, G., et al., "Coupling Confocal Fluorescence Microscopy and Microfluidic Device for Single Molecule Detection," *SPIE Proceedings—Microfluidics, BioMEMS, and Medical Microsystems VII*, Vol. 7207, San Jose, CA, 2009.

[71] Fu, L. -M., et al., "High Performance Microfluidic Capillary Electrophoresis Devices," *Biomedical Microdevices*, Vol. 9, No. 3, 2007, pp. 405–412.

[72] Hofmann, O., et al., "Adaptation of Capillary Isoelectric Focusing to Microchannels on a Glass Chip," *Analytical Chemistry*, Vol. 71, No. 3, 1999, pp. 678–686.

[73] McClain, M. A., et al., "Flow Cytometry of Escherichia Coli on Microfluidic Devices," *Analytical Chemistry*, Vol. 73, No. 21, 2001, pp. 5334–5338.

[74] Santiago, J. G., et al., "Particle Image Velocimetry System for Microfluidics," *Experiments in Fluids*, Vol, 25, No. 4, 1998, pp. 316–319.

[75] Koster, S., and E. Verpoorte, "A Decade of Microfluidic Analysis Coupled with Electrospray Mass Spectrometry: An Overview," *Lab on a Chip*, Vol. 7, No. 11, 2007, pp. 1394–1412.

[76] Kazarian, S. G., "Enhancing High-Throughput Technology and Microfluidics with FTIR Spectroscopic Imaging," *Analytical and Bioanalytical Chemistry*, Vol. 388, No. 3, 2007, pp. 529–532.

[77] McDonnell, E. E., et al., "NMR Analysis on Microfluidic Devices by Remote Detection," *Analytical Chemistry*, Vol. 77, No. 24, 2005, pp. 8109–8114.

List of Acronyms and Abbreviations

AFM atomic force microscope/microscopy

ALD atomic layer deposition

BCB benzocyclobutene

BioMEMS biological microelectromechanical systems

C_4F_8 octofluorocyclobutane

CD critical dimension

CE capillary electrophoresis

CF_4 carbon tetrafluoride

CHF_3 trifluoromethane

CMOS complementary metal-oxide-semiconductor

CMP chemical-mechanical polishing

CNC computer numerical control

COC cyclic olefin copolymer

CTE coefficient of thermal expansion

CVD chemical vapor deposition

DEP dielectrophoresis

DPN dip-pen nanolithography

DRIE deep reactive ion etching

DUV deep ultraviolet

EBL electron beam lithography

EDP ethylenediamine pyrocatechol

EOF electro-osmotic flow

EUV extreme ultraviolet

EWOD electrowetting-on-dielectric

FACS fluorescence-activated cell sorting

FIB focused ion beam

FTIR Fourier transform infrared

HCl hydrochloric acid

HDT heat deflection temperature

HF hydrofluoric acid

HMDS hexamethyldisilazane

IBE ion beam etching

ICP inductively coupled plasma

ITO indium tin oxide

KOH potassium hydroxide

LIF laser-induced fluorescence

LIGA lithographie, galvanoformung, abformung

LoC lab-on-chip

LPCVD low pressure chemical vapor deposition

LTCC low temperature cofired ceramic

MEMS microelectromechanical systems

μCP microcontact printing

μTAS micro total analysis system

MST microsystems technology

NIL nanoimprint lithography

NMR nuclear magnetic resonance

PBW proton beam writing

PCB printed circuit board

PDMS polydimethylsiloxane

PECVD plasma-enhanced chemical vapor deposition

PEEK polyetheretherketone

PET polyethylene terephthalate

PLD pulsed laser deposition

PMMA polymethyl methacrylate

PTFE polytetrafluoroethylene

PVD physical vapor deposition

PZT lead zirconate titanate

RF radio frequency

RF MEMS radio frequency microelectromechanical systems

RIE reactive ion etching

SAM self-assembled monolayer

SAW surface acoustic wave

SEM scanning electron microscope/microscopy

SF_6 sulfur hexafluoride

Si silicon

Si_3N_4 silicon nitride (stoichiometric)

SiNx silicon nitride

SiO_2 silicon dioxide

SMA shape memory alloy

SOG spin-on-glass

SOI silicon-on-insulator

SPM scanning probe microscope/microscopy

TEOS tetraethyl orthosilicate

Tg glass transition temperature

Tm melting temperature

TMAH tetramethyl ammonium hydroxide

UV ultraviolet

About the Authors

Sang-Joon John Lee is an associate professor of mechanical engineering at San José State University (SJSU), California, where he has been a full-time faculty member since 2002. At SJSU he is the director of the Microelectromechanical Systems (MEMS) Laboratory. His research focuses primarily on polymer microfluidics, with recent attention on fluid-structure interaction, microchannel flow dynamics, and surface engineering. Under National Science Foundation support, some of his curricular innovations have been in the areas of hands-on MEMS fabrication, microsystems design, and microfluidics simulation. At SJSU he is actively involved in collaborative faculty leadership for the Microscale Process Engineering Laboratory and the Materials Characterization and Metrology Center. In recent years he has been serving as co-principal investigator of the Nanoscale Materials and Device Characterization Program at SJSU (under the auspices of the Defense Microelectronic Activity), as well as serving as an advisory board member for an instructional video series on MEMS and nanotechnology by Silicon Run Productions.

Prior to this, Dr. Lee acquired much of his hands-on experience with microfabrication processes in the Stanford Nanofabrication Facility, as a research associate in the Rapid Prototyping Laboratory at Stanford University. His familiarity with semiconductor equipment design was acquired while working as a systems engineer at Applied Materials. Dr. Lee earned a B.S. in mechanical engineering from Stanford University and an M.S. and a Ph.D. in mechanical engineering from the Massachusetts Institute of Technology. At M.I.T. his graduate studies focused on manufacturing process innovation and control representation for a point-by-point additive fabrication process called Three-Dimensional Printing. His early teaching experience prior to SJSU came

through part-time instruction at Santa Clara University, where he developed new courses in MEMS and rapid prototyping. Dr. Lee is the coinventor of 10 U.S. patents in the areas of manufacturing process innovation and micro fuel design. His publications have been in the areas of microfluidics, microfabrication, and micro fuel cell technology.

Narayan Sundararajan is the chief technology officer of the Grameen-Intel joint venture (JV), a social business dedicated to social and economic development for the impoverished segment of the world population using information and communications technology solutions.. Dr. Sundararajan also oversees strategy and direction for the JV, including collaborations, identifying key focus areas for the JV and associated social impact and business model analyses. He also is a key member of the emerging markets healthcare strategy team at Intel responsible for driving the global mobile health workers program.

Previously, Dr. Sundararajan traversed various technical, business, and management roles at Intel working in diverse groups such as the New Business Initiatives (NBI), Digital Health Group (DHeG), and Corporate Technology Group (CTG). In NBI, he initiated projects using new platform concepts and business models to address opportunities related to remote healthcare solutions in the developing world. As part of CTG and DHeG, he helped launch the very first biotechnology research group at Intel as one of its early members, and invented several key microfluidics and biochip fabrication techniques such as 3D hydrodynamic focusing and planar pneumatic valves for use in single molecule DNA sequencing applications. He founded and managed programs in microfluidics and early cancer detection using biomarker discovery in collaboration with the Fred Hutchinson Cancer Research Center and Cedars Sinai Hospital. Dr. Sundararajan holds 11 patents issued, with 50 pending. He also has published 23 peer-reviewed papers and presented more than 20 talks including invited talks at conferences and academic institutions in the United States, Europe, Japan, Korea, and India. He was a member of the Technical Program Committee for International Conference on Transducers from 2005 to 2007 and was the member of the Industrial Advisory Board of Vital-IT, a high-performance computer center for bioinformatics, from 2004 to 2006. Dr. Sundararajan received a B.Tech. (Hons) in chemical engineering from the Indian Institute of Technology, Kharagpur, and an M.S. and a Ph.D. in materials science and engineering from Cornell University.

Index

Recent Titles in the Artech House Integrated Microsystems Series

Acoustic Wave and Electromechanical Resonators: Concept to Key Applications, Humberto Campanella

Adaptive Cooling of Integrated Circuits Using Digital Microfluidics, Philip Y. Paik, Krishnendu Chakrabarty, and Vamsee K. Pamula

Fundamentals and Applications of Microfluidics, Second Edition, Nam-Trung Nguyen and Steven T. Wereley

Integrated Interconnect Technologies for 3D Nanoelectronic Systems, Muhannad S. Bakir and James D. Meindl, editors

Introduction to Microelectromechanical (MEM) Microwave Systems, Héctor J. De Los Santos

An Introduction to Microelectromechanical Systems Engineering, Nadim Maluf

MEMS Mechanical Sensors, Stephen Beeby et al.

Micro and Nano Manipulations for Biomedical Applications, Tachung C. YihIlie Talpasanu

Microfabrication for Microfluidics, Sang-Joon John Lee and Narayan Sundararajan

Microfluidics for Biotechnology, Second Edition, Jean Berthier and Pascal Silberzan

Organic and Inorganic Nanostructures, Alexei Nabok

Post-Processing Techniques for Integrated MEMS, Sherif Sedky

Pressure-Driven Microfluidics, Václav Tesař

RFID-Enabled Sensor Design and Applicatons, Amin Rida, Li Yang, and Manos Tentzeris

RF MEMS Circuit Design for Wireless Communications, Héctor J. De Los Santos

Wafer-Level Testing and Test During Burn-in for Integrated Circuits, Sudarshan Bahukudumbi Krishnendu Chakrabarty

Wireless Sensor Network, Nirupama Bulusu and Sanjay Jha

For further information on these and other Artech House titles, including previously considered out-of-print books now available through our In-Print-Forever® (IPF®) program, contact:

Artech House
685 Canton Street
Norwood, MA 02062
Phone: 781-769-9750
Fax: 781-769-6334
e-mail: artech@artechhouse.com

Artech House
16 Sussex Street
London SW1V 4RW UK
Phone: +44 (0)20 7596-8750
Fax: +44 (0)20 7630-0166
e-mail: artech-uk@artechhouse.com

Find us on the World Wide Web at: www.artechhouse.com